ISSUE 2006

PROGRESS IN PHYSICS

VOLUME 3

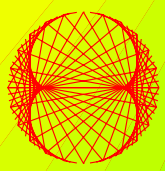

ISSN 1555-5534

The Journal on Advanced Studies in Theoretical and Experimental Physics, including Related Themes from Mathematics

PROGRESS IN PHYSICS

A quarterly issue scientific journal, registered with the Library of Congress (DC, USA). This journal is peer reviewed and included in the abstracting and indexing coverage of: Mathematical Reviews and MathSciNet (AMS, USA), DOAJ of Lund University (Sweden), Zentralblatt MATH (Germany), Referativnyi Zhurnal VINITI (Russia), etc.

Electronic version of this journal:
http://www.geocities.com/ptep_online

To order printed issues of this journal, contact the Editor in Chief.

Department of Mathematics, University of New Mexico, 200 College Road, Gallup, NM 87301, USA

ISSN: 1555-5534 (print)
ISSN: 1555-5615 (online)

Standard Address Number: 297-5092
Printed in the United States of America

JULY 2006 **VOLUME 3**

CONTENTS

Information for Authors and Subscribers

Progress in Physics has been created for publications on advanced studies in theoretical and experimental physics, including related themes from mathematics. All submitted papers should be professional, in good English, containing a brief review of a problem and obtained results.

All submissions should be composed in LaTeX format using the *Progress in Physics* template. This template can be downloaded from the *Progress in Physics* home page http://www.geocities.com/ptep_online. An abstract and the necessary information about authors should be included in the papers. To submit a paper, mail the files to the Editor in Chief.

All submitted papers should be as brief as possible. Beginning from 2006 we accept only papers no longer than 8 journal pages. Short articles are preferable.

Before preparing your paper please contact Editor in Chief for the current terms and conditions.

All material accepted for the online issue of *Progress in Physics* is printed in the paper version of the journal. To order printed issues, contact the Editor in Chief.

This journal is a non-commercial, academic edition. It is printed from private donations.

Open Letter by the Editor-in-Chief: Declaration of Academic Freedom (Scientific Human Rights)
*The Dutch Translation**

Declaratie van Academische Vrijheid

(Wetenschappelijke Mensenrechten)

Artikel 1: Preambule

Meer dan welke tijd dan ook in de geschiedenis van de mensheid weerspiegelt het begin van de 21e eeuw de diepgaande betekenis van de rol van wetenschap en technologie in menselijke aangelegenheden.

Het krachtige doordringende karakter van de moderne wetenschap en technologie heeft de algemene opvatting doen ontstaan dat verdere hoofdontdekkingen in principe alleen gemaakt kunnen worden door grote onderzoeksgroepen die gesubsidieerd worden door de overheid of het bedrijfsleven en die de beschikking hebben over uitzonderlijk dure instrumentatie en geassisteerd worden door hordes ondersteunend personeel.

Deze algemene opvatting is echter van mythische aard en is in tegenspraak met hoe wetenschappelijke ontdekkingen werkelijk gedaan worden. Grote en kostbare technologische projecten, hoe complex ook, zijn slechts het resultaat van het toepassen van diepe wetenschappelijke inzichten van kleine groepen toegewijde onderzoekers of alleen werkende wetenschappers die vaak in een isolement werken. Een wetenschapper die alleen werkt is nu en in de toekomst, net als in het verleden, in staat om een ontdekking te doen die een substantiële invloed heeft op het lot van de mensheid en die het aangezicht van de hele planeet waar we zo onbetekenend op verblijven verandert.

Fundamentele ontdekkingen worden over het algemeen gedaan door individuen op ondergeschikte posities binnen overheidsinstellingen, onderzoeks- en opleidingsinstituten of commerciële ondernemingen. Onderzoekers worden maar al te vaak beperkt en onderdrukt door instituten en bedrijfsdirecteuren die met een andere agenda werken en vanuit persoonlijke belangen of in het belang van het instituut of het bedrijf of door grootheidswaanzin wetenschappelijke ontdekkingen en onderzoek proberen te controleren en/of toe te passen.

De annalen van de wetenschap zijn bezaaid met wetenschappelijke ontdekkingen die onderdrukt en bespot werden door de gevestigde orde, maar die in latere jaren bekendheid kregen en in het gelijk gesteld werden door de onverbiddelijke opmars van praktische noodzakelijkheid en intellectuele verlichting. Daarnaast zijn de wetenschappelijke annalen bevlekt en besmeurd door plagiaat en opzettelijk valse voorstellingen, daden begaan door mensen zonder scrupules, mensen die gemotiveerd werden door jaloezie en hebzucht. En zo is het nog steeds.

Het doel van deze declaratie is het ondersteunen en bevorderen van het grondbeginsel dat stelt dat wetenschappelijk onderzoek vrij moet zijn van verborgen en openlijk onderdrukkende invloeden van bureaucratische, politieke, religieuze en commerciële aard en dat wetenschappelijke creatie niet minder een mensenrecht is dan andere soortgelijke rechten en wanhopige ondernemingen zoals die voorgesteld zijn in internationale verdragen en het internationale recht.

Wetenschappers die deze declaratie ondersteunen behoren zich eraan houden als teken van solidariteit en betrokkenheid met de internationale wetenschapsgemeenschap en als waarborg voor de rechten van alle wereldburgers om naar vermogen individuele vaardigheden en aanleg te gebruiken voor ongeremde wetenschappelijke creatie, dit ter bevordering van de wetenschap en, naar hun uiterste vermogen als betamelijke burgers in een onbetamelijke wereld, voor de vooruitgang van de mensheid. Wetenschap en technologie zijn veel te lang dienaren van onderdrukking geweest.

Artikel 2: Wie is een wetenschapper

Een wetenschapper is ieder persoon die aan wetenschap doet. Ieder persoon die met een wetenschapper samenwerkt in het ontwikkelen, produceren en voorstellen van ideeën en data tijdens onderzoek of toepassing is ook een wetenschapper.

Artikel 3: Waar wordt er wetenschap geproduceerd

Wetenschappelijk onderzoek kan overal worden uitgevoerd, bijvoorbeeld op een werkplek, tijdens een formele educatiecursus, tijdens een gesponsord academisch programma, in groepen, of als individu die thuis onafhankelijk onderzoek doet.

Artikel 4: Vrijheid van keuze van onderzoeksthema

Veel wetenschappers die werken voor een hogere onderzoeksgraad of in andere onderzoeksprogramma's op academische instituten zoals universiteiten of hogescholen worden verhinderd om te werken aan een onderzoeksonderwerp naar eigen keuze door begeleidende academici en/of administra-

*Original text published in English: *Progress in Physics*, 2006, v. 1, 57–60. Online — http://www.geocities.com/ptep_online/.

Originele Engelse versie door Dmitri Rabounski, hoofdredacteur van het tijdschrift *Progress in Physics*. E-mail: rabounski@yahoo.com.

Vertaald door Eit Gaastra. E-mail: eitgaastra@freeler.nl.

tieve ambtenaren, niet vanwege het ontbreken van ondersteunende faciliteiten maar omdat de academische hiërarchie en/of andere ambtenaren doodeenvoudig de onderzoeksrichting niet goedkeuren als het voorgestelde onderzoek de potentie heeft om voor onrust te zorgen ten aanzien van heersende dogma's en favoriete theorieën, of als het voorgestelde onderzoek de subsidies van andere projecten in gevaar kan brengen. Het gezag van de orthodoxe meerderheid meent zeer vaak een onderzoeksproject te moeten torpederen zodat gezag en budgetten onaangetast blijven. Deze alledaagse praktijken zijn weloverwogen belemmeringen om vrije wetenschappelijke gedachten tegen te houden, ze zijn extreem onwetenschappelijk en crimineel. Ze mogen niet getolereerd worden.

Een wetenschapper die werkt voor een academisch instituut, autoriteit of instelling behoort volkomen vrij te zijn ten aanzien van de keuze van het onderzoeksonderwerp en mag enkel beperkt worden door de materiële ondersteuning en intellectuele vaardigheden die geboden worden door het opleidingsinstituut, de instelling of de autoriteit. Als de wetenschapper een onderzoek uitvoert als lid van een samenwerkende groep behoren de onderzoeksdirecteuren en teamleiders zich te beperken tot een adviserende en consulterende rol met betrekking tot de keuze van een relevant onderzoeksthema door een wetenschapper in de groep.

Artikel 5: Vrijheid van keuze van onderzoeksmethoden

Het gebeurt vaak dat er op een wetenschapper druk wordt uitgeoefend door administratief personeel of begeleidende academici met betrekking tot een onderzoeksprogramma dat in een academische omgeving wordt uitgevoerd. Deze druk wordt uitgeoefend om een wetenschapper er toe te dwingen om andere onderzoeksmethoden te gebruiken dan de wetenschapper heeft gekozen, dit vanwege geen andere reden dan persoonlijke voorkeur, vooroordeel, institutioneel beleid, redactionele voorschriften of verenigde autoriteit. Deze praktijk, die zeer wijdverbreid is, is een weloverwogen ontkenning van de vrijheid van gedachten en kan niet toegestaan worden.

Een non-commerciële of academische wetenschapper heeft het recht om een onderzoeksthema te ontwikkelen op elke redelijke manier en met alle redelijke middelen die hij als het meest effectief beschouwt. De uiteindelijke beslissing ten aanzien van hoe het onderzoek uitgevoerd zal worden behoort te worden gemaakt door de wetenschapper zelf.

Als een non-commerciële of academische wetenschapper werkt als lid van een samenwerkend non-commercieel of academisch team van wetenschappers behoren de projectleiders en onderzoeksdirecteuren enkel adviserende en consulterende rechten te hebben en behoren zij niet op een andere manier de onderzoeksmethoden of het onderzoeksthema van de wetenschapper in de groep te beïnvloeden, matigen of beperken.

Artikel 6: Vrijheid van samenwerking en deelname in een onderzoek

Er is een aanzienlijke hoeveelheid institutionele rivaliteit in de alledaagse praktijk van de moderne wetenschap die samengaat met gevallen van persoonlijke jaloezie en het ten koste van alles zorgen voor het behoud van reputaties, ongeacht het wetenschappelijke wezen. Dit heeft er vaak toe geleid dat wetenschappers belet werden de hulp in te roepen van competente collega's van rivaliserende instituten of anderen zonder enige binding met een academisch instituut. Ook deze praktijken zijn weloverwogen belemmeringen van wetenschappelijke vooruitgang.

Als een non-commerciële wetenschapper assistentie van een ander persoon nodig heeft en deze andere persoon stemt daarin toe dan heeft de wetenschapper de vrijheid om die persoon uit te nodigen om enige of alle mogelijke assistentie te verlenen mits de assistentie binnen het aan het onderzoek verbonden budget valt. Als de assistentie onafhankelijk is van budgetoverwegingen heeft de wetenschapper de vrijheid om de assisterende persoon naar eigen goeddunken in dienst te nemen, vrij van enige bemoeienis door welk ander persoon dan ook.

Artikel 7: Vrijheid van meningsverschil in wetenschappelijke discussies

Door heimelijke jaloezie en oude gevestigde belangen verafschuwt de moderne wetenschap openlijke discussie en verbant zij moedwillig wetenschappers die twijfelen aan de orthodoxe standpunten. Zeer vaak worden uitzonderlijk bekwame wetenschappers die op de tekortkomingen in de gangbare theorieën of interpretatie van data wijzen gelabeld als zonderlingen, zodat hun denkbeelden probleemloos genegeerd kunnen worden. Ze worden publiekelijk en privé bespot en het wordt hen systematisch belet om conferenties, seminaries en colloquia te bezoeken, zodat hun ideeën geen publiek kunnen vinden. Opzettelijke vervalsing van data en het verkeerd voorstellen van theorieën zijn nu veel gebruikte werktuigen van onscrupuleuzen in het onderdrukken van feiten, zowel technisch als historisch. Er hebben zich internationale commissies van wetenschappelijke onverlaten gevormd en deze commissies treden als gastheer op tijdens door henzelf in het leven geroepen internationale conferenties waar alleen hun volgelingen toegestaan wordt om lezingen te presenteren, ongeacht de kwaliteit van de inhoud. Deze commissies halen enorme sommen geld uit de publieke portemonnee om hun gesponsorde projecten te subsidiëren door hun toevlucht te nemen tot misleiding en leugens. Iedere op wetenschappelijke gronden berustende tegenwerping ten aanzien van hun voorstellen wordt op hun instigatie volledig doodgezwegen, zodat geld naar hun projecten kan blijven stromen en hun goedbetaalde banen gegarandeerd blijven. Opponerende wetenschappers zijn in

hun opdracht ontslagen; anderen is het belet om zekerheidbiedende academische aanstellingen te krijgen door een netwerk van corrupte medeplichtigen. In andere situaties zijn sommigen verdreven van een kandidatuur voor programma's voor een hogere graad, zoals promotie naar een doctortitel, omdat ze ideeën hebben geuit die de gangbare theorie zouden kunnen ondermijnen, hoe oud die orthodoxe theorie ook was. Het fundamentele feit dat geen wetenschappelijke theorie definitief noch onschendbaar is en daarom open staat voor discussie en her-evaluatie wordt door hen grondig genegeerd. Ook negeren ze het feit dat een fenomeen meerdere aannemelijke verklaringen kan hebben en brengen ze iedere verklaring die niet in overeenstemming is met de orthodoxe opinie kwaadaardig in diskrediet. Zonder aarzelen nemen ze hun toevlucht tot het gebruik van onwetenschappelijke argumenten om hun vooringenomen mening te rechtvaardigen.

Alle wetenschappers behoren vrij te zijn om over hun onderzoek en het onderzoek van anderen te discussiëren zonder angst om publiekelijk of privé zonder wezenlijke argumenten belachelijk gemaakt te worden of te worden beschuldigd, gekleineerd, betwist of anderszins in diskrediet gebracht te worden door ongefundeerde aantijgingen. Geen wetenschapper mag in een positie gebracht worden waar levensonderhoud of reputatie in gevaar zijn als gevolg van het uiten van een wetenschappelijke mening. Vrijheid van wetenschappelijke expressie behoort een uiterst hoog goed te zijn. Het gebruik van macht in het weerleggen van een wetenschappelijk argument is niet wetenschappelijk en behoort niet gebruikt te worden om te muilkorven, onderdrukken, intimideren, verbannen of anderszins een wetenschapper te dwingen of uit te sluiten. Opzettelijke onderdrukking van wetenschappelijke feiten of argumenten, zowel actief door daad als passief door weglaten, en opzettelijke vervalsing van data om een argument te ondersteunen of om een opponerende opvatting in diskrediet te brengen is wetenschappelijke fraude en dient beschouwd te worden als een wetenschappelijke misdaad. Grondbeginselen ten aanzien van bewijsmateriaal behoren iedere wetenschappelijke discussie te begeleiden, of het bewijsmateriaal nu experimenteel, theoretisch of een combinatie van die twee is.

Artikel 8: Vrijheid van publicatie van wetenschappelijke resultaten

Een betreurenswaardige censuur is nu de standaardpraktijk geworden bij redacties van de belangrijke wetenschapstijdschriften en elektronische archieven en hun bendes zogenaamde deskundige referees. De referees worden voor het grootste deel beschermd door anonimiteit zodat de auteur niet hun zogenaamde deskundigheid kan verifiëren. Stukken worden momenteel routinematig geweigerd als de auteur de dominante theorie en gangbare orthodoxie verwerpt of weerlegt. Veel stukken worden nu automatisch geweigerd omdat bij de referenties een wetenschapper staat die in ongenade is gevallen bij de redacteuren, referees of andere deskundige censoren, zonder dat men zich ook maar enigszins over de inhoud van het stuk bekommert. Er bestaat een zwarte lijst van wetenschappers die een afwijkende mening hebben en deze lijst gaat over en weer tussen participerende redacties. Dit alles draagt bij aan grove vooringenomenheid en een misdadige onderdrukking van vrije gedachten en dient veroordeeld te worden door de internationale wetenschapsgemeenschap.

Alle wetenschappers behoren het recht te hebben om hun wetenschappelijke onderzoeksresultaten geheel of gedeeltelijk te presenteren op relevante wetenschapconferenties en hetzelfde te publiceren in gedrukte wetenschapstijdschriften, elektronische archieven en welke andere media dan ook. Van geen enkele wetenschapper behoren stukken of verslagen die ter publicatie aangeboden worden aan wetenschapstijdschriften, elektronische archieven of andere media geweigerd te worden alleen maar omdat het werk de gangbare meerderheidsmening ter discussie stelt, in conflict is met de opvattingen van de redactie, de bases ondermijnt van andere in gang gezette of geplande onderzoeksprojecten van andere wetenschappers, of botst met een politiek dogma, religieus geloof of persoonlijke mening van een ander, en geen enkele wetenschapper behoort op een zwarte lijst te staan of anderszins gecensureerd te worden noch verhinderd te worden om tot publicatie te komen door welk ander persoon dan ook. Geen wetenschapper behoort door de belofte van een geschenk of andere vergoeding ter omkoping de publicatie van het werk van een andere wetenschapper te blokkeren, modificeren of anderszins met de publicatie van het werk te interfereren.

Artikel 9: Het co-auteurschap van wetenschappelijke artikelen

Het is een slecht verborgen gehouden geheim binnen wetenschappelijke kringen dat veel co-auteurs van onderzoeksartikelen eigenlijk weinig of niks van doen hebben met het onderzoek waarover gerapporteerd wordt. Veel supervisors van afstuderende studenten bijvoorbeeld zijn er niet afkerig van om hun namen op artikelen te zetten van personen die slechts nominaal onder hun supervisie werken. In veel van die gevallen heeft degene die het artikel schrijft een superieur begrip ten aanzien van de materie vergeleken met de supervisor. In andere situaties, ook nu weer met als doel algemene bekendheid, reputatie, geld, prestige en dergelijke, worden niet-participerende personen aan het artikel toegevoegd als co-auteur. De werkelijke auteurs van dergelijke artikelen kunnen hiertegen enkel protesteren in het besef dat ze het risico lopen om later hiervoor gestraft te worden of, naar gelang de omstandigheden, zelfs uitgesloten te worden van de kandidatuur voor een hogere onderzoeksgraad of van de onderzoeksgroep. Velen zijn feitelijk ver-

bannen onder dergelijke omstandigheden. Deze ontstellende praktijken kunnen niet getolereerd worden. Alleen de personen verantwoordelijk voor het onderzoek behoren als auteur geaccrediteerd te worden.

Geen wetenschapper behoort een ander persoon uit te nodigen om toegevoegd te worden en geen wetenschapper behoort het toe te staan dat zijn of haar naam toegevoegd wordt als co-auteur van een wetenschappelijk artikel als hij of zij niet significant heeft bijgedragen aan het onderzoek waarover gerapporteerd wordt in het artikel. Geen wetenschapper behoort het toe te staan dat hij of zij door een vertegenwoordiger van een academisch instituut, corporatie, overheidsinstelling of enig ander persoon als co-auteur toegevoegd wordt aan een artikel dat een onderzoek betreft waar hij of zij niet significant aan heeft bijgedragen, en geen wetenschapper behoort het toe te staan dat zijn of haar naam gebruikt wordt als co-auteur met als tegenprestatie welk geschenk of andere vergoeding ter omkoping dan ook. Geen persoon behoort een wetenschapper op wat voor manier dan ook ertoe te bewegen of proberen ertoe te bewegen om het toe te staan dat de naam van de wetenschapper toegevoegd wordt als co-auteur van een wetenschappelijk artikel dat een inhoud heeft waar hij of zij niet significant aan heeft bijgedragen.

Artikel 10: Onafhankelijkheid van affiliatie

Veel wetenschappers zijn nu in dienst met een korte termijn contract. Met de beëindiging van het dienstverband komt er ook een einde aan de academische affiliatie. Redacties voeren vaak het beleid dat personen zonder een academische of commerciële affiliatie niet gepubliceerd worden. Zonder affiliatie kan een wetenschapper van veel middelen niet gebruik maken en de mogelijkheden om lezingen te geven en artikelen te presenteren op conferenties worden er door beperkt. Dit is een verdorven praktijk die gestopt moet worden. Wetenschap herkent geen affiliatie.

Geen wetenschapper behoort belet te worden om artikelen te presenteren op conferenties, colloquia te geven op seminaries, te publiceren in welke media dan ook, toegang te krijgen tot academische bibliotheken of wetenschappelijke publicaties, wetenschappelijke bijeenkomsten bij te wonen of lezingen te geven, vanwege het niet geaffilieerd zijn met een academisch instituut, wetenschappelijk instituut, overheids- of bedrijfslaboratorium, of welke andere organisatie dan ook.

Artikel 11: Vrije toegang tot wetenschappelijke informatie

De meeste gespecialiseerde boeken over wetenschappelijke aangelegenheden en veel wetenschappelijke tijdschriften leveren weinig tot geen winst op zodat commerciële uitgevers niet bereid zijn ze te publiceren zonder een geldbijdrage van academische instituten, overheidsinstellingen, filantropische stichtingen en dergelijke. Onder zulke omstandigheden zouden commerciële uitgevers vrije toegang tot elektronische versies van de publicaties toe moeten staan en ernaar moeten streven de kosten van het gedrukte materiaal tot een minimum te beperken.

Alle wetenschappers behoren ernaar te streven dat hun onderzoeksartikelen gratis beschikbaar zijn voor de internationale wetenschapsgemeenschap of, als dat niet mogelijk is, beschikbaar zijn voor zo weinig mogelijk kosten. Alle wetenschappers zouden actief maatregelen moeten nemen om hun technische boeken verkrijgbaar te maken voor zo weinig mogelijk kosten, zodat de wetenschappelijke informatie beschikbaar kan zijn voor een bredere internationale wetenschapsgemeenschap.

Artikel 12: Ethische verantwoordelijkheid van wetenschappers

De geschiedenis toont ons dat wetenschappelijke ontdekkingen gebruikt worden voor zowel goed als kwaad en dat ze sommigen ten goede komen en anderen vernietigen. Omdat de vooruitgang van wetenschap en technologie niet kan stoppen zullen er bepaalde middelen moeten komen om kwaadaardige toepassingen te voorkomen. Enkel een democratisch gekozen regering die vrij is van religieuze, raciale en andere vooroordelen kan de beschaafde wereld waarborgen. Enkel democratisch gekozen regeringen, tribunalen en commissies kunnen het recht van vrije wetenschappelijke creatie waarborgen. Momenteel zijn er verscheidene ondemocratische staten en totalitaire regimes die actief onderzoek uitvoeren op het gebied van nucleaire fysica, chemie, virologie, genetische manipulatie, etc. om nucleaire, chemische en biologische wapens te produceren. Geen wetenschapper behoort vrijwillig samen te werken met ondemocratische staten of totalitaire regimes. Iedere wetenschapper die gedwongen wordt om te werken aan het ontwikkelen van wapens voor zulke staten behoort wegen en middelen te vinden om de vooruitgang van de onderzoeksprogramma's te vertragen en de wetenschappelijke output te beperken, zodat beschaving en democratie ten slotte kunnen zegevieren.

Alle wetenschappers dragen een morele verantwoordelijkheid voor hun wetenschappelijke creaties en ontdekkingen. Geen wetenschapper behoort zich vrijwillig bezig te houden met het ontwerpen of vervaardigen van wapens van welke soort dan ook voor ondemocratische staten of totalitaire regimes, of toestaan dat zijn of haar wetenschappelijke vaardigheden of kennis gebruikt wordt voor de ontwikkeling van wat dan ook dat de mensheid kan beschadigen. Een wetenschapper behoort te leven met het dictum dat iedere ondemocratische regering en iedere schending van de mensenrechten misdadig is.

28 maart 2006

On Isotropic Coordinates and Einstein's Gravitational Field

Stephen J. Crothers

Queensland, Australia

E-mail: thenarmis@yahoo.com

It is proved herein that the metric in the so-called "isotropic coordinates" for Einstein's gravitational field is a particular case of an infinite class of equivalent metrics. Furthermore, the usual interpretation of the coordinates is erroneous, because in the usual form given in the literature, the alleged coordinate length $\sqrt{dx^2+dy^2+dz^2}$ is not a coordinate length. This arises from the fact that the geometrical relations between the components of the metric tensor are invariant and therefore bear the same relations in the isotropic system as those of the metric in standard Schwarzschild coordinates.

1 Introduction

Petrov [1] developed an algebraic classification of Einstein's field equations. Einstein's field equations can be written as,

$$R_{\alpha\beta} - \frac{1}{2} R g_{\alpha\beta} = \kappa T_{\alpha\beta} - \lambda g_{\alpha\beta} ,$$

where κ is a constant, and λ the so-called cosmological constant. If $T_{\alpha\beta} \propto g_{\alpha\beta}$, the associated space is called an Einstein space. Thus, Einstein spaces include those described by partially degenerate metrics of this form. Consequently, such metrics become non-Einstein only when

$$g = \det \|g_{\alpha\beta}\| = 0 .$$

A simple source is a spherically symmetric mass (a mass island), without charge or angular momentum. A simple source giving rise to a static gravitational field in vacuum, where space is isotropic and homogeneous, constitutes a Schwarzschild space. The associated field equations external to the simple source are

$$R_{\alpha\beta} - \frac{1}{2} R g_{\alpha\beta} = 0 ,$$

or, more simply,

$$R_{\alpha\beta} = 0 .$$

Thus, a Schwarzschild space is an Einstein space. There are four types of Einstein spaces. The Schwarzschild space is a type 1 Einstein space. It gives rise to a spherically symmetric gravitational field.

The simple source interacts with a "test" particle, which has no charge, no angular momentum, and effectively no mass, or so little mass that its own gravitational field can be neglected entirely. A similar concept is utilised in electrodynamics in the notion of a "test" charge.

The only solutions known for Einstein's field equations involve a single gravitating source interacting with a test particle. There are no known solutions for two or more interacting comparable masses. In fact, it is not even known if Einstein's field equations admit of solutions for multi-body configurations, as no existence theorem has even been adduced. It follows that there is no theoretical sense to concepts such as black hole binaries, or colliding or merging black holes, notwithstanding the all too common practice of assuming them well-posed theoretical problems allegedly substantiated by observations.

The metric for Einstein's gravitational field in the usual isotropic coordinates is, in relativistic units ($c = G = 1$),

$$ds^2 = \frac{\left(1-\frac{m}{2r}\right)^2}{\left(1+\frac{m}{2r}\right)^2} dt^2 - \left(1+\frac{m}{2r}\right)^4 \left[dr^2 + r^2\left(d\theta^2 + \sin^2\theta\, d\varphi^2\right)\right] = \tag{1a}$$

$$= \frac{\left(1-\frac{m}{2r}\right)^2}{\left(1+\frac{m}{2r}\right)^2} dt^2 - \left(1+\frac{m}{2r}\right)^4 \left(dx^2+dy^2+dz^2\right), \tag{1b}$$

having set $r = \sqrt{x^2+y^2+z^2}$. This metric describes a Schwarzschild space.

By virtue of the factor $(dx^2+dy^2+dz^2)$ it is usual that $0 \leqslant r < \infty$ is taken. However, this standard range on r is due entirely to assumption, based upon the misconception that because $0 \leqslant r < \infty$ is defined on the usual Minkowski metric, this must also hold for (1a) and (1b). Nothing could be further from the truth, as I shall now prove.

2 Proof

Consider the standard Minkowski metric,

$$\begin{aligned} ds^2 &= dt^2 - dx^2 - dy^2 - dz^2 \equiv \\ &\equiv dt^2 - dr^2 - r^2(d\theta^2 + \sin^2\theta d\varphi^2) , \\ &0 \leqslant r < \infty . \end{aligned} \tag{2}$$

The spatial components of this metric describe a sphere of radius $r \geqslant 0$, centred at $r = 0$. The quantity r is an Efcleeth-

ean* distance since Minkowski space is pseudo-Efcleethean.

Now (2) is easily generalised [2] to

$$ds^2 = dt^2 - dr^2 - (r - r_0)^2(d\theta^2 + \sin^2\theta\, d\varphi^2) = \tag{3a}$$

$$= dt^2 - \frac{(r - r_0)^2}{|r - r_0|^2}\, dr^2 - |r - r_0|^2(d\theta^2 + \sin^2\theta\, d\varphi^2)\,, \tag{3b}$$

$$= dt^2 - d|r - r_0|^2 - |r - r_0|^2(d\theta^2 + \sin^2\theta\, d\varphi^2)\,, \tag{3c}$$

$$0 \leqslant |r - r_0| < \infty\,.$$

The spatial components of equations (3) describe a sphere of radius $R_c(r) = |r - r_0|$, centred at a point located anywhere on the 2-sphere r_0. Only if $r_0 = 0$ does (3) describe a sphere centred at the origin of the coordinate system. With respect to the underlying coordinate system of (3), $R_c(r)$ is the radial distance between the 2-spheres $r = r_0$ and $r \neq r_0$.

The usual practice is to supposedly generalise (2) as

$$ds^2 = A(r)dt^2 - B(r)\big(dr^2 + r^2 d\theta^2 + r^2\sin^2\theta\, d\varphi^2\big) \tag{4}$$

to finally obtain (1a) in the standard way, with the assumption that $0 \leqslant r < \infty$ on (2) must hold also on (4), and hence on equations (1). However, this assumption has never been proved by the theoreticians. The assumption is demonstrably false. Furthermore, this procedure does not produce a generalised solution in terms of the parameter r, but instead a particular solution.

Since (3) is a generalisation of (2), I use it to generalise (4) to

$$ds^2 = e^{\nu}dt^2 - e^{\mu}\big(dh^2 + h^2 d\theta^2 + h^2\sin^2\theta\, d\varphi^2\big) \tag{5}$$

$$h = h(r) = h(|r - r_0|),\quad \nu = \nu(h(r)),\quad \mu = \mu(h(r))\,.$$

Note that (5) can be written in the mixed form

$$ds^2 = e^{\nu}dt^2 - e^{\mu}\left[\left(\frac{dh}{dr}\right)^2 dr^2 + h^2 d\theta^2 + h^2\sin^2\theta d\varphi^2\right], \tag{6}$$

from which the particular form (4) usually used is recovered if $h(|r - r_0|) = r$. However, no particular form for $h(|r - r_0|)$ should be pre-empted. Doing so, in the routine fashion of the majority of the relativists, produces only a particular solution in terms of the Minkowski r, with all the erroneous assumptions associated therewith.

Now (5) must satisfy the energy-momentum tensor equations for the simple, static, vacuum field:

$$0 = e^{-\mu}\left(\frac{\mu'^2}{4} + \frac{\mu'\nu'}{2} + \frac{\mu' + \nu'}{h}\right)$$

$$0 = e^{-\mu}\left(\frac{\mu''}{2} + \frac{\nu''}{2} + \frac{\nu'^2}{r} + \frac{\mu' + \nu'}{2h}\right)$$

$$0 = e^{-\mu}\left(\mu'' + \frac{\mu'^2}{4} + \frac{2\mu'}{h}\right),$$

where the prime indicates d/dh. This gives, in the usual way,

$$ds^2 = \frac{\left(1 - \frac{m}{2h}\right)^2}{\left(1 + \frac{m}{2h}\right)^2}\, dt^2 - \\ - \left(1 + \frac{m}{2h}\right)^4\left[dh^2 + h^2\left(d\theta^2 + \sin^2\theta\, d\varphi^2\right)\right], \tag{7}$$

from which the admissible form for $h(|r - r_0|)$ and the value of the constant r_0 must be rigorously ascertained from the intrinsic geometrical properties of the metric itself.

Now the intrinsic geometry of the metric (2) is the same on all the metrics given herein in terms of the spherical coordinates of Minkowski space, namely, the radius of curvature R_c in the space described by the metric is always the square root of the coefficient of the angular terms of the metric and the proper radius R_p is always the integral of the square root of the component containing the differential element of the radius of curvature. Thus, on (2),

$$R_c(r) \equiv r,\quad R_p(r) \equiv \int_0^r dr = r \equiv R_c(r)\,,$$

and on (3),

$$R_c(r) \equiv |r - r_0|\,,$$

$$R_p(r) \equiv \int_0^{|r - r_0|} dr = |r - r_0| \equiv R_c(r)\,,$$

whereby it is clear that $R_c(r)$ and $R_p(r)$ are identical, owing to the fact that the spatial coordinates of (2) and (3) are Efcleethean.

Now consider the general metric of the form

$$ds^2 = A(r)dt^2 - B(r)dr^2 - C(r)(d\theta^2 + \sin^2\theta\, d\varphi^2) \tag{8}$$

$$A, B, C > 0.$$

In this case,

$$R_c(r) = \sqrt{C(r)},\quad R_p(r) = \int\sqrt{B(r)}\, dr\,.$$

I remark that although (8) is mathematically valid, it is misleading. In the cases of (2) and (3), the respective metrics are given in terms of the radius of curvature and its differential element. This is not the case in (8) where the first and second components are in terms of the parameter r of the radius of curvature, not the radius of curvature itself. I therefore write (8) in terms of only the radius of curvature on (8), thus

$$ds^2 = A^*\big(\sqrt{C(r)}\big)dt^2 - B^*\big(\sqrt{C(r)}\big)d\sqrt{C(r)}^{\,2} - \\ - C(r)(d\theta^2 + \sin^2\theta\, d\varphi^2)\,, \tag{9a}$$

$$A^*, B^*, C > 0\,.$$

*Due to Efcleethees, incorrectly Euclid, so the geometry is rightly Efcleethean.

Note that (9a) can be written as,

$$ds^2 = A^*\left(\sqrt{C(r)}\right)dt^2 - B^*\left(\sqrt{C(r)}\right)\left(\frac{d\sqrt{C(r)}}{dr}\right)^2 dr^2 - \\ - C(r)\left(d\theta^2 + \sin^2\theta\, d\varphi^2\right), \tag{9b}$$

$$A^*, B^*, C > 0,$$

and by setting

$$B^*\left(\sqrt{C(r)}\right)\left(\frac{d\sqrt{C(r)}}{dr}\right)^2 = B(r),$$

equation (8) is recovered, proving that (8) and equations (9) are mathematically equivalent, and amplifying the fact that (8) is a mixed-term metric. Note also that if $C(r)$ is set equal to r^2, the alleged general form used by most relativists is obtained. However, the form of $C(r)$ should not be pre-empted, for by doing so only a particular parametric solution is obtained, and with the form chosen by most relativists, the properties of r in Minkowski space are assumed (incorrectly) to carry over into the metric for the gravitational field.

It is also clear from (8) and equations (9) that $|r - r_0|$ is the Efcleethean distance between the centre of mass of the field source and a test particle, in Minkowski space, and which is mapped into $R_c(r)$ and $R_p(r)$ of the gravitational field by means of functions determined by the structure of the gravitational metric itself, namely the functions given by

$$R_c(r) = \sqrt{C(r)},$$

$$R_p(r) = \int \sqrt{B^*\left(\sqrt{C(r)}\right)}\, d\sqrt{C(r)} = \int \sqrt{B(r)}\, dr.$$

In the case of the usual metric the fact that $|r - r_0|$ is the Efcleethean distance between the field source and a test particle in Minkowski space is suppressed by the choice of the particular function $\sqrt{C(r)} = r^2$, so that it is not immediately apparent that when r goes down to $\alpha = 2m$ on that metric, the parametric distance between field source and test particle has gone down to zero. Generally, as the parametric distance goes down to zero, the proper radius in the gravitational field goes down to zero, irrespective of the location of the field source in parameter space. Thus, the field source is always located at $R_p = 0$ as far as the metric for the gravitational field is concerned.

It has been proved elsewhere [3, 4] that in the case of the simple "point-mass" (a fictitious object), metrics of the form (8) or (9) are characterised by the following scalar invariants,

$$R_p(r_0) \equiv 0, \quad R_c(r_0) \equiv 2m, \quad g_{00}(r_0) \equiv 0, \tag{10}$$

so that the actual value of r_0 is completely irrelevant.

Now (7) can be written as

$$ds^2 = \frac{\left(1 - \frac{m}{2h}\right)^2}{\left(1 + \frac{m}{2h}\right)^2} dt^2 - \\ - \left(1 + \frac{m}{2h}\right)^4 dh^2 - h^2\left(1 + \frac{m}{2h}\right)^4 \left(d\theta^2 + \sin^2\theta\, d\varphi^2\right), \tag{11}$$

$$h = h(r) = h(|r - r_0|).$$

Since the geometrical relations between the components of the metric tensor are invariant it follows that on (11),

$$R_c(r) = h(r)\left(1 + \frac{m}{2h(r)}\right)^2, \tag{12a}$$

$$R_p(r) = \int \left(1 + \frac{m}{2h(r)}\right)^2 dh(r) = \\ = h(r) + m\ln h(r) - \frac{m^2}{2}\frac{1}{h(r)} + K,$$

where $K = \text{constant}$,

$$R_p(r) = h(r) + m\ln\frac{h(r)}{K_1} - \frac{m^2}{2}\frac{1}{h(r)} + K_2 \tag{12b}$$

where K_1 and K_2 are constants.

It is required that $R_p(r_0) \equiv 0$, so

$$0 = h(r_0) + m\ln\frac{h(r_0)}{K_1} - \frac{m^2}{2}\frac{1}{h(r_0)} + K_2,$$

which is satisfied only if

$$h(r_0) = K_1 = K_2 = \frac{m}{2}. \tag{13}$$

Therefore,

$$R_p(r) = h(r) + m\ln\left(\frac{2h(r)}{m}\right) - \frac{m^2}{2}\frac{1}{h(r)} + \frac{m}{2}. \tag{14}$$

According to (12a), and using (13),

$$R_c(r_0) = \frac{m}{2}\left(1 + \frac{m}{2\frac{m}{2}}\right)^2 = 2m,$$

satisfying (10) as required.

Now from (11),

$$g_{00}(r) = \frac{\left(1 - \frac{m}{2h(r)}\right)^2}{\left(1 + \frac{m}{2h(r)}\right)^2},$$

and using (13),

$$g_{00}(r_0) = \frac{\left(1 - \frac{2m}{2m}\right)^2}{\left(1 + \frac{2m}{2m}\right)^2} = 0,$$

satisfying (10) as required.

It remains now to ascertain the general admissible form of $h(r) = h(|r - r_0|)$.

By (6),

$$\frac{dh}{dr} \neq 0 \quad \forall \quad r \neq r_0.$$

It is also required that (11) become Minkowski in the infinitely far field, so

$$\lim_{|r-r_0|\to\infty} \frac{h^2(r)\left(1+\frac{m}{2h(r)}\right)^4}{|r-r_0|^2} \to 1\,,$$

must be satisfied.

When there is no matter present ($m=0$), $h(r)$ must reduce the metric to Minkowski space.

Finally, $h(r)$ must be able to be arbitrarily reduced to r by a suitable choice of arbitrary constants so that the usual metric (1a) in isotropic coordinates can be recovered at will.

The only form for $h(r)$ that satisfies all the requirements is

$$h(r)=\left[|r-r_0|^n+\left(\frac{m}{2}\right)^n\right]^{\frac{1}{n}}, \qquad n\in\Re^+,\quad r_0\in\Re,\quad r\neq r_0\,, \tag{15}$$

where n and r_0 are entirely arbitrary constants. The condition $r\neq r_0$ is necessary since the "point-mass" is not a physical object.

Setting $n=1$, $r_0=\frac{m}{2}$, and $r>r_0$ in (15) gives the usual metric (1a) in isotropic coordinates. Note that in this case $r_0=\frac{m}{2}$ is the location of the fictitious "point-mass" in parameter space (i. e. in Minkowski space) and thus as the distance between the test particle and the source, located at $r_0=\frac{m}{2}$, goes to zero in parameter space, the proper radius in the gravitational field goes to zero, the radius of curvature goes to $2m$, and g_{00} goes to zero. Thus, the usual claim that the term $dr^2+r^2(d\theta^2+\sin^2\theta\,d\varphi^2)$ (or $dx^2+dy^2+dz^2$) describes a coordinate length is false. Note that in choosing this case, the resulting metric suppresses the true nature of the relationship between the r-parameter and the gravitational field because, as clearly seen by (15), $r_0=\frac{m}{2}$ drops out. Note also that (15) generalises the mapping so that distances on the real line are mapped into the gravitational field.

Consequently, there is no black hole predicted by the usual metrics (1) in isotropic coordinates. The black hole concept has no validity in General Relativity (and none in Newton's theory either since the Michell-Laplace dark body is not a black hole [5, 6]).

The singularity at $R_p(r_0)\equiv 0$ is insurmountable because

$$\lim_{|r-r_0|\to 0} \frac{2\pi R_c(r)}{R_p(r)} \to \infty\,,$$

according to the admissible forms of $R_p(r)$, $R_c(r)$, and $h(r)$.

Note also that only in the infinitely far field are $R_c(r)$ and $R_p(r)$ identical; where the field becomes Efcleethean (i. e. Minkowski),

$$\lim_{|r-r_0|\to\infty} \frac{2\pi R_c(r)}{R_p(r)} \to 2\pi\,.$$

It has been proved elsewhere [3, 2] that there are no curvature singularities in Einstein's gravitational field. In particular the Riemann tensor scalar curvature invariant (the Kretschmann scalar) $f=R_{\alpha\beta\sigma\rho}R^{\alpha\beta\sigma\rho}$ is finite everywhere, and and in the case of the fictitious point-mass takes the invariant value

$$f(r_0)\equiv\frac{12}{(2m)^4}\,,$$

completely independent of the value of r_0.

Since the intrinsic geometry of the metric is invariant, (11) with (15) must also satisfy this invariant condition. A tedious calculation gives the Kretschmann scalar for (11) at

$$f(r)=\frac{48m^2}{h^6\left(1+\frac{m}{2h}\right)^{12}}\,,$$

which by (15) is

$$f(r)=\frac{48m^2}{\left[|r-r_0|^n+\left(\frac{m}{2}\right)^n\right]^{\frac{6}{n}}\left(1+\frac{m}{2\left[|r-r_0|^n+\left(\frac{m}{2}\right)^n\right]^{\frac{1}{n}}}\right)^{12}}\,.$$

Then

$$f(r_0)\equiv\frac{12}{(2m)^4}\,,$$

completely independent of the value of r_0, as required by the very structure of the metric.

The structure of the metric is also responsible for the Ricci flatness of Einstein's static, vacuum gravitational field (satisfying $R_{\alpha\beta}=0$). Consequently, all the metrics herein are Ricci flat (i. e. $R=0$). Indeed, all the given metrics can be transformed into

$$ds^2=\left(1-\frac{2m}{R_c}\right)dt^2-\left(1-\frac{2m}{R_c}\right)^{-1}dR_c^2-\\ -R_c^2(d\theta^2+\sin^2\theta\,d\varphi^2)\,, \tag{16}$$

$$R_c=R_c(r)=\sqrt{C(r)}\,,\quad 2m<R_c(r)<\infty\,,$$

which is Ricci flat for any analytic function $R_c(r)$, which is easily verified by using the variables

$$x^0=t\,,\quad x^1=R_c(r)\,,\quad x^2=\theta\,,\quad x^3=\varphi\,,$$

in the calculation of the Ricci curvature from (16), using,

$$R=g^{\mu\nu}\left\{\frac{\partial^2}{\partial x^\mu\partial x^\nu}\left(\ln\sqrt{|g|}\right)-\right.\\ \left.-\frac{1}{\sqrt{|g|}}\frac{\partial}{\partial x^\rho}\left(\sqrt{|g|}\,\Gamma^\rho_{\mu\nu}\right)+\Gamma^\rho_{\mu\sigma}\Gamma^\sigma_{\rho\nu}\right\}.$$

Setting

$$\frac{\chi}{2\pi}=R_c(r)=h(r)\left(1+\frac{m}{2h(r)}\right)^2,$$

transforms the metric (7) into,

$$ds^2 = \left(1 - \frac{2\pi\alpha}{\chi}\right) dt^2 - \left(1 - \frac{2\pi\alpha}{\chi}\right)^{-1} \frac{d\chi^2}{4\pi^2} - \\ - \frac{\chi^2}{4\pi^2}(d\theta^2 + \sin^2\theta d\varphi^2)\,, \qquad (17)$$

$$2\pi\alpha < \chi < \infty\,, \quad \alpha = 2m\,,$$

which is the metric for Einstein's gravitational field in terms of the only theoretically measurable distance in the field – the circumference χ of a great circle [2]. This is a truly coordinate independent expression. There is no need of the r-parameter at all.

Furthermore, equation (17) is clear as to what quantities are radii in the gravitational field, *viz.*

$$R_c(\chi) = \frac{\chi}{2\pi}\,,$$

$$R_p(\chi) = \int_{2\pi\alpha}^{\chi} \sqrt{\frac{\frac{\chi}{2\pi}}{\left(\frac{\chi}{2\pi} - \alpha\right)}}\, \frac{d\chi}{2\pi} = \\ = \sqrt{\frac{\chi}{2\pi}\left(\frac{\chi}{2\pi} - \alpha\right)} + \alpha \ln \left| \frac{\sqrt{\frac{\chi}{2\pi}} + \sqrt{\frac{\chi}{2\pi} - \alpha}}{\sqrt{\alpha}} \right|.$$

3 Epilogue

The foregoing is based, as has all my work to date, upon the usual manifold with boundary, $[0\,, +\infty[\times S^2$. By using the very premises of most relativists, including their $[0, +\infty[\times S^2$, I have demonstrated herein that black holes (see also [4, 7]), and elsewhere as a logical consequence [8], that big bangs are not consistent with General Relativity. Indeed, cosmological solutions for isotropic, homogeneous, type 1 Einstein spaces do not exist. Consequently, there is currently no valid relativistic cosmology at all. The Standard Cosmological Model, the Big Bang, is false.

Stavroulakis [9] has argued that $[0, +\infty[\times S^2$ is inadmissible because it destroys the topological structure of $\mathbb{R}^3$. He has maintained that the correct topological space for Einstein's gravitational field should be $\mathbb{R} \times \mathbb{R}^3$. He has also shown that black holes are not predicted by General Relativity in $\mathbb{R} \times \mathbb{R}^3$.

However, the issue of whether or not $[0, +\infty[\times S^2$ is admissible is not relevant to the arguments herein, given the objectives of the analysis.

Although χ is measurable in principle, it is apparently beyond measurement in practice. This severely limits the utility of Einstein's theory.

The historical analysis of Einstein's gravitational field proceeded in ignorance of the fact that only the circumference χ of a great circle is significant. It has also failed to realise that there are two different immeasurable radii defined in Einstein's gravitational field, as an inescapable consequence of the intrinsic geometry on the metric, and that these radii are identical only in the infinitely far field where space becomes Efcleethean (i. e. Minkowski). Rejection summarily of the oddity of two distinct immeasurable radii is tantamount to complete rejection of General Relativity; an issue I have not been concerned with.

Minkowski's metric in terms of χ is,

$$ds^2 = dt^2 - \frac{d\chi^2}{4\pi^2} - \frac{\chi^2}{4\pi^2}(d\theta^2 + \sin^2\theta\, d\varphi^2)\,,$$

$$0 \leqslant \chi < \infty\,.$$

It is generalised to

$$ds^2 = A\left(\frac{\chi}{2\pi}\right) dt^2 - B\left(\frac{\chi}{2\pi}\right)^{-1} \frac{d\chi^2}{4\pi^2} - \\ - \frac{\chi^2}{4\pi^2}(d\theta^2 + \sin^2\theta\, d\varphi^2)\,, \qquad (18)$$

$$\chi_0 < \chi < \infty\,, \qquad A, B > 0\,,$$

which leads, in the usual way, to the line-element of (17), from which χ_0 and the radii associated with the gravitational field are determined via the intrinsic and invariant geometry of the metric.

Setting $R_c(r) = \sqrt{C(r)}$ in (16) gives,

$$ds^2 = \left(1 - \frac{\alpha}{\sqrt{C(r)}}\right) dt^2 - \left(1 - \frac{\alpha}{\sqrt{C(r)}}\right)^{-1} d\sqrt{C(r)}^{\,2} - \\ - C(r)(d\theta^2 + \sin^2\theta d\varphi^2)\,, \qquad (19)$$

where [2]

$$C(r) = \left(\left|r - r_0\right|^n + \alpha^n\right)^{\frac{2}{n}}, \qquad (20)$$

$$n \in \Re^+, \quad r_0 \in \Re\,, \quad \alpha = 2m\,, \quad r \neq r_0\,,$$

and where n and r_0 are entirely arbitrary constants. Note that if $n = 1$, $r_0 = \alpha$, $r > r_0$, the usual line-element is obtained, but the usual claim that r can go down to zero is clearly false, since when $r = \alpha$, the parametric distance between field source and test particle is zero, which is reflected in the fact that the proper radius on (19) is then zero, $R_c = \alpha = 2m$, and $g_{00} = 0$, as required. The functions (20) are called Schwarzschild forms [4, 7], and they produce an infinite number of equivalent Schwarzschild metrics.

The term $\sqrt{dx^2 + dy^2 + dz^2}$ of the standard metric in "isotropic coordinates" is not a coordinate length as commonly claimed. This erroneous idea stems from the fact that the usual choice of $C(r) = r^2$ in the metric (19) suppresses the true nature of the mapping of parametric distances into the true radii of the gravitational field. This arises from the additional fact that the location of the field source at $r_0 = \alpha$

in parameter space drops out of the functional form $C(r)$ as given by (20), in this particular case. The subsequent usual transformation to the usual metric (1a) carries with it the erroneous assumptions about r, inherited from the misconceptions about r in (19) with the reduction of $C(r)$ to r^2, which, in the usual conception, violates (20), and hence the entire structure of the metric for the gravitational field. Obtaining (1a) from first principles using the expression (5) with $h(r) = r^2$ and the components of the energy-momentum tensor, already presupposes the form of $h(r)$ and generates the suppression of the true nature of r in similar fashion.

The black hole, as proved herein and elsewhere [4, 7], and the Big Bang, are due to a serious neglect of the intrinsic geometry of the gravitational metric, a failure heretofore to understand the structure of type 1 Einstein spaces, with the introduction instead, of extraneous and erroneous hypotheses by which the intrinsic geometry is violated.

Since Nature does not make point-masses, the point-mass referred to Einstein's gravitational field must be regarded as merely the mathematical artifice of a centre-of-mass of the source of the field. The fact that the gravitational metric for the point-mass disintegrates at the point-mass is a theoretical indication that the point-mass is not physical, so that the metric is undefined when $r = r_0$ in parameter space, which is at $R_p(r_0) \equiv 0$ on the metric for the gravitational field. The usual concept of gravitational collapse itself collapses.

To fully describe the gravitational field there must therefore be two metrics, one for the interior of an extended gravitating body and one for the exterior of that field source, with a transition between the two at the surface of the body. This has been achieved in the idealised case of a sphere of incompressible and homogeneous fluid in vacuum [10, 11]. No singularities then arise, and gravitational collapse to a "point-mass" is impossible.

Acknowledgements

I thank Dr. Dmitri Rabounski for his comments concerning elaboration upon certain points I addressed too succinctly in an earlier draft, or otherwise took for granted that the reader would already know.

References

1. Petrov A. Z. Einstein spaces. Pergamon Press, London, 1969.
2. Crothers S. J. On the geometry of the general solution for the vacuum field of the point-mass. *Progress in Physics*, v. 2, 3–14, 2005.
3. Abrams L. S. Black holes: the legacy of Hilbert's error. *Can. J. Phys.*, 1989, v. 67, 919 (see also in arXiv: gr-qc/0102055).
4. Crothers S. J. On the general solution to Einstein's vacuum field and it implications for relativistic degeneracy. *Progress in Physics*, v. 1, 68–73, 2005.
5. Crothers S. J. A short history of black holes. *Progress in Physics*, v. 2, 54–57, 2006.
6. McVittie G. C. Laplace's alleged "black hole". *The Observatory*, 1978, v. 98, 272; http://www.geocities.com/theometria/McVittie.pdf.
7. Crothers S. J. On the ramifications of the Schwarzschild space-time metric. *Progress in Physics*, v. 1, 74–80, 2005.
8. Crothers S. J. On the general solution to Einstein's vacuum field for the point-mass when $\lambda \neq 0$ and its consequences for relativistic cosmology. *Progress in Physics*, v. 2, 7–18, 2005.
9. Stavroulakis N. Non-Euclidean geometry and gravitation. *Progress in Physics*, v. 2, 68–75, 2006.
10. Schwarzschild K. On the gravitational field of a sphere of incompressible fluid according to Einstein's theory. *Sitzungsber. Preuss. Akad. Wiss., Phys. Math. Kl.,* 1916, v. 424 (see also in arXiv: physics/9912033).
11. Crothers S. J. On the vacuum field of a sphere of incompressible fluid. *Progress in Physics*, v. 2, 43–47, 2005.

S-Denying of the Signature Conditions Expands General Relativity's Space

Dmitri Rabounski, Florentin Smarandache, Larissa Borissova

Department of Mathematics, University of New Mexico, Gallup, NM 87301, USA

E-mail: rabounski@yahoo.com; fsmarandache@yahoo.com; lborissova@yahoo.com

We apply the S-denying procedure to signature conditions in a four-dimensional pseudo-Riemannian space — i. e. we change one (or even all) of the conditions to be partially true and partially false. We obtain five kinds of expanded space-time for General Relativity. Kind I permits the space-time to be in collapse. Kind II permits the space-time to change its own signature. Kind III has peculiarities, linked to the third signature condition. Kind IV permits regions where the metric fully degenerates: there may be non-quantum teleportation, and a home for virtual photons. Kind V is common for kinds I, II, III, and IV.

1 Einstein's basic space-time

Euclidean geometry is set up by Euclid's axioms: (1) given two points there is an interval that joins them; (2) an interval can be prolonged indefinitely; (3) a circle can be constructed when its centre, and a point on it, are given; (4) all right angles are equal; (5) if a straight line falling on two straight lines makes the interior angles on one side less than two right angles, the two straight lines, if produced indefinitely, meet on that side. Non-Euclidean geometries are derived from making assumptions which deny some of the Euclidean axioms. Three main kinds of non-Euclidean geometry are conceivable — Lobachevsky-Bolyai-Gauss geometry, Riemann geometry, and Smarandache geometry.

In Lobachevsky-Bolyai-Gauss (hyperbolic) geometry the fifth axiom is denied in the sense that there are infinitely many lines passing through a given point and parallel to a given line. In Riemann (elliptic) geometry*, the axiom is satisfied formally, because there is no line passing through a given point and parallel to a given line. But if we state the axiom in a broader form, such as "through a point not on a given line there is only one line parallel to the given line", the axiom is also denied in Riemann geometry. Besides that, the second axiom is also denied in Riemann geometry, because herein the straight lines are closed: an infinitely long straight line is possible but then all other straight lines are of the same infinite length.

In Smarandache geometry one (or even all) of the axioms is false in at least two different ways, or is false and also true [1, 2]. This axiom is said to be Smarandachely denied (S-denied). Such geometries have mixed properties of Euclidean, Lobachevsky-Bolyai-Gauss, and Riemann geometry. Manifolds that support such geometries were introduced by Iseri [3].

Riemannian geometry is the generalization of Riemann geometry, so that in a space of Riemannian geometry:

(1) The differentiable field of a 2nd rank non-degenerate symmetric tensor $g_{\alpha\beta}$ is given so that the distance ds between any two infinitesimally close points is given by the quadratic form

$$ds^2 = \sum_{0\leqslant\alpha,\beta\leqslant n} g_{\alpha\beta}(x)\, dx^\alpha dx^\beta = g_{\alpha\beta}\, dx^\alpha dx^\beta,$$

known as the Riemann metric†. The tensor $g_{\alpha\beta}$ is called the fundamental metric tensor, and its components define the geometrical structure of the space;

(2) The space curvature may take different numerical values at different points in the space.

Actually, a Riemann geometry space is the space of the Riemannian geometry family, where the curvature is constant and has positive numerical value.

In the particular case where $g_{\alpha\beta}$ takes the diagonal form

$$g_{\alpha\beta} = \begin{pmatrix} 1 & 0 & \dots & 0 \\ 0 & 1 & \dots & 0 \\ \vdots & \vdots & \ddots & \vdots \\ 0 & 0 & \dots & 1 \end{pmatrix},$$

the Riemannian space becomes Euclidean.

Pseudo-Riemannian spaces consist of specific kinds of Riemannian spaces, where $g_{\alpha\beta}$ (and the Riemannian metric ds^2) has sign-alternating form so that its diagonal components bear numerical values of opposite sign.

Einstein's basic space-time of General Relativity is a four-dimensional pseudo-Riemannian space having the sign-alternating signature $(+---)$ or $(-+++)$, which reserves one dimension for time $x^0 = ct$ whilst the remaining three are reserved for three-dimensional space, so that the space metric is‡

$$ds^2 = g_{\alpha\beta}\, dx^\alpha dx^\beta = g_{00}\, c^2 dt^2 + 2g_{0i}\, c\, dt\, dx^i + g_{ik}\, dx^i dx^k.$$

**Elleipein* — "to fall short"; *hyperballein* — "to throw beyond" (Greek).

†Here is a space of n dimensions.

‡Landau and Lifshitz in *The Classical Theory of Fields* [4] use the signature $(-+++)$, where the three-dimensional part of the four-dimensional impulse vector is real. We, following Eddington [5], use the signature $(+---)$, because in this case the three-dimensional *observable impulse*, being the projection of the four-dimensional impulse vector on an observer's spatial section, is real. Here $\alpha, \beta = 0, 1, 2, 3$, while $i, k = 1, 2, 3$.

In general the four-dimensional pseudo-Riemannian space is curved, inhomogeneous, gravitating, rotating, and deforming (any or all of the properties may be anisotropic). In the particular case where the fundamental metric tensor $g_{\alpha\beta}$ takes the strictly diagonal form

$$g_{\alpha\beta} = \begin{pmatrix} 1 & 0 & 0 & 0 \\ 0 & -1 & 0 & 0 \\ 0 & 0 & -1 & 0 \\ 0 & 0 & 0 & -1 \end{pmatrix},$$

the space becomes four-dimensional pseudo-Euclidean

$$ds^2 = g_{\alpha\beta}\, dx^\alpha dx^\beta = c^2 dt^2 - dx^2 - dy^2 - dz^2,$$

which is known as Minkowski's space (he had introduced it first). It is the basic space-time of Special Relativity.

2 S-denying the signature conditions

In a four-dimensional pseudo-Riemannian space of signature $(+---)$ or $(-+++)$, the basic space-time of General Relativity, there are *four signature conditions* which define this space as pseudo-Riemannian.

Question: What happens if we S-deny one (or even all) of the four signature conditions in the basic space-time of General Relativity? What happens if we postulate that one (or all) of the signature conditions is to be denied in two ways, or, alternatively, to be true and false?

Answer: If we S-deny one or all of the four signature conditions in the basic space-time, we obtain a new expanded basic space-time for General Relativity. There are five main kinds of such expanded spaces, due to four possible signature conditions there.

Here we are going to consider each of the five kinds of expanded spaces.

Starting from a purely mathematical viewpoint, the signature conditions are derived from sign-alternation in the diagonal terms g_{00}, g_{11}, g_{22}, g_{33} in the matrix $g_{\alpha\beta}$. From a physical perspective, see §84 in [4], the signature conditions are derived from the requirement that the three-dimensional observable interval

$$d\sigma^2 = h_{ik}\, dx^i dx^k = \left(-g_{ik} + \frac{g_{0i} g_{0k}}{g_{00}} \right) dx^i dx^k$$

must be positive. Hence the three-dimensional observable metric tensor $h_{ik} = -g_{ik} + \frac{g_{0i} g_{0k}}{g_{00}}$, being a 3×3 matrix defined in an observer's reference frame accompanying its references, must satisfy three obvious conditions

$$\det \| h_{11} \| = h_{11} > 0\,,$$

$$\det \begin{Vmatrix} h_{11} & h_{12} \\ h_{21} & h_{22} \end{Vmatrix} = h_{11}\, h_{22} - h_{12}^2 > 0\,,$$

$$h = \det \| h_{ik} \| = \det \begin{Vmatrix} h_{11} & h_{12} & h_{13} \\ h_{21} & h_{22} & h_{23} \\ h_{31} & h_{32} & h_{33} \end{Vmatrix} > 0\,.$$

From here we obtain the signature conditions in the fundamental metric tensor's matrix $g_{\alpha\beta}$. In a space of signature $(+---)$, the signature conditions are

$$\det \| g_{00} \| = g_{00} > 0\,, \qquad \text{(I)}$$

$$\det \begin{Vmatrix} g_{00} & g_{01} \\ g_{10} & g_{11} \end{Vmatrix} = g_{00}\, g_{11} - g_{01}^2 < 0\,, \qquad \text{(II)}$$

$$\det \begin{Vmatrix} g_{00} & g_{01} & g_{02} \\ g_{10} & g_{11} & g_{12} \\ g_{20} & g_{21} & g_{22} \end{Vmatrix} > 0\,, \qquad \text{(III)}$$

$$g = \det \| g_{\alpha\beta} \| = \det \begin{Vmatrix} g_{00} & g_{01} & g_{02} & g_{03} \\ g_{10} & g_{11} & g_{12} & g_{13} \\ g_{20} & g_{21} & g_{22} & g_{23} \\ g_{30} & g_{31} & g_{32} & g_{33} \end{Vmatrix} < 0\,. \qquad \text{(IV)}$$

An expanded space-time of kind I: In such a space-time the first signature condition $g_{00} > 0$ is S-denied, while the other signature conditions remain unchanged. Given the expanded space-time of kind I, the first signature condition is S-denied in the following form

$$\det \| g_{00} \| = g_{00} \geqslant 0\,,$$

which includes two particular cases, $g_{00} > 0$ and $g_{00} = 0$, so $g_{00} > 0$ is partially true and partially false.

Gravitational potential is $\mathrm{w} = c^2(1 - \sqrt{g_{00}})$ [6, 7], so the S-denied first signature condition $g_{00} \geqslant 0$ means that in such a space-time $\mathrm{w} \leqslant c^2$, i. e. two different states occur

$$\mathrm{w} < c^2\,, \qquad \mathrm{w} = c^2.$$

The first one corresponds to the regular space-time, where $g_{00} > 0$. The second corresponds to a special space-time state, where the first signature condition is simply denied $g_{00} = 0$. This is the well-known condition of gravitational collapse.

Landau and Lifshitz wrote, "nonfulfilling of the condition $g_{00} > 0$ would only mean that the corresponding system of reference cannot be accomplished with real bodies" [4].

Conclusion on the kind I: An expanded space-time of kind I ($g_{00} \geqslant 0$) is the generalization of the basic space-time of General Relativity ($g_{00} > 0$), including regions where this space-time is in a state of collapse, ($g_{00} = 0$).

An expanded space-time of kind II: In such a space-time the second signature condition $g_{00}\, g_{11} - g_{01}^2 < 0$ is S-denied, the other signature conditions remain unchanged. Thus, given the expanded space-time of kind II, the second signature condition is S-denied in the following form

$$\det \begin{Vmatrix} g_{00} & g_{01} \\ g_{10} & g_{11} \end{Vmatrix} = g_{00}\, g_{11} - g_{01}^2 \leqslant 0\,,$$

which includes two different cases

$$g_{00}\,g_{11} - g_{01}^2 < 0\,, \qquad g_{00}\,g_{11} - g_{01}^2 = 0\,,$$

whence the second signature condition $g_{00}\,g_{11} - g_{01}^2 < 0$ is partially true and partially false.

The component g_{00} is defined by the gravitational potential $\mathrm{w} = c^2(1 - \sqrt{g_{00}})$. The component g_{0i} is defined by the space rotation linear velocity (see [6, 7] for details)

$$v_i = -c\frac{g_{0i}}{\sqrt{g_{00}}}\,, \quad v^i = -c\,g^{0i}\sqrt{g_{00}}\,, \quad v_i = h_{ik}\,v^k.$$

Then we obtain the S-denied second signature condition $g_{00}\,g_{11} - g_{01}^2 \leqslant 0$ (meaning the first signature condition is not denied $g_{00} > 0$) as follows

$$g_{11} - \frac{1}{c^2}\,v_1^2 \leqslant 0\,,$$

having two particular cases

$$g_{11} - \frac{1}{c^2}\,v_1^2 < 0\,, \qquad g_{11} - \frac{1}{c^2}\,v_1^2 = 0\,.$$

To better see the physical sense, take a case where g_{11} is close to -1.* Then, denoting $v^1 = v$, we obtain

$$v^2 > -c^2, \qquad v^2 = -c^2.$$

The first condition $v^2 > -c^2$ is true in the regular basic space-time. Because the velocities v and c take positive numerical values, this condition uses the well-known fact that positive numbers are greater than negative ones.

The second condition $v^2 = -c^2$ has no place in the basic space-time; it is true as a particular case of the common condition $v^2 \geqslant -c^2$ in the expanded spaces of kind II. This condition means that as soon as the linear velocity of the space rotation reaches light velocity, the space signature changes from $(+---)$ to $(-+++)$. That is, given an expanded space-time of kind II, the transit from a non-isotropic sub-light region into an isotropic light-like region implies change of signs in the space signature.

Conclusion on the kind II: An expanded space-time of kind II ($v^2 \geqslant -c^2$) is the generalization of the basic space-time of General Relativity ($v^2 > -c^2$) which permits the peculiarity that the space-time changes signs in its own signature as soon as we, reaching the light velocity of the space rotation, encounter a light-like isotropic region.

An expanded space-time of kind III: In this space-time the third signature condition is S-denied, the other signature conditions remain unchanged. So, given the expanded space-time of kind III, the third signature condition is

$$\det \begin{Vmatrix} g_{00} & g_{01} & g_{02} \\ g_{10} & g_{11} & g_{12} \\ g_{20} & g_{21} & g_{22} \end{Vmatrix} \geqslant 0\,,$$

*Because we use the signature $(+---)$.

which, taking the other form of the third signature condition into account, can be transformed into the formula

$$\det \begin{Vmatrix} h_{11} & h_{12} \\ h_{21} & h_{22} \end{Vmatrix} = h_{11}\,h_{22} - h_{12}^2 \geqslant 0\,,$$

that includes two different cases

$$h_{11}\,h_{22} - h_{12}^2 > 0\,, \qquad h_{11}\,h_{22} - h_{12}^2 = 0\,,$$

so that the third initial signature condition $h_{11}\,h_{22} - h_{12}^2 > 0$ is partially true and partially false. This condition is not clear. Future research is required.

An expanded space-time of kind IV: In this space-time the fourth signature condition $g = \det\|g_{\alpha\beta}\| < 0$ is S-denied, the other signature conditions remain unchanged. So, given the expanded space-time of kind IV, the fourth signature condition is

$$g = \det\|g_{\alpha\beta}\| = \det \begin{Vmatrix} g_{00} & g_{01} & g_{02} & g_{03} \\ g_{10} & g_{11} & g_{12} & g_{13} \\ g_{20} & g_{21} & g_{22} & g_{23} \\ g_{30} & g_{31} & g_{32} & g_{33} \end{Vmatrix} \leqslant 0\,,$$

that includes two different cases

$$g = \det\|g_{\alpha\beta}\| < 0\,, \qquad g = \det\|g_{\alpha\beta}\| = 0\,,$$

so that the fourth signature condition $g < 0$ is partially true and partially false: $g < 0$ is true in the basic space-time, $g = 0$ could be true in only he expanded spaces of kind IV.

Because the determinants of the fundamental metric tensor $g_{\alpha\beta}$ and the observable metric tensor h_{ik} are connected as follows $\sqrt{-g} = \sqrt{h}\,\sqrt{g_{00}}$ [6, 7], degeneration of the fundamental metric tensor ($g = 0$) implies that the observable metric tensor is also degenerate ($h = 0$). In such fully degenerate areas the space-time interval ds^2, the observable spatial interval $d\sigma^2 = h_{ik}\,dx^i dx^k$ and the observable time interval $d\tau$ become zero†

$$ds^2 = c^2 d\tau^2 - d\sigma^2 = 0\,, \qquad c^2 d\tau^2 = d\sigma^2 = 0\,.$$

Taking formulae for $d\tau$ and $d\sigma$ into account, and also the fact that in the accompanying reference frame we have $h_{00} = h_{0i} = 0$, we write $d\tau^2 = 0$ and $d\sigma^2 = 0$ as

$$d\tau = \left[1 - \frac{1}{c^2}\left(\mathrm{w} + v_i u^i\right)\right] dt = 0\,, \qquad dt \neq 0\,,$$

$$d\sigma^2 = h_{ik}\,dx^i dx^k = 0\,,$$

where the three-dimensional coordinate velocity $u^i = dx^i/dt$ is different to the observable velocity $\mathrm{v}^i = dx^i/d\tau$.

†Note, $ds^2 = 0$ is true not only at $c^2 d\tau^2 = d\sigma^2 = 0$, but also when $c^2 d\tau^2 = d\sigma^2 \neq 0$ (in the isotropic region, where light propagates). The properly observed time interval is determined as $d\tau = \sqrt{g_{00}}\,dt + \frac{g_{0i}}{c\sqrt{g_{00}}}dx^i$, where the coordinate time interval is $dt \neq 0$ [4, 5, 6, 7].

With $h_{ik} = -g_{ik} + \frac{1}{c^2} v_i v_k$, we obtain aforementioned physical conditions of degeneration in the final form

$$\mathrm{w} + v_i u^i = c^2, \qquad g_{ik} u^i u^k = c^2 \Big(1 - \frac{\mathrm{w}}{c^2}\Big)^2 .$$

As recently shown [8, 9], the degenerate conditions permit non-quantum teleportation and also virtual photons in General Relativity. Therefore we expect that, employing an expanded space of kind IV, one may join General Relativity and Quantum Electrodynamics.

Conclusion on the kind IV: An expanded space-time of kind IV ($g \leqslant 0$) is the generalization of the basic space-time of General Relativity ($g < 0$) including regions where this space-time is in a fully degenerate state ($g = 0$). From the viewpoint of a regular observer, in a fully degenerate area time intervals between any events are zero, and spatial intervals are zero. Thus, such a region is observable as a point.

An expanded space-time of kind V: In this space-time all four signature conditions are S-denied, therefore given the expanded space-time of kind V the signature conditions are

$$\det \| g_{00} \| = g_{00} \geqslant 0 ,$$

$$\det \begin{Vmatrix} g_{00} & g_{01} \\ g_{10} & g_{11} \end{Vmatrix} = g_{00}\, g_{11} - g_{01}^2 \leqslant 0 ,$$

$$\det \begin{Vmatrix} g_{00} & g_{01} & g_{02} \\ g_{10} & g_{11} & g_{12} \\ g_{20} & g_{21} & g_{22} \end{Vmatrix} \geqslant 0 ,$$

$$g = \det \| g_{\alpha\beta} \| = \det \begin{Vmatrix} g_{00} & g_{01} & g_{02} & g_{03} \\ g_{10} & g_{11} & g_{12} & g_{13} \\ g_{20} & g_{21} & g_{22} & g_{23} \\ g_{30} & g_{31} & g_{32} & g_{33} \end{Vmatrix} \leqslant 0 ,$$

so all four signature conditions are partially true and partially false. It is obvious that an expanded space of kind V contains expanded spaces of kind I, II, III, and IV as particular cases, it being a common space for all of them.

Negative S-denying expanded spaces: We could also S-deny the signatures with the possibility that say $g_{00} > 0$ for kind I, but this means that the gravitational potential would be imaginary, or, even take into account the "negative" cases for kind II, III, etc. But most of them are senseless from the geometrical viewpoint. Hence we have only included five main kinds in our discussion.

3 Classification of the expanded spaces for General Relativity

In closing this paper we repeat, in brief, the main results.

There are currently three main kinds of non-Euclidean geometry conceivable — Lobachevsky-Bolyai-Gauss geometry, Riemann geometry, and Smarandache geometries. A four-dimensional pseudo-Riemannian space, a space of the Riemannian geometry family, is the basic space-time of General Relativity. We employed S-denying of the signature conditions in the basic four-dimensional pseudo-Riemannian space, when a signature condition is partially true and partially false. S-denying each of the signature conditions (or even all the conditions at once) gave an expanded space for General Relativity, which, being an instance of the family of Smarandache spaces, include the pseudo-Riemannian space as a particular case. There are four signature conditions. So, we obtained five kinds of the expanded spaces for General Relativity:

Kind I Permits the space-time to be in collapse;

Kind II Permits the space-time to change its own signature as reaching the light speed of the space rotation in a light-like isotropic region;

Kind III Has some specific peculiarities (not clear yet), linked to the third signature condition;

Kind IV Permits full degeneration of the metric, when all degenerate regions become points. Such fully degenerate regions provide trajectories for non-quantum teleportation, and are also a home space for virtual photons.

Kind V Provides an expanded space, which has common properties of all spaces of kinds I, II, III, and IV, and includes the spaces as particular cases.

The foregoing results are represented in detail in the book [10], which is currently in print.

4 Extending this classification: mixed kinds of the expanded spaces

We can S-deny one axiom only, or two axioms, or three axioms, or even four axioms simultaneously. Hence we may have: $C_4^1 + C_4^2 + C_4^3 + C_4^4 = 2^4 - 1 = 15$ kinds of expanded spaces for General Relativity, where C_n^i denotes combinations of n elements taken in groups of i elements, $0 \leqslant i \leqslant n$. And considering the fact that each axiom can be S-denied in three different ways, we obtain $15 \times 3 = 45$ kinds of expanded spaces for General Relativity. Which expanded space would be most interesting?

We collect all such "mixed" spaces into a table. Specific properties of the mixed spaces follow below.

1.1.1: $g_{00} \geqslant 0$, $h_{11} > 0$, $h_{11} h_{22} - h_{12}^2 > 0$, $h > 0$. At $g_{00} = 0$, we have the usual space-time permitting collapse.

1.1.2: $g_{00} > 0$, $h_{11} \geqslant 0$, $h_{11} h_{22} - h_{12}^2 > 0$, $h > 0$. At $h_{11} = 0$ we have $h_{12}^2 < 0$ that is permitted for imaginary values of h_{12}: we obtain a complex Riemannian space.

1.1.3: $g_{00} > 0$, $h_{11} > 0$, $h_{11} h_{22} - h_{12}^2 \geqslant 0$, $h > 0$. At $h_{11} h_{22} - h_{12}^2 = 0$, the spatially observable metric $d\sigma^2$ permits purely spatial isotropic lines.

1.1.4: $g_{00} > 0$, $h_{11} > 0$, $h_{11} h_{22} - h_{12}^2 > 0$, $h \geqslant 0$. At $h = 0$, we have the spatially observed metric $d\sigma^2$ completely degenerate. An example — zero-space [9], obtained as a completely degenerate Riemannian space. Because $h = -\frac{g}{g_{00}}$, the

Positive S-denying spaces, $N \geqslant 0$		Negative S-denying spaces, $N \leqslant 0$		S-denying spaces, where $N > 0 \cup N < 0$	
Kind	Signature conditions	Kind	Signature conditions	Kind	Signature conditions
One of the signature conditions is S-denied					
1.1.1	$I \geqslant 0,\ II > 0,\ III > 0,\ IV > 0$	1.2.1	$I \leqslant 0,\ II > 0,\ III > 0,\ IV > 0$	1.3.1	$I \gtrless 0,\ II > 0,\ III > 0,\ IV > 0$
1.1.2	$I > 0,\ II \geqslant 0,\ III > 0,\ IV > 0$	1.2.2	$I > 0,\ II \leqslant 0,\ III > 0,\ IV > 0$	1.3.2	$I > 0,\ II \gtrless 0,\ III > 0,\ IV > 0$
1.1.3	$I > 0,\ II > 0,\ III \geqslant 0,\ IV > 0$	1.2.3	$I > 0,\ II > 0,\ III \leqslant 0,\ IV > 0$	1.3.3	$I > 0,\ II > 0,\ III \gtrless 0,\ IV > 0$
1.1.4	$I > 0,\ II > 0,\ III > 0,\ IV \geqslant 0$	1.2.4	$I > 0,\ II > 0,\ III > 0,\ IV \leqslant 0$	1.3.4	$I > 0,\ II > 0,\ III > 0,\ IV \gtrless 0$
Two of the signature conditions are S-denied					
2.1.1	$I \geqslant 0,\ II \geqslant 0,\ III > 0,\ IV > 0$	2.2.1	$I \leqslant 0,\ II \leqslant 0,\ III > 0,\ IV > 0$	2.3.1	$I \gtrless 0,\ II \gtrless 0,\ III > 0,\ IV > 0$
2.1.2	$I \geqslant 0,\ II > 0,\ III \geqslant 0,\ IV > 0$	2.2.2	$I \leqslant 0,\ II > 0,\ III \leqslant 0,\ IV > 0$	2.3.2	$I \gtrless 0,\ II > 0,\ III \gtrless 0,\ IV > 0$
2.1.3	$I \geqslant 0,\ II > 0,\ III > 0,\ IV \geqslant 0$	2.2.3	$I \leqslant 0,\ II > 0,\ III > 0,\ IV \leqslant 0$	2.3.3	$I \gtrless 0,\ II > 0,\ III > 0,\ IV \gtrless 0$
2.1.4	$I > 0,\ II \geqslant 0,\ III > 0,\ IV \geqslant 0$	2.2.4	$I > 0,\ II \leqslant 0,\ III > 0,\ IV \leqslant 0$	2.3.4	$I > 0,\ II \gtrless 0,\ III > 0,\ IV \gtrless 0$
2.1.5	$I > 0,\ II \geqslant 0,\ III \geqslant 0,\ IV > 0$	2.2.5	$I > 0,\ II \leqslant 0,\ III \leqslant 0,\ IV > 0$	2.3.5	$I > 0,\ II \gtrless 0,\ III \gtrless 0,\ IV > 0$
2.1.6	$I > 0,\ II > 0,\ III \geqslant 0,\ IV \geqslant 0$	2.2.6	$I > 0,\ II > 0,\ III \leqslant 0,\ IV \leqslant 0$	2.3.6	$I > 0,\ II > 0,\ III \gtrless 0,\ IV \gtrless 0$
Three of the signature conditions are S-denied					
3.1.1	$I > 0,\ II \geqslant 0,\ III \geqslant 0,\ IV \geqslant 0$	3.2.1	$I > 0,\ II \leqslant 0,\ III \leqslant 0,\ IV \leqslant 0$	3.3.1	$I > 0,\ II \gtrless 0,\ III \gtrless 0,\ IV \gtrless 0$
3.1.2	$I \geqslant 0,\ II > 0,\ III \geqslant 0,\ IV \geqslant 0$	3.2.2	$I \leqslant 0,\ II > 0,\ III \leqslant 0,\ IV \leqslant 0$	3.3.2	$I \gtrless 0,\ II > 0,\ III \gtrless 0,\ IV \gtrless 0$
3.1.3	$I \geqslant 0,\ II \geqslant 0,\ III > 0,\ IV \geqslant 0$	3.2.3	$I \leqslant 0,\ II \leqslant 0,\ III > 0,\ IV \leqslant 0$	3.3.3	$I \gtrless 0,\ II \gtrless 0,\ III > 0,\ IV \gtrless 0$
3.1.4	$I \geqslant 0,\ II \geqslant 0,\ III \geqslant 0,\ IV > 0$	3.2.4	$I \leqslant 0,\ II \leqslant 0,\ III \leqslant 0,\ IV > 0$	3.3.4	$I \gtrless 0,\ II \gtrless 0,\ III \gtrless 0,\ IV > 0$
All the signature conditions are S-denied					
4.1.1	$I \geqslant 0,\ II \geqslant 0,\ III \geqslant 0,\ IV \geqslant 0$	4.2.1	$I \leqslant 0,\ II \leqslant 0,\ III \leqslant 0,\ IV \leqslant 0$	4.3.1	$I \gtrless 0,\ II \gtrless 0,\ III \gtrless 0,\ IV \gtrless 0$

Table 1: The expanded spaces for General Relativity (all 45 mixed kinds of S-denying). The signature conditions are denoted by Roman numerals

metric ds^2 is also degenerate.

1.2.1: $g_{00} \leqslant 0,\ h_{11} > 0,\ h_{11}h_{22} - h_{12}^2 > 0,\ h > 0$. At $g_{00} = 0$, we have kind 1.1.1. At $g_{00} < 0$ physically observable time becomes imaginary $d\tau = \frac{g_{0i}\,dx^i}{c\sqrt{g_{00}}}$.

1.2.2: $g_{00} > 0,\ h_{11} \leqslant 0,\ h_{11}h_{22} - h_{12}^2 > 0,\ h > 0$. At $h_{11} = 0$, we have kind 1.1.2. At $h_{11} < 0$, distances along the axis x^1 (i. e. the values $\sqrt{h_{11}}dx^1$) becomes imaginary, contradicting the initial conditions in General Relativity.

1.2.3: $g_{00} > 0,\ h_{11} > 0,\ h_{11}h_{22} - h_{12}^2 \leqslant 0,\ h > 0$. This is a common space built on a particular case of kind 1.1.3 where $h_{11}h_{22} - h_{12}^2 = 0$ and a subspace where $h_{11}h_{22} - h_{12}^2 < 0$. In the latter subspace the spatially observable metric $d\sigma^2$ becomes sign-alternating so that the space-time metric has the signature $(+-+-)$ (this case is outside the initial statement of General Relativity).

1.2.4: $g_{00} > 0,\ h_{11} > 0,\ h_{11}h_{22} - h_{12}^2 > 0,\ h \leqslant 0$. This space is built on a particular case of kind 1.1.2 where $h = 0$ and a subspace where $h < 0$. At $h < 0$ we have the spatial metric $d\sigma^2$ sign-alternating so that the space-time metric has the signature $(+--+)$ (this case is outside the initial statement of General Relativity).

1.3.1: $g_{00} \gtrless 0,\ h_{11} > 0,\ h_{11}h_{22} - h_{12}^2 > 0,\ h > 0$. Here we have the usual space-time area ($g_{00} > 0$) with the signature $(+---)$, and a sign-definite space-time ($g_{00} < 0$) where the signature is $(----)$. There are no intersections of the areas in the common space-time; they exist severally.

1.3.2: $g_{00} > 0,\ h_{11} \gtrless 0,\ h_{11}h_{22} - h_{12}^2 > 0,\ h > 0$. Here we have a common space built on two separated areas where $(+---)$ (usual space-time) and a subspace where $(++--)$. The areas have no intersections.

1.3.3: $g_{00} > 0,\ h_{11} > 0,\ h_{11}h_{22} - h_{12}^2 \gtrless 0,\ h > 0$. This is a common space built on the usual space-time and a particular space-time of kind 1.2.3, where the signature is $(+-+-)$. The areas have no intersections.

1.3.4: $g_{00} > 0,\ h_{11} > 0,\ h_{11}h_{22} - h_{12}^2 > 0,\ h \gtrless 0$. This is a common space built on the usual space-time and a particular space-time of kind 1.2.4, where the signature is $(+--+)$. The areas have no intersections.

2.1.1: $g_{00} \geqslant 0,\ h_{11} \gtrless 0,\ h_{11}h_{22} - h_{12}^2 > 0,\ h > 0$. This is a complex Riemannian space with a complex metric $d\sigma^2$, permitting collapse.

2.1.2: $g_{00} \gtrless 0,\ h_{11} > 0,\ h_{11}h_{22} - h_{12}^2 \gtrless 0,\ h > 0$. This space permits collapse, and purely spatial isotropic directions.

2.1.3: $g_{00} \gtrless 0,\ h_{11} > 0,\ h_{11}h_{22} - h_{12}^2 > 0,\ h \gtrless 0$. This space permits complete degeneracy and collapse. At $g_{00} = 0$ and $h = 0$, we have a collapsed zero-space.

2.1.4: $g_{00} > 0,\ h_{11} \gtrless 0,\ h_{11}h_{22} - h_{12}^2 > 0,\ h \gtrless 0$. Here we have a complex Riemannian space permitting complete degeneracy.

2.1.5: $g_{00} > 0,\ h_{11} \geqslant 0,\ h_{11}h_{22} - h_{12}^2 \geqslant 0,\ h > 0$. At

$h_{11}=0$, we have $h_{12}^2=0$: a partial degeneration of the spatially observable metric $d\sigma^2$.

2.1.6: $g_{00}>0,\ h_{11}>0,\ h_{11}h_{22}-h_{12}^2\geqslant 0,\ h\geqslant 0$. This space permits the spatially observable metric $d\sigma^2$ to completely degenerate: $h=0$.

2.2.1: $g_{00}\leqslant 0,\ h_{11}\leqslant 0,\ h_{11}h_{22}-h_{12}^2>0,\ h>0$. At $g_{00}=0$ and $h_{11}=0$, we have a particular space-time of kind 2.1.1. At $g_{00}<0,\ h_{11}<0$ we have a space with the signature $(----)$ where time is like a spatial coordinate (this case is outside the initial statement of General Relativity).

2.2.2: $g_{00}\leqslant 0,\ h_{11}>0,\ h_{11}h_{22}-h_{12}^2\leqslant 0,\ h>0$. At $g_{00}=0$ and $h_{11}h_{22}-h_{12}^2=0$, we have a particular space-time of kind 2.1.2. At $g_{00}<0$ and $h_{11}h_{22}-h_{12}^2<0$, we have a space with the signature $(-+-+)$ (it is outside the initial statement of General Relativity).

2.2.3: $g_{00}\leqslant 0,\ h_{11}>0,\ h_{11}h_{22}-h_{12}^2>0,\ h\leqslant 0$. At $g_{00}=0$ and $h=0$, we have a particular space-time of kind 2.1.3. At $g_{00}<0$ and $h_{11}h_{22}-h_{12}^2<0$, we have a space-time with the signature $(---+)$ (it is outside the initial statement of General Relativity).

2.2.4: $g_{00}>0,\ h_{11}\leqslant 0,\ h_{11}h_{22}-h_{12}^2\leqslant 0,\ h>0$. At $h_{11}=0$ and $h_{11}h_{22}-h_{12}^2=0$, we have a particular space-time of kind 2.1.5. At $h_{11}<0$ and $h_{11}h_{22}-h_{12}^2<0$, we have a space-time with the signature $(++-+)$ (outside the initial statement of General Relativity).

2.2.5: $g_{00}>0,\ h_{11}\leqslant 0,\ h_{11}h_{22}-h_{12}^2\geqslant 0,\ h\leqslant 0$. At $h_{11}=0$ and $h=0$, we have a particular space-time of kind 2.1.4. At $h_{11}<0$ and $h<0$, a space-time with the signature $(+--+)$ (outside the initial statement of General Relativity).

2.2.6: $g_{00}>0,\ h_{11}>0,\ h_{11}h_{22}-h_{12}^2\leqslant 0,\ h\leqslant 0$. At $h_{11}h_{22}-h_{12}^2=0$ and $h=0$, we have a particular space-time of kind 2.1.6. At $h_{11}h_{22}-h_{12}^2<0$ and $h<0$, we have a space-time with the signature $(+-++)$ (outside the initial statement of General Relativity).

2.3.1: $g_{00}\gtrless 0,\ h_{11}\gtrless 0,\ h_{11}h_{22}-h_{12}^2>0,\ h>0$. This is a space built on two areas. At $g_{00}>0$ and $h_{11}>0$, we have the usual space-time. At $g_{00}<0$ and $h_{11}<0$, we have a particular space-time of kind 2.2.1. The areas have no intersections: the common space is actually built on non-intersecting areas.

2.3.2: $g_{00}\gtrless 0,\ h_{11}>0,\ h_{11}h_{22}-h_{12}^2\gtrless 0,\ h>0$. This space is built on two areas. At $g_{00}>0$ and $h_{11}h_{22}-h_{12}^2>0$, we have the usual space-time. At $g_{00}<0$ and $h_{11}h_{22}-h_{12}^2<0$, we have a particular space-time of kind 2.2.2. The areas, building a common space, have no intersections.

2.3.3: $g_{00}\gtrless 0,\ h_{11}>0,\ h_{11}h_{22}-h_{12}^2>0,\ h\gtrless 0$. This space is built on two areas. At $g_{00}>0$ and $h_{11}>0$, we have the usual space-time. At $g_{00}<0$ and $h_{11}<0$, a particular space-time of kind 2.2.3. The areas, building a common space, have no intersections.

2.3.4: $g_{00}>0,\ h_{11}\gtrless 0,\ h_{11}h_{22}-h_{12}^2>0,\ h\gtrless 0$. This space is built on two areas. At $h_{11}>0$ and $h>0$, we have the usual space-time. At $h_{11}<0$ and $h<0$, a particular space-time of kind 2.2.4. The areas, building a common space, have no intersections.

2.3.5: $g_{00}>0,\ h_{11}\gtrless 0,\ h_{11}h_{22}-h_{12}^2\gtrless 0,\ h>0$. This space is built on two areas. At $h_{11}>0$ and $h_{11}h_{22}-h_{12}^2>0$, we have the usual space-time. At $h_{11}<0$ and $h_{11}h_{22}-h_{12}^2<0$, a particular space-time of kind 2.2.5. The areas, building a common space, have no intersections.

2.3.6: $g_{00}>0,\ h_{11}>0,\ h_{11}h_{22}-h_{12}^2\gtrless 0,\ h\gtrless 0$. This space is built on two areas. At $h_{11}h_{22}-h_{12}^2>0$ and $h>0$, we have the usual space-time. At $h_{11}h_{22}-h_{12}^2<0$ and $h<0$, a particular space-time of kind 2.2.6. The areas, building a common space, have no intersections.

3.1.1: $g_{00}>0,\ h_{11}\geqslant 0,\ h_{11}h_{22}-h_{12}^2\geqslant 0,\ h\geqslant 0$. This space permits complete degeneracy. At $h_{11}>0,\ h_{11}h_{22}-h_{12}^2>0,\ h>0$, we have the usual space-time. At $h_{11}=0,\ h_{11}h_{22}-h_{12}^2=0,\ h=0$, we have a particular case of a zero-space.

3.1.2: $g_{00}\geqslant 0,\ h_{11}>0,\ h_{11}h_{22}-h_{12}^2\geqslant 0,\ h\geqslant 0$. At $g_{00}>0,\ h_{11}h_{22}-h_{12}^2>0,\ h>0$, we have the usual space-time. At $g_{00}=0,\ h_{11}h_{22}-h_{12}^2=0,\ h=0$, we have a particular case of a collapsed zero-space.

3.1.3: $g_{00}\geqslant 0,\ h_{11}\geqslant 0,\ h_{11}h_{22}-h_{12}^2>0,\ h\geqslant 0$. At $g_{00}>0,\ h_{11}>0,\ h>0$, we have the usual space-time. At $g_{00}=0,\ h_{11}=0,\ h=0$, we have a collapsed zero-space, derived from a complex Riemannian space.

3.1.4: $g_{00}\geqslant 0,\ h_{11}\geqslant 0,\ h_{11}h_{22}-h_{12}^2\geqslant 0,\ h>0$. At $g_{00}>0,\ h_{11}>0,\ h_{11}h_{22}-h_{12}^2>0$, we have the usual space-time. At $g_{00}=0,\ h_{11}=0,\ h_{11}h_{22}-h_{12}^2=0$, we have the usual space-time in a collapsed state, while there are permitted purely spatial isotropic directions $\sqrt{h_{11}}dx^1$.

3.2.1: $g_{00}>0,\ h_{11}\leqslant 0,\ h_{11}h_{22}-h_{12}^2\leqslant 0,\ h\leqslant 0$. At $h_{11}=0,\ h_{11}h_{22}-h_{12}^2=0$ and $h=0$, we have a particular space-time of kind 3.1.1. At $h_{11}<0,\ h_{11}h_{22}-h_{12}^2<0$ and $h<0$, we have a space-time with the signature $(++++)$ (outside the initial statement of General Relativity).

3.2.2: $g_{00}\leqslant 0,\ h_{11}>0,\ h_{11}h_{22}-h_{12}^2\leqslant 0,\ h\leqslant 0$. At $g_{00}=0,\ h_{11}h_{22}-h_{12}^2=0$ and $h=0$, we have a particular space-time of kind 3.1.2. At $h_{11}<0,\ h_{11}h_{22}-h_{12}^2<0$ and $h<0$, we have a space-time with the signature $(--++)$ (outside the initial statement of General Relativity).

3.2.3: $g_{00}\leqslant 0,\ h_{11}\leqslant 0,\ h_{11}h_{22}-h_{12}^2>0,\ h\leqslant 0$. At $g_{00}=0,\ h_{11}=0$ and $h=0$, we have a particular space-time of kind 3.1.3. At $h_{11}<0,\ h_{11}h_{22}-h_{12}^2<0$ and $h<0$, we have a space-time with the signature $(-+-+)$ (outside the initial statement of General Relativity).

3.2.4: $g_{00}\leqslant 0,\ h_{11}\leqslant 0,\ h_{11}h_{22}-h_{12}^2\leqslant 0,\ h>0$. At $g_{00}=0,\ h_{11}=0$ and $h_{11}h_{22}-h_{12}^2=0$, we have a particular space-time of kind 3.1.4. At $g_{00}<0,\ h_{11}<0$ and $h_{11}h_{22}-h_{12}^2<0$, we have a space-time with the signature $(-++-)$ (outside the initial statement of General Relativity).

3.3.1: $g_{00}>0,\ h_{11}\gtrless 0,\ h_{11}h_{22}-h_{12}^2\gtrless 0,\ h\gtrless 0$. This is a space built on two areas. At $h_{11}>0,\ h_{11}h_{22}-h_{12}^2>0$ and $h_{11}>0$, we have the usual space-time. At $h_{11}<0,\ h_{11}h_{22}-h_{12}^2<0$ and $h_{11}<0$, we have a particular space-time of kind 3.2.1. The areas have no intersections: the

common space is actually built on non-intersecting areas.

3.3.2: $g_{00} \gtrless 0,\ h_{11} > 0,\ h_{11}h_{22} - h_{12}^2 \gtrless 0,\ h \gtrless 0$. This space is built on two areas. At $g_{00} > 0$, $h_{11}h_{22} - h_{12}^2 > 0$ and $h > 0$, we have the usual space-time. At $g_{00} < 0$, $h_{11}h_{22} - h_{12}^2 < 0$ and $h < 0$, we have a particular space-time of kind 3.2.2. The areas, building a common space, have no intersections.

3.3.3: $g_{00} \gtrless 0,\ h_{11} \gtrless 0,\ h_{11}h_{22} - h_{12}^2 > 0,\ h \gtrless 0$. This space is built on two areas. At $g_{00} > 0$, $h_{11} > 0$ and $h > 0$, we have the usual space-time. At $g_{00} < 0$, $h_{11} < 0$ and $h < 0$, we have a particular space-time of kind 3.2.3. The areas, building a common space, have no intersections.

3.3.4: $g_{00} \gtrless 0,\ h_{11} \gtrless 0,\ h_{11}h_{22} - h_{12}^2 \gtrless 0,\ h > 0$. This space is built on two areas. At $g_{00} > 0$, $h_{11} > 0$ and $h_{11}h_{22} - h_{12}^2 > 0$, we have the usual space-time. At $g_{00} < 0$, $h_{11} < 0$ and $h_{11}h_{22} - h_{12}^2 < 0$, a particular space-time of kind 3.2.4. The areas, building a common space, have no intersections.

4.4.1: $g_{00} \geqslant 0,\ h_{11} \geqslant 0,\ h_{11}h_{22} - h_{12}^2 \geqslant 0,\ h \geqslant 0$. At $g_{00} > 0$, $h_{11} > 0$, $h_{11}h_{22} - h_{12}^2 \geqslant 0$ and $h \geqslant 0$, we have the usual space-time. At $g_{00} = 0$, $h_{11} = 0$, $h_{11}h_{22} - h_{12}^2 = 0$ and $h = 0$, we have a particular case of collapsed zero-space.

4.4.2: $g_{00} \leqslant 0,\ h_{11} \leqslant 0,\ h_{11}h_{22} - h_{12}^2 \leqslant 0,\ h \leqslant 0$. At $g_{00} = 0$, $h_{11} = 0$, $h_{11}h_{22} - h_{12}^2 = 0$ and $h = 0$, we have a particular case of space-time of kind 4.4.1. At $g_{00} < 0$, $h_{11} < 0$, $h_{11}h_{22} - h_{12}^2 < 0$ and $h < 0$, we have a space-time with the signature $(----)$ (outside the initial statement of General Relativity). The areas have no intersections.

4.4.3: $g_{00} \gtrless 0,\ h_{11} \gtrless 0,\ h_{11}h_{22} - h_{12}^2 \gtrless 0,\ h \gtrless 0$. At $g_{00} > 0$, $h_{11} > 0$, $h_{11}h_{22} - h_{12}^2 > 0$ and $h > 0$, we have the usual space-time. At $g_{00} < 0$, $h_{11} < 0$, $h_{11}h_{22} - h_{12}^2 < 0$ and $h < 0$, we have a space-time with the signature $(----)$ (outside the initial statement of General Relativity). The areas have no intersections.

References

1. Smarandache F. Paradoxist mathematics. *Collected papers*, v. II, Kishinev University Press, Kishinev, 1997, 5–29.
2. Kuciuk L. and Antholy M. An introduction to Smarandache geometries. *New Zealand Math. Coll.*, Massey Univ., 2001, http://atlas-conferences.com/c/a/h/f/09.htm; Also *Intern. Congress of Mathematicians ICM-2002*, Beijing, China, 2002, http://www.icm2002.org.cn/B/Schedule_Section04.htm.
3. Iseri H. Smarandache manifolds. American Research Press, Rehoboth, 2002.
4. Landau L. D. and Lifshitz E. M. The classical theory of fields. GITTL, Moscow, 1939 (referred with the 4th final expanded edition, Butterworth–Heinemann, 1980).
5. Eddington A. S. The mathematical theory of relativity. Cambridge University Press, Cambridge, 1924 (referred with the 3rd expanded edition, GTTI, Moscow, 1934).
6. Zelmanov A. L. Chronometric invariants. Dissertation, 1944. Published: CERN, EXT-2004-117.
7. Zelmanov A. L. Chronometric invariants and co-moving coordinates in the general relativity theory. *Doklady Acad. Nauk USSR*, 1956, v. 107 (6), 815–818.
8. Borissova L. B. and Rabounski D. D. Fields, vacuum, and the mirror Universe. Editorial URSS, Moscow, 2001, 272 pages (the 2nd revised ed.: CERN, EXT-2003-025).
9. Borissova L. and Rabounski D. On the possibility of instant displacements in the space-time of General Relativity. *Progress in Physics*, 2005, v. 1, 17–19; Also in: *Physical Interpretation of Relativity Theory* (PIRT-2005), Proc. of the Intern. Meeting., Moscow, 2005, 234–239; Also in: *Today's Takes on Einstein's Relativity*, Proc. of the Confer., Tucson (Arizona), 2005, 29–35.
10. Rabounki D., Smarandache F., Borissova L. Neutrosophic Methods in General Relativity. Hexis, Phoenix (Arizona), 2005.

Nonlocal Effects of Chemical Substances on the Brain Produced through Quantum Entanglement

Huping Hu and Maoxin Wu

Biophysics Consulting Group, 25 Lubber Street, Stony Brook, NY 11790, USA

E-mail: hupinghu@quantumbrain.org

Photons are intrinsically quantum objects and natural long-distance carriers of information. Since brain functions involve information and many experiments have shown that quantum entanglement is physically real, we have contemplated from the perspective of our recent hypothesis on the possibility of entangling the quantum entities inside the brain with those in an external chemical substance and carried out experiments toward that end. Here we report that applying magnetic pulses to the brain when an anesthetic or pain medication was placed in between caused the brain to feel the effect of the said substance for several hours after the treatment as if the test subject had actually inhaled the same. The said effect is consistently reproducible. We further found that drinking water exposed to magnetic pulses, laser light or microwave when a chemical substance was placed in between also causes consistently reproducible brain effects in various degrees. Further, through additional experiments we have verified that the said brain effect is the consequence of quantum entanglement between quantum entities inside the brain and those of the chemical substance under study, induced by the photons of the magnetic pulses or applied lights. We suggest that the said quantum entities inside the brain are nuclear and/or electron spins and discuss the profound implications of these results.

1 Introduction

Quantum entanglement is ubiquitous in the microscopic world and manifests itself macroscopically under some circumstances [1, 3, 4]. Further, quantum spins of electrons and photons have now been successfully entangled in various ways for the purposes of quantum computation, memory and communication [5, 6]. In the field of neuroscience, we have recently suggested that nuclear and/or electronic spins inside the brain may play important roles in certain aspects of brain functions such as perception [2]. Arguably, we could test our hypothesis by first attempting to entangle these spins with those of a chemical substance such as a general anaesthetic and then observing the resulting brain effects such an attempt may produce, if any. Indeed, instead of armchair debate on how the suggested experiments might not work, we just went ahead and carried out the experiments over a period of more than a year. Here, we report our results. We point out from the outset that although it is commonly believed that quantum entanglement alone cannot be used to transmit classical information, the function of the brain may not be totally based on classical information [2].

2 Methods, test subjects and materials

Figure 1A (see end sheet) illustrates a typical setup for the first set of experiments. It includes a magnetic coil with an estimated 20 W output placed at one inch above the right side of a test subject's forehead, a small flat glass-container inserted between the magnetic coil and the forehead, and an audio system with adjustable power output and frequency spectrum controls connected to the magnetic coil. When music is played on the audio system, the said magnetic coil produces magnetic pulses with frequencies in the range of 5 Hz to 10 kHz. Experiments were conducted with said container being filled with different general anaesthetics, medications, or nothing/water as control, and the test subject being exposed to the magnetic pulses for 10 min and not being told the content in the container or details of the experiments.

The indicators used to measure the brain effect of the treatment were the first-person experiences of any unusual sensations such as numbness, drowsiness and/or euphoria which the subject felt after the treatment and the relative degrees of these unusual sensations on a scale of 10 with 0 = nothing, 1 = weak, 2 = light moderate, 3 = moderate, 4 = light strong, 5 = strong, 6 = heavily strong, 7 = very strong, 8 = intensely strong, 9 = extremely strong and 10 = intolerable. The durations of the unusual sensations and other symptoms after the treatment, such as nausea or headache, were also recorded.

Figure 1B illustrates a typical setup for the second set of experiments. It includes the magnetic coil connected to the audio system, a large flat glass-container filled with 200 ml fresh tap water and the small flat glass-container inserted between the magnetic coil and larger glass-container. Figure 1C illustrates a typical setup for the second set of experiments when a red laser with a 50 mW output and wavelengths of

635 nm–675 nm was used. All Experiments were conducted in the dark with the small flat glass-container being filled with different general anaesthetics, medications, or nothing/water as control, the large glass-container being filled with 200 ml of fresh tap water and exposed to the magnetic pulses or laser light for 30 min and the test subject consuming the treated tap water but not being told the content in the small container or details of the experiments. The indicators used for measuring the brain effects were the same as those used in the first set of experiments. Experiments were also carried out respectively with a 1200 W microwave oven and a flashlight powered by two size-D batteries. When the microwave oven was used, a glass tube containing 20 ml of fresh tap water was submerged into a larger glass tube containing 50 ml of general anaesthetic and exposed to microwave radiation for 5 sec. The said procedure was repeated numerous times, to collect a total of 200 ml of treated tap water for consumption. When the flashlight was used, the magnetic coil shown in Figure 1B was replaced with the flashlight.

To verify that the brain effects experienced by the test subjects were the consequences of quantum entanglement between quantum entities inside the brain and those in the chemical substances under study, the following additional experiments were carried out. Figure 1D shows a typical setup of the entanglement verification experiments. The setup is the reverse of the setup shown in Figure 1C. In addition, the small flat glass-container with a chemical substance or nothing/water as control was positioned with an angle to the incoming laser light to prevent reflected laser light from re-entering the large glass-container.

In the first set of entanglement verification experiments, the laser light from the red laser first passed through the large glass-container with 200 ml of fresh tap water and then through the small flat glass-container filled with a chemical substance or nothing/water as control located about 300 cm away. After 30 min of exposure to the laser light, a test subject consumed the exposed tap water without being told the content in the small container or details of the experiments and reported the brain effects felt for the next several hours.

In the second set of entanglement verification experiments, 400 ml of fresh tap water in a glass-container was first exposed to the radiation of the magnetic coil for 30 min or that of the 1500W microwave oven for 2 min. Then the test subject immediately consumed one-half of the water so exposed. After 30 min from the time of consumption the other half was exposed to magnetic pulses or laser light for 30 minutes using the setup shown in Figure 1B and Figure 1D respectively. The test subject reported, without being told the content in the small container or details of the experiments, the brain effects felt for the whole period from the time of consumption to several hours after the exposure had stopped. In the third set of entanglement verification experiments, one-half of 400 ml Poland Spring water with a shelve time of at least three months was immediately consumed by the test subject. After 30 min from the time of consumption the other half was exposed to the magnetic pulses or laser light for 30 min using the setup shown in Figure 1B and Figure 1D respectively. Test subject reported, without being told the content in the small container or details of the experiments, the brain effects felt for the whole period from the time of consumption to several hours after the exposure had stopped.

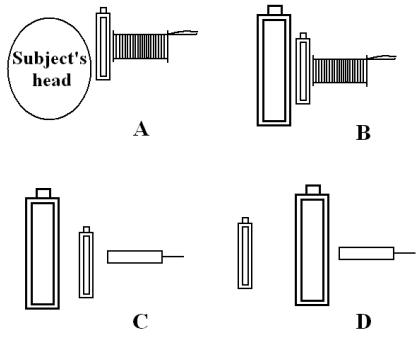

Fig. 1: Schematic view of typical experimental setups used in our study

In the fourth set of entanglement verification experiments, the test subject would take one-half of the 400 ml fresh tap water exposed to microwave for 2 min or magnetic pulses for 30 min to his/her workplace located more than 50 miles away (in one case to Beijing located more than 6,500 miles away) and consumed the same at the workplace at a specified time. After 30 min from the time of consumption, the other half was exposed to magnetic pulses or laser light for 30 min at the original location using the setup shown in Figure 1B and Figure 1D respectively. The test subject reported the brain effects felt without being told the content in the small container or details of the experiments for the whole period from the time of consumption to several hours after the exposure had stopped.

With respect to the test subjects, Subject A and C are respectively the first author and co-author of this paper and Subject B and C are respectively the father and mother of the first author. All four test subjects voluntarily consented to the proposed experiments. To ensure safety, all initial experiments were conducted on Subject A by himself. Further, all general anaesthetics used in the study were properly obtained for research purposes and all medications were either leftover items originally prescribed to Subject C's late mother or items available over the counter. To achieve proper control, repeating experiments on Subject A were carried out by either Subject B or C in blind settings, that is, he was not told whether or what general anaesthetic or medication were applied before the end of the experiments. Further, all experiments on Subject B, C and D were also carried out in blind settings, that is, these test subjects were not told about the details of the experiments on them or whether or what general anaesthetic or medication were applied.

	1st Set: Magn. Coil		2nd Set: Magn. Coil		Red laser		Flashlight		Microwave	
	Test ♯	Effect	Test ♯	Effect	Test ♯	Effect	Test ♯	Effect	Test ♯	Effect
Anaesthetics										
Subject A	13	yes	16	yes	22	yes	8	yes	3	yes
Subject B	2	yes	2	yes	3	yes	0	n/a	1	yes
Subject C	2	yes	6	yes	6	yes	0	n/a	1	yes
Subject D	2	yes	1	yes	5	yes	0	n/a	0	n/a
Medications										
Subject A	17	yes	14	yes	16	yes	1	yes	3	yes
Subject B	1	yes	1	yes	3	yes	0	n/a	2	yes
Subject C	3	yes	1	yes	4	yes	0	n/a	1	yes
Subject D	0	n/a	0	n/a	3	yes	0	n/a	1	yes
Control										
Subject A	12	no	5	no	11	no				
Subject B	3	no	0	n/a	1	no				
Subject C	1	no	2	no	4	no				
Subject D	0	n/a	0	n/a	1	no				

Table 1: Summary of results obtained from the first two sets of experiments

3 Results

Table 1 summarizes the results obtained from the first two sets of experiments described above and Table 2 details the summary into each general anaesthetic studied plus morphine in the case of medications. In the control studies for the first set of experiments, all test subjects did not feel anything unusual from the exposure to magnetic pulses except vague or weak local sensation near the site of exposure. In contrast, all general anaesthetics studied produced clear and completely reproducible brain effects in various degrees and durations as if the test subjects had actually inhaled the same. These brain effects were first localized near the site of treatment and then spread over the whole brain and faded away within several hours. But residual brain effects (hangover) lingered on for more than 12 hours in most cases. Among the general anaesthetics studied, chloroform and deuterated chloroform (chloroform D) produced the most pronounced and potent brain effects in strength and duration followed by isoflorance and diethyl ether. Tribromoethanol dissolved in water (1:50 by weight) and ethanol also produced noticeable effects but they are not summarized in the table.

As also shown in Table 1, while the test subjects did not feel anything unusual from consuming the tap water treated in the control experiments with magnetic pulses or laser light, all the general anaesthetics studied produced clear and completely reproducible brain effects in various degrees and durations respectively similar to the observations in the first set of experiments. These effects were over the whole brain, intensified within the first half hour after the test subjects consumed the treated water and then faded away within the next few hours. But residual brain effects lingered on for more than 12 hours as in the first set of experiments. Among the general anaesthetics studied, again chloroform and deuterated chloroform produced the most pronounced and potent effect in strength and duration followed by isoflorance and diethyl ether as illustrated in Figure 2. Tribromoethanol dissolved in water (1:50 by weight) and ethanol also produced noticeable effects but they are not summarized in the table.

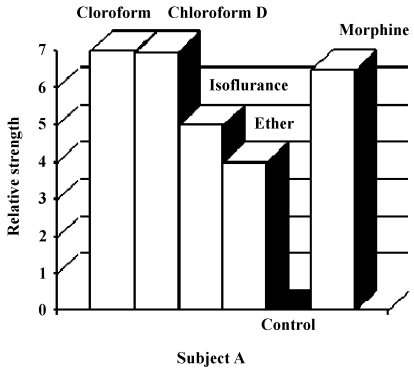

Fig. 2: Illustration of relative strengths of brain effects of several anesthetics and morphine

In addition, available results with flashlight and microwave as photon sources are also summarized in Table 1 respectively. In both cases general anaesthetics studied produced clear and reproducible brain effects. But the brain effects produced with microwave exposure were much stronger than those by flashlight.

Table 1 also summarizes results obtained with several medications including morphine, fentanyl, oxycodone, nicotine and caffeine in first and second sets of experiments. We

found that they all produced clear and completely reproducible brain effects such as euphoria or hastened alertness in various degrees and durations respectively. For example, in the case of morphine in the first set of experiments the brain effect was first localized near the site of treatment and then spread over the whole brain and faded away within several hours. In the case of morphine in the second set of experiments the brain effect was over the whole brain, first intensified within the first half hour after the test subjects consumed the treated water and then faded away within the next a few hours as illustrated in Figure 3.

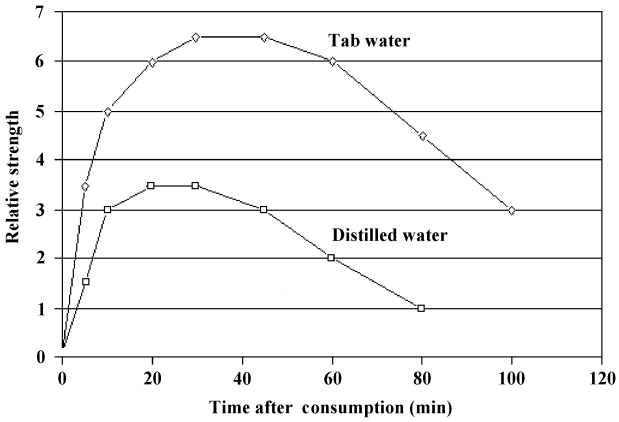

Fig. 3: Illustration of dynamics of brain effects produced by two types of water exposed to morphine

Comparative experiments were also done on Subject A and C with chloroform and diethyl ether by asking them to inhale the vapours of chloroform and diethyl respectively for 5 sec and compare the brain effect felt with those in the two sets of experiments described above. The brain effects induced in these comparative experiments were qualitatively similar to those produced in various experiments described above when chloroform and diethyl ether were respectively used for the exposure to photons of various sources.

Furthermore, through additional experiments we also made the following preliminary observations. First, the brain effects in the first set of experiments could not be induced by a permanent magnet in the place of the magnetic coil. Nor could these effects be produced by a third magnetic coil placed directly above the head of the test subject and connected to a second magnetic coil through an amplifier with the second magnetic coil receiving magnetic pulses from a first magnetic coil after the said magnetic pulses first passed through the anaesthetic sample. That is, the brain effects could not be transmitted through an electric wire. Second, in the second set of experiments the water exposed to magnetic pulses, laser light, microwave and flashlight when a chemical substance was present tasted about the same as that before the exposure. Third, heating tap water exposed to magnetic pulses or laser light in the presence of a chemical substance diminished the brain effect of the said substance. Fourth, when distilled water was used instead of fresh tap water the observed brain effects were markedly reduced as illustrated in Figure 6 in the case of morphine.

Table 3 summarizes the results obtained with the entanglement verification experiments carried out so far with chloroform, deuterated chloroform, diethyl ether and morphine. With all four sets of experiments, clear and consistently reproducible brain effects were experienced by the test subjects above and beyond what were noticeable in the control portions of the experiments under blind settings. More specifically, in the first set of entanglement verification experiments, the brain effects experienced by the test subjects were the same as those in which the setup shown in Figure 1C was used. In the second, third and fourth sets of these experiments, all test subjects did not feel anything unusual in the first half hour after consuming the first half of the water either exposed to microwave/magnetic pulses or just sit on the shelf for more than 3 months. But within minutes after the second half of the same water was exposed to the laser light or magnetic pulses in the presence of general anaesthetics, the test subjects would experience clear and completely reproducible brain effect of various intensities as if they have actually inhaled the general anaesthetic used in the exposure of the second half of the water. The said brain effects were over the whole brain, first intensified within minutes after the exposure began and persisted for the duration of the said exposure and for the next several hours after the exposure had stopped. Further, all other conditions being the same, magnetic coil produced more intense brain effects than the red laser. Furthermore, all other conditions being the same, the water exposed to microwave or magnetic pulses before consumption produced more intense brain effects than water just sitting on the shelve for more than 3 months before consumption.

4 Discussion

With respect to the second, third and fourth sets of entanglement verification experiments, the only possible explanation for the brain effects experienced by the test subjects are that they were the consequences of quantum entanglement because the water consumed by the test subjects was never directly exposed to the magnetic pulses or the laser lights in the presence of the chemical substances. There are other indications that quantum entanglement was the cause of the brain effects experienced by the test subjects. First, the brain effect inducing means could not be transmitted through an electrical wire as already reported above. Second, the said inducing means did not depend on the wavelengths of the photons generated. Thus, mere interactions among the photons, a chemical substance and water will induce brain effects after a test subject consumes the water so interacted.

While designing and conducting the herein described experiments, the first author became aware of the claims

	1st Set: Magn. Coil		2nd Set: Magn. Coil		Red laser		Flashlight		Microwave	
	Test ♯	Effect	Test ♯	Effect	Test ♯	Effect	Test ♯	Effect	Test ♯	Effect
Chloroform										
Subject A	2	yes	2	yes	5	yes	2	yes	3	yes
Subject B	0	n/a	0	n/a	1	yes	0	n/a	1	yes
Subject C	1	yes	2	yes	3	yes	0	n/a	1	yes
Subject D	1	yes	0	n/a	2	yes	0	n/a	0	n/a
Chloroform D										
Subject A	3	yes	2	yes	2	yes	1	yes		
Subject B	1	yes	0	n/a	1	yes	0	n/a		
Subject C	0	n/a	0	n/a	1	yes	0	n/a		
Subject D	0	n/a	0	n/s	0	n/a	0	n/a		
Isoflurance										
Subject A	3	yes	6	yes	5	yes	4	yes		
Subject B	0	n/a	1	yes	0	n/a	0	0		
Subject C	0	n/a	1	yes	1	n/a	0	0		
Subject D	1	yes	1	yes	1	n/a	0	0		
Diethyl Ether										
Subject A	5	yes	6	yes	10	yes	1	yes		
Subject B	1	yes	1	yes	1	yes	0	n/a		
Subject C	1	yes	3	yes	1	yes	0	n/a		
Subject D	0	n/a	0	n/a	2	yes	0	n/a		
Morphine										
Subject A	5	yes	7	yes	5	yes				
Subject B	0	n/a	1	yes	2	yes				
Subject C	0	n/a	1	yes	2	yes				
Subject D	0	n/a	0	n/a	2	yes				
Other Medications										
Subject A	7	yes	4	yes						
Subject B	1	yes	0	n/a						
Subject C	3	yes	0	n/a						
Subject D	0	n/a	0	n/a						

Table 2: Breakdown of the summary in Table 1 into each general anesthetic studied plus morphine in the case of medications

	First Set		Second Set		Third Set		Fourth Set	
	Test ♯	Effect	Test ♯	Effect	Test ♯	Effect	Test ♯	Effect
Subject A	8	yes	8	yes	3	yes	3	yes
Subject B	2	yes	3	yes	2	yes	1	yes
Subject C	3	yes	2	yes	1	yes	1	yes
Control								
Subject A	2	no	8	no	3	no	3	no
Subject B	0	n/a	3	no	2	no	1	no
Subject C	1	no	2	no	1	no	1	no

Table 3: Summary of the results obtained with the entanglement verification experiments carried out so far with chloroform, deuterated chloroform, diethyl ether and morphine

related to the so called "water memory" [7]. However, since these claims were said to be non-reproducible, we do not wish to discuss them further here except to say that we currently do not subscribe to any of the existing views on the subject and readers are encouraged to read our recent online paper on quantum entanglement [8].

We would like to point out that although the indicators used to measure the brain effects were qualitative and subjective, they reflect the first-person experiences of the qualities, intensities and durations of these effects by the test subjects since their brains were directly used as experimental probes. Further, these effects are completely reproducible under blind experimental settings so that possible placebo effects were excluded. However, as with many other important new results, replications by others are the key to independently confirm our results reported here. Our experiments may appear simple and even "primitive" but the results and implications are profound.

We first chose general anaesthetics in our experiments because they are among the most powerful brain-influencing substances. Our expectation was that, if nuclear and/or electronic spins inside the brain are involved in brain functions such as perception as recently hypothesized by us, the brain may be able to sense the effect of an external anaesthetic sample through quantum entanglement between these spins inside the brain and those of the said anaesthetic sample induced by the photons of the magnetic pulses by first interacting with the nuclear and/or electronic spins inside the said anaesthetic sample, thus carrying quantum information about the anaesthetic molecules, and then interacting with the nuclear and/or electronic spins inside the brain.

We suggest here that the said quantum entities inside the brains are likely nuclear and/or electronic spins for the reasons discussed below. Neural membranes and proteins contain vast numbers of nuclear spins such as 1H, 13C, 31P and 15N. These nuclear spins and unpaired electronic spins are the natural targets of interaction with the photons of the magnetic pulses or other sources. These spins form complex intra- and inter-molecular networks through various intramolecular J- and dipolar couplings and both short- and long-range intermolecular dipolar couplings. Further, nuclear spins have relatively long relaxation times after excitations [9]. Thus, when a nematic liquid crystal is irradiated with multi-frequency pulse magnetic fields, its 1H spins can form long-lived intra-molecular quantum coherence with entanglement for information storage [10]. Long-lived (0.05 ms) entanglement of two macroscopic electron spin ensembles at room temperature has also been achieved [3]. Furthermore, spin is a fundamental quantum process with intrinsic connection to the structure of space-time [11] and was shown to be responsible for the quantum effects in both Hestenes and Bohmian quantum mechanics [12, 13]. Thus, we have recently suggested that these spins could be involved in brain functions at a more fundamental level [2].

5 Conclusions

In light of the results from the entanglement verification experiments, we conclude that the brain effects experienced by the test subjects were the consequences of quantum entanglement between quantum entities inside the brains and those of the chemical substances under study induced by the entangling photons of the magnetic pulses or applied lights. More specifically, the results obtained in the first set of experiments can be interpreted as the consequence of quantum entanglement between the quantum entities in the brain and those in the chemical substances induced by the photons of the magnetic pulses. Similarly, the results obtained from the second sets of experiments can be explained as quantum entanglement between the quantum entities in the chemical substance and those in the water induced by the photons of the magnetic pulses, laser light, microwave or flashlight and the subsequent physical transport of the water entangled with the said chemical substance to the brain after consumption by the test subject which, in turn, produced the observed brain effects through the entanglement of the quantum entities inside the brain with those in the consumed water.

Several important conclusions and implications can be drawn from our findings. First, biologically and chemically meaningful information can be communicated via quantum entanglement from one place to another by photons and possibly other quantum objects such as electrons, atoms and even molecules. Second, both classical and quantum information can be transmitted between locations of arbitrary distances through quantum entanglement alone. Third, instantaneous signalling is physically real which implies that Einstein's theory of relativity is in real (not just superficial) conflict with quantum theory. Fourth, brain processes such as perception and other biological processes likely involve quantum information and nuclear and/or electronic spins may play important roles in these processes. Further, our findings provide important new insights into the essence and implications of the mysterious quantum entanglement and clues for solving the long-standing measurement problem in quantum theory including the roles of the observer and/or consciousness. Very importantly, our findings also provide a unified scientific framework for explaining many paranormal and/or anomalous effects such as telepathy, telekinesis and homeopathy, if they do indeed exist, thus transforming these paranormal and anomalous effects into the domains of conventional sciences.

Finally, with respect to applications, our findings enable various quantum entanglement technologies be developed. Some of these technologies can be used to deliver the therapeutic effects of many drugs to various biological systems such as human bodies without physically administrating the same to the said systems. This will dramatically reduce waste and increase productivity because the same drugs can be

repeatedly used to deliver their therapeutic effects to the mass on site or from remote locations of arbitrary distances. Further, many substances of nutritional and recreational values can be repeatedly administrated to desired biological systems such as human bodies through the said technologies either on site or from remote locations. Other such technologies can be used for instantaneous communications between remote locations of arbitrary distances in various ways. Potentially, these technologies can also be used to entangle two or more human minds for legitimate and beneficial purposes.

Acknowledgements

We wish to thank Yongchang Hu and Cuifang Sun for their participation in the experiments and Robert N. Boyd for our visit to his place of research.

References

1. Julsgaard B., Sherson J., Cirac J. I., Fiurasek J., Polzik E. S. Experimental demonstration of quantum memory for light. *Nature*, 2004, v. 432, 482–485.
2. Hu H. P., Wu M. X. Spin-mediated consciousness theory. *Med. Hypotheses*, 2004, v. 63, 633–646; arXiv: quant-ph/0208068.
3. Julsgaard B., Kozhekin A., Polzik E. S. Experimentally long-lived entanglement of two macroscopic objects. *Nature*, 2001, v. 413, 400–403.
4. Ghosh S., Rosenbaum T. F., Aeppli G., Coppersmith S. N. Entangled quantum state of magnetic dipoles. *Nature*, 2003, v. 425, 48–51.
5. Matsukevich D. N., Kuzmich A. Quantum state transfer between matter and light. *Science*, 2004, v. 306, 663–666.
6. Chanelière T. et al. Storage and retrieval of single photons transmitted between remote quantum memory. *Nature*, 2005, v. 438, 833–836.
7. Davenas E. et al. Human basophil degranulation triggered by very dilute antiserum against IgE. *Nature*, 1988, v. 333, 816–818.
8. Hu H. P., Wu M. X. Thinking outside the box: the essence and implications of quantum entanglement. *NeuroQuantology*, 2006, v. 4, 5–16; Cogprints: ID4581.
9. Gershenfeld N., Chuang I. L. Bulk spin resonance quantum computation. *Science*, 1997, v. 275, 350–356.
10. Khitrin A. K., Ermakov V. L., Fung B. M. Information storage using a cluster of dipolar-coupled spins. *Chem. Phys. Lett.*, 2002, v. 360, 160–166.
11. Dirac P. A. M. The quantum theory of the electron. *Proc. R. Soc.*, 1928, v. A117, 610–624.
12. Hestenes D. Quantum mechanics from self-interaction. *Found. Phys.*, 1983, v. 15, 63–78.
13. Salesi G., Recami E. Hydrodynamics of spinning particles. *Phys. Rev.*, 2004, v. A57, 98–105.

The Extended Relativity Theory in Clifford Spaces: Reply to a Review by W. A. Rodrigues, Jr.

Carlos Castro* and Matej Pavšič†

*Center for Theor. Studies of Physical Systems, Clark Atlanta University, Atlanta, USA
E-mail: czarlosromanov@yahoo.com; castro@ctsps.cau.edu

†Jožef Stefan Institute, Jamova 39, 1000 Ljubljana, Slovenia
E-mail: Matej.Pavsic@ijs.si

In a review, W. A. Rodrigues, Jr., wrote that we confused vector and affine spaces, and that we misunderstood the concept of curvature. We reply to those comments, and point out, that in our paper there was an explicit expression for the curvature of a connection. Therefore we were quite aware — contrary to what asserted the reviewer — that the curvature of a manifold has nothing to do with a choice of a frame field which, of course, even in a flat manifold can be position dependent.

In 2005 we published a paper entitled *The Extended Relativity Theory in Clifford Spaces* [1] which was reviewed by W.A. Rodrigues, Jr. [2]. A good review, even if critical, is always welcome, provided that the criticism is correct and relevant. Unfortunately the reviewer produced some statements which need a reply. He wrote:

> "Two kinds of Clifford spaces are introduced in their paper, flat and curved. According to their presentation, which is far from rigorous by any mathematical standard, we learn that flat Clifford space is a vector space, indeed the vector space of a Clifford algebra of real vector space $\mathbb{R}^D$ equipped with a metric of signature $P+Q=D$. As such the authors state that the coordinates of Clifford space are noncommutative Clifford-valued quantities. It is quite obvious for a mathematician that the authors confuse a vector space with an affine space. This is clear when we learn their definition of a curved Clifford space, which is a 16-dimensional manifold where the tangent vectors are position dependent and at any point are generators of a Clifford algebra $C_{P,Q}$. The authors, as is the case of many physicists, seem not to be aware that the curvature of a manifold has to do with the curvature of a connection that we may define on such a manifold, and has nothing to do with the fact that we may choose even in flat manifold a section of the frame bundle consisting of vectors that depend on the coordinates of the manifold points in a given chart of the maximal atlas of the manifold."

When introducing flat C-space we just said that the Clifford-valued polyvector denotes the position of a point in a manifold, called Clifford space, or C-space. It is a common practice to consider coordinates, e. g., four coordinates x^μ, $\mu=0,1,2,3$, of a point $\mathcal{P}$ of a flat spacetime as components of a radius vector from a chosen point $\mathcal{P}_0$ ("the origin") to $\mathcal{P}$. If we did not provide at this point a several pages course on vector and affine spaces, this by no means implies that we were not aware of a distinction of the two kinds of spaces. That position in flat spacetime is described by radius vector is so common that we do not need to provide any further explanation in this respect. Our paper is about *physics* and not mathematics. We just *use* the well established mathematics. Of course a spacetime manifold (including a flat one) is not the same space as a vector space, but, choosing an "origin" in spacetime, to every point there corresponds a vector, so that there is a one-to-one correspondence between the two spaces. This informal description is true, regardless of the fact that there exist corresponding rigorous, formal, mathematical descriptions (to be found in many textbooks on physics and mathematics).

The correspondence between points and vectors does no longer hold in a curved space, at least not according to the standard wisdom practiced in the textbooks on differential geometry. However, there exists an alternative approach adopted by Hestenes and Sobcyk in their book [3], according to which even the points of a curved space are described by vectors. Moreover, there is yet another possibility, described in refs. [4, 5], which employs vector fields $a^\mu(x)\gamma_\mu$ in a curved space $\mathcal{M}$, where γ_μ, $\mu=0,1,2,\ldots,n-1$, are the coordinate basis vector fields. At every point $\mathcal{P}$ the vectors $\gamma_\mu|_\mathcal{P}$ span a tangent space $T_\mathcal{P}\mathcal{M}$ which is a vector space.

A particular case can be such that in a given coordinate system* we have $a^\mu(x)=x^\mu$. Then at every point $\mathcal{P}\in\mathcal{M}$, the object $x(\mathcal{P})=x^\mu(\mathcal{P})\gamma_\mu(\mathcal{P})$ is a tangent vector. So we have one-to-one correspondence between the points $\mathcal{P}$ of $\mathcal{M}$ and the tangent vectors $x(\mathcal{P})=x^\mu(\mathcal{P})\gamma_\mu(\mathcal{P})$, shortly $x^\mu\gamma_\mu$. The set of objects $x(\mathcal{P})$ for all point $\mathcal{P}$ in a region $R\subset\mathcal{M}$ we call the coordinate vector field [4]. So although the manifold is curved, every point in it can be described by a tangent

*"Coordinate system" or simply "coordinates" is an abbreviation for "the coordinates of the manifold points in a given chart of the maximal atlas of the manifold".

vector at that point, the components of the tangent vector being equal to the coordinates of that point.* Those tangent vectors $x^\mu(\mathcal{P})\gamma_\mu(\mathcal{P})$ are now "house numbers" assigned to a point $\mathcal{P}$. We warn the reader not to confuse the tangent vector $x(\mathcal{P})$ at a point $\mathcal{P}$ with the vector pointing from $\mathcal{P}_0$ (a coordinate origin) to a point $\mathcal{P}$, a concept which is ill defined in a curved manifold.

Analogous holds for Clifford space C. It is a manifold whose points $\mathcal{E}$ can be physically interpreted as extended "events". One possible way to describe those points is by means of a *polyvector field* $A(X) = A^M(X)\gamma_M(X) = X^M\gamma_M$, where $\gamma_M|_\mathcal{E}$, $M = 1, 2, \ldots, 2^n$, are tangent polyvectors that at every point $\mathcal{E} \in C$ span a Clifford algebra. At a given point $\mathcal{E} \in C$ it may hold [6, 5]

$$\gamma_M = \gamma_{\mu_1} \wedge \gamma_{\mu_2} \wedge \ldots \wedge \gamma_{\mu_r}\,, \qquad r = 0, 1, 2, \ldots, n \quad (1)$$

i. e., γ_M are defined as wedge product of vectors γ_μ, $\mu = 0, 1, 2, \ldots, n-1$. The latter property cannot hold in a general curved Clifford space [6, 5]. In refs. [7, 1] we considered a particular subclass of curved C-spaces, for which it does hold.

If we choose a particular point $\mathcal{E}_0 \in C$, to which we assign coordinates $X^M(\mathcal{E}_0) = 0$, then we have a correspondence between points $\mathcal{E} \in C$ and Clifford numbers $X^M(\mathcal{E})\,\gamma_M(\mathcal{E})$. In this sense one has to understand the sentence of ref. [1]:

> "An element of C-space is a Clifford number, called also polyvector or Clifford aggregate which we now write in the form $X = s\gamma + x^\mu\gamma_\mu + x^{\mu\nu}\gamma_\mu\wedge\gamma_\nu + \ldots$"

Therefore, a more correct formulation would be, e. g.,

> "An element of C-space is an extended event $\mathcal{E}$, to which one can assign a Clifford number, called polyvector, $X^M(\mathcal{E})\gamma_M(\mathcal{E}) \equiv X^M\gamma_M$."

together with an explanation in the sense as given above. So a rigorous formulation is, not that an element of C-space *is* a Clifford number, but that to a point of C-space there *corresponds* a Clifford number, and that this holds for all points within a domain $\Omega \subset C$ corresponding to a given chart of the maximal atlas of C.

On the one hand we have a 2^n-dimensional manifold $C \equiv \{\mathcal{E}\}$ of points (extended events) $\mathcal{E}$, and on the other hand the 2^n-dimensional space $\{X(\mathcal{E})\}$ of Clifford numbers $X(\mathcal{E}) = X^M(\mathcal{E})\,\gamma\,(\mathcal{E})$ for $\mathcal{E} \in \Omega \subset C$. The latter space $\{X(\mathcal{E})\}$, of course, is not a Clifford algebra. It is a subspace of 2×2^n-dimensional tangent bundle TC of the manifold C. At every point $\mathcal{E} \in C$ there is a also another subspace of TC, namely the 2^n-dimensional tangent space $T_\mathcal{E}C$, which is a Clifford algebra $\mathcal{C}_n$. Since there is a one-to-one correspondence between the spaces $\{X(\mathcal{E})\}$ and $\{\mathcal{E}\}$, the space $\{X(\mathcal{E})\}$ can be used for description of the space $\{\mathcal{E}\}$.

It is true that physicists are often sloppy with mathematical formulations and usage of language, but it is also true that mathematicians often read *physics papers* superficially and see misconceptions, "errors", erroneous mathematical statements, etc., instead of trying to figure out the true content behind an informal (and therefore necessarily imprecise) description, whose emphasis is on physics and not mathematics.

A culmination is when the reviewer writes

> "The authors, as is the case of many physicists, seem not to be aware that curvature... has nothing to do with the fact that we may choose even in flat manifold a section of the frame bundle consisting of vectors that depend on coordinates of the manifold points..."

That curvature has nothing to do with coordinate transformations† is clear to everybody who has ever studied the basis of general relativity. Everyone who has a good faith that the author(s) of a paper have a minimal level of competence would interpret a text such as [1]

> "In flat C-space the basis polyvectors γ_M are constant. In a curved C-space this is no longer true. Each γ_M is a function of C-space coordinates X^M..."

according to

> "In flat C-space one can always find coordinates‡ in which γ_M are constant. In a curved C-space this is no longer true. Each γ_M depends on position in C-space." Or equivalently, "Each γ_M is a function of the C-space coordinates".

However, even our formulation as it stands in ref. [1] makes sense within the context in which we first consider flat space in which we *choose* a constant frame field, i. e., constant basis polyvectors. We denote the latter polyvectors as γ_M. If we then deform§ the flat space into a curved one, then the *same* (poly)vector fields γ_M in general can no longer be independent of position. In this sense the formulation as it stands in our paper is quite correct.

We then define a *connection* on our manifold C, and the corresponding *curvature* (see eqs. (77), (78) of ref. [1]). That

*If we change coordinate system, then $a^\mu(x)\gamma_\mu = x^\mu\gamma_\mu = a'^\mu(x')\gamma'_\mu(x')$, with $a'^\mu = a^\nu(x)(\partial x'^\mu/\partial x^\nu) = x^\nu(\partial x'^\mu/\partial x^\nu)$. In another coordinate system S' one can then take another vector field, such that $b^\mu(x') = x'^\mu$. Let us stress that $b^\mu(x') = x'^\mu$ is a different field from $a'^\mu(x')$, therefore the reader should not think that we say $x'^\mu = x^\nu(\partial x'^\mu/\partial x^\nu)$ which is, of course, wrong. What we say is $a'^\mu(x') = (\partial x'^\mu/\partial x^\nu)a^\nu(x)$, where, in particular, $a^\nu(x) = x^\nu$.

†For instance, in flat spacetime one can introduce a curvilinear coordinate system of coordinates, like the use of polar coordinates in the plane and spherical coordinates in $\mathbb{R}^3$. However, the introduction of a curvilinear coordinate system does not convert the original flat space into a curved one. And vice versa, one can introduce a non-Euclidean metric (non-flat metric) on a two-dim flat surface, for example, like the hyperbolic Lobachevsky metric of constant negative scalar curvature.

‡We renounce to use here the lengthy formulation provided by the reviewer. Usage of the term "coordinates" is sufficient, and it actually means "coordinates of the manifold point in a given chart of the maximal atlas of the manifold".

§This is easy to imagine, if we consider a flat surface embedded in a higher dimensional space, and then deform the surface. In general, we may deform the surface so that is is curved not only extrinsically, but also intrinsically.

the reviewer reproaches us of being ignorant of the fact that the curvature of a manifold has to do with the curvature of a connection is therefore completely out of place, to say at least.

Finally, let us mention that in the review of another paper [8] the same reviewer ascribed to one of us (M.P) an incorrect mathematical statement. But I was quite aware of the well known fact that Clifford algebras associated with vector spaces of different signatures (p, q), with $p + q = n$, are not all isomorphic (in the sense as stated, e. g., in the book by Porteous [9]). What I discussed in that paper was something different. This should be clear from my description, therefore I did not explicitly warn the reader about the difference (although I was aware of the danger that at superficial reading some people might believe me of committing an error). However, in subsequent ref. [1] we did warn the reader about the possibility of such a confusion.

References

1. Castro C. and Pavšič M. The extended relativity theory in Clifford spaces. *Progress in Physics*, 2005, v. 1, 31.
2. Rodrigues W. A., Jr. *Mathematical Reviews*, MR2150508 (2006c:83068).
3. Hestenes D. and Sobcyk G. Clifford algebra to geometric calculus. D. Reidel, Dordrecht, 1984.
4. Pavšič M. The landscape of theoretical physics: a global view; From point particles to the brane world and beyond, in search of a unifying principle. Kluwer Academic Publishers, Amsterdam, 2001.
5. Pavšič M. Spin gauge theory of gravity in Clifford space: A realization of Kaluza-Klein theory in 4-dimensional space-time. arXiv: gr-qc/0507053, to appear in *Int. J. Mod. Phys. A*.
6. Pavšič M. Kaluza-Klein theory without extra dimensions: Curved Clifford space. *Phys. Lett. B*, 2005, v. 614, 85. arXiv: hep-th/0412255.
7. Castro C. and Pavšič M. Higher derivative gravity and torsion from the geometry of C-spaces. *Phys. Lett. B*, 2002, v. 539, 133. arXiv: hep-th/0110079.
8. Pavšič M. Clifford algebra based polydimensional relativity and relativistic dynamics. *Found. Phys.*, 2001, v. 31, 1185. arXiv: hep-th/0011216.
9. Porteous I. R. Topological geometry. Second edition, Cambridge Univ. Press, Cambridge, 1982.

On the Regge-Wheeler Tortoise and the Kruskal-Szekeres Coordinates

Stephen J. Crothers

Queensland, Australia

E-mail: thenarmis@yahoo.com

The Regge-Wheeler tortoise "coordinate" and the the Kruskal-Szekeres "extension" are built upon a latent set of invalid assumptions. Consequently, they have led to fallacious conclusions about Einstein's gravitational field. The persistent unjustified claims made for the aforesaid alleged coordinates are not sustained by mathematical rigour. They must therefore be discarded.

1 Introduction

The Regge-Wheeler tortoise coordinate was not conjured up from thin air. On the contrary, is was obtained *a posteriori* from the Droste/Weyl/(Hilbert) [1, 2, 3] (the DW/H) metric for the static vacuum field; or, more accurately, from Hilbert's corruption of the spacetime metric obtained by Johannes Droste.

The first presentation and misguided use of the Regge-Wheeler coordinate was made by A. S. Eddington [4] in 1924. Finkelstein [5], years later, in 1958, presented much the same; since then virtually canonised in the so-called "Eddington-Finkelstein" coordinates. Kruskal [6], and Szekeres [7], in 1960, compounded the errors with additional errors, all built upon the very same fallacious assumptions, by adding even more fallacious assumptions. The result has been a rather incompetent use of mathematics to produce nonsense on an extraordinary scale.

Orthodox relativists are now so imbued with the misconceptions that they are, for the most part, no longer capable of rational thought on the subject. Although the erroneous assumptions of the orthodox have been previously demonstrated to be false [8–18] they have consistently and conveniently ignored the proofs.

I amplify the erroneous assumptions of the orthodox relativists in terms of the Regge-Wheeler tortoise, and consequently in the Kruskal-Szekeres phantasmagoria.

2 The orthodox confusion and delusion

Consider the DW/H line-element

$$ds^2 = \left(1 - \frac{\alpha}{r}\right) dt^2 - \left(1 - \frac{\alpha}{r}\right)^{-1} dr^2 - \\ - r^2 \left(d\theta^2 + \sin^2\theta \, d\varphi^2\right), \qquad (1)$$

where $\alpha = 2m$. Droste showed that $\alpha < r < \infty$ is the correct domain of definition on (1), as did Weyl some time later. Hilbert however, claimed $0 < r < \infty$. Modern orthodox relativists claim two intervals, $0 < r < \alpha$, $\alpha < r < \infty$, and call the latter the "exterior" Schwarzschild solution and the former a "black hole", notwithstanding that (1) with $0 < r < \infty$ was never proposed by K. Schwarzschild [19]. Astonishingly, the vast majority of orthodox relativists, it seems, have never even heard of Schwarzschild's true solution.

I have proved elsewhere [11, 12, 13] that the orthodox, when considering (1), have made three invalid assumptions, to wit

(a) r is a proper radius;

(b) r can go down to zero;

(c) A singularity must occur where the Riemann tensor scalar curvature invariant (the Kretschmann scalar), $f = R_{\alpha\beta\rho\sigma} R^{\alpha\beta\rho\sigma}$, is unbounded.

None of these assumptions have ever been proved true with the required mathematical rigour by any orthodox relativist. Notwithstanding, they blindly proceed on the assumption that they are all true. The fact remains however, that they are all demonstrably false.

Consider assumption (a). By what rigorous argument have the orthodox identified r as a radial quantity on (1)? Moreover, by what rigorous mathematical means have they ever indicated what they mean by a radial quantity on (1)? Even a cursory reading of the literature testifies to the fact that the orthodox relativists have never offered any mathematical rigour to justify assumption (a). Mathematical rigour actually proves that this assumption is false.

Consider assumption (b). By what rigorous means has it ever been proved that r can go down to zero on (1)? The sad fact is that the orthodox have never offered a rigorous argument. All they have ever done is inspect (1) and claim that there are singularities at $r = \alpha$ and at $r = 0$, and thereafter concocted means to make one of them ($r = 0$) a "physical" singularity, and the other a "coordinate" singularity, and vaguely refer to the latter as a "pathology" of coordinates, whatever that means. The allegation of singularities at $r = \alpha$ and at $r = 0$ also involves the unproven assumption (a). Evidently the orthodox consider that assumptions (a) and (b) are self-evident, and so they don't even think about them. However, assumptions (a) and (b) are not self-evident and if they are to be justifiably used, they must first be proved. No

orthodox relativist has ever bothered to attempt the necessary proofs. Indeed, none it would seem have ever seen the need for proofs, owing to their "self-evident" assumptions.

Assumption (c) is an even more curious one. Indeed, it is actually a bit of legerdemain. Having just assumed (a) and (b), the orthodox needed some means to identify their "physical" singularity. They went looking for it at a suitable unbounded curvature scalar, found it in the Kretschmann scalar, after a series of misguided transformations of "coordinates" leading to the Kruskal-Szekeres "extension", and thereafter have claimed singularity of the Kretschmann type in the static vacuum field.

Furthermore, using these unproved assumptions, the orthodox relativists have claimed a process of "gravitational collapse" to a "point-mass". And with this they have developed what they have called grandiosely and misguidedly, "singularity theorems", by which it is alleged that "physical" singularities and "trapped surfaces" are a necessary consequence of gravitational collapse, and even cosmologically, called Friedmann singularities.

The orthodox relativists must first prove their assumptions by rigorous mathematics. Unless they do this, their analyses are unsubstantiated and cannot be admitted.

Since the orthodox assumptions have in fact already been rigorously proved entirely false, the theory that the orthodox have built upon them is also false.

3 The Regge-Wheeler tortoise; the Kruskal-Szekeres phantasmagoria

Since the Regge-Wheeler tortoise does not come from thin air, from where does it come?

First consider the general static line-element

$$ds^2 = A\left(\sqrt{C(r)}\right)dt^2 - B\left(\sqrt{C(r)}\right)d\sqrt{C(r)}^2 - \\ - C(r)\left(d\theta^2 + \sin^2\theta\, d\varphi^2\right), \quad (2)$$

$$A, B, C > 0\,.$$

It has the solution

$$ds^2 = \left(1-\frac{\alpha}{\sqrt{C(r)}}\right)dt^2 - \left(1-\frac{\alpha}{\sqrt{C(r)}}\right)^{-1} d\sqrt{C(r)}^2 - \\ - C(r)\left(d\theta^2 + \sin^2\theta\, d\varphi^2\right), \quad (3)$$

and setting $R_c(r) = \sqrt{C(r)}$ for convenience, this becomes

$$ds^2 = \left(1-\frac{\alpha}{R_c(r)}\right)dt^2 - \left(1-\frac{\alpha}{R_c(r)}\right)^{-1} dR_c^2(r) - \\ - R_c^2(r)\left(d\theta^2 + \sin^2\theta d\varphi^2\right), \quad (4)$$

for some analytic function $R_c(r)$. Clearly, if $R_c(r)$ is set equal to r, then (1) is obtained.

Reduce (4) to two dimensions, thus

$$ds^2 = \left(1-\frac{\alpha}{R_c(r)}\right)dt^2 - \left(1-\frac{\alpha}{R_c(r)}\right)^{-1} dR_c^2(r)\,. \quad (5)$$

The null geodesics are given by

$$ds^2 = 0 = \left(1-\frac{\alpha}{R_c(r)}\right)dt^2 - \left(1-\frac{\alpha}{R_c(r)}\right)^{-1} dR_c^2(r)\,.$$

Consequently

$$\left(\frac{dt}{dR_c(r)}\right)^2 = \left(\frac{R_c(r)}{R_c(r)-\alpha}\right)^2,$$

and therefore,

$$t = \pm\left[R_c(r) + \alpha\ln\left|\frac{R_c(r)}{\alpha} - 1\right|\right] + \text{const.}$$

Now

$$R^*(r) = R_c(r) + \alpha\ln\left|\frac{R_c(r)}{\alpha} - 1\right| \quad (6)$$

is the so-called Regge-Wheeler tortoise coordinate. If $R_c(r) = r$, then

$$r^* = r + \alpha\ln\left|\frac{r}{\alpha} - 1\right|, \quad (7)$$

which is the standard expression used by the orthodox. They never use the general expression (6) because they only ever consider the particular case $R_c(r) = r$, owing to the fact that they do not know that their equations relate to a particular case. Furthermore, with their unproven and invalid assumptions (a) and (b), many orthodox relativists claim

$$0 = 0 + \alpha\ln\left|\frac{0}{\alpha} - 1\right| \quad (8)$$

so that $r_0^* = r_0 = 0$. But as explained above, assuming $r_0 = 0$ in (1) has no rigorous basis, so (8) is rather misguided.

Let us now consider (2). I identify therein the radius of curvature $R_c(r)$ as the square root of the coefficient of the angular terms, and the proper radius $R_p(r)$ as the integral of the square root of the component of the metric tensor containing the squared differential element of the radius of curvature. Thus, on (2),

$$R_c(r) = \sqrt{C(r)}\,, \\ R_p(r) = \int\sqrt{B(\sqrt{C(r)})}\; d\sqrt{C(r)} + \text{const.} \quad (9)$$

In relation to (4) it follows that,

$$R_c(r) \quad \text{is the radius of curvature,} \\ R_p(r) = \int\sqrt{\frac{R_c(r)}{(R_c(r)-\alpha)}}\; dR_c(r) + K\,, \quad (10)$$

where K is a constant to be rigorously determined by a boundary condition. Note that according to (10) there is no *a priori* reason for $R_p(r)$ and $R_c(r)$ to be identical in Einstein's gravitational field.

Now consider the usual Minkowski metric,

$$ds^2 = dt^2 - dr^2 - r^2\left(d\theta^2 + \sin^2\theta d\varphi^2\right), \qquad (11)$$

$$0 \leqslant r < \infty,$$

where

$$R_c(r) = r, \qquad R_p(r) = \int_0^r dr = r \equiv R_c(r). \qquad (12)$$

In this case $R_p(r)$ is identical to $R_c(r)$. The identity is due to the fact that the spatial components of Minkowski space are Efcleethean*. But (4), and hence (10), are non-Efcleethean, and so there is no reason for $R_p(r)$ and $R_c(r)$ to be identical therein.

The geometry of a spherically symmetric line-element is an intrinsic and invariant property, by which radii are rigorously determined. The radius of curvature is always the square root of the coefficient of the angular terms and the proper radius is always the integral of the square root of the component containing the square of the differential element of the radius of curvature. Note that in general $R_c(r)$ and $R_p(r)$ are analytic functions of r, so that r is merely a parameter, and not a radial quantity in (2) and (4). So $R_c(r)$ and $R_p(r)$ map the parameter r into radii (i. e. distances) in the gravitational field. Note further that r is actually defined in Minkowski space. Thus, a distance in Minkowski space is mapped into corresponding distances in Einstein's gravitational field by the mappings $R_c(r)$ and $R_p(r)$.

It has been proved [11, 12] that the admissible form for $R_c(r)$ is,

$$R_c(r) = \left(\left|r - r_0\right|^n + \alpha^n\right)^{\frac{1}{n}}, \qquad (13)$$

$$n \in \Re^+, \quad r_0 \in \Re, \quad \alpha = 2m, \quad r \neq r_0,$$

where n and r_0 are entirely arbitrary constants, and that

$$R_p(r) = \sqrt{R_c(r)\left(R_c(r) - \alpha\right)} + \alpha \ln\left|\frac{\sqrt{R_c(r)} + \sqrt{R_c(r) - \alpha}}{\sqrt{\alpha}}\right|.$$

If $n=1$, $r_0=\alpha$, $r>r_0$ are chosen, then by (13), $R_c(r)=r$ and equation (1) is recovered; but by (13), $\alpha < r < \infty$ is then the range on the r-parameter. Note that in this case

$$R_c(\alpha) = \alpha, \qquad R_p(\alpha) = 0,$$

and that in general,

$$R_c(r_0) = \alpha, \qquad R_p(r_0) = 0,$$

$$\alpha < R_c(r) < \infty,$$

since the value of r_0 is immaterial. I remark in passing that if $n=3$, $r_0=0$, $r>0$ are chosen, Schwarzschild's original solution results.

Returning now to the Regge-Wheeler tortoise, it is evident that

$$-\infty < R^*(r) < \infty,$$

and that $R^*(r)=0$ when $R(r) \approx 1.278465\,\alpha$. Now according to (13), $\alpha < R_c(r) < \infty$, so the Regge-Wheeler tortoise can be written generally as,

$$R^*(r) = R_c(r) + \alpha \ln\left(\frac{R_c(r)}{\alpha} - 1\right), \qquad (14)$$

which is, in the particular case invariably used by the orthodox relativists,

$$r^* = r + \alpha \ln\left(\frac{r}{\alpha} - 1\right),$$

and so, by (13) and (14), the orthodox claim that

$$0 = 0 + \alpha \ln\left|\frac{0}{\alpha} - 1\right|,$$

is nonsense. It is due to the invalid assumptions (a) and (b) which the orthodox relativists have erroneously taken for granted. Of course, the tortoise, r^*, cannot be interpreted as a radius of curvature, since in doing so would violate the intrinsic geometry of the metric. This is clearly evident from (13), which specifies the permissible form of a radius of curvature on a metric of the form (4).

So what is the motivation to the Regge-Wheeler tortoise and the subsequent Kruskal-Szekeres extension? Very simply this, to rid (1) of the singularity at $r=\alpha$ and make $r=0$ a "physical" singularity, satisfying the *ad hoc* assumption (c), under the mistaken belief that† $r=\alpha$ is not a physical singularity (but it is a true singularity, however, not a Kretschmann curvature-type). This misguided notion is compounded by a failure to realise that there are two radii in Einstein's gravitational field and that they are never identical, except in the infinitely far field where spacetime becomes Minkowski, and that what they treat as a proper radius in the gravitational field is in fact the radius of curvature in their particular metric, which cannot go down to zero. Only the proper radius can approach zero, although it cannot take the value of zero, i. e. $r \neq r_0$ in (13), since $R_p(r_0) \equiv 0$ marks the location of the centre of mass of the source of the field, which is not a physical object.

*Owing to the geometry due to Efcleethees, for those ignorant of Greek; usually and incorrectly Euclid.

†Indeed, that $\left(R_c(r_0) \equiv \alpha\right) \equiv \left(R_p(r_0) \equiv 0\right)$.

The mechanical procedure to the Kruskal-Szekeres extension is well-known, so I will not reproduce it here, suffice to say that it proposes the following null coordinates u and v,

$$u = t - R^*(r)\,,$$
$$v = t + R^*(r)\,,$$

which is always given by the orthodox relativists in the particular case

$$u = t - r^*\,,$$
$$v = t + r^*\,.$$

Along the way to the Kruskal-Szekeres extension, the sole purpose of which is to misguidedly drive the radius of curvature r in (1) down to zero, owing to their invalid assumptions (a), (b) and (c), the orthodox obtain

$$ds^2 = -\frac{\alpha e^{-\frac{r}{\alpha}}}{r}\, e^{\frac{(v-u)}{2\alpha}}\, du\, dv\,,$$

which in general terms is

$$ds^2 = -\frac{\alpha e^{-\frac{R_c(r)}{\alpha}}}{R_c(r)}\, e^{\frac{(v-u)}{2\alpha}}\, du\, dv\,,$$

and erroneously claim that the metric components of (1) have been factored into a piece, $\frac{e^{-r/\alpha}}{r}$, which is non-singular as $r \to \alpha$, times a piece with u and v dependence [20]. The claim is of course completely spurious, since it is based upon the false assumptions (a), (b), and (c). The orthodox relativists have not, contrary to their claims, developed a coordinate patch to cover a part of an otherwise incompletely covered manifold. What they have actually done, quite unwittingly, is invent a completely separate manifold, which they glue onto the manifold of the true Schwarzschild field, and confound this new and separate manifold as a part of the original manifold, and by means of the Kruskal-Szekeres extension, leap between manifolds in the mistaken belief that they are moving between coordinate patches on one manifold. The whole procedure is ludicrous; and patently false. Loinger [21] has also noted that the alleged "interior" of the Hilbert solution is a different manifold.

The fact that the Hilbert solution is not diffeomorphic to Schwarzschild's solution was proved by Abrams [9], who showed that the Droste/Weyl metric is diffeomorphic to Schwarzschild's original solution. This is manifest in (13), and can be easily demonstrated alternatively by a simple transformation, as follows. In the Hilbert metric, denote the radius of curvature by r^*, and equate this to Schwarzschild's radius of curvature thus,

$$r^* = \left(r^3 + \alpha^3\right)^{\frac{1}{3}}\,. \qquad (15)$$

Since $0 < r < \infty$ in Schwarzschild's original solution, it follows from this that

$$\alpha < r^* < \infty\,,$$

which is precisely what Droste obtained; later confirmed by Weyl. There is no "interior" associated with the DW/H metric, and no "trapped surface". The transformation (15) simply shifts the location of the centre of mass of the source in parameter space from $r_0 = 0$ to $r_0 = \alpha$, as given explicitly in (13).

4 Recapitulation and general comments

The standard school of relativists has never attempted to rigorously prove its assumptions about the variable r appearing in the line-element (1). It has never provided any rigorous argument as to what constitutes a radial quantity in Einstein's gravitational field. It has invented a curvature condition, in the behaviour of the Kretschmann scalar, as an *ad hoc* basis for singularity in Einstein's gravitational field.

The Regge-Wheeler tortoise has been thoroughly misinterpreted by the standard school of relativists. The Kruskal-Szekeres extension is a misguided procedure, and does not lead to a coordinate patch, but in fact, to a completely separate manifold having nothing to do with a Schwazschild space. The motivation to the Eddington-Finkelstein coordinates and the Kruskal-Szekeres extension is due to the erroneous assumptions that the variable r in (1) is a proper radius and can therefore go down to zero.

The standard school has failed to see that there are two radii in Einstein's gravitational field, which are determined by the intrinsic geometry of the metric. Thus, it has failed to understand the geometrical structure of type 1 Einstein spaces. Consequently, the orthodox relativists have incorrectly treated the variable r in (1) as a proper radius, failing to see that it is in fact the radius of curvature in (1), and that the proper radius must in fact be calculated by the geometrical relations intrinsic to the metric. They have failed to realise that the quantity r is in general nothing more than a parameter, defined in Minkowski space, which is mapped into the radii of the gravitational field, thereby making Minkowski space a parameter space from which Efcleethean distance is mapped into the corresponding true radii of Einstein's pseudo-Riemannian gravitational field.

The so-called "singularity theorems" are not theorems at all, as they are based upon false concepts. The "point-mass" is actually nothing more than the location of the centre of mass of the source of the gravitational field, and has no physical significance. Moreover, the alleged theorems are based upon the invalid construction of "trapped surfaces", essentially derived from the false assumptions (a), (b) and (c). The Friedmann singularities simply do not exist at all, either physically or mathematically, as it has been rigorously proved that cosmological solutions for isotropic type 1 Einstein spaces do not even exist [14], so that the Standard Cosmological model is completely invalid.

My own experience has been that most orthodox relativists just ignore the facts, resort to aggressive abuse when

confronted with them, and merrily continue with their demonstrably false assumptions. But here is a revelation: abuse and ignorance are not scientific methods. Evidently, scientific method is no longer required in science.

I have in the past, invited certain very substantial (and some not so substantial) elements of the orthodox relativists, literally under a torrent of vicious abuse, both gutter and eloquent, depending upon the person, (to which I have on occasion responded in kind after enduring far too much), to prove their assumptions (a), (b), and (c). Not one of them took up the invitation. I have also invited them to prove me wrong by simply providing a rigorous demonstration that the radius of curvature is not always the square root of the coefficient of the angular terms of the metric, and that the proper radius is not always the integral of the square root of the component containing the square of the differential element of the radius of curvature. Not one of them has taken up that invitation either. To refute my analysis is very simple in principle — rigorously prove the foregoing.

Alas, the orthodox are evidently unwilling to do so, being content instead to foist their errors upon all and sundry in the guise of profundity, to salve their need of vainglory, and ignore or abuse those who ask legitimate questions as to their analyses. And quite a few persons who have pointed out serious errors in the standard theory, have been refused any and all opportunity to publish papers on these matters in those journals and electronic archives which constitute the stamping grounds of the orthodox.

I give the foregoing in illustration of how modern science is now being deliberately censored and falsified. This cannot be allowed to continue, and those responsible must be exposed and penalised. It is my view that what the modern orthodox relativists have done amounts to scientific fraud. The current situation is so appalling that to remain silent would itself be criminal.

References

1. Droste J. The field of a single centre in Einstein's theory of gravitation, and the motion of a particle in that field. *Ned. Acad. Wet., S.A.*, v. 19, 1917, 197 (www.geocities.com/theometria/Droste.pdf).
2. Weyl H. Zur Gravitationstheorie. *Ann. Phys.*, (*Leipzig*), 1917, v. 54, 117.
3. Hilbert D. *Nachr. Ges. Wiss. Gottingen, Math. Phys. Kl.*, v. 53, 1917 (see also in arXiv: physics/0310104).
4. Eddington A. S. A comparison of Whitehead's and Einstein's formulas. *Nature*, 1924, v. 113, 192.
5. Finkelstein D. Past-future asymmetry of the gravitational field of a point particle. *Phys. Rev.*, 1958, v. 110, 965.
6. Kruskal M. D. Maximal extension of Schwarzschild metric. *Phys. Rev.*, 1960, v. 119, 1743.
7. Szekeres G. On the singularities of a Riemannian manifold. *Math. Debreca.*, 1960, v. 7, 285.
8. Brillouin M. The singular points of Einstein's Universe. *Journ. Phys. Radium*, 1923, v. 23, 43 (see also in arXiv: physics/0002009).
9. Abrams L. S. Black holes: the legacy of Hilbert's error. *Can. J. Phys.*, 1989, v. 67, 919 (see also in arXiv: gr-qc/0102055).
10. Abrams L. S. The total space-time of a point charge and its consequences for black holes. *Int. J. Theor. Phys.*, v. 35, 1996, 2661 (see also in arXiv: gr-qc/0102054).
11. Crothers S. J. On the general solution to Einstein's vacuum field and it implications for relativistic degeneracy. *Progress in Physics*, 2005, v. 1, 68–73.
12. Crothers S. J. On the ramifications of the Schwarzschild spacetime metric. *Progress in Physics*, 2005, v. 1, 74–80.
13. Crothers S. J. On the geometry of the general solution for the vacuum field of the point-mass. *Progress in Physics*, 2005, v. 2, 3–14.
14. Crothers S. J. On the general solution to Einstein's vacuum field for the point-mass when $\lambda \neq 0$ and its consequences for relativistic cosmology. *Progress in Physics*, 2005, v. 3, 7–14.
15. Stavroulakis N. A statical smooth extension of Schwarzschild's metric. *Lettere al Nuovo Cimento*, 1974, v. 11, 8 (see also in www.geocities.com/theometria/Stavroulakis-3.pdf).
16. Stavroulakis N. On the principles of General Relativity and the $S\Theta(4)$-invariant metrics. *Proc. 3rd Panhellenic Congr. Geometry*, Athens, 1997, 169 (see also in www.geocities.com/theometria/Stavroulakis-2.pdf).
17. Stavroulakis N. On a paper by J. Smoller and B. Temple. *Annales de la Fondation Louis de Broglie*, 2002, v. 27, 3 (see also in www.geocities.com/theometria/Stavroulakis-1.pdf).
18. Stavroulakis N. Non-Euclidean geometry and gravitation *Progress in Physics*, 2006, v. 2, 68–75.
19. Schwarzschild K. On the gravitational field of a mass point according to Einstein's theory. *Sitzungsber. Preuss. Akad. Wiss., Phys. Math. Kl.*, 1916, 189 (www.geocities.com/theometria/schwarzschild.pdf).
20. Wal R. M. General Relativity. The University of Chicago Press, Chicago, 1984.
21. Loinger A. On black holes and gravitational waves. *La Goliardica Pavese*, Pavia, 2002, 22–25; arXiv: gr-qc/0006033.

Complexity Science for Simpletons

Craig Alan Feinstein

2712 Willow Glen Drive, Baltimore, Maryland 21209, USA

E-mail: cafeinst@msn.com

In this article, we shall describe some of the most interesting topics in the subject of Complexity Science for a general audience. Anyone with a solid foundation in high school mathematics (with some calculus) and an elementary understanding of computer programming will be able to follow this article. First, we shall explain the significance of the P versus NP problem and solve it. Next, we shall describe two other famous mathematics problems, the Collatz $3n+1$ Conjecture and the Riemann Hypothesis, and show how both Chaitin's incompleteness theorem and Wolfram's notion of "computational irreducibility" are important for understanding why no one has, as of yet, solved these two problems.

1 Challenge

Imagine that you have a collection of one billion lottery tickets scattered throughout your basement in no particular order. An official from the lottery announces the number of the winning lottery ticket. For a possible prize of one billion dollars, is it a good idea to search your basement until you find the winning ticket or until you come to the conclusion that you do not possess the winning ticket? Most people would think not — even if the winning lottery ticket were in your basement, performing such a search could take $10^9/(60 \times 60 \times 24 \times 365.25)$ years, over thirty work-years, assuming that it takes you at least one second to examine each lottery ticket. Now imagine that you have a collection of only one thousand lottery tickets in your basement. Is it a good idea to search your basement until you find the winning ticket or until you come to the conclusion that you do not possess the winning ticket? Most people would think so, since doing such would take at most a few hours.

From these scenarios, let us postulate a general rule that the maximum time that it may take for one person to search N unsorted objects for one specific object is directly proportional to N. This is clearly the case for physical objects, but what about abstract objects? For instance, let us suppose that a dating service is trying to help n single women and n single men to get married. Each woman gives the dating service a list of characteristics that she would like to see in her potential husband, for instance, handsome, caring, athletic, domesticated, etc. And each man gives the dating service a list of characteristics that he would like to see in his potential wife, for instance, beautiful, obedient, good cook, thrifty, etc. The dating service is faced with the task of arranging dates for each of its clients so as to satisfy everyone's preferences.

Now there are $n!$ (which is shorthand for $n \times (n-1) \times (n-2) \times \cdots \times 2 \times 1$) possible ways for the dating service to arrange dates for each of its clients, but only a fraction of such arrangements would satisfy all of its clients. If $n = 100$, it would take too long for the dating service's computer to evaluate all 100! possible arrangements until it finds an arrangement that would satisfy all of its clients. (100! is too large a number of possibilities for any modern computer to handle.) Is there an efficient way for the dating service's computer to find dates with compatible potential spouses for each of the dating service's clients so that everyone is happy, assuming that it is possible to do such? Yes, and here is how:

Matchmaker algorithm — Initialize the set $M = \emptyset$. Search for a list of compatible relationships between men and women that alternates between a compatible relationship $\{x_1, x_2\}$ not contained in set M, followed by a compatible relationship $\{x_2, x_3\}$ contained in set M, followed by a compatible relationship $\{x_3, x_4\}$ not contained in set M, followed by a compatible relationship $\{x_4, x_5\}$ contained in set M, and so on, ending with a compatible relationship $\{x_{m-1}, x_m\}$ not contained in set M, where both x_1 and x_m are not members of any compatible relationships contained in set M. Once such a list is found, for each compatible relationship $\{x_i, x_{i+1}\}$ in the list, add $\{x_i, x_{i+1}\}$ to M if $\{x_i, x_{i+1}\}$ is not contained in M or remove $\{x_i, x_{i+1}\}$ from M if $\{x_i, x_{i+1}\}$ is contained in M. (Note that this procedure must increase the size of set M by one.) Repeat this procedure until no such list exists.

Such an algorithm is guaranteed to **efficiently** find an arrangement M that will satisfy all of the dating service's clients whenever such an arrangement exists [30]. So we see that with regard to abstract objects, it is not necessarily the case that the maximum time that it may take for one to search N unsorted objects for a specific object is directly proportional to N; in the dating service example, there are $n!$ possible arrangements between men and women, yet it is not necessary for a computer to examine all $n!$ arrangements in order to find a satisfactory arrangement. One might think that the problem of finding a satisfactory dating arrangement is easy for a modern computer to solve because the list of pairs of men and women who are compatible is relatively small (of size at most n^2, which is much smaller than the number of possible arrangements $n!$) and because it is

easy to verify whether any particular arrangement will make everyone happy. But this reasoning is invalid, as we shall demonstrate.

2 The SUBSET-SUM problem

Consider the following problem: You are given a set $A = \{a_1, \ldots, a_n\}$ of n integers and another integer b which we shall call the *target integer*. You want to know if there exists a subset of A for which the sum of its elements is equal to b. (We shall consider the sum of the elements of the empty set to be zero.) This problem is called the *SUBSET-SUM problem* [10]. Now, there are 2^n subsets of A, so one could naïvely solve this problem by exhaustively comparing the sum of the elements of each subset of A to b until one finds a subset-sum equal to b, but such a procedure would be infeasible for even the fastest computers in the world to implement when $n = 100$. Is there an algorithm which can considerably reduce the amount of work for solving the SUBSET-SUM problem? Yes, there is an algorithm discovered by Horowitz and Sahni in 1974 [21], which we shall call the *Meet-in-the-Middle algorithm*, that takes on the order of $2^{n/2}$ steps to solve the SUBSET-SUM problem instead of the 2^n steps of the naïve exhaustive comparison algorithm:

Meet-in-the-Middle algorithm — First, partition the set A into two subsets, $A^+ = \{a_1, \ldots, a_{\lceil \frac{n}{2} \rceil}\}$ and $A^- = \{a_{\lceil \frac{n}{2} \rceil + 1}, \ldots, a_n\}$. Let us define S^+ and S^- as the sets of subset-sums of A^+ and A^-, respectively. Sort sets S^+ and $b - S^-$ in ascending order. Compare the first elements in both of the lists. If they match, then stop and output that there is a solution. If not, then compare the greater element with the next element in the other list. Continue this process until there is a match, in which case there is a solution, or until one of the lists runs out of elements, in which case there is no solution.

This algorithm takes on the order of $2^{n/2}$ steps, since it takes on the order of $2^{n/2}$ steps to sort sets S^+ and $b - S^-$ (assuming that the computer can sort in linear-time) and on the order of $2^{n/2}$ steps to compare elements from the sorted lists S^+ and $b - S^-$. Are there any faster algorithms for solving SUBSET-SUM? $2^{n/2}$ is still a very large number when $n = 100$, even though this strategy is a vast improvement over the naïve strategy. It turns out that no algorithm with a better worst-case running-time has ever been found since the Horowitz and Sahni paper [40]. And the reason for this is because it is impossible for such an algorithm to exist. Here is an explanation why:

Explanation: To understand why there is no algorithm with a faster worst-case running-time than the Meet-in-the-Middle algorithm, let us travel back in time seventy-five years, long before the internet. If one were to ask someone back then what a computer is, one would have gotten the answer, "a person who computes (usually a woman)" instead of the present day definition, "a machine that computes" [18]. Let us imagine that we knew two computers back then named Mabel and Mildred (two popular names for women in the 1930's [34]). Mabel is very efficient at sorting lists of integers into ascending order; for instance she can sort a set of ten integers in 15 seconds, whereas it takes Mildred 20 seconds to perform the same task. However, Mildred is very efficient at comparing two integers a and b to determine whether $a < b$ or $a = b$ or $a > b$; she can compare ten pairs of integers in 15 seconds, whereas it takes Mabel 20 seconds to perform the same task.

Let's say we were to give both Mabel and Mildred the task of determining whether there exists a subset of some four element set, $A = \{a_1, a_2, a_3, a_4\}$, for which the sum of its elements adds up to b. Since Mildred is good at comparing but not so good at sorting, Mildred chooses to solve this problem by comparing b to all of the sixteen subset-sums of A. Since Mabel is good at sorting but not so good at comparing, Mabel decides to solve this problem by using the Meet-in-the-Middle algorithm. In fact, of all algorithms that Mabel could have chosen to solve this problem, the Meet-in-the-Middle algorithm is the most efficient for her to use on sets A with only four integers. And of all algorithms that Mildred could have chosen to solve this problem, comparing b to all of the sixteen subset-sums of A is the most efficient algorithm for her to use on sets A with only four integers.

Now we are going to use the principle of mathematical induction to prove that the best algorithm for Mabel to use for solving the SUBSET-SUM problem for large n is the Meet-in-the-Middle algorithm: We already know that this is true when $n = 4$. Let us assume that this is true for n, i. e., that of all possible algorithms for Mabel to use for solving the SUBSET-SUM problem on sets with n integers, the Meet-in-the-Middle algorithm has the best worst-case running-time. Then we shall prove that this is also true for $n + 1$:

Let S be the set of all subset-sums of the set $A = \{a_1, a_2, \ldots, a_n\}$. Notice that the SUBSET-SUM problem on the set $A \cup \{a'\}$ of $n+1$ integers and target b is equivalent to the problem of determining whether (1) $b \in S$ or (2) $b' \in S$ (where $b' = b - a'$). (The symbol $\in$ means "is a member of".) Also notice that these two subproblems, (1) and (2), are independent from one another in the sense that the values of b and b' are unrelated to each other and are also unrelated to set S; therefore, in order to determine whether $b \in S$ or $b' \in S$, it is necessary to solve both subproblems (assuming that the first subproblem solved has no solution). So it is clear that if Mabel could solve both subproblems in the fastest time possible and also whenever possible make use of information obtained from solving subproblem (1) to save time solving subproblem (2) and whenever possible make use of information obtained from solving subproblem (2) to save time solving subproblem (1), then Mabel would be able to solve the problem of determining whether (1) $b \in S$ or (2) $b' \in S$ in the fastest time possible [15].

We shall now explain why the Meet-in-the-Middle algorithm has this characteristic for sets of size $n+1$: It is clear that by the induction hypothesis, the Meet-in-the-Middle algorithm solves each subproblem in the fastest time possible, since it works by applying the Meet-in-the-Middle algorithm to each subproblem, without loss of generality sorting and comparing elements in lists S^+ and $b-S^-$ and also sorting and comparing elements in lists S^+ and $b'-S^-$ as the algorithm sorts and compares elements in lists S^+ and $b-[S^- \cup (S^-+a')]$. There are two situations in which it is possible for the Meet-in-the-Middle algorithm to make use of information obtained from solving subproblem (1) to save time solving subproblem (2) or to make use of information obtained from solving subproblem (2) to save time solving subproblem (1). And the Meet-in-the-Middle algorithm takes advantage of both of these opportunities:

- Whenever the Meet-in-the-Middle algorithm compares two elements from lists S^+ and $b-S^-$ and the element in list S^+ turns out to be less than the element in list $b-S^-$, the algorithm makes use of information obtained from solving subproblem (1) (the fact that the element in list S^+ is less than the element in list $b-S^-$) to save time, when n is odd, solving subproblem (2) (the algorithm does not consider the element in list S^+ again).
- Whenever the Meet-in-the-Middle algorithm compares two elements from lists S^+ and $b'-S^-$ and the element in list S^+ turns out to be less than the element in list $b'-S^-$, the algorithm makes use of information obtained from solving subproblem (2) (the fact that the element in list S^+ is less than the element in list $b'-S^-$) to save time, when n is odd, solving subproblem (1) (the algorithm does not consider the element in list S^+ again).

Therefore, we can conclude that the Meet-in-the-Middle algorithm whenever possible makes use of information obtained from solving subproblem (1) to save time solving subproblem (2) and whenever possible makes use of information obtained from solving subproblem (2) to save time solving subproblem (1). So we have completed our induction step to prove true for $n+1$, assuming true for n.

Therefore, the best algorithm for Mabel to use for solving the SUBSET-SUM problem for large n is the Meet-in-the-Middle algorithm. But is the Meet-in-the-Middle algorithm the best algorithm for Mildred to use for solving the SUBSET-SUM problem for large n? Since the Meet-in-the-Middle algorithm is not the fastest algorithm for Mildred to use for small n, is it not possible that the Meet-in-the-Middle algorithm is also not the fastest algorithm for Mildred to use for large n? It turns out that for large n, there is no algorithm for Mildred to use for solving the SUBSET-SUM problem with a faster worst-case running-time than the Meet-in-the-Middle algorithm. Why?

Notice that the Meet-in-the-Middle algorithm takes on the order of $2^{n/2}$ steps regardless of whether Mabel or Mildred applies it. And notice that the algorithm of naïvely comparing the target b to all of the 2^n subset-sums of set A takes on the order of 2^n steps regardless of whether Mabel or Mildred applies it. So for large n, regardless of who the computer is, the Meet-in-the-Middle algorithm is faster than the naïve exhaustive comparison algorithm — from this example, we can understand the general principle that the asymptotic running-time of an algorithm does not differ by more than a polynomial factor when run on different types of computers [40, 41]. Therefore, since no algorithm is faster than the Meet-in-the-Middle algorithm for solving SUBSET-SUM for large n when applied by Mabel, we can conclude that no algorithm is faster than the Meet-in-the-Middle algorithm for solving SUBSET-SUM for large n when applied by Mildred. And furthermore, using this same reasoning, we can conclude that no algorithm is faster than the Meet-in-the-Middle algorithm for solving SUBSET-SUM for large n when run on a modern computing machine. □

So it doesn't matter whether the computer is Mabel, Mildred, or any modern computing machine; the fastest algorithm which solves the SUBSET-SUM problem for large n is the Meet-in-the-Middle algorithm. Because once a solution to the SUBSET-SUM problem is found, it is easy to verify (in polynomial-time) that it is indeed a solution, we say that the SUBSET-SUM problem is in class NP [5]. And because there is no algorithm which solves SUBSET-SUM that runs in polynomial-time (since the Meet-in-the-Middle algorithm runs in exponential-time and is the fastest algorithm for solving SUBSET-SUM, as we have shown above), we say that the SUBSET-SUM problem is not in class P [5]. Then since the SUBSET-SUM problem is in class NP but not in class P, we can conclude that $P \neq NP$, thus solving the P versus NP problem [15]. The solution to the P versus NP problem demonstrates that it is possible to hide abstract objects (in this case, a subset of set A) without an abundance of resources — it is, in general, more difficult to find a subset of a set of only one hundred integers for which the sum of its elements equals a target integer than to find the winning lottery-ticket in a pile of one billion unsorted lottery tickets, even though the lottery-ticket problem requires much more resources (one billion lottery tickets) than the SUBSET-SUM problem requires (a list of one hundred integers).

3 Does $P \neq NP$ really matter?

Even though $P \neq NP$, might there still be algorithms which efficiently solve problems that are in NP but not P in the average-case scenario? (Since the $P \neq NP$ result deals only with the worst-case scenario, there is nothing to forbid this from happening.) The answer is yes; for many problems which are in NP but not P, there exist algorithms which efficiently solve them in the average-case scenario [28, 39],

so the statement that $P \neq NP$ is not as ominous as it sounds. In fact, there is a very clever algorithm which solves almost all instances of the SUBSET-SUM problem in polynomial-time [11, 26, 28]. (The algorithm works by converting the SUBSET-SUM problem into the problem of finding the shortest non-zero vector of a lattice, given its basis.) But even though for many problems which are in NP but not P, there exist algorithms which efficiently solve them in the average-case scenario, in the opinion of most complexity-theorists, it is probably false that for all problems which are in NP but not P, there exist algorithms which efficiently solve them in the average-case scenario [3].

Even though $P \neq NP$, might it still be possible that there exist polynomial-time *randomized* algorithms which correctly solve problems in NP but not in P with a high probability regardless of the problem instance? (The word "randomized" in this context means that the algorithm bases some of its decisions upon random variables. The advantage of these types of algorithms is that whenever they fail to output a solution, there is still a good chance that they will succeed if they are run again.) The answer is probably no, as there is a widely believed conjecture that $P = BPP$, where BPP is the class of decision problems for which there are polynomial-time randomized algorithms that correctly solve them at least two-thirds of the time regardless of the problem instance [22].

4 Are quantum computers the answer?

A *quantum computer* is any computing device which makes direct use of distinctively quantum mechanical phenomena, such as superposition and entanglement, to perform operations on data. As of today, the field of practical quantum computing is still in its infancy; however, much is known about the theoretical properties of a quantum computer. For instance, quantum computers have been shown to efficiently solve certain types of problems, like factoring integers [35], which are believed to be difficult to solve on a *classical computer*, e. g., a human-computer like Mabel or Mildred or a machine-computer like an IBM PC or an Apple Macintosh.

Is it possible that one day quantum computers will be built and will solve problems like the SUBSET-SUM problem efficiently in polynomial-time? The answer is that it is generally suspected by complexity theorists to be impossible for a quantum computer to solve the SUBSET-SUM problem (and all other problems which share a characteristic with the SUBSET-SUM problem in that they belong to a subclass of NP problems known as *NP-complete* problems [5]) in polynomial-time. A curious fact is that if one were to solve the SUBSET-SUM problem on a quantum computer by brute force, the algorithm would have a running-time on the order of $2^{n/2}$ steps, which (by coincidence?) is the same asymptotic running-time of the fastest algorithm which solves SUBSET-SUM on a classical computer, the Meet-in-the-Middle algorithm [1, 4, 19].

In any case, no one has ever built a practical quantum computer and some scientists are even of the opinion that building such a computer is impossible; the acclaimed complexity theorist, Leonid Levin, wrote: "QC of the sort that factors long numbers seems firmly rooted in science fiction. It is a pity that popular accounts do not distinguish it from much more believable ideas, like Quantum Cryptography, Quantum Communications, and the sort of Quantum Computing that deals primarily with locality restrictions, such as fast search of long arrays. It is worth noting that the reasons why QC must fail are by no means clear; they merit thorough investigation. The answer may bring much greater benefits to the understanding of basic physical concepts than any factoring device could ever promise. The present attitude is analogous to, say, Maxwell selling the Daemon of his famous thought experiment as a path to cheaper electricity from heat. If he did, much of insights of today's thermodynamics might be lost or delayed" [25].

5 Unprovable conjectures

In the early twentieth century, the famous mathematician, David Hilbert, proposed the idea that all mathematical facts can be derived from only a handful of self-evident axioms. In the 1930's, Kurt Gödel proved that such a scenario is impossible by showing that for any proposed finite axiom system for arithmetic, there must always exist true statements that are unprovable within the system, if one is to assume that the axiom system has no inconsistencies. Alan Turing extended this result to show that it is impossible to design a computer program which can determine whether any other computer program will eventually halt. In the latter half of the 20th century, Gregory Chaitin defined a real number between zero and one, which he calls Ω, to be the probability that a computer program halts. And Chaitin proved that:

Theorem 1: For any mathematics problem, the bits of Ω, when Ω is expressed in binary, completely determine whether that problem is solvable or not.

Theorem 2: The bits of Ω are random and only a finite number of them are even possible to know.

From these two theorems, it follows that the very structure of mathematics itself is random and mostly unknowable! [8]

Even though Hilbert's dream to be able derive every mathematical fact from only a handful of self-evident axioms was destroyed by Gödel in the 1930's, this idea has still had an enormous impact on current mathematics research [43]. In fact, even though mathematicians as of today accept the incompleteness theorems proven by Gödel, Turing, and Chaitin as true, in general these same mathematicians also believe that these incompleteness theorems ultimately have no impact on traditional mathematics research, and they have thus adopted Hilbert's paradigm of deriving mathematical

facts from only a handful of self-evident axioms as a practical way of researching mathematics. Gregory Chaitin has been warning these mathematicians for decades now that these incompleteness theorems are actually very relevant to advanced mathematics research, but the overwhelming majority of mathematicians have not taken his warnings seriously [7]. We shall directly confirm Chaitin's assertion that incompleteness is indeed very relevant to advanced mathematics research by giving very strong evidence that two famous mathematics problems, determining whether the Collatz $3n+1$ Conjecture is true and determining whether the Riemann Hypothesis is true, are impossible to solve:

The Collatz $3n+1$ Conjecture — Here's a fun experiment that you, the reader, can try: Pick any positive integer, n. If n is even, then compute $n/2$ or if n is odd, then compute $(3n+1)/2$. Then let n equal the result of this computation and perform the whole procedure again until $n=1$. For instance, if you had chosen $n=11$, you would have obtained the sequence $(3\times11+1)/2=17$, $(3\times17+1)/2=26$, $26/2=13, 20, 10, 5, 8, 4, 2, 1$.

The Collatz $3n+1$ Conjecture states that such an algorithm will always eventually reach $n=1$ and halt [23]. Computers have verified this conjecture to be true for all positive integers less than $224\times2^{50}\approx2.52\times10^{17}$ [33]. Why does this happen? One can give an informal argument as to why this may happen [12] as follows: Let us assume that at each step, the probability that n is even is one-half and the probability that n is odd is one-half. Then at each iteration, n will decrease by a multiplicative factor of about $\left(\frac{3}{2}\right)^{1/2}\left(\frac{1}{2}\right)^{1/2}=$ $=\left(\frac{3}{4}\right)^{1/2}$ on average, which is less than one; therefore, n will eventually converge to one with probability one. But such an argument is **not** a rigorous mathematical proof, since the probability assumptions that the argument is based upon are not well-defined and even if they were well-defined, it would still be possible (although extremely unlikely, with probability zero) that the algorithm will never halt for some input.

Is there a rigorous mathematical proof of the Collatz $3n+1$ Conjecture? As of today, no one has found a rigorous proof that the conjecture is true and no one has found a rigorous proof that the conjecture is false. In fact, Paul Erdös, who was one of the greatest mathematicians of the twentieth century, commented about the Collatz $3n+1$ Conjecture: "Mathematics is not yet ready for such problems" [23]. We can informally demonstrate that there is no way to deductively prove that the conjecture is true, as follows:

Explanation: First, notice that in order to be certain that the algorithm will halt for a given input n, it is necessary to know whether the value of n at the beginning of each iteration of the algorithm is even or odd. (For a rigorous proof of this, see *The Collatz Conjecture is Unprovable* [16].) For instance, if the algorithm starts with input $n=11$, then in order to know that the algorithm halts at one, it is necessary to know that 11 is odd, $(3\times11+1)/2=17$ is odd, $(3\times17+1)/2=26$ is even, $26/2=13$ is odd, 20 is even, 10 is even, 5 is odd, 8 is even, 4 is even, and 2 is even. We can express this information (odd, odd, even, odd, even, even, odd, even, even, even) as a vector of zeroes and ones, $(1,1,0,1,0,0,1,0,0,0)$. Let us call this vector the *parity vector* of n. (If n never converges to one, then its parity vector must be infinite-dimensional.) If one does not know the parity vector of the input, then it is impossible to know what the algorithm does at each iteration and therefore impossible to be certain that the algorithm will converge to one. So any proof that the algorithm applied to n halts must specify the parity vector of n. Next, let us give a definition of a *random vector*:

Definition — We shall say that a vector $\mathbf{x}\in\{0,1\}^m$ is *random* if $\mathbf{x}$ cannot be specified in less than m bits in a computer text-file [6].

Example 1 — The vector of one million concatenations of the vector $(0,1)$ is **not** random, since we can specify it in less than two million bits in a computer text-file. (We just did.)

Example 2 — The vector of outcomes of one million coin-tosses has a good chance of fitting our definition of "random", since much of the time the most compact way of specifying such a vector is to simply make a list of the results of each coin-toss, in which one million bits are necessary.

Now let us suppose that it were possible to prove the Collatz $3n+1$ Conjecture and let B be the number of bits in a hypothetical computer text-file containing such a proof. And let $(x_0,x_1,x_2,\ldots,x_B)$ be a random vector, as defined above. (It is not difficult to prove that at least half of all vectors with $B+1$ zeroes and ones are random [6].) There is a mathematical theorem [23] which says that there must exist a number n with the first $B+1$ bits of its parity vector equal to $(x_0,x_1,x_2,\ldots,x_B)$; therefore, any proof of the Collatz $3n+1$ Conjecture must specify vector $(x_0,x_1,x_2,\ldots,x_B)$ (as we discussed above), since such a proof must show that the Collatz algorithm halts when given input n. But since vector $(x_0,x_1,x_2,\ldots,x_B)$ is random, $B+1$ bits are required to specify vector $(x_0,x_1,x_2,\ldots,x_B)$, contradicting our assumption that B is the number of bits in a computer text-file containing a proof of the Collatz $3n+1$ Conjecture; therefore, a formal proof of the Collatz $3n+1$ Conjecture cannot exist [16]. □

The Riemann Hypothesis — There is also another famous unresolved conjecture, the Riemann Hypothesis, which has a characteristic similar to that of the Collatz $3n+1$ Conjecture, in that it too can never be proven true. In the opinion of many mathematicians, the Riemann Hypothesis is the most important unsolved problem in mathematics [13]. The reason why it is so important is because a resolution of the Riemann Hypothesis would shed much light on the distribution of prime numbers: It is well known that the number of prime numbers less than n is approximately $\int_2^n\frac{dx}{\log x}$. If the Riemann Hypothesis is true, then for large n, the error in this approxi-

mation must be bounded by $cn^{1/2}\log n$ for some constant $c>0$ [38], which is also a bound for a *random walk*, i. e., the sum of n independent random variables, X_k, for $k=1,2,\ldots,n$ in which the probability that $X_k=-c$ is one-half and the probability that $X_k=c$ is one-half.

The Riemann-Zeta function $\zeta(s)$ is a complex function which is defined to be $\zeta(s)=\frac{s}{s-1}-s\int_1^\infty\frac{x-\lfloor x\rfloor}{x^{s+1}}dx$ when the real part of the complex number s is positive. The Riemann Hypothesis states that if $\rho=\sigma+ti$ is a complex root of ζ and $0<\sigma<1$, then $\sigma=1/2$. It is well known that there are infinitely many roots of ζ that have $0<\sigma<1$. And just like the Collatz $3n+1$ Conjecture, the Riemann Hypothesis has been verified by high-speed computers — for all $|t|<T$ where $T\approx 2.0\times 10^{20}$ [29]. But it is still unknown whether there exists a $|t|\geqslant T$ such that $\zeta(\sigma+ti)=0$, where $\sigma\neq 1/2$. And just like the Collatz $3n+1$ Conjecture, one can give a heuristic probabilistic argument that the Riemann Hypothesis is true [17], as follows:

It is well known that the Riemann Hypothesis follows from the assertion that for large n, $M(n)=\Sigma_{k=1}^{n}\mu(k)$ is bounded by $cn^{1/2}\log n$ for some constant $c>0$, where μ is the Möbius Inversion function defined on $\mathbb{N}$ in which $\mu(k)=-1$ if k is the product of an odd number of distinct primes, $\mu(k)=1$ if k is the product of an even number of distinct primes, and $\mu(k)=0$ otherwise. If we were to assume that $M(n)$ is distributed as a random walk, which is certainly plausible since there is no apparent reason why it should not be distributed as a random walk, then by probability theory, $M(n)$ is bounded for large n by $cn^{1/2}\log n$ for some constant $c>0$, with probability one; therefore, it is very likely that the Riemann Hypothesis is true. We shall now explain why the Riemann Hypothesis is unprovable, just like the Collatz $3n+1$ Conjecture:

Explanation: The Riemann Hypothesis is equivalent to the assertion that for each $T>0$, the number of real roots t of $\zeta(1/2+ti)$, where $0<t<T$, is equal to the number of roots of $\zeta(s)$ in $\{s=\sigma+ti\colon 0<\sigma<1,\ 0<t<T\}$. It is well known that there exists a continuous **real** function $Z(t)$ (called the Riemann-Siegel function) such that $|Z(t)|=|\zeta(1/2+ti)|$, so the real roots t of $\zeta(1/2+ti)$ are the same as the real roots t of $Z(t)$. (The formula for $Z(t)$ is $\zeta(1/2+ti)e^{i\vartheta(t)}$, where $\vartheta(t)=\arg\left[\Gamma(\frac{1}{4}+\frac{1}{2}it)\right]-\frac{1}{2}t\ln\pi$.) Then because the formula for the real roots t of $\zeta(1/2+ti)$ cannot be reduced to a formula that is simpler than the equation, $\zeta(1/2+ti)=0$, the only way to determine the number of real roots t of $\zeta(1/2+ti)$ in which $0<t<T$ is to count the changes in sign of the real function $Z(t)$, where $0<t<T$ [31].

So in order to prove that the number of real roots t of $\zeta(1/2+ti)$, where $0<t<T$, is equal to the number of roots of $\zeta(s)$ in $\{s=\sigma+ti:\ 0<\sigma<1,\ 0<t<T\}$, which can be computed via a theorem known as the *Argument Principle* **without** counting the changes in sign of $Z(t)$, where $0<t<T$ [27, 31, 32], it is necessary to count the changes in sign of $Z(t)$, where $0<t<T$. (Otherwise, it would be possible to determine the number of real roots t of $\zeta(1/2+ti)$, where $0<t<T$, without counting the changes in sign of $Z(t)$ by computing the number of roots of $\zeta(s)$ in $\{s=\sigma+ti\colon 0<\sigma<1,\ 0<t<T\}$ via the Argument Principle.) As T becomes arbitrarily large, the time that it takes to count the changes in sign of $Z(t)$, where $0<t<T$, approaches infinity for the following reasons: (1) There are infinitely many changes in sign of $Z(t)$. (2) The time that it takes to evaluate the sign of $Z(t)$ approaches infinity as $t\to\infty$ [31]. Hence, an infinite amount of time is required to prove that for each $T>0$, the number of real roots t of $\zeta(1/2+ti)$, where $0<t<T$, is equal to the number of roots of $\zeta(s)$ in $\{s=\sigma+ti:\ 0<\sigma<1,\ 0<t<T\}$ (which is equivalent to proving the Riemann Hypothesis), so the Riemann Hypothesis is unprovable. □

Chaitin's incompleteness theorem implies that mathematics is filled with facts which are both true and unprovable, since it states that the bits of Ω completely determine whether any given mathematics problem is solvable and only a finite number of bits of Ω are even knowable [8]. And we have shown that there is a very good chance that both the Collatz $3n+1$ Conjecture and the Riemann Hypothesis are examples of such facts. Of course, we can never formally prove that either one of these conjectures is both true and unprovable, for obvious reasons. The best we can do is prove that they are unprovable and provide computational evidence and heuristic probabilistic reasoning to explain why these two conjectures are most likely true, as we have done. And of course, it is conceivable that one could find a counter-example to the Collatz $3n+1$ Conjecture by finding a number n for which the Collatz algorithm gets stuck in a nontrivial cycle or a counter-example to the Riemann Hypothesis by finding a complex root, $\rho=\sigma+ti$, of ζ for which $0<\sigma<1$ and $\sigma\neq 1/2$. But so far, no one has presented any such counter-examples.

The theorems that the Collatz $3n+1$ Conjecture and the Riemann Hypothesis are unprovable illustrate a point which Chaitin has been making for years, that mathematics is not so much different from empirical sciences like physics [8, 14]. For instance, scientists universally accept the law of gravity to be true based on experimental evidence, but such a law is by no means absolutely certain — even though the law of gravity has been observed to hold in the past, it is not inconceivable that the law of gravity may cease to hold in the future. So too, in mathematics there are conjectures like the Collatz $3n+1$ Conjecture and the Riemann Hypothesis which are strongly supported by experimental evidence but can never be proven true with absolute certainty.

6 Computational irreducibility

Up until the last decade of the twentieth century, the most famous unsolved problem in all of mathematics was to prove

the following conjecture:

Fermat's Last Theorem (FLT) — When $n > 2$, the equation $x^n + y^n = z^n$ has no nontrivial integer solutions.

After reading the explanations in the previous section, a skeptic asked the author what the difference is between the previous argument that the Collatz $3n+1$ Conjecture is unprovable and the following argument that Fermat's Last Theorem is unprovable (which cannot possibly be valid, since Fermat's Last Theorem was proven by Wiles and Taylor in the last decade of the twentieth century [37]):

Invalid Proof that FLT is unprovable: Suppose that we have a computer program which computes $x^n + y^n - z^n$ for each $x, y, z \in \mathbb{Z}$ and $n > 2$ until it finds a nontrivial (x, y, z, n) such that $x^n + y^n - z^n = 0$ and then halts. Obviously, Fermat's Last Theorem is equivalent to the assertion that such a computer program can never halt. In order to be certain that such a computer program will never halt, it is necessary to compute $x^n + y^n - z^n$ for each $x, y, z \in \mathbb{Z}$ and $n > 2$ to determine that $x^n + y^n - z^n \neq 0$ for each nontrivial (x, y, z, n). Since this would take an infinite amount of time, Fermat's Last Theorem is unprovable. □

This proof is invalid, because the assertion that "it is necessary to compute $x^n + y^n - z^n$ for each $x, y, z \in \mathbb{Z}$ and $n > 2$ to determine that $x^n + y^n - z^n \neq 0$ for each nontrivial (x, y, z, n)" is false. In order to determine that an equation is false, it is not necessary to compute both sides of the equation — for instance, it is possible to know that the equation $6x + 9y = 74$ has no integer solutions without evaluating $6x + 9y$ for every $x, y \in \mathbb{Z}$, since one can see that if there were any integer solutions, the left-hand-side of the equation would be divisible by three but the right-hand-side would not be divisible by three.

Question — So why can't we apply this same reasoning to show that the proof that the Collatz $3n + 1$ Conjecture is unprovable is invalid? Just as it is not necessary to compute $x^n + y^n - z^n$ in order to determine that $x^n + y^n - z^n \neq 0$, is it not possible that one can determine that the Collatz algorithm will converge to one without knowing what the algorithm does at each iteration?

Answer — Because what the Collatz algorithm does at each iteration **is** what determines whether or not the Collatz sequence converges to one [16], it is necessary to know what the Collatz algorithm does at each iteration in order to determine that the Collatz sequence converges to one. Because the exact values of $x^n + y^n - z^n$ are **not** relevant to knowing that $x^n + y^n - z^n \neq 0$ for each nontrivial (x, y, z, n), it is not necessary to compute each $x^n + y^n - z^n$ in order to determine that $x^n + y^n - z^n \neq 0$ for each nontrivial (x, y, z, n).

Exercise — You are given a deck of n cards labeled $1, 2, 3, \ldots, n$. You shuffle the deck. Then you perform the following "reverse-card-shuffling" procedure: Look at the top card labeled k. If $k = 1$, then stop. Otherwise, reverse the order of the first k cards in the deck. Then look at the top card again and repeat the same procedure. For example, if $n = 7$ and the deck were in order 5732416 (where 5 is the top card), then you would obtain $4237516 \to 7324516 \to 6154237 \to \to 3245167 \to 4235167 \to 5324167 \to 1423567$. Now, we present two problems:

- Prove that such a procedure will always halt for any n and any shuffling of the n cards.
- Find a closed formula for the maximum number of iterations that it may take for such a procedure to halt given the number of cards in the deck, or prove that no such formula exists. (The maximum number of iterations for $n = 1, 2, 3, \ldots, 16$ are $0, 1, 2, 4, 7, 10, 16, 22, 30, 38, 51, 65, 80, 101, 113, 139$ [36].)

It is easy to use the principle of mathematical induction to solve the first problem. As for the second problem, it turns out that there is no closed formula; in other words, in order to find the maximum number of iterations that it may take for such a procedure to halt given the number of cards n in the deck, it is necessary to perform the reverse-card-shuffling procedure on every possible permutation of $1, 2, 3, \ldots, n$. This property of the Reverse-Card-Shuffling Problem in which there is no way to determine the outcome of the reverse-card-shuffling procedure without actually performing the procedure itself is called *computational irreducibility* [42]. Notice that the notion of computational irreducibility also applies to the Collatz $3n+1$ Conjecture and the Riemann Hypothesis in that an infinite number of irreducible computations are necessary to prove these two conjectures.

Stephen Wolfram, who coined the phrase "computational irreducibility", argues in his famous book, *A New Kind of Science* [42], that our universe is computationally irreducible, i.e., the universe is so complex that there is no general method for determining the outcome of a natural event without either observing the event itself or simulating the event on a computer. The dream of science is to be able to make accurate predictions about our natural world; in a computationally irreducible universe, such a dream is only possible for very simple phenomena or for events which can be accurately simulated on a computer.

7 Open problems in mathematics

In the present year of 2006, the most famous unsolved number theory problem is to prove the following:

Goldbach's Conjecture — Every even number greater than two is the sum of two prime numbers.

Just like the Collatz $3n + 1$ Conjecture and the Riemann Hypothesis, there are heuristic probabilistic arguments which support Goldbach's Conjecture, and Goldbach's Conjecture has been verified by computers for a large number of even numbers [20]. The closest anyone has come to proving Goldbach's Conjecture is a proof of the following:

Chen's Theorem — Every sufficiently large even integer is either the sum of two prime numbers or the sum of a prime number and the product of two prime numbers [9].

Although the author cannot prove it, he believes the following:

Conjecture 1 — Goldbach's Conjecture is unprovable.

Another famous conjecture which is usually mentioned along with Goldbach's Conjecture in mathematics literature is the following:

The Twin Primes Conjecture — There are infinitely many prime numbers p for which $p + 2$ is also prime [20].

Just as with Goldbach's Conjecture, the author cannot prove it, but he believes the following:

Conjecture 2 — The Twin Primes Conjecture is undecidable, i. e., it is impossible to know whether the Twin Primes Conjecture is true or false.

8 Conclusion

The $P \neq NP$ problem, the Collatz $3n+1$ Conjecture, and the Riemann Hypothesis demonstrate to us that as finite human beings, we are all severely limited in our ability to solve abstract problems and to understand our universe. The author hopes that this observation will help us all to better appreciate the fact that there are still so many things which G-d allows us to understand.

Acknowledgements

I thank G-d, my parents, my wife, and my children for their support.

References

1. Aaronson S. NP-complete problems and physical reality. *SIGACT News*, *Complexity Theory Column*, March 2005.
2. Belaga E. Reflecting on the $3x + 1$ mystery: Outline of a scenario. Univ. Strasbourg preprint, 10 pages, 1998.
3. Ben-David S., Chor B., Goldreich O., and Luby M. *Journal of Computer and System Sciences*, 1992, v. 44, No. 2, 193–219.
4. Bennett C., Bernstein E., Brassard G., and Vazirani U. *SIAM J. Comput.*, 1997, v. 26(5), 1510–1523.
5. Bovet P. B. and Crescenzi P. Introduction to the theory of complexity. Prentice Hall, 1994.
6. Chaitin G. J. Algorithmic information theory. Rev. 3rd ed., Cambridge University Press, 1990.
7. Chaitin G. J. arXiv: math/0306042.
8. Chaitin G. J. Meta Math! Pantheon, October 2005.
9. Chen J. R. *Kexue Tongbao*, 1966, v. 17, 385–386.
10. Cormen T. H., Leiserson C. E., and Rivest R. L., Introduction to algorithms. McGraw-Hill, 1990.
11. Coster M. J., Joux A., LaMacchia B. A., Odlyzko A. M., Schnorr C. P., and Stern J. *Computational Complexity*, 1992, No. 2, 111–128.
12. Crandall R. E. *Math. Comp.*, 1978, v. 32, 1281–1292.
13. Derbyshire J. Prime obsession. Joseph Henry Press, 2003.
14. Dombrowski K. *Progress in Physics*, 2005, v. 1, 65–67.
15. Feinstein C. A. arXiv: cs/0310060.
16. Feinstein C. A. arXiv: math/0312309.
17. Good I. J. and Churchhouse R. F. *Math. Comp.*, 1968, v. 22, 857–861.
18. Grier D. A. When computers were human. Princeton University Press, 2005.
19. Grover L. K. *Proc. 28th Annual ACM Symp. on the Theory of Computing*, May 1996, 212–219.
20. Guy R. K. Unsolved problems in number theory. 3rd ed., New York, Springer-Verlag, 2004.
21. Horowitz E. and Sahni S. *Journal of the ACM*, 1974, v. 2l, No. 2, 277–292.
22. Impagliazzo R. and Wigderson A. *Proc. of the Twenty-Ninth Annual ACM Symp. on Theory of Computing*, 1997, 220–229.
23. Lagarias J. C. *Amer. Math. Monthly*, 1985, v. 92, 3–23. Repr. in: *Conf. on Organic Math.*, Canad. Math. Soc. Conf. Proc., v. 20, 1997, 305–331; http://www.cecm.sfu.ca/organics/papers.
24. Lagarias J. C. arXiv: math/0309224.
25. Levin L. A. *Probl. Inform. Transmis.*, 2003, v. 39(1), 92–103.
26. Menezes A., van Oorschot P., and Vanstone S. Handbook of applied cryptography. CRC Press, 1996.
27. Odlyzko A. M. *Math. of Computation 1943-1993*, W. Gautschi (ed.), AMS, Proc. Symp. Appl. Math., v. 48, 1994, 451–463.
28. Odlyzko A. M. *Cryptol. and Comput. Num. Theory*, C. Pomerance (ed.), AMS, Proc. Symp. Appl. Math., 1990, v. 42, 75–88.
29. Odlyzko A.M. *Supercomputing'89, Conf. Proc.*, L.P. Kartashev and S.I. Kartashev (eds.), Int. Supercomp. Inst., 1989, 348–352.
30. Papadimitriou C. H. and Steiglitz K. Combinatorial optimization: Algorithms and complexity. Prentice-Hall, Englewood Cliffs, NJ, 1982.
31. Pugh G. R. Master's thesis, Univ. of British Columbia, 1998.
32. Rao M. and Stetkaer H. Complex analysis. World Sci., 1991.
33. Roosendaal E. http://personal.computrain.nl/eric/wondrous/.
34. Shackleford M. W. *Actuarial Note 139*, Social Security Admin., May 1998; http://www.ssa.gov/OACT/babynames/.
35. Shor P. *Proc. 35th Ann. Symp. on Found. of Computer Sci., Santa Fe, NM, USA, 1994*, IEEE Comp. Soc. Press, 124–134.
36. Sloane N.J.A. *Online Enc. of Integer Seq.*, No. A000375, 2005.
37. Weisstein E. W. Fermat's last theorem. *Concise Enc. of Math.*, 2nd ed., CRC Press, Boca Raton (FL), 2003, 1024–1027.
38. Weisstein E. W. Riemann Hypothesis. *Ibid.*, 2550–2551.
39. Wilf H. S. *Inform. Proc. Lett.*, 1984, v. 18, 119–122.
40. Woeginger G. J. *Lecture Notes in Computer Sci.*, Springer-Verlag Heidelberg, 2003, v. 2570, 185–207.
41. Wolfram S. *Phys. Rev. Lett.*, 1985, v. 54, 735–738.
42. Wolfram S. A new kind of science. Wolfram Media, Champaign, IL, 2002.
43. Zach R. arXiv: math/0508572.

Steady Particle States of Revised Electromagnetics

Bo Lehnert

Alfvén Laboratory, Royal Institute of Technology, S-10044, Stockholm, Sweden

E-mail: Bo.Lehnert@ee.kth.se

A revised Lorentz invariant electromagnetic theory leading beyond Maxwell's equations, and to a form of extended quantum electrodynamics, has been elaborated on the basis of a nonzero electric charge density and a nonzero electric field divergence in the vacuum state. Among the applications of this theory, there are steady electromagnetic states having no counterpart in conventional theory and resulting in models of electrically charged and neutral leptons, such as the electron and the neutrino. The analysis of the electron model debouches into a point-charge-like geometry with a very small characteristic radius but having finite self-energy. This provides an alternative to the conventional renormalization procedure. In contrast to conventional theory, an integrated radial force balance can further be established in which the electron is prevented from "exploding" under the action of its net self-charge. Through a combination of variational analysis and an investigation of the radial force balance, a value of the electronic charge has been deduced which deviates by only one percent from that obtained in experiments. This deviation requires further investigation. A model of the neutrino finally reproduces some of the basic features, such as a small but nonzero rest mass, an angular momentum but no magnetic moment, and long mean free paths in solid matter.

1 Introduction

Maxwell's equations in a vacuum state with a vanishing electric field divergence have served as a basis for quantum electrodynamics (QED) in its conventional form [1]. This theory has been very successful in many applications, but as stated by Feynman [2], there still exist areas within which it does not provide fully adequate descriptions of physical reality. When applying conventional theory to attempted models of the electron, there thus appear a number of incomprehensible and unwieldy problems. These include the existence of a steady particle state, the unexplained point-charge-like geometry, the question of infinite self-energy and the associated physical concept of renormalization with extra added counter terms [3], the lack of radial force balance of the electron under the action of its self-charge [4], and its unexplained quantized charge. Also the models of an electrically neutral state of the neutrino include a number of questions, such as those of a nonzero but small rest mass, a nonzero angular momentum and a vanishing magnetic moment, and excessively long mean free paths for interaction with solid matter.

The limitations of conventional theory have caused a number of authors to elaborate modified electromagnetic approaches aiming beyond Maxwell's equations. Among these there is a theory [5–12] to be described in this paper. It is based on a vacuum state that can give rise to local space charges and an associated nonzero electric field divergence, leading to a current in addition to the displacement current. The field equations are then changed in a substantial manner, to result in a form of extended quantum electrodynamics ("EQED").

In applications of the present theory to photon physics, the nonzero electric field divergence appears as a small quantity, but it still comes out to have an essential effect on the end results [11, 12]. For the steady particle states to be treated here, the field equations contain electric field divergence terms which appear as large contributions already at the outset.

2 Basic field equations

The basic physical concept of the present theory is the appearance of a local electric charge density in the vacuum state in which there are quantum mechanical electromagnetic fluctuations. This charge density is associated with a nonzero electric field divergence. When imposing the condition of Lorentz invariance on the system, there arises a local "space-charge current density" in addition to the displacement current. The detailed deductions are described in earlier reports by the author [5–12]. The revised field equations *in the vacuum* are given by

$$\operatorname{curl}\mathbf{B}/\mu_0 = \varepsilon_0(\operatorname{div}\mathbf{E})\,\mathbf{C} + \varepsilon_0\partial\mathbf{E}/\partial t\,, \tag{1}$$

$$\operatorname{curl}\mathbf{E} = -\partial\mathbf{B}/\partial t\,, \tag{2}$$

$$\mathbf{B} = \operatorname{curl}\mathbf{A}\,, \qquad \operatorname{div}\mathbf{B} = 0\,, \tag{3}$$

$$\mathbf{E} = -\nabla\phi - \partial\mathbf{A}/\partial t\,, \qquad \operatorname{div}\mathbf{E} = \bar{\rho}/\varepsilon_0 \tag{4}$$

for the electric and magnetic fields $\mathbf{E}$ and $\mathbf{B}$, the electric

charge density $\bar{\rho}$, the magnetic vector potential $\mathbf{A}$, the electrostatic potential ϕ, and the velocity vector $\mathbf{C}$, where $\mathbf{C}^2 = c^2$. In analogy with the direction to be specified for the current density in conventional theory, the unit vector $\mathbf{C}/c$ depends on the geometry of the particular configuration to be studied.

Using well-known vector identities, equations (1) and (2) can be recast into the local momentum equation

$$\operatorname{div} {}^2\mathbf{S} = \bar{\rho}\,(\mathbf{E} + \mathbf{C} \times \mathbf{B}) + \varepsilon_0 \frac{\partial}{\partial t}\,\mathbf{g} \tag{5}$$

and the local energy equation

$$-\operatorname{div} \mathbf{S} = \bar{\rho}\,\mathbf{E} \cdot \mathbf{C} + \frac{1}{2}\,\varepsilon_0 \frac{\partial}{\partial t}\,w_f\,. \tag{6}$$

Here ${}^2\mathbf{S}$ is the electromagnetic stress tensor,

$$\mathbf{g} = \varepsilon_0\,\mathbf{E} \times \mathbf{B} = \frac{1}{c^2}\,\mathbf{S} \tag{7}$$

can be interpreted as an electromagnetic momentum density with $\mathbf{S}$ denoting the Poynting vector, and

$$w_f = \frac{1}{2}\left(\varepsilon_0\,\mathbf{E}^2 + \mathbf{B}^2/\mu_0\right) \tag{8}$$

representing the electromagnetic field energy density. An electromagnetic source energy density

$$w_s = \frac{1}{2}\,\bar{\rho}\,(\phi + \mathbf{C} \cdot \mathbf{A}) \tag{9}$$

can also be deduced and related to the density (8) as shown earlier [12].

As distinguished from Maxwell's equations, the present theory includes steady electromagnetic states in which all explicit time derivatives vanish in equations (1)–(6). The volume integrals of w_f and w_s then become equal for certain configurations which are limited in space.

3 Steady axisymmetric states

Among the steady axisymmetric states the analysis is here restricted to particle-shaped ones where the configuration is bounded both in the axial and radial directions. There are also string-shaped states being uniform in the axial directions, as described elsewhere [7, 12].

3.1 General features of particle-shaped states

In particle-shaped geometry a frame (r, θ, φ) of spherical coordinates is introduced, where all relevant quantities are independent of the angle φ. The analysis is further limited to a current density $\mathbf{j} = (0, 0, C\bar{\rho})$ and a vector potential $\mathbf{A} = (0, 0, A)$. Here $C = \pm\, c$ represents the two possible spin directions. The basic equations (1)–(4) then take the form

$$\frac{(r_0\,\rho)^2\,\bar{\rho}}{\varepsilon_0} = D\phi = \left[D + (\sin\theta)^{-2}\right](CA)\,, \tag{10}$$

where the dimensionless radial variable $\rho = r/r_0$ has been introduced with r_0 as a characteristic radial dimension, and where the operator $D = D_\rho + D_\theta$ is defined by

$$D_\rho = -\frac{\partial}{\partial\rho}\left(\rho^2 \frac{\partial}{\partial\rho}\right), \qquad D_\theta = -\frac{\partial^2}{\partial\theta^2} - \frac{\cos\theta}{\sin\theta}\frac{\partial}{\partial\theta}\,. \tag{11}$$

The general solution of equations (10) is obtained in terms of a *generating function*

$$F(r, \theta) = CA - \phi = G_0 \cdot G(\rho, \theta)\,, \tag{12}$$

where G_0 stands for a characteristic amplitude and G for a normalized dimensionless part. The solutions become

$$CA = -(\sin^2\theta)\,DF\,, \tag{13}$$

$$\phi = -\left[1 + (\sin^2\theta)\,D\right]F\,, \tag{14}$$

$$\bar{\rho} = -\left(\frac{\varepsilon_0}{r_0^2\,\rho^2}\right) D\left[1 + (\sin^2\theta)\,D\right]F\,. \tag{15}$$

The extra degree of freedom introduced by the nonzero electric field divergence and the inhomogeneity of equations (10) are underlying this general result.

Using expressions (13)–(15), (9), and the functions

$$f(\rho, \theta) = -(\sin\theta)\,D\left[1 + (\sin^2\theta)\,D\right]G\,, \tag{16}$$

$$g(\rho, \theta) = -\left[1 + 2(\sin^2\theta)\,D\right]G \tag{17}$$

integrated field quantities can be obtained which represent a net electric charge q_0, magnetic moment M_0, mass m_0, and angular momentum s_0. The magnetic moment is obtained from the local contributions of the current density, and the mass and angular momentum from those of w_s/c^2 and the energy relation by Einstein. The current density behaves as a common convection current. The mass flow originates from the velocity vector, having the same direction for positive and negative charge elements. Thus the integrated quantities become

$$q_0 = 2\pi\varepsilon_0\,r_0\,G_0\,J_q\,, \qquad I_q = f\,, \tag{18}$$

$$M_0 = \pi\varepsilon_0\,C\,r_0^2\,G_0\,J_M\,, \qquad I_M = \rho\,(\sin\theta) f\,, \tag{19}$$

$$m_0 = \pi(\varepsilon_0/c^2)\,r_0\,G_0^2\,J_m\,, \qquad I_m = fg\,, \tag{20}$$

$$s_0 = \pi(\varepsilon_0 C/c^2)\,r_0^2\,G_0^2\,J_s\,, \qquad I_s = \rho\,(\sin\theta) fg \tag{21}$$

with the normalized integrals

$$J_k = \int_{\rho_k}^{\infty}\!\!\int_0^{\pi} I_k\,d\rho\,d\theta\,, \qquad k = q, M, m, s\,. \tag{22}$$

Here ρ_k are small radii of circles centered around the origin $\rho = 0$ when G is divergent there, and $\rho_k = 0$ when G is convergent at $\rho = 0$.

At this point a further step is taken by restricting the analysis to a separable generating function

$$G(\rho, \theta) = R(\rho) \cdot T(\theta)\,. \tag{23}$$

The integrands of the normalized forms then become

$$I_q = \tau_0 R + \tau_1 (D_\rho R) + \tau_2 D_\rho (D_\rho R) , \quad (24)$$

$$I_M = \rho (\sin\theta) I_q , \quad (25)$$

$$I_m = \tau_0\tau_3 R^2 + (\tau_0\tau_4 + \tau_1\tau_3) R (D_\rho R) + \tau_1\tau_4 (D_\rho R)^2 + + \tau_2\tau_3 R D_\rho (D_\rho R) + \tau_2\tau_4 (D_\rho R) [D_\rho (D_\rho R)] , \quad (26)$$

$$I_s = \rho (\sin\theta) I_m , \quad (27)$$

where

$$\tau_0 = -(\sin\theta)(D_\theta T) - (\sin\theta) D_\theta \left[(\sin^2\theta)(D_\theta T)\right] , \quad (28)$$

$$\tau_1 = -(\sin\theta) T - (\sin\theta) D_\theta \left[(\sin^2\theta) T\right] - \sin^3\theta (D_\theta T) , \quad (29)$$

$$\tau_2 = -(\sin^3\theta) T , \quad (30)$$

$$\tau_3 = -T - 2(\sin^2\theta)(D_\theta T) , \quad (31)$$

$$\tau_4 = -2(\sin^2\theta) T . \quad (32)$$

The restriction (23) of separability becomes useful here for configurations having sources $\bar{\rho}$ and $\mathbf{j}$ that are mainly localized to a region near the origin, such as for a particle of limited extent. The analysis further concerns a radial function R which can become convergent or divergent at the origin, and a finite polar function T with finite derivatives which can be symmetric or antisymmetric in respect to the "equatorial plane" (midplane) defined by $\theta = \pi/2$. Repeated partial integration of expressions (22) for J_q and J_M leads to the following results as described in detail elsewhere [7, 8, 12]:

- The integrated charge q_0 and magnetic moment M_0 vanish in all cases where R is convergent at the origin and T has top-bottom symmetry as well as antisymmetry in respect to the equatorial plane. These cases lead to models of electrically neutral particles, such as the neutrino;
- The charge q_0 and magnetic moment M_0 are both nonzero provided that R is divergent at the origin and T has top-bottom symmetry. This case leads to models of charged particles, such as the electron. As will be seen from the analysis to follow, the *divergence* of R can still becomes reconcilable with *finite* values of q_0, M_0, m_0, and s_0 provided that the characteristic radius r_0 is made to shrink to the very small values of a point-charge-like state, as also being supported by experimental observations.

3.2 Quantum conditions of steady states

In this analysis a simplified road is chosen by imposing relevant quantum conditions afterwards on the obtained general solutions of the field equations. This is expected to be a rather good approximation to a rigorous approach where the extended field equations are quantized from the outset. The quantized equations namely become equivalent to the original ones in which the field quantities are replaced by their expectation values according to Heitler [13].

The angular momentum (spin) condition to be imposed on a model of the electron in the capacity of a fermion particle, as well as of the neutrino, is combined with equation (21) to result in

$$s_0 = \pi \left(\varepsilon_0 C / c^2\right) r_0^2 G_0^2 J_s = \pm h/4\pi . \quad (33)$$

In particular, for a charged particle such as the electron, muon, tauon or their antiparticles, equations (18) and (33) combine to

$$q^* \equiv |q_0/e| = \sqrt{f_0 J_q^2 / 2 J_s} , \qquad f_0 = 2\varepsilon_0 c h / e^2 . \quad (34)$$

Here q^* is a dimensionless charge which is normalized with respect to the experimentally determined elementary charge "e", and $f_0 \cong 137.036$ is the inverted value of the fine-structure constant.

According to Dirac, Schwinger, and Feynman [14] the quantum condition of the magnetic moment of a charged particle such as the electron becomes

$$M_0 m_0 / q_0 s_0 = 1 + \delta_M , \qquad \delta_M = 1/2\pi f_0 , \quad (35)$$

which shows excellent agreement with experiments. Here the unity term of the right hand member is due to Dirac who obtained the correct Landé factor, and δ_M is a small quantum mechanical correction due to Schwinger and Feynman. Conditions (33) and (35) can also be made plausible by elementary physical arguments based on the present picture of a particle-shaped state of "self-confined" radiation [7, 12].

In a charged particle-shaped state the electric current distribution generates a total magnetic flux Γ_{tot}. Here we consider the electron to be a system having both quantized angular momentum s_0 and a quantized charge q_0. The magnetic flux should then be quantized as well, and be given by the specific values of the two quantized concepts s_0 and q_0. This leads to the relation

$$\Gamma_{tot} = |s_0/q_0| . \quad (36)$$

4 A model of the electron

The analysis in this section will show that finite and nonzero integrated field quantities can be obtained in terms of the shrinking characteristic radius of a point-charge-like state. This does not imply that r_0 has to become strictly equal to zero, which would end up into the unphysical situation of a structureless point.

4.1 The integrated field quantities

The generating function to be considered has the parts

$$R = \rho^{-\gamma} e^{-\rho}, \qquad \gamma > 0 , \quad (37)$$

$$T = 1 + \sum_{\nu=1}^{n} \left\{ a_{2\nu-1} \sin[(2\nu-1)\theta] + a_{2\nu} \cos(2\nu\theta) \right\} . \quad (38)$$

The radial part (37) appears at first glance to be somewhat special. Generally one could have introduced a negative power series of ρ. However, for a limited number of terms, that with the largest negative power will in any case dominate at the origin. Due to the analysis which follows the same series has further to contain one term only, with a locked special value of γ. Moreover, the exponential factor in the form (37) secures the convergence of any moment with R, but will not appear in the end result.

The radial form (37) is now inserted into the integrands (24)–(27). Then the integrals (22) take a form $J_k = J_{k\rho} J_{k\theta}$. Here $J_{k\rho}$ is a part resulting from the integration with respect to ρ, and which is dominated by terms of the strongest negative power. The part $J_{k\theta}$ further results from the integration with respect to θ. In the integrals $J_{k\rho}$ divergences appear when the lower limits ρ_k approach zero. To outbalance this, we introduce a shrinking characteristic radius

$$r_0 = c_0\,\varepsilon\,, \qquad c_0 > 0\,, \qquad 0 < \varepsilon \ll 1\,, \tag{39}$$

where ε is a dimensionless smallness parameter. The integrated field quantities (18)–(21) then become

$$q_0 \;=\; 2\pi\varepsilon_0 c_0 G_0\,[J_{q\theta}/(\gamma-1)]\,(\varepsilon/\rho_q^{\gamma-1})\,, \tag{40}$$

$$M_0 m_0 \;=\; \pi^2(\varepsilon_0^2 C/c^2)c_0^3 G_0^3\cdot \\ \cdot\,[J_{M\theta}J_{m\theta}/(\gamma-2)(2\gamma-1)]\,(\varepsilon^3/\rho_M^{\gamma-2}\rho_m^{2\gamma-1})\,, \tag{41}$$

$$s_0 \;=\; \pi(\varepsilon_0 C/c^2)c_0^2 G_0^2\,[J_{s\theta}/2(\gamma-1)]\,(\varepsilon/\rho_s^{\gamma-1})^2. \tag{42}$$

The reason for introducing the compound quantity $M_0 m_0$ in expression (41) is that this quantity appears as a single entity in all finally obtained relations of the present analysis. The configuration with its integrated quantities is now required to scale in such a way that the geometry is preserved by becoming independent of ρ_k and ε. Such a uniform scaling implies that

$$\rho_q = \rho_M = \rho_m = \rho_s = \varepsilon \tag{43}$$

and that the parameter γ has to approach the value 2 from above, as specified by

$$\gamma(\gamma-1) = 2+\tilde{\delta}\,, \quad 0 \leqslant \tilde{\delta} \ll 1\,, \quad \gamma \approx 2+\tilde{\delta}/3\,. \tag{44}$$

As a result of this

$$J_{k\theta} = \int_0^{\pi} I_{k\theta}\,d\theta\,, \tag{45}$$

where

$$I_{q\theta} \;=\; -2\tau_1 + 4\tau_2\,, \tag{46}$$

$$I_{M\theta}/\tilde{\delta} \;=\; (\sin\theta)(-\tau_1+4\tau_2)\,, \tag{47}$$

$$I_{m\theta} \;=\; \tau_0\tau_3 - 2(\tau_0\tau_4+\tau_1\tau_3) + \\ +\,4(\tau_1\tau_4+\tau_2\tau_3) - 8\tau_2\tau_4\,, \tag{48}$$

$$I_{s\theta} \;=\; (\sin\theta)\,I_{m\theta}\,. \tag{49}$$

Then

$$q_0 \;=\; 2\pi\varepsilon_0 c_0 G_0 A_q\,, \tag{50}$$

$$M_0 m_0 \;=\; \pi^2(\varepsilon_0^2 C/c^2)c_0^3 G_0^3 A_M A_m\,, \tag{51}$$

$$s_0 \;=\; (1/2)\pi(\varepsilon_0 C/c^2)c_0^2 G_0^2 A_s \tag{52}$$

with $A_q \equiv J_{q\theta}$, $A_M \equiv J_{M\theta}/\tilde{\delta}$, $A_m \equiv J_{m\theta}$, and $A_s \equiv J_{s\theta}$.

The uniform scaling due to relations (39) and (43) in the range of small ε requires the characteristic radius r_0 to be very small, but does not specify its absolute value. One possibility of estimating this radius is by a crude modification of the field equations by an effect of General Relativity originating from the circulatory spin motion [7, 12]. This yields an upper limit of r_0 of about 10^{-19} meters for which this modification can be neglected.

As expressed by equations (39) and (43), the present results also have an impact on the question of Lorentz invariance of the electron radius. In the limit $\varepsilon \to 0$ the deductions will thus in a formal way satisfy such an invariance, in terms of a vanishing radius. At the same time the range of small ε becomes applicable to the physically relevant case of a very small but nonzero radius of a configuration having an internal structure.

4.2 The magnetic flux

According to equation (13) the magnetic flux function becomes

$$\Gamma = 2\pi r\,(\sin\theta)A = -2\pi r_0\,(G_0/c)\,\rho(\sin^3\theta)\,DG\,. \tag{53}$$

Making use of equations (37) and (39), it takes the form

$$\Gamma = 2\pi(c_0 G_0/C)\sin^3\theta\,\big\{\big[\gamma(\gamma-1)+2(\gamma-1)\rho+\rho^2\big]\,T - \\ -\;D_\theta\,T\big\}\,\big(\varepsilon/\rho^{\gamma-1}\big)\,e^{-\rho}\,. \tag{54}$$

To obtain a nonzero and finite magnetic flux function at the spherical surface $\rho = \varepsilon$ when γ approaches the value 2 from above, one has then to choose a corresponding dimensionless lower radius limit $\rho_\Gamma = \varepsilon$, in analogy with the condition (43).

In the further analysis a normalized flux function

$$\Psi \equiv \Gamma_{(\rho=\varepsilon,\theta)}/2\pi(c_0 G_0/C) = \sin^3\theta\,(D_\theta T - 2T) \tag{55}$$

is introduced at $\rho = \varepsilon$. A detailed study [8, 9, 12] of this function shows that there is a main magnetic flux

$$\Psi_0 = \Psi(\pi/2) \equiv A_\Gamma\,, \tag{56}$$

which intersects the equatorial plane, and that the total flux of equation (36) also includes that of two separate magnetic "islands" situated above and below the equatorial plane. As a consequence, the derivative $d\Psi/d\theta$ has two zero points at θ_1 and $\theta_2 > \theta_1$ in the range $0 \leqslant \theta \leqslant \pi/2$. These define the particular fluxes Ψ_1 in the range $0 < \theta \leqslant \theta_1$ and Ψ_2 in the

range $\theta_2 < \theta < \pi/2$. The total normalized magnetic flux thus becomes

$$\Psi_{tot} = f_{\Gamma f}\,\Psi_0\,, \quad f_{\Gamma f} = \left[2(\Psi_1 + \Psi_2) - \Psi_0\right]/\Psi_0\,, \quad (57)$$

where $f_{\Gamma f} > 1$ is the *obtained* flux factor including the additional contributions from the magnetic islands.

4.3 Quantum conditions

For the angular momentum and its associated charge relation (34) the quantum condition becomes

$$q^* = \sqrt{f_0 A_q^2/A_s} \quad (58)$$

according to equations (50) and (52). The magnetic moment condition (35) further reduces to

$$A_M A_m/A_q A_s = 1 + \delta_M\,. \quad (59)$$

Combination of equations (36), (50), (52), and (56) finally yields

$$8\pi f_{\Gamma q} A_\Gamma A_q = A_s\,, \quad (60)$$

where $f_{\Gamma q}$ is the flux factor being *required* by the quantum condition. For a self-consistent solution the two flux factors of equations (57) and (60) have to become equal to a common factor $f_\Gamma = f_{\Gamma f} = f_{\Gamma q}$.

4.4 Variational analysis of the integrated charge

Since the elementary electronic charge appears to represent the smallest quantum of free charge, the question may be raised whether there is a more profound reason for such a charge to exist, possibly in terms of variational analysis. In a first attempt efforts have therefore been made to search for an extremum of the normalized charge (58), under the two subsidiary quantum conditions (59) and (60) and including Lagrange multipliers. The available variables are then the amplitudes (a_1, a_2, a_3, ...) of the polar function (38). However, such a conventional procedure is found to be upset by difficulties. It namely applies when there are well-defined and localized points of extremum, but not when such single points are replaced by a flat plateau in parameter space.

The plateau behaviour is in fact what occurs here, and an alternative analysis is then applied in terms of an increasing number of amplitudes that are "swept" (scanned) across their entire range of variation [9, 12]. One illustration of this is presented in Fig. 1 for the first four amplitudes, and with a flux factor $f_\Gamma = 1.82$. The figure shows the behaviour of the normalized charge q^* when scanning the ranges of the remaining amplitudes a_3 and a_4. There is a steep barrier in the upper part of Fig. 1, from which q^* drops down to a flat plateau being quite close to the level $q^* = 1$ which represents the experimental value:

- A detailed analysis of the four-amplitude case clearly demonstrates the asymptotic flat plateau behaviour at large amplitudes a_3 and a_4. The self-consistent minimum values of q^* obtained along the perimeter of the plateau have been found to vary from $q^* = 0.969$ for $f_\Gamma = 1.81$ to $q^* = 1.03$ for $f_\Gamma = 1.69$. Consequently, the plateau is found to be slightly "warped", being partly below and partly above the level $q^* = 1$;
- For an increasing number of amplitudes beyond four there is a similar plateau behaviour, with only a slight increase in the level. This is not in conflict with the principle of the variational analysis. Any function q^* can thus have minima in the hyperspace of amplitudes at points where some of these amplitudes vanishes;
- The preserved plateau behaviour at an increasing number of amplitudes can be understood from the fact that the ratio A_q^2/A_s in equation (58) becomes a slow function of the higher "multipole" terms of the expansion (38);
- With these plateau solutions the normalized charge q^* is still left with some additional degrees of freedom. These are eliminated by the analysis of the force balance in the following subsection. There it will be shown that the lowest value of q^* obtained from the variational analysis solely does not become reconcilable with the radial force balance.

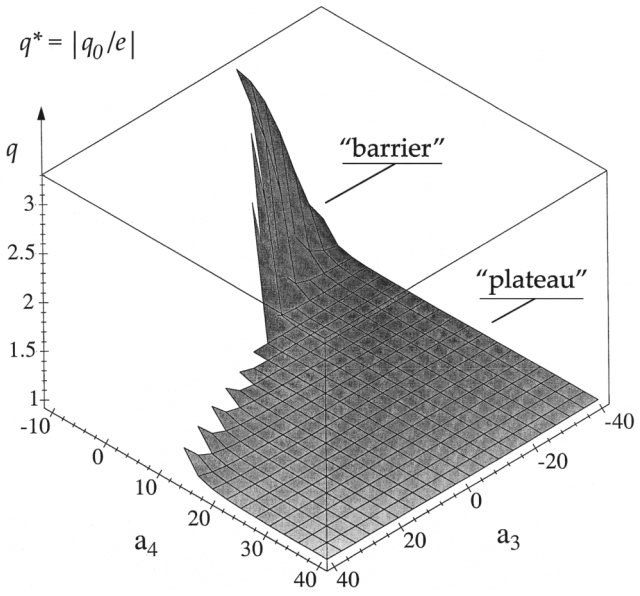

Fig. 1: The normalized electron charge $q^* \equiv |q_0/e|$ as a function of the two amplitudes a_3 and a_4 in the four amplitude case.

4.5 The radial force balance

The fundamental description of a charged particle in conventional theory is deficient also in respect to its radial force balance. Thus, an equilibrium cannot be maintained by the classical electrostatic force $\bar{\rho}\,\mathbf{E}$ in equation (5) only, but

is then assumed to require forces of a nonelectromagnetic character to be present as described by Jackson [4]. In other words, the electron would otherwise "explode" under the action of its self-charge.

Turning to the present revised theory, however, there is an additional magnetic term $\bar{\rho}\,\mathbf{C}\times\mathbf{B}$ in equation (5) which under certain conditions provides the radial force balance of an equilibrium. With the already obtained results based on equations (10)–(15), the integrated radial force of the right-hand member in equation (5) becomes

$$F_r = -2\pi\varepsilon_0 G_0^2 \iint \left[DG + D\left(s^2 DG\right)\right] \cdot \cdot \left[\frac{\partial G}{\partial \rho} - \frac{1}{\rho}\, s^2 DG\right] \rho^2 s\, d\rho\, d\theta\,, \qquad (61)$$

where $s \equiv \sin\theta$. For the point-charge-like model of Sections 4.1–4.4 this force is represented by the form

$$F_r = I_+ - I_-\,, \qquad (62)$$

where I_+ and I_- are the positive and negative contributions to F_r. The results are as follows [10]:

- The ratio I_+/I_- in the plateau region of the four-amplitude case decreases from 1.27 at $q^* = 0.98$ to 0.37 at $q^* = 1.01$, thereby passing a sharply defined equilibrium point $I_+/I_- = 1$ at $q^* \cong 0.988$. The remaining degrees of freedom of this case have then been used up;
- With more than four amplitudes slightly higher values of q^* have been obtained in a corresponding plateau region. Even when there exists a force balance at higher values of q^* than that of the four-amplitude solution, the latter still corresponds to the lowest q^* for an integrated radial force balance;
- The obtained small deviation of $q^* \cong 0.988$ from the experimental value $q^* = 1$ is a remaining problem. One possible explanation could be provided by a small quantum mechanical correction of the magnetic flux condition (60), in analogy with the correction δ_M of the magnetic moment condition (59). Another possibility to be further examined is simply due to some uncertainty in the numerical calculations of a rather complex system of relations, being subject to iterations in several consecutive steps;
- The present analysis of the integrated (total) forces, performed instead of a treatment of their local parts, is in full analogy with the earlier deductions of the integrated charge, magnetic moment, mass, and angular momentum.

With the obtained radial force balance, we finally return to the radial constant c_0 of equation (39). As shown earlier [7], the mass and magnetic moment become $m_0 = K_m/c_0$ and $M_0 = K_M c_0$ where K_m and K_M include the normalized integrals A_m, A_M, and A_s. Introducing the relation $h\nu = m_0 c^2$ by Planck and Einstein and the related Compton wavelength $\lambda_C = c/\nu = h/m_0 c$ combination with $m_0 = K_m/c_0$ then yields $6\pi c_0/\lambda_C = A_m/A_s$. In the radial force balance $A_m/A_s = 1.07$. Choosing the three-fold circumference based on the radius c_0 to be equal to the Compton wavelength then results in masses of the electron, muon, and tauon which deviate by only seven percent from the experimental values. This three-fold circumference requires further investigation.

5 A model of the neutrino

The electrically neutral steady states described in Section 3.1 will now be used as a basis for models of the neutrino. Since the analysis is restricted to a steady particle-shaped configuration, it includes the concept of a nonzero rest mass. This is supported by the observed neutrino oscillations. The present neutrino models are described in detail elsewhere [7, 12, 15], and will only be outlined in this section.

5.1 A convergent generating function

A separable generating function is now adopted, having a convergent radial part R and a polar part T of top-bottom symmetry, as given by

$$R = \rho^\gamma e^{-\rho}\,, \qquad T = \sin^\alpha\theta\,, \qquad (63)$$

where $\gamma \gg \alpha \gg 1$. At increasing values of ρ the part R first reaches a maximum at $\rho = \hat{\rho} = \hat{r}/r_0 = \gamma$, after which it drops steeply to zero at large ρ. Therefore $\hat{r} = \gamma r_0$ can be taken as an effective radius of the configuration. Inserting the forms (63) into equations (24)–(32) and the integrated expressions (20)–(22) for the total mass and angular momentum, we obtain the ratio

$$J_m/J_s = 15/38\,\gamma\,. \qquad (64)$$

Combination of equations (20), (21), (64), and the quantum condition (33) then yields the mass-radius relation

$$m_0\hat{r} = m_0\gamma r_0 = 15h/152\pi c \cong 7{\times}10^{-44}\ [\mathrm{kg}{\times}\mathrm{m}]\,. \qquad (65)$$

For a case with top-bottom antisymmetry of T there is little difference as compared to the result obtained here.

5.2 A divergent generating function

We now turn to a generating function having a divergent radial part of the same form (37) as that for the electron model, and with a polar part of top-bottom antisymmetry. When $\rho = r/r_0$ increases from $\rho = 0$, the radial part decreases from a high level, down to $R = 1/e$ at $\rho = 1$, and further to very small values. Thus $\hat{r} = r_0$ can here be taken as an effective radius of the configuration.

The analysis of the radial integrals is analogous to that of the electron model. To obtain nonzero and finite values of mass m_0 and angular momentum s_0, a shrinking effective radius $\hat{r}$ and a shrinking amplitude factor G_0 are introduced through the relations

$$\hat{r} = r_0 = c_r \cdot \varepsilon\,, \qquad G_0 = c_G \cdot \varepsilon^{\beta}, \tag{66}$$

where c_r, c_G, and β are positive constants and $0 < \varepsilon \ll 1$. Expressions (20) and (21) then take the forms

$$m_0 = \pi(\varepsilon_0/c^2) c_r c_G^2 (2\gamma-1)^{-1} J_{m\theta}\left[\varepsilon^{1+2\beta}/\rho_m^{2\gamma-1}\right], \tag{67}$$

$$s_0 = \pi(\varepsilon_0 C/c^2) c_r^2 c_G^2 [2\,(\gamma-1)]^{-1} J_{s\theta}\left[\varepsilon^{2(1+\beta)}/\rho_s^{2(\gamma-1)}\right], \tag{68}$$

where the lower limits ρ_m and ρ_s of the integrals (22) have been introduced. For nonzero and finite values of m_0 and s_0 it is then required that

$$\rho_m = \varepsilon^{(1+2\beta)/(2\gamma-1)}\,, \qquad \rho_s = \varepsilon^{(1+\beta)/(\gamma-1)}\,. \tag{69}$$

With the quantum condition (33) relations (66)–(69) further combine to

$$m_0 \hat{r} = \frac{h}{2\pi c}\,\frac{\gamma-1}{2\gamma-1}\,(J_{m\theta}/J_{s\theta})\,\varepsilon\,. \tag{70}$$

The ratio $J_{m\theta}/J_{s\theta}$ is here expected to become a slow function of the profile shapes of $T(\theta)$ and $I_{m\theta}$, as obtained for a number of test functions for $I_{m\theta}$. An additional specific example with $\gamma = 3$ and $\beta = 3/2$ yields $\rho_m = \varepsilon^{4/5}$ and $\rho_s = \varepsilon^{5/4}$ making ρ_m and ρ_s almost linear functions of ε. In a first crude approximation relation (70) can therefore be written as

$$m_0 \hat{r} \cong 2{\times}10^{-43}\,\varepsilon\ [\mathrm{kg{\times}m}]\,. \tag{71}$$

5.3 Neutrino penetration into solid matter

The mass m_0 has to be reconcilable with observed data. The upper bounds of the neutrino mass are about 4.7 eV for the electron-neutrino, 170 keV for the muon-neutrino, and 18 MeV for the tauon-neutrino. Neutrinos can travel as easily through the Earth as a bullet through a bank of fog. They pass through solid matter consisting of nucleons, each having a radius $r_N \cong 6{\times}10^{-15}$ meters. Concerning the present neutrino models, there are the following options:

- With the result (65) the ratio $\hat{r}/r_N$ becomes about 10^6, 40, and 0.4 for the electron-neutrino, muon-neutrino, and the tauon-neutrino. The interaction with the electron-neutrino is then expected to take place between the short-range nucleon field as a whole and a very small part of the neutrino field. The latter field could then "heal" itself in terms of a restoring tunneling effect. Then the electron-neutrino would represent the "fog" and the nucleon the "bullet". The mean free paths of the muon- and tauon-neutrinos would on the other hand become short for this option;
- With the result (71) the corresponding values of $\hat{r}/r_N$ become about $4{\times}10^6\,\varepsilon$, $100\,\varepsilon$, and ε, respectively. Here sufficiently small values of ε would make the neutrino play the role of the "bullet" and the nucleon that of the "fog".

6 Conclusions

The present steady electromagnetic equilibria, and their applications to leptons, have no counterparts in conventional theory. The electron model, and that of the muon, tauon and corresponding antiparticles, embrace new aspects and explanations of a number of so far unsolved problems:

- To possess a nonzero electric net charge, the characteristic radius of the particle-shaped states has to shrink to that of a point-charge-like geometry. This agrees with experimental observation;
- Despite the success of the conventional renormalization procedure, physically more satisfactory ways are needed in respect to the infinite self-energy problem of a point-charge, and to the extra added counter terms by which a finite result is obtained from the difference of two "infinities". Such a situation is avoided through the present theory where the "infinity" (divergence) of the generating function is outbalanced by the "zero" of a shrinking characteristic radius;
- In the present approach the Lorentz invariance of the electron radius is formally satisfied at the limit $r_0 \to 0$. At the same time the theory includes a parameter range of small but nonzero radii being reconcilable with an internal structure;
- In contrast to conventional theory, an integrated radial force balance can be provided by the present space-charge current density which prevents the electron from "exploding" under the action of its electric self-charge. Possibly a corresponding situation may arise for the bound quarks in the interior of baryons. Here the strong force provides an equilibrium for their mutual interactions, but this does not fully explain how the individual quarks are kept in equilibrium in respect to their self-charges;
- The variational analysis results in a parameter range of the normalized charge q^* which is close to the experimental value $q^* = 1$. Within this range the remaining degrees of freedom in the analysis become exhausted when imposing the additional condition of an integrated radial force balance. This results in $q^* \cong 0.99$ which deviates by only one percent from the experimental value. The reason for the deviation is not clear at the present stage, but it should on the other hand be small enough to be regarded as an experimental support of the theory. It can also be taken as an indirect confirmation of a correctly applied value

of the Landé factor, because a change of the latter by a factor of two would result in entirely different results. Provided that the value $q^* = 1$ can be obtained after relevant correction, the elementary charge would no longer remain as an independent constant of nature, but is then derived from the velocity of light, Planck's constant, and the permittivity of the vacuum.

The steady states having a vanishing net charge also form possible models for a least some of the basic properties of the neutrino:

- A small but nonzero rest mass is in conformity with the analysis;
- The steady state includes an angular momentum, but no magnetic moment;
- Long mean free paths are predicted in solid matter, but their detailed comparison with observed data is so far an open question.

References

1. Schiff L. I. Quantum Mechanics. McGraw-Hill Book Comp. Inc., New York, 1949, Ch XIV.
2. Feynman R. P. Lectures in physics: mainly electromagnetism and matter. Addison-Wesley, Reading, Massachusetts, 1964, p. 28–1.
3. Ryder L. H. Quantum field theory. Second edition. Cambridge Univ. Press, 1996, Ch. 9.3.
4. Jackson J. D. Classical Electrodynamics. John Wiley and Sons, Inc., New York–London–Sydney, 1962, Ch. 17.4.
5. Lehnert B. An extended formulation of Maxwell's equations. *Spec. Sci. Technol.*, 1986, v. 9, 177–184.
6. Lehnert B. Basic concepts of an extended electromagnetic theory. *Spec. Sci. Technol.*, 1994, v. 17, 259–273.
7. Lehnert B., Roy S. Extended electromagnetic theory. World Scientific Publishers, Singapore, 1998.
8. Lehnert B. Optical effects of an extended electromagnetic theory. In: *Advances in Chemical Physics*, v. 119. Edited by M. W.Evans, I. Prigogine, and S. A. Rice, John Wiley and Sons, Inc., New York, 2001, 1–77.
9. Lehnert B., Scheffel J. On the minimum elementary charge of an extended electromagnetic theory. *Physica Scripta*, 2002, v. 65, 200–207.
10. Lehnert B. The electron as a steady-state confinement system. *Physica Scripta*, 2004, v. T113, 41–44.
11. Lehnert B. Photon physics of revised electromagnetics. *Progress in Physics*, 2006, v. 2, 78–85.
12. Lehnert B. Revised electromagnetics with fundamental applications. Report TRITA-ALF-2004-02, Fusion Plasma Physics, Alfvén Laboratory, Royal Institute of Technology, Stockholm, 2004, 1–126.
13. Heitler W. The quantum theory of radiation. Third edition. Clarendon Press, Oxford, 1954, Appendix, p. 409
14. Feynman R. P. QED: The strange theory of light and matter, Penguin, London, 1990.
15. Lehnert B. Neutral particle states of an extended electromagnetic theory. In: *Dirac equation, neutrinos and beyond*, Edited by V. V. Dvoeglazov. *Ukrainian Journal: Electromagnetic Phenomena*, 2003, T. 3, v. 9, 49–55.

Positive, Neutral and Negative Mass-Charges in General Relativity

Larissa Borissova and Florentin Smarandache
Department of Mathematics, University of New Mexico, Gallup, NM 87301, USA
E-mail: lborissova@yahoo.com; fsmarandache@yahoo.com

As shown, any four-dimensional proper vector has two observable projections onto time line, attributed to our world and the mirror world (for a mass-bearing particle, the projections posses are attributed to positive and negative mass-charges). As predicted, there should be a class of neutrally mass-charged particles that inhabit neither our world nor the mirror world. Inside the space-time area (membrane) the space rotates at the light speed, and all particles move at as well the light speed. So, the predicted particles of the neutrally mass-charged class should seem as light-like vortices.

1 Problem statement

As known, neutrosophy is a new branch of philosophy which extends the current dialectics by the inclusion of neutralities. According to neutrosophy [1, 2, 3], any two opposite entities <A> and <Anti-A> exist together with a whole class of neutralities <Neut-A>.

Neutrosophy was created by Florentin Smarandache and then applied to mathematics, statistics, logic, linguistic, and other branches of science. As for geometry, the neutrosophic method expanded the Euclidean set of axioms by denying one or more of them in at least two distinct ways, or, alternatively, by accepting one or more axioms true and false in the same space. As a result, it was developed a class of Smarandache geometries [4], that includes Euclidean, Riemann, and Lobachevski-Gauss-Bolyai geometries as partial cases.

In nuclear physics the neutrosophic method theoretically predicted "unmatter", built on particles and anti-particles, that was recently observed in CERN and Brookhaven experiments (see [5, 6] and References there). In General Relativity, the method permits the introduction of entangled states of particles, teleportation of particles, and also virtual particles [7], altogether known before in solely quantum physics. Aside for these, the method permits to expand the basic space-time of General Relativity (the four-dimensional pseudo-Riemannian space) by a family of spaces where one or more space signature conditions is permitted to be both true and false [8].

In this research we consider another problem: mass-charges of particles. Rest-mass is a primordial property of particles. Its numerical value remains unchanged. On the contrary, relativistic mass has "charges" dependent from relative velocity of particles. Relativistic mass displays itself in only particles having interaction. Therefore theory considers relativistic mass as mass-charge.

Experimental physics knows two kinds of regular particles. Regular mass-bearing particles possessing non-zero rest-masses and relativistic masses (masses-in-motion). Massless light-like particles (photons) possess zero rest-masses, while their relativistic masses are non-zeroes. Particles of other classes (as virtual photons, for instance) can be considered as changed states of mass-bearing or massless particles.

Therefore, following neutrosophy, we do claim:

Aside for observed positively mass-charged (i. e. mass-bearing) particles and neutrally mass-charged (light-like) particles, there should be a third class of "negatively" mass-charged particles unknown in today's experimental physics.

We aim to establish such a class of particles by the methods of General Relativity.

2 Two entangled states of a mass-charge

As known, each particle located in General Relativity's space-time is characterized by its own four-dimensional impulse vector. For instance, for a mass-bearing particle the proper impulse vector P^α is

$$P^\alpha = m_0 \frac{dx^\alpha}{ds}\,, \quad P_\alpha P^\alpha = 1\,, \quad \alpha = 0,1,2,3\,, \qquad (1)$$

where m_0 is the rest-mass of this particle. Any vector or tensor quantity can be projected onto an observer's time line and spatial section. Namely the projections are physically observable quantities for the observer [9]. As recently shown [10, 11], the four-dimensional impulse vector (1) has two projections onto the time line*

$$\frac{P_0}{\sqrt{g_{00}}} = \pm m\,, \qquad \text{where } m = \frac{m_0}{\sqrt{1-\mathrm{v}^2/c^2}}\,, \qquad (2)$$

and solely the projection onto the spatial section

$$P^i = \frac{m}{c}\,\mathrm{v}^i = \frac{1}{c}\,p^i, \quad \text{where } \mathrm{v}^i = \frac{dx^i}{d\tau}\,, \quad i = 1,2,3\,, \quad (3)$$

where p_i is the three-dimensional observable impulse. Therefore, we conclude:

*Where $d\tau = \sqrt{g_{00}}dt + \frac{g_{0i}}{c\sqrt{g_{00}}}dx^i$ is the properly observed time interval [9, 12].

> Any mass-bearing particle, having two time projections, exists in two observable states, entangled to each other: the positively mass-charged state is observed in our world, while the negatively mass-charged state is observed in the mirror world.

The mirror world is almost the same that ours with the following differences:

1. The particles bear negative mass-charges and energies;
2. "Left" and "right" have meanings opposite to ours;
3. Time flows oppositely to that in our world.

From the viewpoint of an observer located in the mirror world, our world will seem the same that his world for us.

Because both states are attributed to the same particle, and entangled, both our world and the mirror world are two entangled states of the same world-object.

To understand why the states remain entangled and cannot be joined into one, we consider the third difference between them — the time flow.

Terms "direct" and "opposite" time flows have a solid mathematical ground in General Relativity. They are connected to the sign of the derivative of the coordinate time interval by the proper time interval . The derivative arrives from the purely geometrical law that the square of a unit four-dimensional vector remains unchanged in a four-dimensional space. For instance, the four-dimensional velocity vector

$$U^\alpha U_\alpha = g_{\alpha\beta}\, U^\alpha U^\beta = 1\,, \qquad U^\alpha = \frac{dx^\alpha}{ds}\,. \tag{4}$$

Proceeding from by-component notation of this formula, and using $\mathrm{w} = c^2(1-\sqrt{g_{00}})$ and $v_i = -c\frac{g_{0i}}{\sqrt{g_{00}}}$, we arrive to a square equation

$$\left(\frac{dt}{d\tau}\right)^2 - \frac{2v_i\mathrm{v}^i}{c^2\left(1-\frac{\mathrm{w}}{c^2}\right)}\frac{dt}{d\tau} + \\ + \frac{1}{\left(1-\frac{\mathrm{w}}{c^2}\right)^2}\left(\frac{1}{c^4}\,v_iv_k\mathrm{v}^i\mathrm{v}^k - 1\right) = 0\,, \tag{5}$$

which solves with two roots

$$\left(\frac{dt}{d\tau}\right)_{1,2} = \frac{1}{1-\frac{\mathrm{w}}{c^2}}\left(\frac{1}{c^2}\,v_i\mathrm{v}^i \pm 1\right). \tag{6}$$

Observer's proper time lows anyhow directly $d\tau > 0$, because this is a relative effect connected to the his viewpoint at clocks. Coordinate time t flows independently from his views. Accordingly, the direct flow of time is characterized by the time function $dt/d\tau > 0$, while the opposite flow of time is $dt/d\tau < 0$.

If $dt/d\tau = 0$ happens, the time flow stops. This is a boundary state between two entangled states of a mass-charged particle, one of which is located in our world (the positively directed time flow $dt/d\tau > 0$), while another — in the mirror world (where the time flow is negatively directed $dt/d\tau < 0$).

From purely geometric standpoints, the state $dt/d\tau = 0$ describes a space-time area, which, having special properties, is the boundary space-time membrane between our world and the mirror world (or the mirror membrane, in other word). Substituting $dt/d\tau = 0$ into the main formula of the space-time interval $ds^2 = g_{\alpha\beta}\, dx^\alpha dx^\beta$

$$ds^2 = c^2dt^2 + 2g_{0i}cdtdx^i + g_{ik}\, dx^i dx^k, \tag{7}$$

we obtain the metric of the space within the area

$$ds^2 = g_{ik}\, dx^i dx^k. \tag{8}$$

So, the mirror membrane between our world and the mirror world has a purely spatial metric which is also stationary.

As Kotton showed [13], any three-dimensional Riemannian space permits a holonomic orthogonal reference frame, in respect to which the three-dimensional metric can be reduced to the sum of Pythagorean squares. Because our initially four-dimensional metric ds^2 is sign-alternating with the signature $(+---)$, the three-dimensional metric of the mirror membrane between our world and the mirror world is negatively defined and has the form

$$ds^2 = -H_1^2(dx^1)^2 - H_2^2(dx^2)^2 - H_3^2(dx^3)^2, \tag{9}$$

where $H_i\,(x^1, x^2, x^3)$ are Lamé coefficients (see for Lamé coefficients and the tetrad formalism in [14]). Determination of this metric is connected to the proper time of observer, because we mean therein.

Substituting $dt = 0$ into the time function (6), we obtain the physical conditions inside the area (mirror membrane)

$$v_i\, dx^i = \pm c^2 d\tau\,. \tag{10}$$

Owning the definition of the observer's proper time

$$d\tau = \sqrt{g_{00}}\, dt + \frac{g_{0i}\, dx^i}{\sqrt{g_{00}}} = \left(1-\frac{\mathrm{w}}{c^2}\right)dt - \frac{1}{c^2}\, v_i dx^i, \tag{11}$$

and using $dx^i = v^i d\tau$ therein, we obtain: the observer's proper state $d\tau > 0$ can be satisfied commonly with the state $dt = 0$ inside the membrane only if there is*

$$v_i\mathrm{v}^i = -c^2 \tag{12}$$

thus we conclude:

> The space inside the mirror membrane between our world and the mirror world seems as the rotating at the light speed, while all particles located there move at as well the light speed. So, particles that inhabit the space inside the membrane seem as light-like vortices.

*Here is a vector product of two vectors v_i and v^i, dependent on the cosine between them (which can be both positive and negative). Therefore the modules may not be necessarily imaginary quantities.

Class of mass-charge	Particles	Energies	Class of motion	Area
Positive mass-charges, $m > 0$	mass-bearing particles	$E > 0$	move at sub-light speeds	our world
Neutral mass-charges, $m = 0$	massless (light-like) particles	$E > 0$	move at the light speed	our world
	light-like vortices	$E = 0$	move at the light speed within the area, rotating at the light speed	the membrane
	massless (light-like) particles	$E < 0$	move at the light speed	the mirror world
Negative mass-charges, $m < 0$	mass-bearing particles	$E < 0$	move at sub-light speeds	the mirror world

This membrane area is the "barrier", which prohibits the annihilation between positively mass-charged particles and negatively mass-charged particles — the barrier between our world and the mirror world. In order to find its mirror twin, a particle should be put in an area rotating at the light speed, and accelerated to the light speed as well. Then the particle penetrates into the space inside the membrane, where annihilates with its mirror twin.

As a matter of fact, no mass-bearing particle moved at the light speed: this is the priority of massless (light-like) particles only. Therefore:

> Particles that inhabit the space inside the membrane seem as light-like vortices.

Their relativistic masses are zeroes $m = 0$ as those of massless light-like particles moving at the light speed. However, in contrast to light-like particles whose energies are non-zeroes, the particles inside the membrane possess zero energies $E = 0$ because the space metric inside the membrane (8) has no time term.

The connexion between our world and the mirror world can be reached by matter only filled in the light-like vortical state.

3 Two entangled states of a light-like matter

As known, each massless (light-like) particle located in General Relativity's space-time is characterized by its own four-dimensional wave vector

$$K^\alpha = \frac{\omega}{c}\frac{dx^\alpha}{d\sigma}\,, \qquad K_\alpha K^\alpha = 0\,, \tag{13}$$

where ω is the proper frequency of this particle linked to its energy $E = \hbar\omega$, and $d\sigma = \left(-g_{ik} + \frac{g_{0i}g_{0k}}{g_{00}}\right)dx^i dx^k$ is the measured spatial interval. (Because massless particles move along isotropic trajectories, the trajectories of light, one has $ds^2 = 0$, however the measured spatial interval and the proper interval time are not zeroes.)

As recently shown [10, 11], the four-dimensional wave vector has as well two projections onto the time line

$$\frac{K_0}{\sqrt{g_{00}}} = \pm\omega\,, \tag{14}$$

and solely the projection onto the spatial section

$$K^i = \frac{\omega}{c}c^i = \frac{1}{c}p^i, \quad \text{where } c^i = \frac{dx^i}{d\tau}\,, \tag{15}$$

while c^i is the three-dimensional observable vector of the light velocity (its square is the world-invariant c^2, while the vector's components c^i can possess different values). Therefore, we conclude:

> Any massless (light-like) particle, having two time projections, exists in two observable states, entangled to each other: the positively energy-charged state is observed in our world, while the negatively energy-charged state is observed in the mirror world.

Because along massless particles' trajectories $ds^2 = 0$, the mirror membrane between the positively energy-charged massless states and their entangled mirror twins is characterized by the metric

$$ds^2 = g_{ik}\,dx^i dx^k = 0\,, \tag{16}$$

or, expressed with Lamé coefficients $H_i\,(x^1, x^2, x^3)$,

$$ds^2 = -H_1^2(dx^1)^2 - H_2^2(dx^2)^2 - H_3^2(dx^3)^2 = 0\,. \tag{17}$$

As seen, this is a particular case, just considered, the membrane between the positively mass-charged and negatively mass-charge states.

4 Neutrosophic picture of General Relativity's world

As a result we arrive to the whole picture of the world provided by the purely mathematical methods of General Relativity, as shown in Table.

It should be noted that matter inside the membrane is not the same as the so-called zero-particles that inhabit fully degenerated space-time areas (see [15] and [8]), despite the fact they posses zero relativistic masses and energies too. Fully degenerate areas are characterized by the state $w + v_i u^i = c^2$ as well as particles that inhabit them*. At first, inside the membrane the space is regular, non-degenerate. Second. Even in the absence of gravitational fields, the zero-space state becomes $v_i u^i = c^2$ that cannot be trivially reduced to $v_i u^i = -c^2$ as inside the membrane.

*Here $u^i = dx^i/dt$ is so-called the coordinate velocity.

Particles inside the membrane between our world and the mirror world are filled into a special state of light-like vortices, unknown before.

This is one more illustration to that, between the opposite states of positively mass-charge and negatively mass-charge, there are many neutral states characterized by "neutral" mass-charge. Probably, further studying light-like vortices, we'd find more classes of neutrally mass-charged states (even, probably, an infinite number of classes).

References

1. Smarandache F. Neutrosophy/neutrosophic probability, set, and logic. American Research Press, Rehoboth, 1998.
2. Smarandache F. A unifying field in logic: neutrosophic logic. Neutrosophy, neutrosophic set, neutrosophic probability. 3rd ed., American Research Press, Rehoboth, 2003.
3. Smarandache F. and Liu F. Neutrosophic dialogues. Xiquan Publishing House, Phoenix, 2004.
4. Iseri H. Smarandache manifolds. American Research Press, Rehoboth, 2002.
5. Smarandache F. A new form of matter — unmatter, composed of particles and anti-particles. *Progress in Physics*, 2005, v. 1, 9–11.
6. Smarandache F. and Rabounski D. Unmatter entities inside nuclei, predicred by the Brightsen Nucleon Cluster Model. *Progress in Physics*, 2006, v. 1, 14–18.
7. Rabounki D., Borissova L., Smarandache F. Entangled particles and quantum causality threshold in the General Theory of Relativity. *Progress in Physics*, 2005, v. 2, 101–107.
8. Rabounki D., Smarandache F., Borissova L. Neutrosophic methods in General Relativity. Hexis, Phoenix (Arizona), 2005.
9. Zelmanov A. L. Chronometric invariants and co-moving coordinates in the general relativity theory. *Doklady Acad. Nauk USSR*, 1956, v. 107(6), 815–818.
10. Borissova L. and Rabounski D. Fields, vacuum, and the mirror Universe. Editorial URSS, Moscow, 2001, 272 pages (2nd rev. ed.: CERN, EXT-2003-025).
11. Rabounski D. D. and Borissova L. B. Particles here and beyond the Mirror. Editorial URSS, Moscow, 2001, 84 pages.
12. Landau L. D. and Lifshitz E. M. The classical theory of fields. GITTL, Moscow, 1939 (ref. with the 4th final exp. edition, Butterworth-Heinemann, 1980).
13. Kotton E. Sur les variétés a trois dimensions. *Ann. Fac. Sci. Toulouse* (2), v. 1, Thése, Paris, 1899.
14. Petrov A. Z. Einstein spaces. Pergamon, Oxford, 1969.
15. Borissova L. and Rabounski D. On the possibility of instant displacements in the space-time of General Relativity. *Progress in Physics*, 2005, v. 1, 17–19; Also in: *Physical Interpretation of Relativity Theory* (PIRT-2005), Proc. of the Intern. Meeting., Moscow, 2005, 234–239; Also in: *Today's Take on Einstein's Relativity*, Proc. of the Confer., Tucson (Arizona), 2005, 29–35.

Much Ado about Nil: Reflection from Moving Mirrors and the Interferometry Experiments

Christo I. Christov

Dept. of Mathematics, University of Louisiana at Lafayette, Lafayette, LA 70504, USA

E-mail: christov@louisiana.edu

The emitter and receiver Doppler effects are re-examined from the point of view of boundary condition on a moving boundary. Formulas are derived for the frequencies of the waves excited on receiver's and emitter's surfaces by the waves traveling thorough the medium. It is shown that if the emitting source and the reflection mirror are moving with the same speed in the same direction relative to a medium at rest, there is no observable Doppler effect. Hence, the nil effect of Michelson and Morley experiment (MME) is the only possible outcome and cannot be construed as an indication about the existence or nonexistence of an absolute continuum. The theory of a new experiment that can give conclusive information is outlined and the possible experimental set-up is sketched.

5 Introduction

Since the groundlaying work of Fizeau, interferometry has been one of the most often used methods to investigate the properties of light. The idea of interferometry was also applied to detecting the presence of an absolute medium in the Michelson and Morley experiment (MME) [1]. The expected effect was of second order $O(v^2/c^2)$ with respect to the ratio between the Earth speed v and speed of light c and it is generally accepted now that Michelson-Morley experiment yielded a nil result, in the sense that the fringes that were observed corresponded to a much smaller (assumed to be negligible) speed than actual Earth's speed. Around the end of Nineteen Century, the nil result of MME prompted Fitz-Gerald and Lorentz to surmise that the lengths are contracted in the direction of motion by the Lorentz factor $\sqrt{1 - v^2/c^2}$ that cancels exactly the expected effect. Since then the Lorentz contraction has been many times verified and can be considered now as an established fact. The Lorentz contraction does not need MME anymore in order to survive as the main vehicle of the modern physics of processes at high speeds.

On another note, the nil effect of MME was eventually interpreted as an indication that there exists no absolute (resting) medium where the light propagates. The problem with this conclusion is that nobody *actually* proposed a theory for MME in which a continuous medium was considered with the correct boundary conditions. Rather, the emission theory of light was used whose predictions contradicted the experimental evidence. In the present paper we show that if a medium at rest is assumed and if this medium is not entrained by the moving bodies, the exact effect from MME is nil, i. e., the expected second-order effect was an artifact from the fact that the emission theory of light (essentially corpuscular in its nature) was applied to model the propagation of light in a continuous medium.

The best way to judge about the existence of the absolute medium is to stage first-order experiments (one way experiments). Along these lines are organized many experimental works, most notably [2, 3] where the sought effect was the anisotropy of speed of light. In our opinion, it is not quite clear how one can discriminate between an anisotropic speed of light on one hand and a first-order Doppler effect, on the other. Yet, we believe that the solution of the conundrum about the existence or nonexistence of an absolute continuum will be solved by a first-order experiment. To this end we also propose an interference experiment that should be able to measure the first-order effect. The most important thing is that first-order effect has actually been observed (see [2, 3], among others). This being said, one should be aware that the "second-order" re-interpretations of the slightly nontrivial results of [4] are also a valid avenue of research in the quest for detecting the absolute medium (or as the modern euphemism goes "the preferred frame"). In this connection, an important contribution seems to be [5]. Another source of higher-order effects can also be the local dependence of speed of light on the strength of the gravitational field. This kind of dependence is very important in any experiment conducted on Earth and in order to figure out the more subtle effects, one should use a theory in which the fundamental tensor of space affects the propagation of light. In the framework of the present approach it will result into a wave equation for the light which has non-constant coefficients, the latter depending on the curvature tensor. It goes beyond the scope of the present short note to delve into this more complicated case.

The aim of the present paper is to be understood in a very limited fashion: we show that the main effect of MME must be zero when it is considered in a purely Euclidean space without gravitational effects on the propagation of light. We

pose correctly the problem of propagation and reflection of waves in a resting medium when both the source and the mirror are moving with respect to the medium. We show that the strict result from the interference is nil which invalidates most of the conclusions drawn from the perceived nil effect of MME.

6 Conditions on moving boundaries

Here we follow [6] (see also [7] for application to MME) where emitter's Doppler effect was explained with boundary conditions (b. c.) on a moving boundary. Consider the $(1+1)\,D$ linear wave equation

$$\phi_{tt} = c^2 \phi_{xx}\,, \tag{1}$$

whose solution is the harmonic wave.

$$\phi\,(x,t) = e^{i\hat{k}x \pm i\hat{\omega}t}, \quad \text{where} \quad \hat{k} = \frac{\hat{\omega}}{c}\,, \tag{2}$$

where c is the characteristic speed and "$\pm$" signs refer to the left- and right-going waves, respectively.

Consider now a boundary (a point in 1D) moving with velocity u, at which a wave with temporal frequency ω is created. This means that the wave propagating inside the medium satisfies the following boundary condition

$$\begin{aligned}\phi\,(ut,t) = e^{i(\omega_1 t - k_1 x)} = e^{i\omega_1 (t - x/c)} = \\ = e^{i\omega_1 t(1-u/c)} = e^{i\omega t},\end{aligned} \tag{3}$$

where it is tacitly assumed that the right going wave is of interest. The above b. c. gives that

$$\omega_1 \left(1 - \frac{u}{c}\right) = \omega, \quad \rightarrow \quad \omega_1 = \frac{\omega}{1 - u/c}\,. \tag{4}$$

The last formula is the well known emitter's Doppler effect which shows how the frequency of the propagating wave is related to the frequency of the moving emitter

If the receiver is at rest, it will measure a frequency ω_1. The situation is completely different if the receiver is also moving, say with velocity v in the positive x-direction (to the right). Then due to the b. c. $\phi\,(vt,t) = e^{i\omega_1 t - i\frac{\omega_1}{c} vt} = e^{i\omega_2 t}$, the traveling wave of frequency ω_1 and wave number $k_1 = \frac{\omega_1}{c}$ will generate an oscillation of frequency ω_2 at the moving boundary point $x = vt$:

$$\omega_2 = \omega_1 \left(1 - \frac{v}{c}\right) = \omega\, \frac{1 - v/c}{1 - u/c}\,, \tag{5}$$

i. e., the measuring instruments in the moving frame of the receiver will detect a standing wave of frequency ω_2. We observe here that if the receiver is moving exactly with the speed of the emitter, then the frequency measured in receiver's frame will be exactly equal to emitter's frequency. In other words, a receiver that is moving with the same speed as the emitter does not observe a Doppler effect and cannot discover the motion.

This conclusion appears in an implicit form in the standard texts, e. g. [8, 9, p.164], where it is claimed that a Doppler effect is observed only for relative motion of the emitter and the receiver. Unfortunately, this correct observation did not lead to posing the question about the relevance of MME despite of the conspicuous lack of *relative motion* between the emitter and the receiver (mirror) in MME. The explanation in [8] was that "[F]or electromagnetic waves there evidently exists *no preferred frame*". We believe that the rigorous statement is that absolute rest (the "preferred frame") *cannot be detected* from measurements of Doppler effect between a source and a receiver which are moving together with identical speed through the absolute continuum.

After a consensus has been reached between the present work and the literature that the luminiferous continuum cannot be detected from an experiment in which a single source and a receiver are moving together as a non-deformable system, then the interesting question which remains is whether the absolute continuum can be detected when the emitter and the mirror are in relative motion, i. e. when they move with different speeds relative to the resting frame. To this end, consider now the situation when the receiver is a mirror which sends back a left going wave $e^{i\omega_3 t + ik_3 x}$ generated by the oscillations with frequency ω_2 at the point $x = vt$ namely, $e^{i\omega_3 t + ik_3 vt} = e^{i\omega_2 t}$. Then

$$\omega_3\,(1 + v/c) = \omega_2, \;\; \Rightarrow \;\; \omega_3 = \omega\, \frac{1 - v/c}{(1 + v/c)(1 - u/c)}\,. \tag{6}$$

Now, the wave of frequency ω_3 is traveling through the continuum to the left. The frequency, ω_4, of the wave excited on the *moving* surface of the emitter by this traveling wave has to satisfy the moving b. c. $e^{i\hat{\omega}_4} = e^{i(\hat{\omega}_3 t + \omega_3 \frac{u}{c} t)}$. Then

$$\omega_4 = \omega_3 \left(1 + \frac{u}{c}\right), \;\; \Rightarrow \quad \omega_4 = \omega\, \frac{(1 - v/c)(1 + u/c)}{(1 + v/c)(1 - u/c)}\,. \tag{7}$$

The above result is illustrated in Fig. 1.

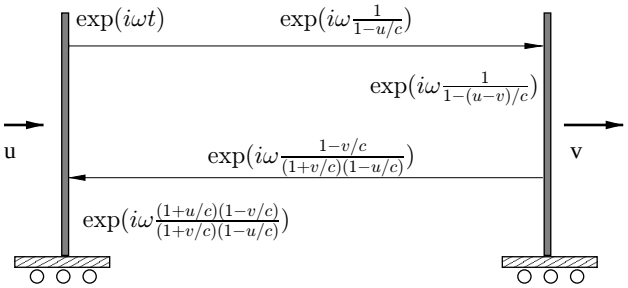

Fig. 1: Moving emitter and receiver

The case of waves propagating transversely to the emitter and receiver gives a trivial result in 1D, in the sense that the frequency and wave number of the propagating wave are not affected by the motion of the source or the receiver. The most general treatment for point source in 3D is given by

the eikonal equation [6, p.225] for the inhomogeneous wave equation that is obtained in a frame moving with prescribed speed in certain direction.

An interesting limiting case is presented when $u, v \ll c$. Then the product uv/c^2 can be neglected in comparison with $(u-v)/c$ (provided that $u-v \simeq \mathrm{O}(u)$) and the above formula reduces to

$$\omega_4 = \frac{1+(u-v)/c}{1-(u-v)/c},$$

which is the formula from [8, 9] for zero angle between the relative speed and the line of the emitter and observer. The discrepancies of order (uv/c^2) can be the cause of the so-called Pioneer anomaly [10]. It will be interesting to reexamine the raw data from Pioneer 10 eliminating the formula for relativistic Doppler effect and using in its place Eq. 7. Then what appears as an anomaly, can actually give the information about the absolute velocities of Earth and of the space ship. It is not necessary, of course, to go as far as Pioneer 10 and 11 went. The experiment can be done with an interferometer whose arms are the distances between two different satellites moving with different orbital speeds in the vicinity of Earth.

7 Michelson-Morley experiment (MME)

It was argued that because of the motion of the experimental equipment (the interferometer), the time taken by light to travel in the direction of motion will be different from the time needed to return, and these times together will differ from the time to travel in lateral direction. The argument that led to the prediction that the effect is of second order (see, [11, p.149], [1]) was typically corpuscular in its nature. The emission theory of light assumed that the "particles" of light were supposed to move in a resting continuum with velocity c. However when these particles were emitted by a moving surface in the direction of motion, they acquired speed $c+v$, whereas the particles emitted against the motion would move with speed $c-v$. The emission theory claimed that the total time for a ray to complete the full path in longitudinal direction is

$$t_1 = \frac{l}{c+v} + \frac{l}{c-v} = \frac{2l}{c(1-v^2/c^2)}, \qquad (8)$$

where l is the length of the longitudinal and transverse arms of the interferometer. The arguments about the nature of reflections in the transverse arm of the interferometer are similarly based on the emission theory. In the transverse direction the length of the path traveled by one light corpuscle is calculated using the Pythagorean theorem and the total time needed for the light particle to complete the return trip to the lateral mirror is given by (see [1])

$$t_2 = \frac{2l}{c}\sqrt{1+\frac{v^2}{c^2}}. \qquad (9)$$

Then the difference in the times needed to traverse the longitudinal and the transverse arms is

$$t_1 - t_2 \approx \frac{2l}{c}\left[1+2\frac{v^2}{c^2}-1-\frac{v^2}{c^2}+\mathrm{O}\left(\frac{v^4}{c^4}\right)\right] \approx l\,\frac{v^2}{c^2}. \qquad (10)$$

Under the standard analogies of corpuscular approach, at this point the arguments usually go back to the wave theory of light assuming that the change in travel time of light particles somehow materializes as change of the emitted or received frequency.

Although the scientific community gradually elevated MME to the status of one of the *experimenta crucis* for the theory of relativity, the above argument was never critically revisited after the postulate of the constancy of speed of light was accepted. The only work known to the present author is [12] where the emission theory and wave theory of Doppler effect are compared and shown to coincide within the first order in v/c but no conclusions about the actual applicability of the above corpuscular-based formula are made.

The problem with applying a corpuscular approach to a wave phenomenon in a medium is that a propagation speed $c+v$ is impossible since all propagation speeds are limited by the characteristic speed of the medium. Yet, the above derivations were repeated in [11, 13] and now feature prominently in many of the most authoritative modern textbooks, such as [9, 14]. So we are faced with a very peculiar situation: The formula used to explain the results of one of the most important for relativity theory experiments contradict the second postulate of the same theory.

The fallacy of the argumentation is as follows:

(i) The existence of a continuous medium in which the light propagates is stipulated (luminiferous continuum);

(ii) An irrelevant to continuum description theoretical formula is derived using the corpuscular concept of light (emission theory of light);

(iii) An experiment is designed for which it is believed that it can allow the measurement of the variable involved in the irrelevant theoretical formula;

(iv) Measurements obtained from the experiment do not show the expected effect;

(v) Conclusion is drawn that the contradiction is due to the fact that the original assumption of the presence of a continuum at rest is wrong;

(vi) The concept of existing of a material luminiferous continuum (i) is abandoned altogether.

This kind of fallacy is called *ignoratio elenchi* ("pure and simple irrelevance") and consists in using an argument that is supposed to prove one proposition but succeeds only in proving a different one. Clearly, there can be at least two causes for the nil result of the experiment. Before assuming that (i) is wrong, one has to examine (ii) from the point of view of the wave theory of light under the condition of

constancy of speed of light. The only way to pass judgment on the presence or absence of an absolute continuum is to derive a formula for the interference effect that is based on the assumption that the space between the different parts of the equipment is filled with a continuous medium in which the propagation speed of linear waves is a given constant. In doing so, the reflection from the mirror has to be treated as an excitation of a wave on moving material surface. Then the frequency of the excited wave (which then travels back as the reflected wave) is subject to the motion of the mirror itself. In this short note we make an attempt to correctly pose the problem (using the adequate mathematical approach to solving the wave equation with b. c. on moving boundaries) and to show the consequences of this for the interpretation of interferometry experiments involving moving mirrors that are moving translatory with respect to the supposed absolute continuum. Only after the proper theoretical formula based on the idea that the continuum is at rest and that the equipment is moving relative to it, is derived and only after the predictions of this *relevant* formula are found to contradict the experimental evidence, one rule out the existence of an absolute continuum at rest in which the light waves are propagating as shear waves in a material medium.

It has been shown above that if the source of light and the mirror are moving together with the same velocity relative to the resting medium, then the Doppler effect is strictly equal to zero. This means that no Doppler effect can be detected from an experiment in which the emitter and the mirror are moving together through a quiescent continuum. This means that a nil effect from the celebrated experiment of Michelson and Morley should be interpreted as an evidence about the existence of a material continuum at rest and that this absolute continuum is not entrained by the moving bodies. The flawed arguments of the emission theory of light introduced an error of $\mathrm{O}(v^2/c^2)$ in the formulas which was, in fact, the perceived effect in MME. At the same time, the correct solution (see the previous section) shows that the effect must be strictly nil provided that an absolute continuum fills the space between the different parts of the interferometer and that this continuum is not entrained.

8 A possible experimental set-up

If MME is irrelevant to detecting the absolute medium, then the question arises of is it possible at all to detect the latter by means of an interferometry experiment whose parts are moving together with the Earth. The answer (as already suggested in [7]) is in the positive if one can use two *independent* sources of light of virtually identical frequencies and avoid reflections. This means that one has to aim the beams against each other as shown in Fig. 2.

Assume now that two waves of identical frequencies are excited at two *different* points that are moving together in the same direction with the same velocity relative to the resting medium. The interference between the right-going wave from the left source and the left-going wave from the right source is given by

$$\begin{aligned} e^{i\omega(t-x/c)/(1-u/c)} + e^{i\omega(t+x/c)/(1+u/c)} = \\ = \left[\cos(\omega_1 t - k_1 x) + \cos(\omega_2 t + k_2 x)\right] + \\ + i\left[\sin(\omega_1 t - k_1 x) + \sin(\omega_2 t + k_2 x)\right] = \\ = 2\cos(\tilde{\omega} t + \hat{k} x)\exp\left[i(\hat{\omega} t + \tilde{k} x)\right], \end{aligned} \tag{11}$$

where

$$\tilde{\omega} = \frac{\omega_1+\omega_2}{2} = \omega\left(1-\frac{u^2}{c^2}\right), \quad \hat{\omega} = \frac{\omega_2-\omega_1}{2} = -\frac{u}{c}\tilde{\omega},$$

are the carrier and beat frequencies, and $\tilde{k} = \tilde{\omega}/c$, $\hat{k} = \hat{\omega}/c$. The wave excited at certain point, say $x = 0$, is

$$2\cos(\tilde{\omega} t)\exp(i\hat{\omega} t). \tag{12}$$

In Fig. 2 we show a possible experimental set-up which makes use of two independent sources of coherent light. Note that using two lasers, does not make our experiment similar to the set-up used in [15] because the latter involves mirrors and as it has been shown above, using mirrors dispels any possible effect.

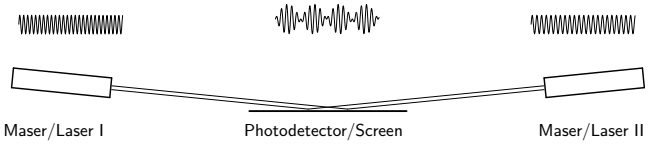

Fig. 2: Experimental set-up involving two lasers/masers

One of the ways to find the beat frequency is to use a photodetector in a point of the region of interference of the two waves. Note that the carrier frequency of the visible light is very high and cannot be detected in principle. The problem is that and even the beat frequency, Eq. 12, can be too high for the resolution of the available photodetectors. Apart from the fact that mirrors were used in [16], the high beat frequency could be another reason why it was not detected in those experiments. In fact they were after the beat frequency connected with the second-order effects and found practically no beat which is exactly what is to be expected in the light of the theory above presented. This is additional confirmation of the theory proposed here because we claim that no effect (neither first- nor second-order not higher-order) can exist if reflections are involved.

The other way to conduct the experiment is to measure the beat wave number $\hat{k}$ by taking a snapshot of the wave at certain moment of time. Then the spatial distribution of the wave amplitude is

$$2\cos(\hat{k}x)\,\exp(i\tilde{k}x), \tag{13}$$

which will produce an interference pattern in the resting continuum that can be observed on a screen (as shown

alternatively in Fig. 2). Note that in this case the screen is "parallel" or "tangent" to the vibrating part of the absolute continuum, and what is observed, are the dark and light strips corresponding the the different values of the amplitude of the beat wave. Clearly, the effect will be best observed if the two lasers beams have identical polarization.

The requirements for the frequency stabilization of the sources of light stem from the magnitudes of the beat frequency. It is accepted nowadays that the speed of the so-called Local Standard of Rest (LSR) to which solar system belongs, is of order of $v \approx 300$ km/s relative to the center of the local cluster of galaxies [17]. The speed of LSR is an upper estimate of the speed with respect to the absolute medium. This maximum can be reached only if the center of cluster of galaxies is at rest relative to the medium. Thus, the upper limit for the dimensionless parameter $\varepsilon = v/c$ is 10^{-3}, which places very stringent requirements on the resolution in case that a photodetector is involved. For red-light lasers, the beat frequency is of order of 600 GHz which is well beyond the sensitivity of the available photodetectors. This means that one should opt for terahertz masers when the beat frequency ω_b will be smaller than 1–3 GHz.

In the alternative implementation of the experimental set-up a detecting screen is used to get the spatial distribution of the interference pattern. In such a case, one can use standard visible-light lasers. For instance, the red light has wavelength approximately in the range of $600\,\mathrm{m}^{-9}$, then the beat wave length is expected to be $\varepsilon^{-1} \approx 1000$ times longer. This means 0.6 mm which is technically feasible to observe on a screen. Conversely, using terahertz masers in this case could make the wave length of the beat wave of order of 20–50 cm.

Now, in order to have reliable results from the proposed interferometry experiment, one needs frequency stabilization a couple of orders of magnitude better than the sought effect. To be on the safe side, we mention that the lowest value for ε is 10^{-4} which corresponds to the orbital speed of Earth. Then the best stabilization of the frequency needed is 10^{-7}. This is well within the stabilization limits for the currently available low-power lasers. For example, Coherent, Inc. offers the series 899-21 that are Actively Stabilized, Scanning Single-Frequency Ring Lasers with stabilization 10^{-9}.

9 Conclusion

The theory of Michelson-Morley interference experiment is revisited from the point of view of the wave theory of light. The fallacy of using the accepted formula based on the emission theory of light is shown and new formulas are derived based on the correct posing of the boundary conditions at moving boundaries for a hyperbolic equation. It is shown that when the source of light and the reflector are moving with the same speed through a non-entrained absolute continuum, the reflected wave as received back at the emitter's place shows no Doppler shift, and hence no fringes can be expected. The situation is different if the emitter and the reflector are in relative motion with respect to each other. The meaning of the results of the present work is that the only correct conclusion from a nil effect from interferometry experiment involving reflection is not that absolute medium does not exist, but that an absolute continuum exist which is not entrained by the motion of the measuring instrument (the system of emitters and mirrors). Naturally, the nil effect of Michelson-Morley experiment should not be used as the sole verification of the absolute medium and to this end a new experimental set-up is proposed.

References

1. Michelson A. A., Morley E. W. On the relat. motion of the earth and the luminiferous ether. *Am. J. Sci.*, 1887, v.34, 333–345.
2. Torr D. G., Kolen P. An experiment to measure relative variations in the one-way velocity of light. *Prec. Measur. Fund. Const. II*, Natl. Bur. Stand. (US), Sp. Publ. 617, 1984, 675–679.
3. Krisher T.P., Maleki L., Lutes G.F., Primas L.E., Logan R.T., Anderson J. D. Test of isotropy of the one-way speed of light using hydrogen-maser standards. *Phys. Rev. D*, 1990, v. 42, 731–734.
4. Miller D. C. The ether-drift experiment and the determination of the absolute motion of earth. *Reviews of Modern Physics*, 1933, v. 5, 203–242.
5. Cahill R. T. The Michelson and Morley 1887 experiment and the discovery of absolute motion. *Progress in Physics*, 2005, v. 3, 25–29.
6. Whitham G. B. Linear and nonlinear waves. Wiley, NY, 1974.
7. Christov C. I. Discrete out of continuous: Dynamics of phase patterns in continua. *Continuum Models and Discrete Systems — Proc. of CMDS8*, World Sci., Singapore, 1996, 370–394.
8. Elmore W. C., Heald M. A. Physics of waves. Dover, NY, 1969.
9. Dichtburn R. W. Light, volume 1. Acad. Press, London, 1976.
10. Anderson J. D., Laing P. A., Lau E. L., Liu A. S., Nieto M. M., Turyshev S. G. Study of the anomalous acceleration of Pioneer 10 and 11. *Phys. Rev. D*, 2002, v. 65, 082004.
11. Michelson A. A. Studies in optics. Univ. Chicago Press, 1927.
12. Tolman R. C. The second postulate of relativity. *Physical Review*, 1910, v. 31, 26–40.
13. Lorentz H. A. The theory of electrons and its applications to the phenomena of light and radiant heat. Dover, NY, 1952.
14. Hecht E., Zajaz A. Optics. Adison-Wesley, Reading, 1974.
15. Jaseda T. S., Javan A., Townes C. H. Frequency stability of He-Ne masers and measurements of length. *Phys. Rev. Lett.*, 1963, v. 10, 165–167.
16. Jaseda T. S., Javan A., Murray J, Townes C. H. Test of special relativity or of the isotropy of space by use of infrared masers. *Phys. Rev. A*, 1964, v. 113, 1221–1225.
17. Smoot G. F., Gorenstein M. V., Miller R. A. Detection of anisotropy in the Cosmic Blackbody Radiation. *Phys. Rev. Lett.*, 1977, v. 39, 898–901.

The Roland De Witte 1991 Experiment (to the Memory of Roland De Witte)

Reginald T. Cahill

School of Chemistry, Physics and Earth Sciences, Flinders University, Adelaide 5001, Australia

E-mail: Reg.Cahill@flinders.edu.au

In 1991 Roland De Witte carried out an experiment in Brussels in which variations in the one-way speed of RF waves through a coaxial cable were recorded over 178 days. The data from this experiment shows that De Witte had detected absolute motion of the earth through space, as had six earlier experiments, beginning with the Michelson-Morley experiment of 1887. His results are in excellent agreement with the extensive data from the Miller 1925/26 detection of absolute motion using a gas-mode Michelson interferometer atop Mt. Wilson, California. The De Witte data reveals turbulence in the flow which amounted to the detection of gravitational waves. Similar effects were also seen by Miller, and by Torr and Kolen in their coaxial cable experiment. Here we bring together what is known about the De Witte experiment.

Preface of the Editor-in-Chief

Today, on the 15th anniversary of De Witte's experiment, I would like to comment on an erroneous discussion of the "supposed disparity" between the De Witte results and Einstein's Principle of Relativity, and the whole General Theory of Relativity, due to the measured anisotropy of the velocity of light. The same should be said about the Torr-Kolen experiment (1981, Utah State Univ., USA) and the current experiment by Cahill (Flinders Univ., Australia).

The discussion was initiated by people having a poor knowledge of General Relativity, having learnt it from "general purpose" books, and bereft of native abilities to learn even the basics of tensor calculus and Riemannian geometry — mainly so-called "anti-relativists" and mere anti-semites, to whom Einstein's genius and discoveries give no rest.

Roland De Witte was excellent experimentalist, not a master in theory. He was misled about the "disparity" by the anti-relativists, that resulted his deep depression and death.

It is well known that in a four-dimensional pseudo-Riemannian space (the basic space-time of General Relativity), the velocity of light c is said to be general covariantly invariant; its value is independent of the reference frame we use. However a real observer is located in his three-dimensional spatial section $x^0 = \text{const}$ (inhomogeneous, curved, and deforming), pierced by time lines $x^i = \text{const}$ (also inhomogeneous and curved). The space can bear a gravitational potential $\mathrm{w} = c^2(1-\sqrt{g_{00}})$, and be non-holonomic — the time lines are non-othogonal to the spatial section, that is displayed as the space three-dimensional rotation at the linear velocity $v_i = -c\frac{g_{0i}}{\sqrt{g_{00}}}$. These factors lead to the fact that the physically observable time interval is $d\tau = \sqrt{g_{00}}\,dt - \frac{1}{c^2}\,v_i dx^i$, which is different to the coordinate time interval dt. Anyone can find all this in *The Classical Theory of Fields* by Landau and Lifshitz [1], the bible of General Relativity, and other literature.

The complete theory of physically observable quantities was developed in the 1940's by Abraham Zelmanov, by which the observable quantities are determined by the projections of four-dimensional quantities onto an observer's real time line and spatial section. (See [2,3,4,5] and References therein.) From this we see that the physically observable velocity of light is a three-dimensional vector $c^i = \frac{dx^i}{d\tau}$ dependent on the gravitational potential and the space non-holonomity (rotation) through the physically observable time interval $d\tau$. In particular, c^i can be distributed anisotropically in the spatial section, if it completely rotates. At the same time the complete general covariantly invariant c remains unchanged.

Therefore the anisotropy of the observed value of the velocity of light does not contradict Einstein's Principle of Relativity. On the contrary, such an experimental result can be viewed as a new verification of Einstein's theory.

Moreover, as already shown by Zelmanov [2] in the 1940's, General Relativity's space permits absolute reference frames connected to the anisotropy of the fields of the spatial non-holonomity or deformation, i. e. connected to globally polarized fields which are likely a global background giro. Therefore, absolute reference frames connected to the spatial anisotropy of the velocity of light or the Cosmic Microwave Background can also be viewed as additional verifications of General Relativity.

Roland De Witte didn't published his experimental results. All we possess subsequent to his death is his public letter of 1998 and letters to his colleagues wherein he described his experimental set up in detail. I therefore asked Prof. Cahill to prepare a brief description of the De Witte experiment so that any interested person may thereby have a means of referring to De Witte's results as published. Reginald T. Cahill is an expert in such experimental techniques and currently prepares a new experiment, similar to that by De Witte (but with a precision in measurement a thousand times greater using current technologies). Therefore his description of the De Witte experiment is accurate.

Dmitri Rabounski

[1] Landau L. D., Lifshitz E. M. The classical theory of fields. 4th ed., Butterworth–Heinemann, 1980.

[2] Zelmanov A. L. Chronometric invariants. Dissertation thesis, 1944. 2nd ed., American Research Press, Rehoboth (NM), 2006.

[3] Zelmanov A. L. Chronometric invariants and co-moving coordinates in the general relativity theory. *Doklady Acad. Nauk USSR*, 1956, v. 107(6).

[4] Zelmanov A. L., Agakov V. G. Elements of General Relativity. Moscow, Nauka, 1988.

[5] Rabounski D. Zelmanov's anthropic principle and the infinite relativity principle. *Progress in Physics*, 2006, v. 1.

1 Introduction


R. De Witte

Ever since the 1887 Michelson-Morley experiment [1] to detect absolute motion, that is motion relative to space, by means of the anisotropy of the speed of light, physicists in the main have believed that such absolute motion was unobservable, and even meaningless. This was so after Einstein proposed as one of his postulates for his Special Theory of Relativity that the speed of light is invariant quantity. However the Michelson-Morley experiment did observe small fringe shifts of the form indicative of an anisotropy of the light speed*. The whole issue has been one of great confusion over the last 100 years or so. This confusion arose from deep misunderstandings of the theoretical structure of Special Relativity, but also because ongoing detections of the anisotropy of the speed of light were treated with contempt, rather than being rationally discussed. The intrinsic problem all along has been that the observed anisotropy of the speed of light also affects the very apparatus being used to measure the anisotropy. In particular the Lorentz-Fitzgerald length contraction effect must be included in the analysis of the interferometer when the calibration constant for the device is calculated. The calibration constant determines what value of the speed of light anisotropy is to be determined from an observed fringe shift as the apparatus is rotated. Only in 2002 was it discovered that the calibration constant is very much smaller than had been assumed [2, 3], and that the observed fringe shifts corresponded to a speed in excess of 0.1% of the speed of light. That discovery showed that the presence of a gas in the light path is essential if the interferometer is to act as a detector of absolute motion, and that a vacuum operated interferometer is totally incapable of detecting absolute motion. That physics has suppressed this effect for over 100 years is a major indictment of physics. There have been in all seven detections of such anisotropy, with five being Michelson interferometer experiments [1, 4, 5, 6, 7], and two being one-way RF coaxial cable propagation time experiments, see [9, 10] for extensive discussion and analysis of the experimental data. The most thorough interferometer experiment was by Miller in 1925/26. He accumulated sufficient data that in conjunction with the new calibration understanding, the velocity of motion of the solar system could be determined† as ($\alpha = 5.2^{\text{hr}}$, $\delta = -67^\circ$), with a speed of 420 ± 30 km/s. This local (in the galactic sense) absolute motion is different from the Cosmic Microwave Background (CMB) anisotropy determined motion, in the direction ($\alpha = 11.20^{\text{hr}}$, $\delta = -7.22^\circ$) with speed 369 km/s; this is motion relative to the source of the CMB, namely relative to the distant universe.

*The older terminology was that of detecting motion relative to an *ether* that was embedded in a geometrical space. However the more modern understanding does away with both the ether and a geometrical space, and uses a structured dynamical *3-space*, as in [9, 10].

†There is a possibility that the direction is opposite to this direction.

The first one-way coaxial cable speed-of-propagation experiment was performed at the Utah State University in 1981 by Torr and Kolen [8]. This involved two rubidium vapor clocks placed approximately 500 m apart with a 5 MHz sinewave RF signal propagating between the clocks via a buried nitrogen filled coaxial cable maintained at a constant pressure of ~ 2 psi. Unfortunately the cable was orientated in an East-West direction which is not a favourable orientation for observing absolute motion in the Miller direction. There is no reference to Miller's result in the Torr and Kolen paper, otherwise they would presumably not have used this orientation. Nevertheless there is a small projection of the absolute motion velocity onto the East-West cable and Torr and Kolen did observe an effect in that, while the round speed time remained constant within $0.0001\%\, c$, variations in the one-way travel time were observed. The maximum effect occurred, typically, at the times predicted using the Miller velocity [9, 10]. So the results of this experiment are also in remarkable agreement with the Miller direction, and the speed of 420 km/s. As well Torr and Kolen reported fluctuations in both the magnitude, from 1–3 ns, and the time of maximum variations in travel time.

However during 1991 Roland De Witte performed the most extensive RF travel time experiment, accumulating data over 178 days. His data is in complete agreement with the 1925/26 Miller experiment. These two experiments will eventually be recognised as two of the most significant experiments in physics, for independently and using different experimental techniques they detected the same velocity of absolute motion. But also they detected turbulence in the flow of space past the earth; non other than gravitational waves. Both Miller and De Witte have been repeatably attacked for their discoveries. Of course the experiments indicated the anisotropy of the speed of light, but that is not in conflict with the confirmed correctness of various relativistic effects. While Miller was able to publish his results [4], and indeed the original data sheets were recently discovered at Case Western Reserve University, Cleveland, Ohio, De Witte was never permitted to publish his data in a physics journal. The only source of his data was from a e-mail posted in 1998, and a web page that he had established. This paper is offered as a resource so that De Witte's extraordinary discoveries may be given the attention and study that they demand, and that others may be motivated to repeat the experiment, for that is the hallmark of science‡.

2 The De Witte experiment

In a 1991 research project within Belgacom, the Belgium telcommunications company, another (serendipitous) detection of absolute motion was performed. The study was undertaken by Roland De Witte. This organisation had two sets of atomic

‡The author has been developing and testing new techniques for doing one-way RF travel time experiments.

clocks in two buildings in Brussels separated by 1.5 km and the research project was an investigation of the task of synchronising these two clusters of atomic clocks. To that end 5 MHz radio frequency (RF) signals were sent in both directions through two buried coaxial cables linking the two clusters. The atomic clocks were caesium beam atomic clocks, and there were three in each cluster: A1, A2 and A3 in one cluster, and B1, B2, and B3 at the other cluster. In that way the stability of the clocks could be established and monitored. One cluster was in a building on Rue du Marais and the second cluster was due south in a building on Rue de la Paille. Digital phase comparators were used to measure changes in times between clocks within the same cluster and also in the propagation times of the RF signals. Time differences between clocks within the same cluster showed a linear phase drift caused by the clocks not having exactly the same frequency, together with short term and long term noise. However the long term drift was very linear and reproducible, and that drift could be allowed for in analysing time differences in the propagation times between the clusters.

The atomic clocks (OSA 312) and the digital phase comparators (OS5560) were manufactured by Oscilloquartz, Neuchâtel, Switzerland. The phase comparators produce a change of 1 V for a phase variation of 200 ns between the two input signals. At both locations the comparison between local clocks, A1–A2 and A1–A3, and between B1–B2, B1–B3, yielded linear phase variations in agreement with the fact that the clocks have not exactly the same frequencies due to the limited reproducible accuracy together with a short term and long term phase noise (A. O. Mc Coubrey, *Proc. of the IEEE*, Vol. 55, No. 6, June, 1967, 805–814). Even if the long term frequency instability were 2×10^{-13} this is able to produce a phase shift of 17 ns a day, but this instability was not often observed and the ouputs of the phase comparators have shown that the local instability was typically only a few nanoseconds a day (5 ns) between two local clocks.

But between distant clocks A1 toward B1 and B1 toward A1, in addition to the same linear phase variations (but with identical positive and negative slopes, because if one is fast, the other is slow), there is also an additional clear sinusoidal-like phase undulation ($\approx$ 24 h period) of the order of 28 ns peak to peak.

The possible instability of the coaxial lines cannot be responsible for the phase effects observed because these signals are in phase opposition and also because the lines are identical (same place, length, temperature, etc. . .) causing the cancellation of any such instabilities. As well the experiment was performed over 178 days, making it possible to measure with accuracy ($\pm$ 25 s) the period of the phase signal to be the sidereal day (23 h 56 min), thus permitting to conclude that absolute motion had been detected, even with apparent turbulence.

According to the manufacturer of the clocks, the typical humidity sensitivity is $df/f = 10^{-14}$ % humidity, so the effect observed between two distant clocks (24 ns in 12 h) needs, for example, a differential step of variation of humidity of 55%, two times a day, over 178 days. So the humidity variations cannot be responsible for the persistent periodic phase shift observed. As for pressure effects, the manufacturer confirmed that no measurable frequency change during pressure variations around 760 mm Hg had been observed. When temperature effects are considered, the typical sensitivity around room temperature is $df/f = 0.25\times10^{-13}$ °C and implies, for example, a differential step of room temperature variation of 24°C, two times a day, over 178 days to produce the observed time variations. Moreover the room temperature was maintained at nearly a constant around 20°C by the thermostats of the buildings. So the possible temperature variations of the clocks could not be responsible for the periodic phase shift observed between distant clocks. As well the heat capacity of the housings of the clocks would even further smooth out possible temperature variations. Finally, the typical magnetic sensitivity of $df/f = 1.4\times10^{-13}$ Gauss needs, for example, differential steps of field induction of 4 Gauss variation, two times a day, over 178 days. But the terrestrial magnetic induction in Belgium is only in the order of 0.2 Gauss and thus its variations are much less (except during a possible magnetic storm). As for possible parasitic variable DC currents in the vicinity of the clocks, a 4 Gauss change needs a variation of 2000 amperes in a conductor at 1 m, and thus can be excluded as a possible effect. So temperature, pressure, humidity and magnetic induction effects on the frequencies of the clocks were thus completely negligible in the experiment.

Changes in propagation times were observed over 178 days from June 3 1991 7 h 19 m GMT to 27 Nov 19 h 47 m GMT and recorded. A sample of the data, plotted against sidereal time for just three days, is shown in Fig. 1. De Witte recognised that the data was evidence of absolute motion but he was unaware of the Miller experiment and did not realise that the Right Ascension for minimum/maximum propagation time agreed almost exactly with Miller's direction ($\alpha = 5.2^{\mathrm{hr}}$, $\delta = -67°$). In fact De Witte expected that the direction of absolute motion should have been in the CMB direction, but that would have given the data a totally different sidereal time signature, namely the times for maximum/minimum would have been shifted by 6 hrs. The declination of the velocity observed in this De Witte experiment cannot be determined from the data as only three days of data are available. However assuming exactly the same declination as Miller the speed observed by De Witte appears to be also in excellent agreement with the Miller speed, which in turn is in agreement with that from the Michelson-Morley and other experiments.

Being 1st-order in v/c the Belgacom experiment is easily analysed to sufficient accuracy by ignoring relativistic effects, which are 2nd-order in v/c. Let the projection of the

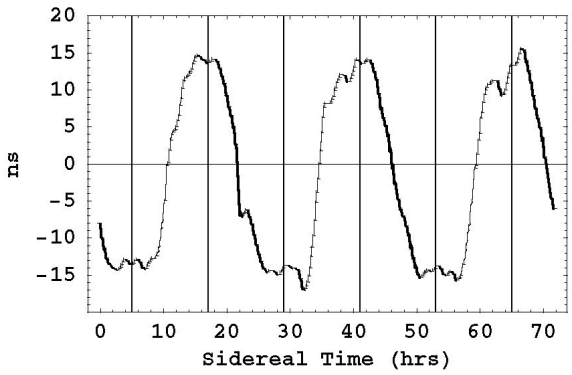

Fig. 1: Variations in twice the one-way travel time, in ns, for an RF signal to travel 1.5 km through a buried coaxial cable between Rue du Marais and Rue de la Paille, Brussels, by subtracting the Paille Street phase shift data from the Marais Street phase shift data. An offset has been used such that the average is zero. The cable has a North-South orientation, and the data is $\pm$ difference of the travel times for NS and SN propagation. The sidereal time for maximum effect of $\sim$5 hr (or $\sim$17 hr) (indicated by vertical lines) agrees with the direction found by Miller [4]. Plot shows data over 3 sidereal days and is plotted against sidereal time. The main effect is caused by the rotation of the earth. The superimposed fluctuations are evidence of turbulence i.e gravitational waves. Removing the earth induced rotation effect we obtain the first experimental data of the turbulent structure of space, and is shown in Fig. 2. De Witte performed this experiment over 178 days, and demonstrated that the effect tracked sidereal time and not solar time, as shown in Fig. 3.

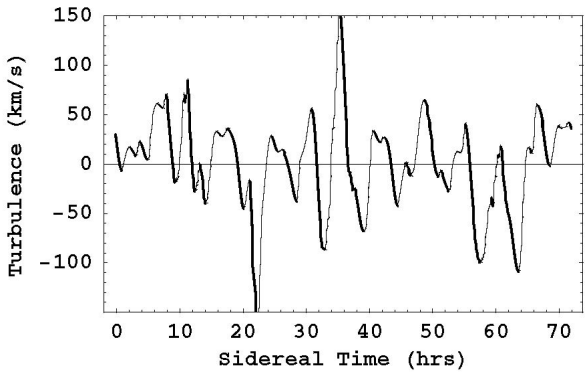

Fig. 2: Shows the speed fluctuations, essentially "gravitational waves" observed by De Witte in 1991 from the measurement of variations in the RF coaxial-cable travel times. This data is obtained from that in Fig. 1 after removal of the dominant effect caused by the rotation of the earth. Ideally the velocity fluctuations are three-dimensional, but the De Witte experiment had only one arm. This plot is suggestive of a fractal structure to the velocity field. This is confirmed by the power law analysis shown in Fig. 4. From [11].

absolute velocity vector $\mathbf{v}$ onto the direction of the coaxial cable be v_P. Then the phase comparators reveal the *difference* between the propagation times in NS and SN directions. Consider a simple analysis to establish the magnitude of the observed speed.

$$\Delta t = \frac{L}{\frac{c}{n} - v_P} - \frac{L}{\frac{c}{n} + v_P} = \\ = 2\,\frac{L}{c/n}\,n\,\frac{v_P}{c} + \mathrm{O}\left(\frac{v_P^2}{c^2}\right) \approx 2t_0\,n\,\frac{v_P}{c}\,.$$

Here $L = 1.5$ km is the length of the coaxial cable, $n = 1.5$ is the assumed refractive index of the insulator within the coaxial cable, so that the speed of the RF signals is approximately $c/n = 200,000$ km/s, and so $t_0 = nL/c = 7.5\times10^{-6}$ sec is the one-way RF travel time when $v_P = 0$. Then, for example, a value of $v_P = 400$ km/s would give $\Delta t = 30$ ns. De Witte reported a speed of 500 km/s. Because Brussels has a latitude of 51° N then for the Miller direction the projection effect is such that v_P almost varies from zero to a maximum value of $|\mathbf{v}|$. The De Witte data in Fig. 1 shows Δt plotted with a false zero, but shows a variation of some 28 ns. So the De Witte data is in excellent agreement with the Miller's data.

The actual days of the data in Fig. 1 are not revealed by De Witte so a detailed analysis of the data is not possible. If all of De Witte's 178 days of data were available then a detailed analysis would be possible.

De Witte does however reveal the sidereal time of the cross-over time, that is a "zero" time in Fig. 1, for all 178 days of data. This is plotted in Fig. 3 and demonstrates that the time variations are correlated with sidereal time and not local solar time. A least squares best fit of a linear relation to that data gives that the cross-over time is retarded, on average, by 3.92 minutes per solar day. This is to be compared with the fact that a sidereal day is 3.93 minutes shorter than a solar day. So the effect is certainly galactic and not associated with any daily thermal effects, which in any case would be very small as the cable is buried. Miller had also compared his data against sidereal time and established the same property, namely that, up to small diurnal effects identifiable with the earth's orbital motion, the dominant features in the data tracked sidereal time and not solar time, [4].

The De Witte data is also capable of resolving the question of the absolute direction of motion found by Miller. Is the direction ($\alpha = 5.2^{\mathrm{hr}}$, $\delta = -67°$) or the opposite direction? Being a 2nd-order Michelson interferometer experiment Miller had to rely on the earth's orbital effects in order to resolve this ambiguity, but his analysis of course did not take account of the gravitational in-flow effect [9, 10]. The De Witte experiment could easily resolve this ambiguity by simply noting the sign of Δt. Unfortunately it is unclear as to how the sign in Fig. 1 is actually defined, and De Witte does not report a direction expecting, as he did, that the direction should have been the same as the CMB direction.

The dominant effect in Fig. 1 is caused by the rotation of the earth, namely that the orientation of the coaxial cable with respect to the direction of the flow past the earth changes as the earth rotates. This effect may be approximately unfolded from the data, see [9, 10], leaving the gravitational waves shown in Fig. 2. This is the first evidence that the velocity

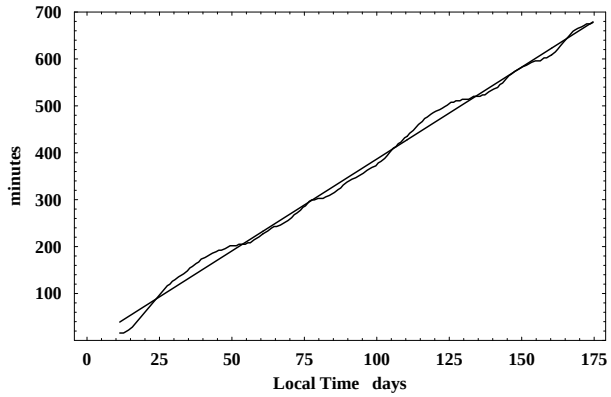

Fig. 3: Plot of the negative of the drift of the cross-over time between minimum and maximum travel-time variation each day (at $\sim 10^{\mathrm{h}} \pm 1^{\mathrm{h}}$ ST) versus local solar time for some 178 days, from June 3 1991 7 h 19 m GMT to 27 Nov 19 h 47 m GMT. The straight line plot is the least squares fit to the experimental data, giving an average slope of 3.92 minutes/day. The time difference between a sidereal day and a solar day is 3.93 minutes/day. This demonstrates that the effect is related to sidereal time and not local solar time.

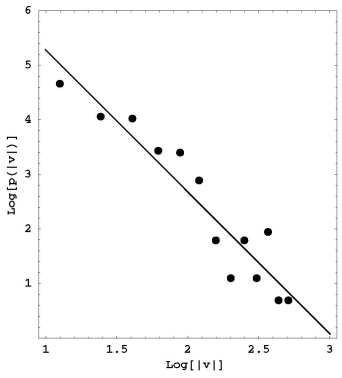

Fig. 4: Shows that the speed fluctuations in Fig. 2 are scale free, as the probability distribution from binning the speeds has the form $p(v) \propto |v|^{-2.6}$. This plot shows $\log[p(v)]$ vs $|v|$. From [11].

field describing the flow of space has a complex structure, and is indeed fractal. The fractal structure, i.e. that there is an intrinsic lack of scale to these speed fluctuations, is demonstrated by binning the absolute speeds $|v|$ and counting the number of speeds $p(|v|)$ within each bin. Plotting $\log[p(|v|)]$ vs $|v|$, as shown in Fig. 4 we see that $p(v) \propto |v|^{-2.6}$. The Miller data also shows evidence of turbulence of the same magnitude. So far the data from three experiments, namely Miller, Torr and Kolen, and De Witte, show turbulence in the flow of space past the earth. This is what can be called gravitational waves [9, 10].

3 Biography of De Witte

These short notes were extracted from De Witte's webpage.

Roland De Witte was born September 29, 1953 in the small village of Halanzy in the south of Belgium. He became the apprentice to an electrician and learned electrical wiring of houses. At the age of fourteen he decided to take private correspondence courses in electronics from the EURELEC company, and obtained a diploma at the age of sixteen. He decided to stop work as an apprentice and go to school. Without a state diploma it was impossible for him to be admitted into an ordinary school with teenagers of his age. After working for a scrap company where he used dynamite, he was finally admitted into a secondary school with the assistance of the director, but with the condition that he pass some tests from the board of the state examiners, called the Central Jury, for the first three years. After having sat the exams he became a legitimate schoolboy. But when he was in the last but one year in secondary school he decided to prepare for the entrance exam in physics at the University of Liège, and became a university student in physics one year before his friends. During secondary school years he was interested in all the scientific activities and became a schoolboy president of the Scientific Youths of the school in Virton. Simple physics experiments were performed: Millikan, photoelectric effect, spectroscopy, etc... and a small electronics laboratory was started. He also took part in different scientific short talks contests, and became a prizewinner for a talk about "special relativity", and received a prize from the Belgian Shell Company which had organised the contest. De Witte even visited the house where Einstein lived for a few months in Belgium when he left Germany. The house is the "Villa Savoyarde" at "Coq-Sur-Mer" Belgium, and is just 200 m from the North Sea. During secondary school De Witte had hobbies such as astronomy and pirate radio transmission on 27 Mhz with a hand-made transmitter, with his best long distance communication being with Denmark.

De Witte says that he is not able to study by "heart", and during secondary school, even with his bad memory which caused problems in history and english, he nevertheless always achieved the maximum of points in physics, chemistry and mathematics and was the top of his class. At University he obtained the diploma from the two year degree in physics but was not able to continue due to the "impossibility to study by heart several thousands of pages of erroneous calculations" like the others did to obtain the graduate diploma. Thus even though considered to be intelligent by several teachers, he decided to leave the University and became the manager of a retail electronic components shop. He did this job for ten years while also performing his physics experiments and studying theoretical physics. He was interested in microwaves and became an IEEE member and reader of the publications of the Microwave Theory & Techniques and Instrumentation & Measurement Societies. During that period he built an electron spin resonance spectrometer for the pleasure of studying the electron and free radicals. By chance he was invited by Dr. Yves Lion of the Physics Institute of the University of Liège to help them for a few weeks in their researches on the photoionisation mechanism of the tryptophan amino-acid with the powerful EPR spectrometer. He was also interested in TV satellite reception and Meteosat images. He built several microwave microstrip circuits such as an 18 dB

low noise amplifier using GaAs-Fets for 11.34 GHz. He also developed some apparatus using microprocessors for a digital storage system for Meteosat's images.

In 1990 he became a civil servant in the Metrology Department of the Transmission Laboratories of Belgacom (Belgium Telephone Company). His job was to test the synchronization of rubidium frequency standards on a distant master ceasium beam clock. It is there that he took the time to compare the phase of distant ceasium clocks and discovered the periodic phase shift signal with a sidereal day period. De Witte retired from the Department, reporting that he had been dismissed, and worked on theoretical physics and philosophy of science, while performing various cheap experiments to test his electron theory and also develop a new working process for a beamless ceasium clock.

De Witte acknowledged assistance from J. Tamborijn, the Engineer Cerfontaine, and particularly Engineer and Executive Director B. Daspremont, all from the Metrology, Fiber Optics and Transmission Laboratory of Belgacom in Brussels, for the use of the six caesium atomic clocks, the comparators, the recorder and the underground lines, and also Paul Pàquet, Director of the Royal Observatory of Belgium, for explanations and documentation provided about the realisation of UTC in Belgium.

4 De Witte's letter

Roland De Witte was not able to have his experimental results published in a physics journal. His only known publications are that of an e-mail posted to the newsgroup sci.physics.research. The e-mail is reproduced here:

> * Subject: Ether-wind detected!
> * From: "DE WITTE Roland" <roland.dewitte@ping.be>
> * Date: 07 Dec 1998 00:00:00 GMT
> * Approved: baez@math.ucr.edu
> * Newsgroups: sci.physics.research
> * Organization: EUnet Belgium, Leuven, Belgium
>
> I have performed an interesting experiment with cesium beam frequency standards.
>
> A 5 Mhz signal from one clock (A) is sent to another clock (B) 1.5 km apart in Brussels by the use of an underground coaxial cable of the Belgium Telephone Company. There, the 5Mhz signal from clock A is compared to the one of clock B, by the use of a digital phase comparator (like those used in PLL).
>
> Incredibly, the output of the phase comparator shows a clear and important sinus-like undulation which permits to conclude of the existence of a periodic variation (24 h period) of the speed of light in the coaxial cable around 500 km/s.
>
> In performing the experiment during 178 days, with six caesium beam clocks, the period of the phase signal has been accurately measured and is 23 h 56 m $\pm$25 s. and thus is the sidereal day.
>
> This result, like the one of D. G. Torr and P. Kolen (Natl. Bur. Stand. (U.S.), Spec. Publ. 617, 1984) is well understood with a new space-time theory based on a new electron theory.
>
> It is also the case for the nearly negative result of the experiment of Krisher et al., with a fiber optics instead of a coaxial cable (Physical Review D, Vol. 42, Number 2, 1990, pp. 731–734).
>
> All the details of the experiment is on my web-site under construction: www.ping.be/electron/belgacom.htm together with already a few arguments against Einstein's special theory of relativity.
>
> DE WITTE Roland
> www.ping.be/electron
>
> [Moderator's note: needless to say, there are many potential causes of daily variations that need to be studied in interpreting an experiment of this sort. — jb]

5 Conclusions

The De Witte experiment was truly remarkable considering that initially it was serendipitous. DeWiite's data like that of Miller is extremely valuable and needs to be made available for detailed analysis. Regrettably Roland De Witte has died, and the bulk of the data was apparently lost when he left Belgacom.

References

1. Michelson A. A. and Morley E. W. *Philos. Mag.*, 1887, S. 5, v. 24, No. 151, 449–463.
2. Cahill R. T. and Kitto K. Michelson-Morley experiments revisited. *Apeiron*, 2003, v. 10(2), 104–117.
3. Cahill R. T. The Michelson and Morley 1887 experiment and the discovery of absolute motion. *Progress in Physics*, 2005, v. 3, 25–29.
4. Miller D. C. *Rev. Mod. Phys.*, 1933, v. 5, 203–242.
5. Illingworth K. K. *Phys. Rev.*, 1927, v. 3, 692–696.
6. Joos G. *Ann. d. Physik* 1930, Bd. 7, 385.
7. Jaseja T. S. *et al. Phys. Rev. A*, 1964, v. 133, 1221.
8. Torr D. G. and Kolen P. *Precision Measurements and Fundamental Constants*, Taylor B. N. and Phillips W. D. eds. Natl. Bur. Stand. (U.S.), Spec. Pub., 1984, v. 617, 675.
9. Cahill R. T. Process Physics: From information theory to quantum space and matter. Nova Science Pub., NY, 2005.
10. Cahill R. T. Absolute motion and gravitational effects. *Apeiron*, 2004, v. 11, 53–111.
11. Cahill R. T. Dynamical fractal 3-Space and the generalised Schrödinger equation: Equivalence principle and vorticity effects. *Progress in Physics*, 2006, v. 1, 27–34.

Effect of Alpha-Particle Energies on CR-39 Line-Shape Parameters using Positron Annihilation Technique

M. A. Abdel-Rahman*, M. Abdel-Rahman*, M. Abo-Elsoud†, M. F. Eissa†, Y. A. Lotfy*, and E. A. Badawi*

*Physics Department, Faculty of Science, Minia University, Egypt
†Physics Department, Faculty of Science, Beni-suef University, Egypt
E-mail: maboelsoud24@yahoo.com <M. Abo-Elsoud>; emadbadawi@yahoo.com <E. A. Badawi>

Polyally diglycol carbonate "CR-39" is widely used as etched track type particle detector. Doppler broadening positron annihilation (DBPAT) provides direct information about core and valance electrons in (CR-39) due to radiation effects. It provides a non-destructive and non-interfering probe having a detecting efficiency. This paper reports the effect of irradiation α-particle intensity emitted from ^{241}Am (5.486 MeV) source on the line shape S- and W-parameters for CR-39 samples. Modification of the CR-39 samples due to irradiation were studied using X-ray diffraction (XRD) and scanning electron microscopy (SEM) techniques.

1 Introduction

Polyallyl diglycol carbonate ($C_{12}H_{18}O_7, \rho = 1310\,kg/m^3$) is a thermoset polymer [1]. Polyallyl diglycol carbonate, CR-39, has been used in heavy ion research such as composition of cosmic rays, heavy ion nuclear reactions, radiation dose due to heavy ions, exploration of extra heavy elements etc. Its availability in excellent quality from different manufactures is also an advantage for further applications [1].

Swift heavy ions (SHI) produce permanent damage in polymeric materials as latent tracks along their path due to dissociation of valence bonds, cross linking and formation of free radicals [2, 3].

Positron Annihilation Technique (PAT) has been employed for the investigating Polymorphism in several organic materials [4] and it has emerged as a unique and potent probe for characterizing the properties of polymers [5]. In PAT, the positron is used as a nuclear probe which is repelled by the ion cores and preferentially localized in the atomic size free-volume holes [6] of the polymeric material. The motion of the electron-positron pair causes a Doppler shift on the energy of the annihilation radiation. As a consequence, the line-shape gives the distribution of the longitudinal momentum component of the annihilating pair. Positron Annihilation Doppler Broadening Spectroscopy (PADBS) is a well established tool to characterize defects [7]. The 0.511 MeV peak is Doppler broadened by the longitudinal momentum of the annihilating pairs. Since the positrons are thermalized, the Doppler broadening measurements provide information about the momentum distributions of electrons at the annihilation site.

Essentially all prior Doppler broadening measurements [8, 9] have been performed using either slow positron beams or wide-energy-spectrum positron beams from radioactive sources. Two parameters S (for shape), and W (for wings) [10] are usually used to characterize the annihilation peak. The S-parameter is more sensitive to the annihilation with low momentum valence and unbound electrons. The S-parameter defined by Mackenzie et al. [11] as the ratio of the integration over the central part of the annihilation line to the total integration. Diffraction peaks are analyzed through common fitting procedures, which result in parameters like the center of gravity and the width of the distribution. The W-parameter is more sensitive to the annihilation with high momentum core electrons and is defined as the ratio of counts in the wing regions of the peak to the total counts in the peak.

Fig. 1 shows Doppler broadening line-shape from which the S- and W-parameters are calculated using the following equations:

$$S = \frac{\int_{xc-g1}^{xc+g1} y(x)dx}{area},$$

$$W = \frac{\int_{xc-g3}^{xc-g2} y(x)dx + \int_{xc-g2}^{xc-g3} y(x)dx}{area},$$

where $area = \int_{g\,\min}^{g\,\max} y(x)dx$, and xc is the center of the peak.

In this regard, the main goal of the positron annihilation technique experiments is to point out the CR-39 line-shape parameters resulting from the effect of α-particle energies.

2 Experimental technique

Track detectors "CR-39" were normally irradiated in air by different α-particle energies with different fluxes from 1476.42 particles/cm^2 at 1.13 MeV to 48130.25 particles/cm^2 at 4.95 MeV from 0.1 μCi ^{241}Am source. Collimators of different thickness were used to change the α-particle energy.

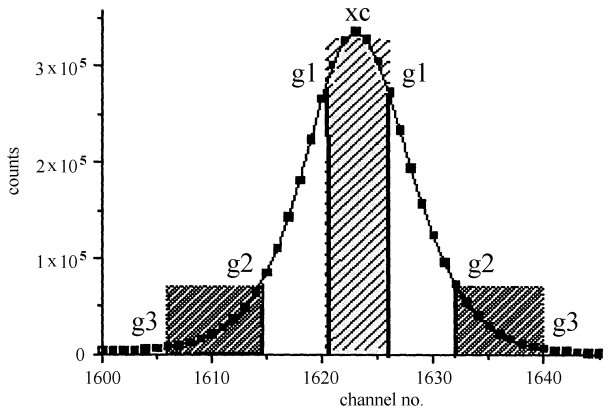

Fig. 1: Definition of the S- and W-parameters [12] (note, that the limits $g1$, $g2$, $g3$ are arbitrary to a certain degree, but have to be the same for all annihilation lines analyzed).

After irradiations, the samples were etched in 6.25 M NaOH solution at 70°C for 6 hr.

The simplest way to guide the positrons into the samples is to use a sandwich configuration as shown in Fig. 2. ^{22}Na is the radioactive isotope used in our experiment.

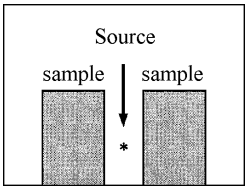

Fig. 2: Sandwich configuration of the positron source respect to a pair of specimen.

The positron source of 1mCi free carrier ^{22}NaCl was evaporated from an aqueous solution of sodium chloride and deposited on a thin Kapton foil of 7.5 μm in thickness. The ^{22}Na decays by positron emission and electron capture (E. C.) to the first excited state (at 1.274 MeV) of ^{22}Na. This excited state de-excites to the ground state by the emission of a 1.274 MeV gamma ray with half life $T_{1/2}$ of 3×10^{-12} sec. The positron emission is almost simultaneous with the emission of the 1.274 MeV gamma ray while the positron annihilation is accompanied by two 0.511 MeV gamma rays. The measurements of the time interval between the emission of 1.274 MeV and 0.511 MeV gamma rays can yield the lifetime τ of positrons. The source has to be very thin so that only small fractions of the positron annihilate in the source.

The system which has been used to determine the Doppler broadening S-and W-parameters consists of an Ortec HPGe detector with an energy resolution of 1.95 keV for 1.33 MeV line of ^{60}Co, an Ortec 5 kV bais supply 659, Ortec amplifier 575 and trump 8 k MCA. Fig. 3 shows a schematic diagram of the experimental setup. Doppler broadening is caused by the distribution of the velocity of the annihilating electrons in the directions of gamma ray emission. The signal coming from the detector enters the input of the preamplifier and the output from the preamplifier is fed to the amplifier. The

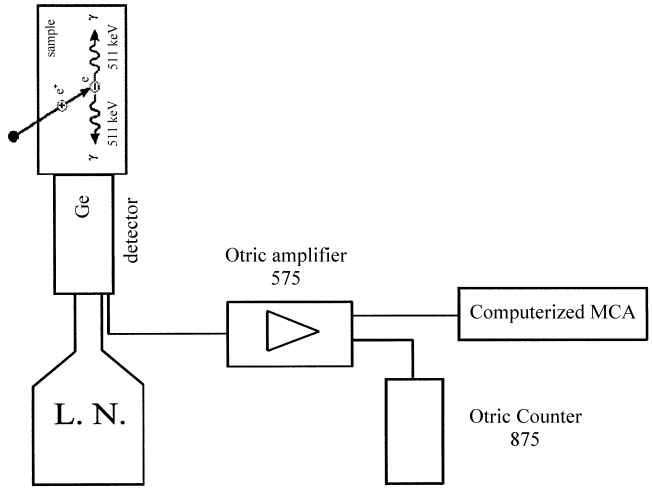

Fig. 3: Block diagram of HPGe-detector and electronics for Doppler broadening line-shape measurements.

input signal is a negative signal. The output signal from the amplifier is fed to a computerized MCA. All sample spectra are acquired for 30 min.

3 Results and discussion

3.1 Positron annihilation measurements

Fig. 4 shows the Doppler broadening line shape parameters measured for unirradiated and irradiated CR-39 samples at α-particle energies of 2.86 and 4.86 MeV. The measured line-shape profiles reveal similar line-shape counts for samples (unirradiated and irradiated with α-particle energy, i. e. 4.86 MeV). A minimum line-shape counts are obtained at 2.86 MeV. The other observation is that the Full Width at Half Maximum (FWHM) for 2.86 MeV irradiated sample is more broadening than others. From such behavior it is clear that either something happened during irradiation with 2.86 MeV and it recovers again at higher energies or some kind of transition occurs at 2.86 MeV of α-particle energy.

The Doppler broadening line-shape S- and W-parameters are calculated using SP ver. 1.0 program [13] which designed to automatically analyze of the positron annihilation line in a fully automated fashion.

The S- and W-parameters calculated using the previous program were correlated as a function of α-particle energy with different fluxes deposit into CR-39 detector, the results are illustrated in Fig. 5. The S-parameters has values around 46% while values of about 15% are obtained for W-parameters. An abrupt change definitely observed at irradiation energy 2.86 MeV of α-particles for both S- and W-parameters. At this energy a drastically decrease in the S-parameter comparable with a drastically increase in the W-parameter. Values of about 35% and 28% were observed for the S- and W-parameters respectively at 2.86 MeV of α-particle energy.

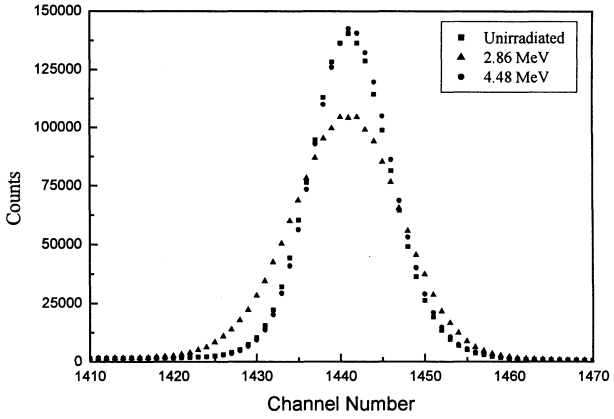

Fig. 4: The line shape spectra of the unirradiated sample and irradiated with α-particle energies of 2.86 and 4.84 MeV.

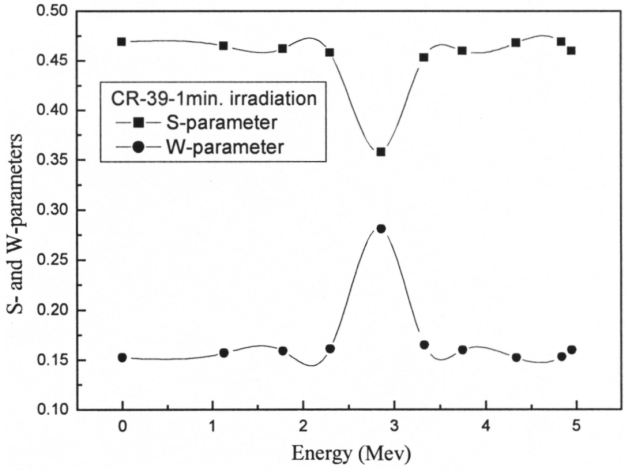

Fig. 5: The behavior of the S- and W-parameters as a function of α-particle energies.

A high concentration of defects, or an increase in the mean size of defects, leads to a larger contribution of annihilation photons from low momentum electrons because positrons are trapped at defects [14]. This is reflected in Doppler broadening measurements by an increase in S-parameter and a decrease in W-parameter. The behavior of S- and W-parameters reveal an abrupt change at the position of the transition. The behavior of the line-shape S- and W-parameters can be related to the different phases. Like many others molecular materials, the use of PAT also proven a very valuable in the study of phase transition in polymers. The same results have been obtained by Schiltz et al. [15]. Walker's et al. [4] measurements have indicated the conversion of one polymorphism to another. Srivastana et al. [16] have investigated polymorphic transitions in DL-norlevcine and hexamethyl benzene.

The transitions in the crystalline phase are related to the lattice transformation from monoclinic to hexagonal and setting in of torsional oscillations in the polymer chain.

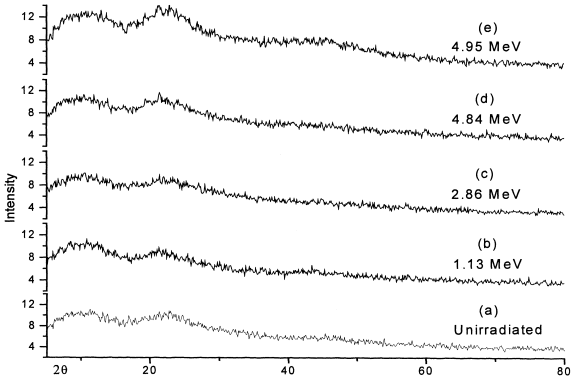

Fig. 6: X-ray diffraction pattern of "CR-39" Polyallyl diglycol carbonate.

3.2 X-ray diffraction pattern (XRD) and Scanning Electron Microscopy (SEM)

The X-ray diffraction analysis was used to obtain information about the transformation as a result of change in α-irradiation intensity. The XRD intensity measurements as a function of diffraction angle (2θ) for unirradiated sample and samples irradiated at different α-particle energies are shown in Fig. 6.

From the X-ray charts it is observed that, an increase in the intensity is obtained at higher α-irradiation intensity 4.84 and 4.95 MeV. At these energies, the XRD chart reveals a new peak that start to appear at 2.86 MeV α-particle energy. The one prominent X-ray peak is located at $2\theta = 21.5^{\circ}$ and it grows up with increasing α-particle energy. The appearance of this peak might be related to phase transition.

A number of papers on the study of polymer show that the amorphous state is altered by structural relaxation and crystallization processes. Positron annihilation behavior in the amorphous state has been described both in terms of topological short range ordering (TSRO) and chemical short-range ordering (CSRO) at the basis of the structural relaxation mechanisms [11, 15, 17–19]. During crystallization the positron behavior is determined by the phase diagram of the amorphous and crystallized system. On our X-ray diffraction patterns might be the first sign of the crystallization onset appears at 2.86 MeV. This sign is increased at higher α-particle energies as shown in the Fig. 6.

The SEM images taken for unirradiated and irradiated CR-39 samples at 4.84 MeV with magnification of 500 are shown in Fig. 7a and b. Tracks are obtained as a result of exposure of α-particle energy. A different magnified (15000) image for one track is shown at Fig. 7c. Cumbrera et al. [19] showed that rings of the structure (metastable structure) were already present in the scanning electron micrographs.

4 Conclusion

Doppler broadening positron annihilation (DBPAT) provides direct information about core and valance electrons in CR-

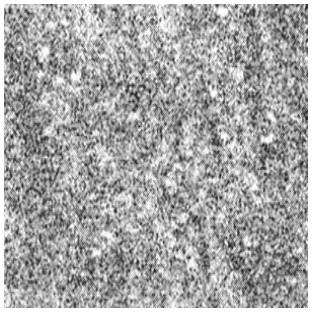

(a) Unirradiated ($M = 500$)

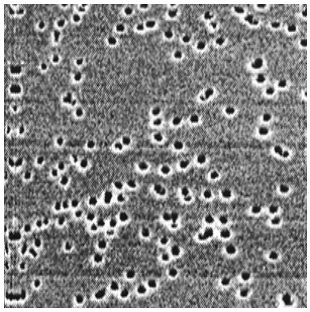

(b) 4.84 MeV ($M = 500$)

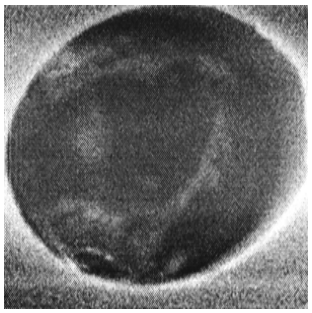

(c) 4.84 MeV ($M = 15\,000$)

Fig. 7: SEM for unirradiated sample and irradiated sample at 4.84 MeV α-particle energies for different magnifications

39 due to radiation effects. The behavior of the S- and W-parameters supports the idea that positrons are trapped by defects and inhomogeneities inherently present in the as-received CR-39 polycarbonate. The annihilation characteristics of positrons are very sensitive to phase transitions. The phase transition in the CR-39 polycarbonate remain complex. XRD pattern and SEM technique of polymers studied in the present work clearly show crystalline and amorphous regions in the samples.

References

1. Rajta I., Baradács E., Bettiol A. A., Csige I., Tökési K., Budai L. and Kiss Á Z. *Nucl. Instr. and Meth. in Phys. Res. B*, 2005, v. 231, 384–388.
2. Myler U., Xu X. L., Coleman M. R. and Simpson P. J. Ion implant-induced change in polimide films monitored by variable energy positron annihilation spectroscopy. *J. Polym. Sci. B. Polym. Phys.*, 1998, v. 36, 2413–2421.
3. Kumar R., Rajguru S., Das D. and Prasad R. *Radiation Measurements*, 2003, v. 36, issues 1–6, 151–154.
4. Walker W. W. and Kline D. C. *J. Chem. Phys.*, 1974, v. 60, 4990.
5. Jean Y. C. In: A. Dupasquier and A. P. Mills Jr., eds., *Positron Spectroscopy of Solids*, IOS Publ., Amsterdam, 1995, 563–569.
6. Schrador D. M., Jean Y. C. (Eds). Positron and positronium chemistry, studies in physical and theoretical. Elsevier, Amsterdam, 1988, v. 57.
7. Dupasquier A., Mills A. P. (Eds.) Positron Spectroscopy of Solids. 1995.
8. Escobar Galindo R., Van Veen A., Alba Garcia A., Schut H., De Hosson J. Th. In: *Proc. of the Twelfth Conf. on Positron Annihilation*, 2000, 499.
9. Hori F., Oshima R. In: *Proc. of the Twelfth Conf. on Positron Annihilation*, 2000, 204.
10. Urban-Klaehen J. M., Quarles C. A. *J. Appl. Phys.*, 1989, v. 86, 355.
11. Mackenzie I. K., Eady J. A. and Gingerich R. R. *Phys. Lett. 33A*, 1970, 279.
12. Priesmeyer H. G., Bokuchava G. *Applied Radiation and Isotopes*, 2005, v. 63, 751–755.
13. http://www.ifj.edu.pl/∼mdryzek.
14. Osipowicz A., Harting M., Hempel M., Britton D. T., Bauer-Kugelmann W., Triftshauser W. *Appl. Surf. Sci.*, 1999, v. 149, 198.
15. Schiltz A., Liolios A., Dalas M. In: *Proc. of the 7th Int. Conf. on Positron Annihilation*, New Delhi, 1985.
16. Srivastana P. K., Singh K. P. and Jain P. C. *Solid state comun.*, 1986, v. 58, 147.
17. Tsumbu M., Segers D., Dorikend M. and Dorikens-Vanpraet L. *Rev. Phys. Appl.*, 1985, v. 20, 831–836.
18. Mbungu T., Segers D. In: *Proc. of the 6th Int. Conf. on Positron Annihilation*, Texas, Arlington, 1982.
19. Cumbrera F. L., Millan M., Conde A., *J. Mater. Sci.*, 1982, v. 17, 861.

Planck Particles and Quantum Gravity

Stephen J. Crothers* and Jeremy Dunning-Davies†

*Queensland, Australia; †Department of Physics, University of Hull, England
E-mail: thenarmis@yahoo.com; j.dunning-davies@hull.ac.uk

The alleged existence of so-called Planck particles is examined. The various methods for deriving the properties of these "particles" are examined and it is shown that their existence as genuine physical particles is based on a number of conceptual flaws which serve to render the concept invalid.

1 Introduction

The idea of the so-called Planck particle seems to have been around for quite some time now but has appeared in a number of totally different contexts. It seems to have been used initially as a means of making equations and expressions dimensionless by making use of suitable combinations of the universal constants c, the speed of light, G, Newton's universal constant of gravitation, and finally Planck's constant. As far as the third and final constant is concerned, it has appeared variously as the original h and in the reduced form $\hbar$. The combinations considered were those which ended up with the dimensions of mass or length or time and so, the idea of a "Planck particle" emerged.

Hence, initially the notion seems to have occurred via expressions deduced from dimensional considerations; no mention of an actual "particle" would have been included at this point presumably. Later, however, other arguments were introduced which lead to the same expressions. These included examining the equivalence of the Compton wavelength and Schwarzschild radius of a particle or drawing on results from Special Relativity and Quantum Mechanics. Finally, because the expressions incorporate the Planck constant, which is normally associated with quantum phenomena, and both the speed of light and the universal constant of gravitation, which are often associated with relativistic and gravitational phenomena, these "particles" seem to have been elevated to a position of importance and even physical reality which is difficult to justify.

Here the various methods of determining the expressions for the various physical quantities, such as mass and length, of these so-called Planck "particles" will be examined, before some conclusions about the actual "particles" themselves — including their physical existence — will be discussed.

2 The "Planck" quantities

(a) Dimensional analysis

Using the fundamental ideas of dimensional analysis allows the derivation of the Planck mass, Planck length, and all the other Planck quantities to be accomplished very easily. Taking c, G and h as the three basic quantities, the expression for the Planck mass is found easily by putting

$$\left(LT^{-1}\right)^{\alpha}\left(ML^2T^{-1}\right)^{\beta}\left(M^{-1}L^3T^{-2}\right)^{\gamma}=M\,,$$

where $\left(LT^{-1}\right)$, $\left(ML^2T^{-1}\right)$, $\left(M^{-1}L^3T^{-2}\right)$ are the dimensions of c, G and h respectively. Equating coefficients immediately gives

$$\text{Planck mass}\equiv\sqrt{\frac{ch}{G}}\,.$$

Similar manipulations give

$$\text{Planck length}\equiv\sqrt{\frac{hG}{c^3}}\quad\text{and}\quad\text{Planck time}\equiv\sqrt{\frac{hG}{c^5}}\,.$$

It is easy to see how expressions such as these could prove useful in making equations dimensionless and so more suitable for numerical work. However, the derivation of these expressions is seen to have been accomplished by a purely mathematical exercise; absolutely no physical argument has been involved!

(b) Compton wavelength and Schwarzschild radius

Another derivation involves the consideration of a body whose Compton wavelength equals its Schwarzschild or gravitational radius [1]. Immediately, this equivalence leads to

$$\frac{h}{mc}=\frac{2Gm}{c^2}\,,$$

from which it follows that

$$m=\sqrt{\frac{hc}{2G}}\,.$$

Corresponding expressions for the Planck length and Planck time follow easily and it is seen that the ratio of Planck mass to Planck length equals $c^2/2G$, which would make such a body, if it truly existed, a Michell-Laplace dark body or a Schwarzschild black hole.

However, the expressions derived by this route are seen to involve an extra figure two. This apparent little problem is overcome by using $\hbar$ instead of h in the dimensional analysis approach and by putting the Compton wavelength equal to π multiplied by the Schwarzschild or gravitational radius in the approach. Since the equivalence is purely arbitrary, introducing an extra arbitrary factor of π is not really a problem.

(c) The quantum/relativity approach

This approach makes use of the Heisenberg uncertainty principle [2]. The starting point is provided by the introduction of a Planck time, t_p, for which quantum fluctuations are felt to exist on the scale of the Planck length which is defined to be equal to $\ell_p = ct_p$. If a Planck density is denoted by ρ_p, a Planck mass may then be $m_p \cong \rho_p \ell_p^3$. Then, using Heisenberg's uncertainty principle in the form

$$\Delta E\, \Delta t \cong m_p c^2 t_p \cong \rho_p \left(ct_p\right)^3 c^2 t_p \cong \frac{c^5 t_p^4}{G t_p^2} \cong \hbar\,,$$

leads to

$$t_p \cong \sqrt{\frac{\hbar G}{c^5}} \cong 5.4{\times}10^{-44}\ \text{sec}\,.$$

Here the reduced Planck constant, $\hbar$, has been used as is more usual. The expressions for both the Planck mass and Planck length follow easily and their numerical values are

$$m_p \cong 2.2{\times}10^{-8}\ \text{kg} \quad \text{and} \quad \ell_p \cong 1.6{\times}10^{-35}\ \text{m}$$

respectively, where the value of the reduced Planck constant has been used.

These are the three basic properties associated with these so-called Planck "particles". It is quite common to note also that the corresponding Planck energy and Planck temperature are then given by

$$E_p = m_p c^2 \cong \sqrt{\frac{\hbar c^5}{G}} \cong 1.2{\times}10^{19}\ \text{GeV}$$

and

$$T_p = \frac{E_p}{k} \cong \sqrt{\frac{\hbar c^5}{G k^2}} \cong 1.4{\times}10^{32}\ \text{K}\,.$$

3 Planck particles as black holes

The arbitrary equality of the Compton wavelength to the alleged "Schwarzschild radius" has resulted in the claim that the so-called Planck particles are black holes. This conclusion is inadmissible for a number of reasons.

The expression

$$R = \frac{2Gm}{c^2}, \tag{1}$$

describes the Michell-Laplace dark body, a theoretical astronomical object having an escape velocity equal to that of light. This expression can be generalised to

$$R \leqslant \frac{2Gm}{c^2}, \tag{2}$$

to include escape velocities greater than that of light.

The radius R described by (1) and (2) is Euclidean, and therefore measurable in principle. The Compton wavelength is also measurable in principle because it too is Euclidean. However, (1) is routinely claimed to be the "Schwarzschild radius", the radius of the event horizon of the alleged black hole. (1) is also claimed to show that the escape velocity associated with a black hole is the velocity of light. Actually this is false. An alleged black hole has no escape velocity since it is claimed also that neither material object nor light may leave the event horizon. On the other hand, an escape velocity does not mean that a material object having an initial velocity less than the escape velocity cannot leave the surface of a gravitating body. A material object possessing an initial velocity less than the escape velocity may leave the surface of the host object, travel radially outward to a finite distance where it comes to rest momentarily before falling radially backwards to the host. If the escape velocity is the velocity of light, then light itself may leave the surface and travel radially outward to infinity and, therefore, escape. Hence, equation (1) does not specify an escape velocity for the alleged black hole. In truth, black holes have no escape velocity associated with them [3, 4].

Furthermore, in the case of the Michell-Laplace dark body, equation (1) specifies a Euclidean radius, whereas, in the case of the alleged black hole, the Schwarzschild radius is non-Euclidean. Moreover, in principle, R is a measurable length in the Euclidean space of Newton's theory, but in General Relativity R is not measurable in principle. Hence equating the Euclidean Compton wavelength to R given by (1) is conceptually flawed. In addition, in Einstein's gravitational field there are two radii — the proper radius and the radius of curvature. These are the same only in the infinitely far field where space-time is asymptotically Minkowski, (that is, pseudo-Euclidean) where the radii coalesce to become identical because, in Euclidean space, the radius of curvature and the proper radius are identical. Therefore, when the Compton wavelength is equated to (1) in the context of the black hole, which non-Euclidean Einstein radius does R specify?

It has been shown [5, 6] that when (1) is interpreted in terms of Einstein's gravitational field, the Schwarzschild radius R is actually the invariant radius of curvature of the fictitious point-mass, which corresponds to an associated invariant proper radius of zero. In ignorance of the fact that Einstein's gravitational field yields two different radii, physicists erroneously interpret R in equation (1) as a proper radius in Einstein's gravitational field and, therefore, allow it to go to zero, which is false! In their conception of R as

a proper radius they also treat R as a measurable quantity in Einstein's gravitational field, as it is in Euclidean space, which is also false!

Hence, even if the equality of the Compton wavelength to the gravitational radius of curvature of a point-mass could be admitted, the alleged Planck particles would necessarily be point-masses, which are not only fictitious but also contradict the very meaning of the Compton wavelength and, indeed, the foundations of Quantum Mechanics. However, there can be no meaning to the equality of a measurable Euclidean length to an immeasurable non-Euclidean length to begin with. Not only that, there can be no meaning to the equality of a Euclidean length which is both the proper radius and the radius of curvature in Euclidean space and a non-Euclidean radius of curvature, which is not the same as the corresponding non-Euclidean proper radius. Consequently, claims that Planck particles are black holes are false, even if black holes actually exist. It might well be noted at this juncture that General Relativity, contrary to widespread claims, doesn't even predict the existence of black holes [5, 6].

Planck particles are presumed to be able to interact with one another. However, the black hole is allegedly derived from a solution to Einstein's gravitational field for a "point-mass". Therefore, the black hole is the result of a solution involving a *single* gravitating body interacting with a "test particle". It is *not* the result of a solution involving the gravitational coupling of two comparable masses. Since there are no known solutions to Einstein's field equations for multi-body configurations and since it is not even known if Einstein's field equations admit multi-body configurations [3], all conceptions of black hole interactions are meaningless. Consequently, Schwarzschild radius Planck particle interactions are also meaningless.

The claim that Planck particles were prolific during the early Universe but are now extremely rare is also erroneous. This follows since it has been proved that cosmological solutions to Einstein's field equations for isotropic type 1 Einstein spaces, from which the expanding Universe and the Big Bang have allegedly been derived, do not even exist.[7].

4 Comments and conclusions

Above, three ways of deducing expressions for the so-called Planck quantities have been outlined. In many ways, the first method indicates a good idea of the physical standing for the so-called Planck "particles". This first method is purely a mathematical manipulation of three man-made constants. At the end of the day, all numbers originate in a man-made model and so these three numbers, although assigned a seemingly exalted status as universal constants, are still members of that group of man-made objects. As mentioned already, the first method contains no physics and makes absolutely no pretensions to contain any. The second and third derivations, on the other hand, do seem to contain some physics as a basis for what follows. However, closer examination casts real doubt on this initial feeling. What physical basis is there in asserting the equivalence of the Compton wavelength and the Schwarzschild or gravitational radius of a particle? If one believes modern ideas, this merely asserts that the said particle is a "Schwarzschild black hole", and does so from the outset. The second of these two is simply a mathematical manipulation of symbols using Heisenberg's uncertainty principle as a starting point. The manipulations, as such, are reasonable enough, but is it valid to then make physical assertions about "particles" whose very existence depends only on these mathematical manipulations?

The alleged link between Quantum mechanics and General Relativity via the interpretation of the Compton wavelength as a Schwarzschild radius is clearly seen to be false. All that remains is an interpretation of Planck particles via equation (1) as it relates to the Michell-Laplace dark body radius. In this case, one may say only that the escape velocity associated with a Planck particle is the velocity of light in the flat three-dimensional Euclidean space of Newton. Of course, the Planck particles are thereby robbed of their more mysterious relativistic qualities and their primordial profusion. Black hole creation in the collision of a high energy photon with a particle and concomitant digestion of the photon is fallacious. Likewise there is no possibility of micro black holes being formed by fermion collision in particle accelerators.

There can be little doubt that Planck "particles" originated purely out of mathematical manipulations and there seems no reason to suppose that they exist or ever have existed as genuine physical particles. It is for that reason that it is worrying to see these objects being assigned an actual physical role in models of the early universe. Most books on this subject seem to regard Planck "particles" as genuine particles — mini black holes — which existed in large numbers during the very early stages of the formation of the universe but are now thought to be extremely rare, if not actually extinct. The grounds for this belief seem very shaky and it is claimed, for example, that the decay of a single Planck "particle" could lead to the production of 5×10^{18} baryons [1]. It is also claimed that theory as presently available doesn't allow examination back beyond a time of approximately 10^{-43} seconds, the Planck "time" because, beyond that time, a theory of quantum gravity would be necessary. Hence, this time is effectively regarded as an actual barrier between the quantum and non-quantum world. Why? The relevance of this question lies in the fact that it is a purely arbitrary figure. The fact that it and the other Planck quantities depend on the reduced Planck constant, which is regarded as being a quantity associated with quantum mechanics, and the speed of light and the universal constant of gravitation, which are associated with relativistic and gravitational phenomena, is something which comes out of human choice not something which occurs naturally. It is

interesting that quantities which have the dimensions of mass, length and time may be constructed from these three constants which appear so frequently in so many areas of theoretical science but that is all it is — interesting! It is not, at least as far as current scientific knowledge is concerned, any more significant than that. Playing around with numbers and combinations of numbers can be very fascinating but, if attempts are made to assign physical reality to the outcomes of such mathematical diversions, scientific chaos could, and probably will, ensue!

References

1. Hoyle F., Burbidge G., Narlikar J. A different approach to cosmology. Cambridge University Press, 2000.
2. Coles P., Lucchin F. Cosmology. John Wiley & Sons.
3. McVittie G. C. Laplace's alleged "black hole". *The Observatory*, v. 98, 1978, 272; http://www.geocities.com/theometria/McVittie.pdf.
4. Crothers S. J. A brief history of black holes. *Progress in Physics*, 2006, v. 2, 54–57.
5. Abrams L. S. Black holes: the legacy of Hilbert's error. *Can. J. Phys.*, 1989, v. 67, 919; arXiv: gr-qc/0102055.
6. Crothers S. J. On the general solution to Einstein's vacuum field and it implications for relativistic degeneracy. *Progress in Physics*, 2005, v. 1, 68–73.
7. Crothers S. J. On the general solution to Einstein's vacuum field for the point-mass when $\lambda \neq 0$ and its consequences for relativistic cosmology. *Progress in Physics*, 2005, v. 3, 7–14.

The Quantum Space Phase Transitions for Particles and Force Fields

Ding-Yu Chung* and Volodymir Krasnoholovets†

*P.O. Box 180661, Utica, Michigan 48318, USA
†Institute for Basic Research, 90 East Winds Court, Palm Harbor, FL 34683, USA
E-mail: chung@wayne.edu; v_kras@yahoo.com

We introduce a phenomenological formalism in which the space structure is treated in terms of attachment space and detachment space. Attachment space attaches to an object, while detachment space detaches from the object. The combination of these spaces results in three quantum space phases: binary partition space, miscible space and binary lattice space. Binary lattice space consists of repetitive units of alternative attachment space and detachment space. In miscible space, attachment space is miscible to detachment space, and there is no separation between attachment space and detachment spaces. In binary partition space, detachment space and attachment space are in two separate continuous regions. The transition from wavefunction to the collapse of wavefuction under interference becomes the quantum space phase transition from binary lattice space to miscible space. At extremely conditions, the gauge boson force field undergoes a quantum space phase transition to a "hedge boson force field", consisting of a "vacuum" core surrounded by a hedge boson shell, like a bubble with boundary.

1 The origin of the space structure

The conventional explanation of the hidden extra space dimensions is the compactization of the extra space dimensions. For example, six space dimensions become hidden by the compactization, so space-time appears to be four dimensional. Papers [1, 2] propose the other explanation of the reduction of >4D space-time into 4D space-time by slicing >4D space-time into infinitely many 4D slices surrounding the 4D core particle. Such slicing of >4D space-time is like slicing 3-space D object into 2-space D object in the way stated by Michel Bounias as follows: "You cannot put a pot into a sheet without changing the shape of the 2-D sheet into a 3-D dimensional packet. Only a 2-D slice of the pot could be a part of sheet".

This paper proposes that the space structure for such reduction of >4D space-time can also be derived from the cosmic digital code [3, 4], which one can consider as "the law of all laws". The cosmic digital code consists of mutually exclusive attachment space and detachment space. Attachment space attaches to an object, while detachment space detaches from the object. The cosmic digital code is analogous to two-value digital code for computer with two mutually exclusive values: 1 and 0, representing *on* and *off*. In terms of the cosmic digital code, attachment space and detachment space are represented as 1 and 0, respectively. The object with >4D space-time attaches to >4D attachment space, which can be represented by

$(i\ 1_{3+k})_m$ as $>$ 4D attachment space with m repetitive units of time (i) and $3+k$ space dimension.

The slicing of >4D attachment space is through 4D detachment space, represented by

$(i\ 0_3)_n$ as detachment space with n repetitive units of time (i) and three space dimension.

The slicing of >4D attachment space by 4D detachment space is the space-time dimension number reduction equation as follows

$$\underbrace{(i\ 1_{3+k})_m}_{\text{4D attachment space}} \xrightarrow{slicing} \underbrace{(i\ 1_3)_m}_{\text{4D core attachment space}} + \underbrace{\sum_{k=1}^{k}((i\ 0_3)\ (i\ 1_3))_{n,k}}_{k\text{ types 4D slices}} \quad (1)$$

The two products of the slicing are the 4D-core attachment space and 4D slices represented by n repetitive units of alternative 4D attachment space and 4D detachment space. They are k types of 4D slices, representing the total number of space dimensions greater than three-dimensional space. For example, the slicing of 10D attachment space produces 4D core attachment space and six types of 4D slices. The value of n approaches to infinity for infinitely many 4D slices.

The core attachment space surrounded by infinitely many 4D slices corresponds to the core particle surrounded by infinitely many small 4D particles. Gauge force fields are made of such small 4D particles surrounding the core particle. The space with repetitive units (of alternative attachment space and detachment space) is binary lattice space.

The combination of attachment space (1) and detachment space (0) results in three quantum space phases: miscible space, binary partition space, or binary lattice space for four-dimensional space-time.

$$\begin{array}{l}(1_4)_n \text{ attachment space} + (0_4)_n \text{ detachment space}\\ \overset{combination}{\longrightarrow} \text{ three quantum space phases:}\\ (1_4\ 0_4)_n \text{ binary lattice space, miscible space, or}\\ (1_4)_n\,(0_4)_n \text{ binary partition space.}\end{array} \tag{2}$$

Binary lattice space consists of repetitive units of alternative attachment space and detachment space. In miscible space, attachment space is miscible to detachment space, and there is no separation of attachment space and detachment space. In binary partition space, detachment space and attachment space are in two separate continuous regions.

2 The quantum space phase transition for particles

Binary lattice space, $(1_40_4)_n$, consists of repetitive units of alternative attachment space and detachment space. Thus, binary lattice space consists of multiple quantized units of attachment space separated from one another by detachment space. Binary lattice space is the space for wavefunction, which thus appears as not an abstract entity but a real one filled with a substance, that is in line with works [5, 6]. In wavefunction

$$|\psi\rangle \;=\; \sum_{i=1}^{n} c_i|\,\phi_i\rangle \tag{3}$$

each individual basis element $|\phi_i\rangle$ attaches to attachment space, and separates from the adjacent basis element by detachment space. Detachment space detaches from object. Binary lattice space with n units of four-dimensional, $(1_40_4)_n$, contains n units of basis elements.

Detachment space contains no object that carries information. Without information, detachment space is outside of the realm of causality. Without causality, distance (space) and time do not matter to detachment space, resulting in non-localizable and non-countable space-time. The requirement for the system (binary lattice space) containing non-localizable and non-countable detachment space is the absence of net information by any change in the space-time of detachment space. All changes have to be coordinated to result in zero net information. This coordinated non-localized binary lattice space corresponds to nilpotent space. All changes in energy, momentum, mass, time, space have to result in zero as defined by the generalized nilpotent Dirac equation [7, 8]

$$\begin{aligned}\big(\mp\mathbf{k}\,\partial/\partial t \pm \mathbf{i}\nabla + \mathbf{j}m\big)\big(\pm i\mathbf{k}E \pm \mathbf{ip} + \mathbf{j}m\big)\times\\ \times\exp\big(i(-Et + \mathbf{pr})\big) = 0\,,\end{aligned} \tag{4}$$

where E, $\mathbf{p}$, m, t and $\mathbf{r}$ are respectively energy, momentum, mass, time, space and the symbols ±1, $\pm i$, $\pm\boldsymbol{i}$, $\pm\boldsymbol{j}$, $\pm\boldsymbol{k}$, $\pm\mathbf{i}$, $\pm\mathbf{j}$, $\pm\mathbf{k}$ are used to represent the respective units required by the scalar, pseudoscalar, quaternion and multivariate vector groups. The changes involve the sequential iterative path from nothing (nilpotent) through conjugation, complexification, and dimensionalization. The non-local property of binary lattice space for wavefunction provides the violation of Bell inequalities [9] in quantum mechanics in terms of faster-than-light influence and indefinite property before measurement. The non-locality in Bell inequalities does not result in net new information.

In binary lattice space, for every attachment space, there is its corresponding adjacent detachment space. Thus, a basis element attached to attachment space can never be at rest with complete localization even at the absolute zero degree. The adjacent detachment space forces the basis element to delocalize.

In binary lattice space, for every detachment space, there is its corresponding adjacent attachment space. Thus, no part of the object can be irreversibly separated from binary lattice space, and no part of a different object can be incorporated in binary lattice space. Binary lattice space represents coherence as wavefunction. Binary lattice space is for coherent system.

Any destruction of the coherence by the addition of a different object to the object causes the collapse of binary lattice space into miscible space. The collapse is a quantum space phase transition from binary lattice space to miscible space.

$$\begin{array}{l}\underbrace{\big((0_4)\ (1_4)\big)_n}\\ \text{binary lattice space}\\ \overset{quantum\ space\ phase\ transition}{\longrightarrow} \text{ miscible space.}\end{array} \tag{5}$$

In miscible space, attachment space is miscible to detachment space, and there is no separation of attachment space and detachment space. In miscible space, attachment space contributes zero speed, while detachment space contributes the speed of light. A massless particle is on detachment space continuously, and detaches from its own space continuously. For a moving massive particle, the massive part with rest mass m_0 belongs to attachment space and the other part of the particle mass, which appears due to the motion, induces an additional energy, namely the kinetic energy K, that changes properties of attachment space and leads to the propagation speed v lesser than the speed of light c.

To maintain the speed of light constant for a moving particle, the time (t) in a moving particle has to be dilated, and the length (L) has to be contracted relative to the rest frame

$$\begin{aligned}t &= \frac{t_0}{\sqrt{1 - v^2/c^2}} = t_0\gamma\,,\\ L &= L_0/\gamma\,,\\ E &= K + m_0c^2 = \gamma m_0c^2,\end{aligned} \tag{6}$$

where $\gamma = 1/\sqrt{1-v^2/c^2}$ is the Lorentz factor for time dilation and length contraction, E is the total energy and K is the kinetic energy.

The information in such miscible space is contributed by the combination of both attachment space and detachment space, so detachment space with information can no longer be non-localize. Any value in miscible space is definite. All observations in terms of measurements bring about the collapse of wavefunction, resulting in miscible space that leads to eigenvalue as definite quantized value. Such collapse corresponds to the appearance of eigenvalue E by a measurement operator H on a wavefunction ψ, i. e.

$$H\psi = E\psi\,. \tag{7}$$

Another way for the quantum space phase transition from binary lattice space to miscible space is gravity. Penrose [10] pointed out that the gravity of a small object is not strong enough to pull different states into one location. On the other hand, the gravity of large object pulls different quantum states into one location to become binary partition space. Therefore, a small object without outside interference is always in binary lattice space, while a large object is never in binary latticespace.

3 The quantum space phase transitions for force fields

At zero temperature or extremely high pressure, binary lattice space for a gauge force field undergoes a quantum space phase transition to become binary partition space. In binary partition space, detachment space and attachment space are in two separate continuous regions as follows

$$\underbrace{(1_4)_m + \sum_{k=1}^{k}\big((0_4)\ (1_4)\big)_{n,k}}_{\text{particle gauge boson field in binary lattice space}} \longrightarrow \underbrace{(1_4)_m}_{\text{hedge particle}} + \underbrace{\sum_{k=1}^{k}(0_4)_{n,k}\ (1_4)_{n,k}}_{\substack{\text{hedge boson field in binary}\\ \text{partition space}}} \tag{8}$$

The force field in binary lattice space is a gauge boson force field, the force field in binary partition space is denoted as a *hedge boson force field*. The detachment space in hedge boson field is a "vacuum" core, while hedge bosons attached to attachment space form the hedge boson shell. Gauge boson force field has no boundary, while the attachment space in the binary partition space acts as the boundary for hedge boson force field. Hedge boson field is like a bubble with core vacuum surrounded by membrane where hedge bosons locate.

Hedge boson force is incompatible to gauge boson force field. The incompatibility of hedge boson force field and gauge boson force field manifests in the Meissner effect, where superconductor repels external magnetism. The energy (stiffness) of hedge boson force field can be determined by the penetration of boson force field into hedge boson force field as expressed by the London equation for the Meissner effect

$$\nabla^2 H = -\lambda^{-2} H\,, \tag{9}$$

where H is an external boson field and λ is the depth of the penetration of magnetism into hedge boson shell. Eq. (9) indicates that the external boson field decays exponentially as it penetrate into hedge boson force field.

The Meissner effect is the base for superconductivity. It is also the base for gravastar, an alternative to black hole [11–13]. Gravastar is a spherical void as Bose-Einstein condensate surrounded by an extremely durable form of matter. This paper proposes gravastar based on hedge boson field.

Before the gravitational collapse of large or supermassive star, the fusion process in the core of the star to create the outward pressure counters the inward gravitational pull of the star's great mass. When the core contains heavy elements, mostly iron, the fusion stops. Instantly, the gravitational collapse starts. The great pressure of the gravity collapses atoms into neutrons. Further pressure collapses neutrons to quark matter and heavy quark matter.

Eventually, the high gravitational pressure transforms the gauge gluon force field into the hedge gluon force field, consisting of a vacuum core surrounded by a hedge gluon shell, like a bubble. The exclusion of gravity by the hedge gluon force field as in the Meissner effect prevents the gravitational collapse into singularity. To keep the hedge gluon force field from collapsing, the vacuum core in the hedge gluon force field acquires a non-zero vacuum energy whose density (ρ) is equal to negative pressure (P). The space for the vacuum core becomes de Sitter space. The vacuum energy of the vacuum core comes from the gravitons in the exterior region surrounding the hedge gluon force field as in the Chapline's dark energy star. The external region surrounding the hedge gluon force field becomes the vacuum exterior region. Thus, the core of gravastar can be divided into three regions: the vacuum core, the hedge gluon shell, and the vacuum exterior region

$$\begin{aligned} &\text{vacuum core region:} && \rho = -P\\ &\text{hedge gluon shell region:} && \rho = +P\\ &\text{vacuum exterior region:} && \rho = P = 0 \end{aligned} \tag{10}$$

Quarks without the strong force field are transformed into the decayed products as electron-positron and neutrino-antineutrino denoted as the "lepton composite"

$$\text{quarks} \xrightarrow{quark\ decay} \underbrace{e^- + e^+ + \bar{\nu} + \nu}_{\text{the lepton composite}} \tag{11}$$

The result is that the core of the collapsed star consists of the lepton composite surrounded by the hedge gluon field. This lepton composite-hedge gluon force field core constitutes the core for gravastar. The star consisting of the lepton composite-hedge gluon field core (LHC) and the matter shell is "gravastar". The matter shell consists of different layers of matters: heavy quark matter layer, quark matter layer, neutron layer, and heavy element layer one after the other:

$$\begin{array}{l}\text{LHC (lepton composite}\\ \qquad\text{— hedge gluon force field core):}\\ \quad\text{lepton composite region:}\quad \rho = +P\\ \quad\text{vacuum core region:}\quad \rho = -P\\ \quad\text{hedge gluon shell region:}\quad \rho = +P\\ \quad\text{vacuum exterior region:}\quad \rho = P = 0\\ \text{MATTER SHELL}\\ \quad\text{(heavy quark layer}\\ \quad\text{quark layer}\\ \quad\text{neutron layer}\\ \quad\text{heavy element layer):}\quad \rho = +P\end{array} \qquad (12)$$

4 Summary

Thus our formal phenomenological approach allows us to conclude that the quantum space phase transition is the quantum phase transition for space. The approach that is developed derives the space structure from attachment space and detachment space. Attachment space attaches to an object, while detachment space detaches from the object. The combination of attachment space and detachment space results in three quantum space phases: binary partition space, miscible space, or binary lattice space. Binary lattice space consists of repetitive units of alternative attachment space and detachment space. In miscible space, attachment space is miscible to detachment space, and there is no separation of attachment space and detachment space. In binary partition space, detachment space and attachment space are in two separate continuous regions. For a particle, the transition from wavefunction to the collapse of wavefuction under interference is the quantum space phase transition from binary lattice space to miscible space.

At zero temperature or extremely high pressure, gauge boson force field undergoes a quantum space phase transition to "hedge boson force field", consisting of a vacuum core surrounded by a hedge boson shell, like a bubble with boundary. In terms of the quantum space phase, gauge boson force field is in binary lattice space, while hedge boson force field is in binary partition space. The hedge boson force fields include superconductivity and gravastar.

References

1. Bounias M. and Krasnoholovets V. Scanning the structure of ill-known spaces: Part 1. Founding principles about mathematical constitution of space. *Kybernetes: The International Journal of Systems and Cybernetics*, 2003, v. 32 (7/8), 945–975. arXiv: physics/0211096.
2. Bounias M. and Krasnoholovets V. Scanning the structure of ill-known spaces: Part 2. Principles of construction of physical space. *Ibid.*, 2003, v. 32 (7/8), 976–1004. arXiv: physics/0211096.
3. Chung D. The cosmic digital code and quantum mechanics. arXiv: quan-ph/0204033.
4. Chung D. and Krasnoholovets V. The cosmic organism theory. arXiv: physics/0512026.
5. Krasnoholovets V. Submicroscopic deterministic quantum mechanics. *Int. J. Computing Anticipatory Systems*, 2002, v. 11, 164–179. arXiv: quant-ph/0109012.
6. Krasnoholovets V. On the origin of conceptual difficulties of quantum mechanics. In: *Developments in Quantum Physics*, Eds.: F. Columbus and V. Krasnoholovets, 2004, Nova Science Publishers Inc., New York, 85–109. arXiv: physics/0412152.
7. Rowlands P. Some interpretations of the Dirac algebra. *Speculat. Sci. Tech.*, 1996, v. 19, 243–51.
8. Rowlands P. and Cullerne J. P. The Dirac algebra and its physical interpretation, 1994. arXiv: quant-ph/0010094.
9. Bell J. S. On the Einstein-Podolsky-Rosen paradox. *Physics*, 1964, v. 1, 195–199.
10. Penrose R. Wavefunction collapse as a real gravitational effect. In: *Mathematical Physics*, eds: by A. Fokas, A. Grigoryan, T. W. B. Kibble and B. Zegarlinski, 2000, Imperial College, London, 266–282.
11. Mazur P. O. and Mottola E. Gravitational condensate stars: an alternative to black holes. Preprint LA-UR-01-5067, 2001. arXiv: gr-qc/0109035.
12. Mazur P. O. and Mottol E. Gravitational condensate stars. *Proc. Nat. Acad. Sci.*, 2004, v. 111, 9545–9550. arXiv: gr-qc/0407075.
13. Chapline G. Dark energy stars. arXiv: astro-ph/0503200.

Spectral Emission of Moving Atom Exhibits always a Redshift

J. X. Zheng-Johansson

Institute of Fundamental Physics Research, 611 93 Nyköping, Sweden
E-mail: jxzj@iofpr.org

A renewed analysis of the H. E. Ives and G. R. Stilwell's experiment on moving hydrogen canal rays (*J. Opt. Soc. Am.*, 1938, v. 28, 215) concludes that the spectral emission of a moving atom exhibits always a redshift which informs not the direction of the atom's motion. The conclusion is also evident from a simple energy relation: atomic spectral radiation is emitted as an orbiting electron consumes a portion of its internal energy on transiting to a lower-energy state which however has in a moving atom an additional energy gain; this results in a redshift in the emission frequency. Based on auxiliary experimental information and a scheme for de Broglie particle formation, we give a vigorous elucidation of the mechanism for deceleration radiation of atomic electron; the corresponding prediction of the redshift is in complete agreement with the Ives and Stilwell's experimental formula.

1 Introduction

Charged de Broglie particles such as the electron and the proton can be decelerated by emitting electromagnetic radiation. This occurs in all different kinds of processes, including atomic spectral emission produced in laboratory [1, 2] or from celestial processes[3], and charged particle synchrotron radiation [4, 5]. The electromagnetic radiation emission from sources of this type is in common converted from a portion of the *internal energy* or the *mass* of a de Broglie particle involved, which often involves a final state in motion, hence moving source. The associated source-motion effect has except for admitting a relativistic effect connected to high source velocity thus far been taken as no different from the ordinary Doppler effect that consists in a red- or blue-shift depending on the source is moving away or toward the observer. The ordinary Doppler effects are directly observable with moving sources of a "conventional type", like an external-field-driven oscillating electron, an automobile horn, and others, that are externally driven into oscillation which does not add directly to the mass of the source. In this paper we first (Sec. 2) examine the property, prominently an invariable redshift, of moving atom radiation as informed by the hydrogen canal ray experiment [1] of Ives and Stilwell performed at the Bell Labs in 1938 for a thorougher investigation of the associated anomalous Doppler effect then known. Combining with auxiliary experimental information and a scheme for de Broglie particle formation[6], we then elucidate (Secs. 3–5) the mechanism for spectral emission of moving atom, or in essence the underlying (relative) deceleration radiation of moving de Broglie electron, and predict Ives and Stilwell's experimental formula for redshift.

2 Indication by Ives-Stilwell's experiment on fast moving hydrogen atoms

In their experiment on fast moving hydrogen canal ray spectral emission[1], Ives and Stilwell let positively charged hydrogen ions H_i^+ of mass M_{H_i} and charge q_i ($i=2,3$) be accelerated into a canal ray of high velocity, v, across accurately controlled electric potential $\mathscr{V}$ correlated with v through the work-energy relation $q\mathscr{V}=\frac{1}{2}M_{\mathrm{H}_i}v^2$; or

$$v/c = A\sqrt{\mathscr{V}} \tag{1}$$

with c the speed of light, and $A=\sqrt{\frac{2q_i}{c^2 M_{\mathrm{H}_i}}}$. For $\mathscr{V}\sim 6700$–20755 volts, $v\sim 10^6$ m/s as from (1). By neutralization and dissociation the ions are at exit converted to excited atoms that are unstable and will transit to ground state by emitting Balmer spectral lines. The wavelength, λ_r, of the emitted Hβ line is then measured using diffraction grating (Fig. 1a) as a function of $\mathscr{V}$. For a finite v, the spectral line produces a first-diffraction peak at $P(v)$, at distance $y(v)=PO$ from the center O; for a hydrogen at rest, $v=0$, the line has a wavelength $\lambda_{r_0}=4861$ angst. and produces a first peak at P_0, $y_0=P_0O$. These have the geometric relations: $\lambda_r=\frac{\lambda_{r_0}}{y_0}y$, and

$$\Delta\lambda_r=\lambda_r-\lambda'_{r_0}=(\lambda_{r_0}/y_0)(y-y_0) \tag{2}$$

$\Delta\lambda_r$ being the mean displacement of the Doppler lines at a given v. The measured spectrogram, Fig. 1b, informs $y-y_0=B'\sqrt{\mathscr{V}}$ with B' a constant; this combining with (2) is:

$$\Delta\lambda_r/\lambda_{r_0}=(\lambda_r-\lambda'_{r_0})/\lambda_{r_0}=B\sqrt{\mathscr{V}} \tag{3}$$

where $B=B'\lambda_{r_0}/y_0$.

If *assuming*

$$\frac{\Delta\lambda_r}{\lambda_{r_0}}=+\frac{v}{c}, \tag{4}$$

then this and (3) give $\frac{v}{c}=B\sqrt{\mathscr{V}}$. But $\frac{v}{c}$ and $\sqrt{\mathscr{V}}$ must satisfy (1); thus $B\equiv A$; that is (3) writes:

$$\Delta\lambda_r/\lambda_{r_0}=A\sqrt{\mathscr{V}}. \tag{3'}$$

In [1], the two variables $\frac{\Delta\lambda_r}{\lambda_{r_0}}$ and $\sqrt{\mathscr{V}}$ are separately

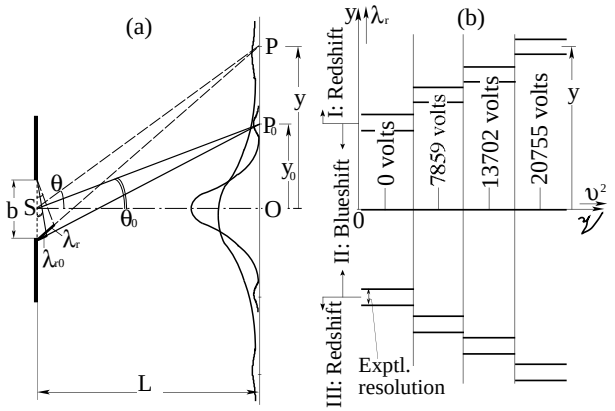

Fig. 1: (a) Schematic single-slit diffraction grating. (b) Experimental spectrogram, peak coordinates $y\,(\propto \lambda_r)$ at several voltages $\mathscr{V}\,(\propto v^2)$, 7859, ..., 20755 volts, after original Fig. of Ref. [1]. Spectral lines at finite $\mathscr{V}$ values all fall in the redshift regions I and III beyond the $\mathscr{V}=0$ ($v^2=0$)-lines illustrated in this plot.

measured and thus given an experimental relation, shown in Fig. 10, of [1, p. 222], which agrees completely with (3′); accordingly (4) is directly confirmed. Furthermore there is a shift of center of gravity of λ'_{r_0} from λ_{r_0}: $\Delta'\lambda_r=\lambda_{r_0}-\lambda'_{r_0}=$ $=\frac{1}{2}(\frac{v}{c})^2$; or $\lambda'_{r_0}=\lambda_{r_0}\left(1-\frac{1}{2}(\frac{v}{c})^2\right)\simeq\lambda_{r_0}\sqrt{1-(v/c)^2}$. With this and (4) in the first equation of (3) or similarly of (2), one gets:

$$\lambda_r=\sqrt{1-(v/c)^2}\,\lambda_{r_0}+(v/c)\lambda_{r_0}; \qquad (5)$$

(5) gives $\lambda_r-\lambda_{r_0}>\frac{v}{c}-\frac{1}{2}(\frac{v}{c})^2\geqslant 0$; or, λ_r is always elongated for $|v|>0$. Furthermore, (4)–(5) are obtained in [1] for both the cases where source and observer move toward and away from each other: The source velocity v is in the fixed $+x$-direction; waves emitted parallel with v (Fig. 2) strike on the diffraction grating D (observer 1) directly (Fig. 2b), and waves antiparallel with v (Fig. 2c) strike on mirror M (observer 2) first and are then reflected to D. That is, (5) is regardless of the direction of the vector c. Therefore from Ives and Stilwell's experiment we conclude:

> The wavelength of spectral line emitted from an atom in motion is always *longer*, or *red-shifted*, than from one at rest, irrespective if the atom is moving away or toward the observer; the faster the atom moves, the longer wavelength its spectral line is shifted to.

This apparently contrasts with the conventional Doppler effect where wavelengths will be $\lambda_r=\lambda_{r_0}(1-v/c)$ and $\lambda_r=$ $=\lambda_{r_0}(1+v/c)$ and show a blue or red shift according to if the source is moving toward or away from the observer.

3 Emission frequency of a moving atom

If a H atom is at rest in the vacuum, its electron, of charge $-e$ in circular motion at velocity u_{n+1} about the atomic nucleus in an excited $n+1$th orbit, has from quantum-mechanical solution (and also solution based on the unification scheme [6]) an eigen energy $\varepsilon_{u.n+1}=-\hbar^2/\left[2m_{e_0}(n+1)^2a_{B_0}^2\right]$, where $n=1,2,\ldots$ and $m_{e_0}=\gamma_0 M_e$, $\gamma_0=1/\left[1-(u_{n+1}/c)^2\right]^{-1/2}$ with u_n being high ($\sim 10^6$ m/s), M_e the electron rest mass, and a_{B_0} Bohr's radius (should already contain $1/\gamma_0$, see below). If now the electron transits to an unoccupied nth orbit, the atom lowers its energy to $\varepsilon_{u.n}$ and emits an electromagnetic wave of frequency

$$\nu_{r_0}=\frac{\varepsilon_{u.n+1}(0)-\varepsilon_{u.n}(0)}{h}=\frac{\hbar^2(2n+1)}{h2m_e(n+1)^2n^2a_B^2}; \qquad (6)$$

accordingly $\lambda_{r_0}=c/\nu_{r_0}$ and $k_{r_0}=2\pi/\lambda_{r_0}=2\pi\nu_{r_0}/c$.

If now the atom is moving at a velocity v in $+x$-direction, $(v/c)^2\gg 0$, then in the motion direction, its orbital radius is Lorentz contracted to $a_B=a_{B_0}/\gamma$, and its mass augmented according to Einstein to $m_e=\gamma m_{e_0}=\gamma\gamma_0 M_e$ (see also the classical-mechanics solutions [6]), where $\gamma=1/\sqrt{1-(v/c)^2}$. With a_B and m_e for a_{B_0} and m_{e_0} in (6), we have $\nu_r=$ $=\frac{\varepsilon_{u.n+1}(v)-\varepsilon_{u.n}(v)}{h}=\gamma\nu_{r_0}$; including in this an additional term $\delta\nu_r$ which we will justify below to result because of an energy gain of the moving source, the spectral frequency for the $n+1\to n$ transition for the moving atom then writes

$$\nu_r=\gamma\left(\nu_{r_0}+\delta\nu_r\right). \qquad (7)$$

4 Atomic spectral emission scheme

We now inspect how an electron transits, from an initial $n+1$th to final nth orbit in an atom moving in general, here at velocity v in $+x$-direction. To the initial-state electron, with a velocity u_{n+1} if $v=0$, the finite v of the traveling atom will at each point on the orbit project a component $v\cos\theta$ onto $u_{n+1}(\theta)$, with θ in $(0,2\pi)$; the average is $\bar{u}_{n+1}=$ $=\int_{\theta=0}^{2\pi}[u_{n+1}+v\cos\theta]d\theta=u_{n+1}$. That is, $\bar{u}_{n+1}$ and any its derivative dynamic quantities of the stationary-state orbiting electron are not affected by v except through the second order factor $\gamma(v)$. The situation however differs during the $n+1\to n$ transition which distinct features may be induced as follows:

(i) The transition ought realistically be a mechanical process in which, in each sampling, the electron comes off orbit $n+1$ at a single definite location, e. g. A in Fig. 2a. That where A is located on the orbit in any sampling, is a statistic event.

(ii) The spectral radiation is a single monochromatic electromagnetic wave emitted in forward direction of the orbiting electron at the point (A) it comes off orbit $n+1$, as based on observations for decelerating electron radiation in a storage ring in synchrotron experiments [4], which is no different from an orbiting atomic electron except for its macroscopic orbital size.

(iii) It follows from (i)–(ii) combined with momentum conservation condition that the transition electron coming off at A, will migrate across shortest-distance AB, perpendicular

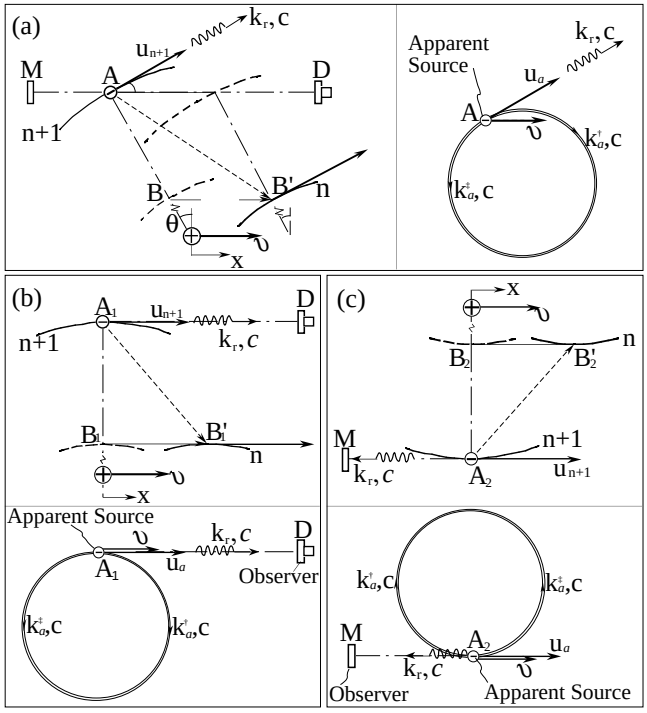

Fig. 2: An atomic electron comes off orbit $n+1$ statistically e. g. at A in (a), emitting in brief time δt a single electromagnetic wave of energy $h\nu_r$ in forward (u_{n+1}) direction, and then migrates (transits) along AB, $\perp u_{n+1}$, to orbit n for an atom of $v = 0$, and across AB' in time $t_{AB'}$ for finite v in $+x$-direction; $\mathrm{BB}' = vt_{AB'}$. In (a): $\angle c, v = \theta$; (b): $c\|v$; (c): $-c\|v$. The insets in (a)-(c) illustrate the radiation from an apparent source.

to u_{n+1}, to orbit n, at B if the atom is at rest, or at B' if the atom is moving at velocity v in x-direction, given after vector addition.

(iv) A stationary-state orbiting electron on orbit n^* ($= n+1$ or n), $\psi_{k_{dn^*}}$, is [6] a (*single*) beat or de Broglie phase wave convoluted from the opposite-traveling component total waves $\{\varphi^j_{kn}\}$ generated by an oscillatory massless (vaculeon) charge $-e$, of wavevectors $k^\dagger_{n^*}$ and $k^\ddagger_{n^*}$, which being Doppler shifted for the source moving at velocity u^j_{n+1}. An $n+1 \to n$ transition emits the difference between the two *single* waves, $\psi_{k_{dn+1}}$ and $\psi_{k_{dn}}$ — the emitted radiation is naturally also a *single* wave. And,

(v) The component total waves making up the electron beat wave at A is generated by the source in a brief time δt when at A, a wave frequency $\sim \mathcal{V} = 511\,\mathrm{keV}/h \simeq 10^{20}\,\mathrm{s}^{-1}$; so the the time for detaching the entire radiation wave trains from the source is estimated $\delta t \sim 1/\mathcal{V} = 8\times10^{-21}$ s. In contrast, the orbiting period of the electron is $\tau_{d.n+1} = 1/\nu_{d.n+1} = (n_1)^2 1.5\times10^{-16}$ s. So in time $\delta t \ll \tau_{d.n+1}$, the electron is essentially not moved along orbit $n+1$ as well as path AB or AB'; hence u_{n^*} ($\simeq u_{n+1}$) (thus c) and v are at fixed angle θ. Specifically if the electron comes off at A_1 and A_2 as in Fig. 2b and c, respectively, we have the approaching and receding source and observer

$$c \,\|\, v \qquad \text{and} \qquad -c \,\|\, v\,. \tag{8}$$

The wave and dynamic variables for the nonstationary transition process would not be a simple difference between solutions of the stationary states. However, we can try to represent the process effectively using an apparent source such that:

(v.1) the total wave detached from the apparent source gives the same observed radiation as due to the actual source; and

(v.2) the apparent source in transition has the same motion as the (actual source of the) transition electron, that is, translating at the velocity v (cf. item iv) in $+x$-direction here.

5 A theoretical formula for the redshift

In fulfilling (v.1), the apparent source ought to be an oscillatory charge (q) executing in stationary state circular motion at velocity u_a on orbit $n+1$ (insets in Fig. 2). Let first the orbit $n+1$ be at rest, $v = 0$, and so must be the apparent source as by (v.2). The apparent source generates two identical monochromatic electromagnetic waves traveling oppositely along orbit $n+1$, of wavevectors $k^\dagger_{a0} = k^\ddagger_{a0} = k_{a0}$, which superpose into a single electromagnetic wave $\psi_{k_{a0}}$. On transition, the source emits the entire $\psi_{k_{a0}}$ in the direction parallel with $u_a(\theta)$, by simply detaching it; thus $k_{a0} \equiv k_{r_0} = 2\pi/\lambda_{r_0}$.

Let now orbit $n+1$ be in motion at velocity v in $+x$-direction, and so must be the apparent source. Let the source comes off orbit $n+1$ at point A_1 (Fig. 2b). In a brief time δt before this, the apparent source was essentially at A_1 and generating two waves $\varphi^\dagger_{k^\dagger_a}$ parallel and antiparallel with u_a, thus v; their wavelengths were owing to the source motion of v Doppler shifted, to $\lambda^\dagger_a = \lambda_{r_0}(1-\frac{v}{c})$, $\lambda^\ddagger_a = \lambda_{r_0}(1+\frac{v}{c})$, and wavevectors $k^\dagger_a = \frac{2\pi}{\lambda^\dagger_a}$, $k^\ddagger_a = \frac{2\pi}{\lambda^\ddagger_a}$ with the Doppler shifts

$$k^\dagger_a - k_{r_0} = \frac{(v/c)k_{r_0}}{1-v/c}\ (a); \quad k_{r_0} - k^\ddagger_a = \frac{(v/c)k_{r_0}}{1+v/c}\ (b). \tag{9}$$

The two waves superpose to $\psi_{k_a} = \varphi^\dagger_{k^\dagger_a} + \varphi^\ddagger_{k^\ddagger_a}$, being according to [6] now a single beat, or de Broglie phase wave of the moving apparent source. On transition the source detaches the entire single beat wave ψ_{k_a}, which is no longer "regulated" by the source and will relax into a pure electromagnetic wave ψ_{k_r}, but in conserving momentum, retains in the single direction parallel with u_a thus v. Similarly, if the source exits at A_2 (Fig. 2c), a single electromagnetic wave will be emitted parallel with $u_a(A_2)$, or, $-v\cdot\psi_{k_a}$ has a de Broglie wavevector given[6] by the geometric mean of (9a) and (b):

$$k_{a.d} = \sqrt{(k^\dagger_a - k_{r_0})(k_{r_0} - k^\ddagger_a)} = \frac{\left(\frac{v}{c}\right)k_{r_0}}{\sqrt{1-(v/c)^2}}$$

$$\text{or} \qquad k_{a.d} = \gamma\left(\frac{v}{c}\right)k_{r_0}\,. \tag{10}$$

We below aim to express the $k_{a.d}$-effected radiation variables k_r, ν_r and λ_r, which being directly observable. Momentum conservation requires $|\hbar k_{a.d}| = |\hbar \delta k_r|$; $k_{a.d}$ is associated with an energy *gain* of the apparent source, $\varepsilon_{a.v} = \frac{(\hbar k_{a.d})^2}{2m_e}$, owing to its motion, and thus an energy *deficit* in the emitted radiation wave ψ_{k_r},

$$\begin{aligned} &\delta\varepsilon_r (= \hbar \delta k_r c) = -\varepsilon_{a.v}\,, \\ &\text{for either} \quad c \parallel v \quad \text{or} \quad -c \parallel v\,, \end{aligned} \tag{11}$$

and accordingly momentum and frequency deficits in the emission

$$\delta k_r = -k_{a.d} = -(v/c) k_{r_0}\,, \tag{12}$$

$$\delta \nu_r = \delta k_r c = -(v/c) k_{r_0} c = -(v/c)\nu_{r_0}\,. \tag{13}$$

With (13) in (7), we have

$$\nu_r = \gamma \left(1 - \frac{v}{c}\right) \nu_{r_0} \simeq \gamma \nu_{r_0} - \left(\frac{v}{c}\right) \nu_{r_0} \tag{14}$$

where γ in front of $\delta\nu_r$ is higher order thus dropped. With (14) we can further compute for the emitted wave:

$$k_r = \frac{2\pi\nu_r}{c} = \gamma \left(1 - \frac{v}{c}\right) k_{r_0} \simeq \gamma k_{r_0} - \left(\frac{v}{c}\right) k_{r_0}\,, \tag{15}$$

$$\lambda_r = \frac{c}{\nu_r} = \frac{c}{\nu_{r_0}(1/\gamma - v/c)} \simeq \frac{\lambda_{r_0}}{\gamma} + \left(\frac{v}{c}\right) \lambda_{r_0}\,. \tag{16}$$

The theoretical prediction (16) for λ_r above is seen to agree exactly with Ives and Stilwell's experimental formula, (5). Notice especially that the prediction gives $\delta\nu_r < 0$ and $\delta\lambda_r > 0$ for both $c \parallel v$ and $-c \parallel v$ as follows from (11); that is, they represent always a redshift in the emission spectral line, regardless if the wave is emitted parallel or antiparallel with v.

6 Discussion

From the forgoing analysis of the direct experimental spectral data of Ives and Stilwell on hydrogen canal rays, and with the elucidation of the underlying mechanism, we conclude without ambiguity that, the spectral emission of a moving hydrogen atom exhibits always a redshift compared to that from an atom at rest; the faster the atom moves, the redder-shift it shows. This is not an ordinary Doppler effect associated with a conventional moving source, but rather is an energy deficiency resulting from the de Broglie electron kinetic energy gain in transition to a moving frame, a common feature elucidated in [7] to be exhibited by the deceleration radiation of all de Broglie particles. This redshift does not inform the direction of motion of the source (the atom).

It is on the other hand possible for an atomic spectral emission to exhibit blue shift for other reasons, for example, when the observer is moving toward the source as based on Galilean transformation. The author thanks P.-I. Johansson for his support of the research and the Studsvik Library for helping acquiring needed literature.

References

1. Ives H. E. and Stilwell G. R. An experimental study of the rate of a moving atomic clock. *J. Opt. Soc. Am.*, 1938, v. 28, 215–226.
2. Kuhn H. G. Atomic spectra. Longmans, London, 1962.
3. Freedman W. L. The Hubble constant and the expansion age of the Universe. *Phys. Rept.*, 2000, v. 333, 13–31; arXiv: astro-ph/9909076; Riess A. G., The case for an accelerating Universe from supernovae. *Pub. of Astronom. Soc. Pacific*, 2000, v. 112, 1284–1299.
4. Crasemann B. Synchrotron radiation in atomic physics. *Can. J. Phys.*, 1998, v. 76, 251–272.
5. Winick H. and Doniach S., editors. Synchrotron radiation research. Plenum Press, New York, 1980.
6. Zheng-Johansson J. X. and Johansson P-I., Fwd. Lundin R., Unification of Classical, Quantum and Relativistic Mechanics and of the four forces. Nova Sci. Pub., NY, 2006; Inference of Schrödinger equation from classical-mechanics solution. *Quantum Theory and Symmetries IV*, ed Dobrev V. K., Heron Press, Sofia, 2006; (with Lundin R.) Cause of gravity. Prediction of gravity between charges in a dielectric medium. *ibid.*; also arxiv: phyiscs/0411134; arxiv physics/0411245; *Bull. Am. Phys. Soc.*, 2006, Topics in Quantum Foundations, B40; *ibid.*, 2004, in: Charm Quark States, D10; *ibid.*, 2004, C1.026; Origin of mass. Mass and mass-energy equation from classical-mechanics solution. arxiv: physics/0501037; *Bull. Am. Phys. Soc.*, 2005, New Ideas in Particle Theory, Y9; Electromagnetic radiation of a decelerating moving de Broglie particle: always a redshift, *ibid.*, 2005, Intermediate Energy Accelerators, Radiation Sources, and New Acceleration Methods, T13; Unification of Classical and Quantum Mechanics, & the theory of relative motion. *Bull. Am. Phys. Soc.*, 2003, General Physics, G35.01; *ibid.*, 2004, General Theory, Y38.
7. Zheng-Johansson J. X. and Johansson P-I., Fwd. Lundin R. Inference of basic laws of Classical, Quantum and Relativistic Mechanics from first-principles classical-mechanics solutions. Nova Sci. Pub., NY, 2006.

Dark Matter and Dark Energy: Breaking the Continuum Hypothesis?

Emilio Casuso Romate and John Beckman
Instituto de Astrofísica de Canarias, E-38200 La Laguna, Tenerife, Spain
E-mail: eca@iac.es

In the present paper an attempt is made to develop a fractional integral and differential, deterministic and projective method based on the assumption of the essential discontinuity observed in real systems (note that more than 99% of the volume occupied by an atom in real space has no matter). The differential treatment assumes continuous behaviour (in the form of averaging over the recent past of the system) to predict the future time evolution, such that the real history of the system is "forgotten". So it is easy to understand how problems such as unpredictability (chaos) arise for many dynamical systems, as well as the great difficulty to connecting Quantum Mechanics (a probabilistic differential theory) with General Relativity (a deterministic differential theory). I focus here on showing how the present theory can throw light on crucial astrophysical problems like dark matter and dark energy.

1 Introduction

In 1999 I published [1] the preliminaries of a new theory: the General Interactivity. It was a sketched presentation of the mathematical basis of the theory, i. e. the fractional integral treatment of time evolution. In the present paper we extend the ideas of General Interactivity to the fractional derivatives, and so we can explain the outer flatness of rotation curves, last measures of SN Ia at high redshifts, the fluctuations in the CMB radiation and the classical cosmology theory.

In 1933 Zwicky [2] found that the Coma cluster of galaxies ought to contain more matter than is inferred from optical observations: many of the thousands of galaxies in the cluster move at speeds faster than the escape velocity expected from the amount of visible matter and from the Newton theory of gravitation. In the 1970's, many authors discovered that the speed of stars and clouds of hydrogen atoms rotating in a galactic disk is nearly constant all the way out to the edge of the galaxy [3, 4]. Using Newton's law of gravitation, this implied that the amount of matter at increasing radius is not falling away, against the observed star-light suggests. Over past two decades, the measured deflection of light from a distant star by a massive object like a galaxy (gravitational lens) points to a mass-to-light ratio for the lensing galaxies of about 150, and yet if galaxies contained only observed stars the expected value would be between 5 and 10 [5]. From the observed cosmic microwave background (CMB, the relic radiation of the Big Bang that fills the Universe) fluctuations, we need that 23% of the Universe is dark matter, and 73% is dark energy [6, 7, 8, 9, 10]. Recent observations of SN Ia brightness show that the expansion of the Universe has been speeding up. This unexpected acceleration is also ascribed to an amount of dark energy that is very similar than 73% of the Universe [11].

In Section 2 we show a review of the theory, in Section 3 we apply the theory to account for the observed dark matter and dark energy, and in Section 4 we develop the conclusions.

2 The model

I start from two hypothesis: (1) the irreversibility in time of natural systems and (2) the interactivity among all the systems in the Universe. These hypotheses imply an intricate, unsettled and discontinuous (and hence non-differentiable) space-time. The differential treatment projects a variable $X(t)$, whose value is known at a time t, to a successive time, $t+\Delta t$, through the assumption of a knowledge of their time derivative, $X'(t)$, as follows: $X(t+\Delta t) = X(t) + + X'(t)\Delta t$. In many cases, to a good approximation, there is proportionality between $X(t)$ and $X'(t)$ so that $X'(t) \propto X(t+\Delta t)$. Here I extend this projection, but with two crucial modifications: (a) I project a complete distribution of real values (a set of measured values ordered in time) instead of individual values at one time, and (b) I generalize the derivative to the Liouville fractional derivative (to take into account the possibility of the discontinuous space-time of the system under study). This then gives the fundamental equation of the new dynamics:

$$\frac{d^{\beta}_{FRAC}}{dt}\, X(t_{past}) \propto X(t_{future})\,. \qquad (1)$$

$X(t_{past})$ being a table of values of the variable X until the present time, $X(t_{future})$ the same number of values of X but from the present time to the future (a projection), and β a value between 0 and 1 that includes the key information about the history of the system.

But for more physical sense, one must take the inverse of equation (1), i. e.

$$X(t_{past}) \propto \frac{1}{\Gamma(\beta)} \int_{t_{past}}^{T} \frac{X(t_{future})}{(t_{past} - t_{future})^{1-\beta}} dt_{future} \qquad (2)$$

which is the fractional integration (or the Riemann-Liouville integral) of $X(t_{future})$, T being a time-period characteristic of each system. The first hypothesis, irreversibility, suggests the necessity of projecting the values of $X(t)$, weighted by a function of time that must be similar to the function characteristic of critical points, such as observed in the well known irreversible phase transitions in Thermodynamics; for example, the form $(T_E - T_{EC})^{-0.64}$ for the time correlation length of an infinite set of spins with a temperature T_E near the critical temperature T_{EC} [12]. Compare this with the term $(t_{past} - t_{future})^{\beta-1}$ in equation (2). I call this weighting "generalized inertia"; it is characteristic of each system in the sense of incorporating into the β exponent the history of all the interactions suffered by the system, including those interactions avoided by the differential approximation (high order terms in Taylor expansions) due to its small values.

To use the fundamental equation (1) with maximum efficiency, I invert equation (2) because this is an Abel integral transform, and there is a technique developed by Simmoneau et al. [13] to optimize the inversion of Abel transforms. This technique consists in making a spectral expansion using a special kind of polynomials whose coefficients are obtained by means of numerical integration, thus avoiding the basic problem of amplification of the errors, a problem inherent in numerical differentiation; in the technique of Simmoneau et al., measurement errors are incorporated into the coefficients of the spectral expansion and then propagate with time without being amplified.

In the present context one can see the time as a critical variable, each "present" being an origin of time coordinates, with two time dimensions: the past and the future. We should note that in Quantum Mechanics two independent wave functions are needed (the real part and the imaginary part of the total wave function) to describe the state of a system at each moment in time.

One can view General Interactivity as a third approximation to reality: the first was the conception of continuous and flat space-time by Newton, the second was that of continuous and curved space-time by Einstein. Here I see a discontinuous space-time whose degree of intricacy measures the essential cause of changing. As in Newtonian Dynamics, where the forces are the causes of changing, and in General Relativity, where modifications of the metric of space-time are the cause of changes in the motion of all massive systems, in General Interactivity the exponent β gives us a measure of the intricacy of the space-time "seen" by each system through a given variable X. But how can we see Gravity from the new point of view of General Interactivity? From (differential) Potential Theory we know that the modulus of the gravity force per unit mass is the following function of mass distribution, $\rho(x)$, in space:

$$F_G(x) = G \int \frac{\rho(x')}{|x' - x|^2} d^3x' \qquad (3)$$

and, comparing with the three-dimensional fractional integration of $\rho(x)$ we have:

$$R_\beta\big[\rho(x)\big] = \pi^{\beta-\frac{\pi}{2}} \frac{\Gamma\left(\frac{3-\beta}{2}\right)}{\Gamma\left(\frac{\beta}{2}\right)} \int \frac{\rho(x')}{|x - x'|^{3-\beta}} d^3x'; \qquad (4)$$

$F_G(x)$ can be identified with the 1-integral of $\rho(x)$ in three-dimensional space ($\beta = 1$) except for a constant. So in the present context the gravity force can be interpreted as a one-dimensional projection of the three-dimensional continuous distribution of matter. It is not, then, a complete integral (this would be $\beta = 3$) and so the sum (integral) for obtaining the gravity is more intricate than the mass distribution (continuous by definition), i. e. the real discontinuity of mass distributions is transferred to the fractional integral instead of working with a discontinuous $\rho(x)$. Gravity, like the electrostatic force, whose expression is very similar to $F_G(x)$, is seen as an inertial reaction of space-time, which would tend to its initial (less intricate,i. e. simpler) state, towards a structure in which the masses were all held together without relative motions; both forces are seen as reactions against the action of progressive intricacy in the general expansion of the Universe following the Big Bang.

We take the total mass-energy of the Universe as the observable magnitude $X(t)$ to evolve in time using Eq. (2). The constancy of this variable gives $1 = \frac{1}{\beta^2}(T^2 - t_{past}^2)^\beta$ (where I take squared variables for simplicity in the use of Simmoneau et al.'s inversion technique). The greater past-time variable, t_{past}, less β indicating that the space-time is more intricate with time; this is the reason for integrating more fractionally (less β). So the parameter β can also be considered as a measure of the entropy of the Universe.

Another key to understand General Interactivity comes from the classical Gaussian and Planckian distribution functions, to which real systems in equilibrium tend. The equilibrium distribution function for systems of particles, for collisional and for collisionless systems (in the non-degenerate limit [14]) is Gaussian; classical Brownian motion is an example [15]; the equilibrium distribution function for systems of waves is a Planckian, and a key example is blackbody radiation. If both distribution functions evolve in time, then, using the inversion of equation (2), we have the same final result: the Planckian distribution. This tells us that whatever the initial distribution at the beginning of the Big Bang (perhaps both the Planckian characteristic of interacting waves and the Gaussian characteristic of interacting particles coexisted), their time evolution leads to a Planckian distribution, thereby connecting with the actual observed spectrum of the Cosmic Microwave Background, which appears to be almost perfectly Planckian.

But, why is the Planckian more stable than the Gaussian with the passing of time? The answer I propose is that successive critical transitions (at each time), due to the complexity caused by interactions at large distances, tend to amplify the Gaussian distribution to all range of energies, making it

flatter. This breaks the thermal homogeneity because of the very different time evolution of many regions, due to the delay in the transmission of information from any one zone to others that are far away (note that the speed of the light is a constant). This amplification goes preferentially to high energies because there is no limit, in contrast with lower energies, for which the limit is the vacuum energy.

In this context, then, the Universe is seen as an expansion of objects that emitting information (electromagnetic waves) in all directions, and one can differentiate between two basic kinds of interactions: (a) at small distances (the distance travelled by light during a time that is characteristic of each system) forming coupled systems showing macroscopic (ensemble) characteristics, such as temperature or density, well differentiated from those of their surroundings; and (b) at large distances, interfering one system from another in a complex manner due to the permanent change in the relative distances due to the constancy of the speed of light, the huge number of interactions and the internal variation of the sources themselves. Note that this distinction between small and large distances can be extended relative to each physical system. For instance, a cloud of water vapour (as in the Earth's atmosphere) constitutes a system of water molecules interacting over short distances, while the interaction between one cloud and another is considered to take place over a large distance. Inside a galaxy, the stars in a cluster are considered to interact over short distances, while the interactions between that cluster and the remaining stars and gas clouds in the galaxy are considered as interactions over large distances.

In General Relativity there are no point objects; instead, all the objects in Nature are considered as systems of other objects, even subatomic particles appearing to be composed of others yet smaller.

I now focus on one of the most puzzling interpretations of Quantum Mechanics: the wave-particle duality. In Quantum Mechanics the objects under study show a double behaviour depending on what type of experiment one makes. An electron behaves as a particle in collisions with other electrons, but the same electron passing through two gaps (enough small and enough near each other) behaves as a wave in that the outcoming electrons form an interference pattern. In General Interactivity each "particle" is considered as a system, and we know that the equilibrium distribution of random particles is Gaussian, and that after the time evolution given by Eq. (2) the distribution transforms into a Planckian (the interaction with the other systems "drives" the random set of particles) which is the distribution to which a set of interacting waves in a cavity naturally tend. Furthermore, the Planckian can be decomposed into a set of Gaussians, so that the double nature of matter/energy is ensured. The fact that a Planckian can be the result of the addition of Gaussians of different centres and amplitudes is interpreted as the Planckian representing an ensemble of random motions in turn represented by Gaussians, which find a series of walls to which resulting in certain reflexion and certain absorption. As already demonstrated [15], both processes, reflexion and absorption by a barrier, are equivalent to the addition and the subtraction, respectively, of two Gaussians: the main Gaussian and that which emerge as a consequence of the barrier (by displacing its centre to the other side of the barrier). A Gaussian, then, converts into a set of several other Gaussians at progressively smaller amplitudes as a consequence of the existence of barriers, and the envelope is a Planckian. There is a partial reflection at each barrier in the direction of higher energies, while the reflection is total to the lower energies and the absorption of unreflected part must be added to the left of the barrier. This argument can be applied to explain the Planckian distribution observed in the Cosmic Microwave Background Radiation: the energy barriers can be thought of as the consequence of the existence of wrinkles in space-time, caused by the finiteness of the Universe (closed box) and the uncoupled expansion of the content with respect to the box, or by breaking of the expansion because of the collision of the outer parts with another medium, or by the succession of several bangs at the beginning, instead of only one bang.

3 Dark Matter and Dark Energy

Another example of application of this theory is the generalization of one of the most important theorems in Field Theory, Gauss's theorem, leading to a possible solution (as a kind of Modified Newtonian Dynamics theory) of the well known problem of the "lost mass" of the Universe and its associated problem of "dark matter" [16]. Assuming the well known observation of the infinitesimal volume occupied by matter relative to holes in Nature (the nucleus of an atom occupy less than 1% of the atom's volume, and gas clouds in the interstellar medium have densities of 1 atom per cubic centimeter or less), one must consider the possibility of relaxing the continuum hypothesis. The Gauss's theorem can be expressed, simplified and for the gravitational field, as

$$\int_S g_N dS = -4\pi GM\,, \tag{5}$$

where g_N is the intensity of the gravity field over a closed surface, S, which contains the mass, M, which is the origin of the field, on the assumption of continuity, and G is the universal gravity constant. So, integrating Eq. (5) on the assumption of $g_N \simeq$ constant over S, we get $g_N = -4\pi GM/S$, with $S = \int_S dS$. If we take as the starting point the differential form of Gauss theorem, and then we take in Eq. (5) the fractional, instead of the full, integral and also assume $g \simeq$ const, we have

$$g(r) = \frac{-4\pi GM}{\frac{\pi^{\beta-1}\Gamma\left(\frac{2-\beta}{2}\right)}{\Gamma\left(\frac{\beta}{2}\right)} \int_S \frac{dX}{|S-X|^{2-\beta}}}\,. \tag{6}$$

Because β is less than 2, g is greater than g_N, and this result could explain the observational fact of g_N being very

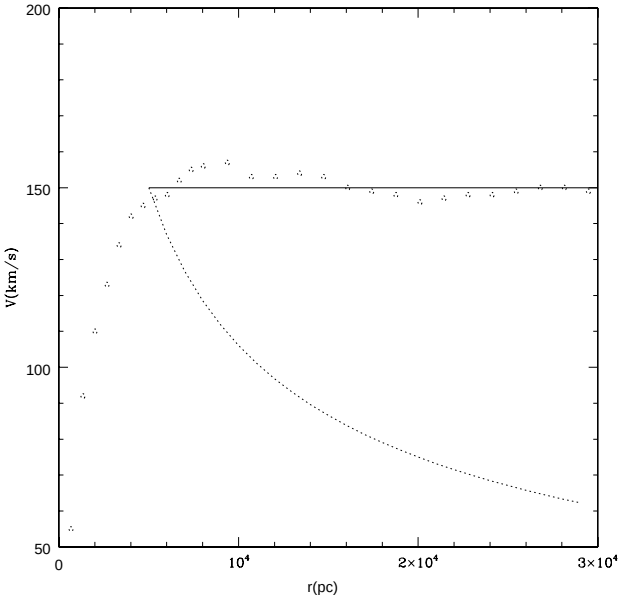

Fig. 1: Rotation curve (kms^{-1}) for NGC3198. Crosses are observational data points taken from van Albada et al. [17]. Full line is the prediction of the present theory, and dashed line is the prediction by the Newton law of gravitation.

small in explaining, for instance, many galactic rotation curves far from the central regions. For, assuming spherical simetry one has:

$$g(r) = g_N \frac{4\pi r^2}{\frac{\pi^{\beta-1}\Gamma\left(\frac{2-\beta}{2}\right)}{\Gamma\left(\frac{\beta}{2}\right)} \int_0^{2\pi} \frac{2\pi r^2 \sin\theta d\theta}{r^{2-\beta}}} \,. \tag{7}$$

And taking $\beta = 1$ one has $g(r) = g_N r$, which introduced in the classical centrifugal equilibrium identity $\frac{V^2}{r} = g$ leads to the amazingly $V = (GM)^{1/2} \simeq$ constant as is observed for flat rotation curves that needs dark matter (see Fig. 1).

More complicated treatment can be made: in the integral treatment one can consider the basic constituents of matter (the atoms) and the infinitesimal size of the volume occupied by the atomic mass (the nucleus) with respect to the size of the atom, and then one finds the necessity of take into account that ubiquitous nature of the big holes existing inside the matter (the atoms and molecules inside the very low density galactic gas clouds amplify the hole effect respect to the whole cloud and then amplify the influence in the macroscopic gravitational (massive) behaviour). So one can consider the hypothesis of continuity as a first approximation, and one can re-examine the Gauss' theorem

$$\int_S g dS = -4\pi G \int_V \rho dV \,, \tag{8}$$

where g is the gravitational field over the surface S, S is any closed surface containing the massive object which is the source of the field, G is the gravitational constant, ρ is the density, and V is the volume contained within the surface S. And one can generalize Eq. (5) in the sense of take both integrals as fractional integrals (α and β respectively) which leads to normal integrals for some especial case. If one assumes, for simplicity, spherical symmetry for the gas mass distribution in the galaxy, one has:

$$\rho = \rho_0 \, e^{\frac{-(r-r_0)}{r'}} \tag{9}$$

and assuming $g \simeq$ constant over the now non-necessary continue surface (the fractional integration takes this into account) one has:

$$g = -\frac{16\pi^2 G\rho_0 C_2(\beta)}{f(\alpha) r^2 C_1(\alpha)} \, r^{2-\alpha} \int r^2 r^{\beta-3} e^{-\frac{r-r_0}{r'}} dr \,, \tag{10}$$

where $f(\alpha)$ is some function of α,

$$C_2(\beta) = \pi^{\beta-3/2} \frac{\Gamma\left(\frac{3-\beta}{2}\right)}{\Gamma\left(\frac{\beta}{2}\right)} \,, \tag{11}$$

$$C_1(\alpha) = \pi^{\alpha-1} \frac{\Gamma\left(\frac{2-\alpha}{2}\right)}{\Gamma\left(\frac{\alpha}{2}\right)} \,, \tag{12}$$

while

$$g_N = -\frac{4\pi G\rho_0}{r^2} \int r^2 e^{-\frac{r-r_0}{r'}} dr \,. \tag{13}$$

So, in the especial case when $\beta = 3$ and $\alpha = 2$ we have $g = g_N$. Then, expanding $r^{\beta-3} \simeq 1 + (\beta-3)\log r + \ldots$ as $\beta \to 3$ and $r^{2-\alpha} \simeq 1 - (\alpha-2)\log r + \ldots$ as $\alpha \to 2$, and including the expansions into Eq. (13) one has

$$\begin{aligned} g \simeq & \frac{8\pi C_2(\beta)}{f(\alpha) C_1(\alpha)} \big(1 - (\alpha-2)\log r\big) \times \\ & \times \left(g_N - \frac{4\pi G\rho_0}{r^2} \int (\beta-3)(\log r) r^2 e^{-\frac{r-r_0}{r'}} dr \right). \end{aligned} \tag{14}$$

And integrating by parts and taking very large values for r, we have

$$g \simeq g_N \frac{8\pi C_2(\beta)}{f(\alpha) C_1(\alpha)} \big(1 + (\alpha-2)(3-\beta)\log^2 r\big) \,. \tag{15}$$

And for typical values of observed flat rotation curves ($5\mathrm{kpc} \leqslant r \leqslant 20\mathrm{kpc}$) we have that $g \propto g_N r$ represents a good approximation. So, for certain values of α and β (α less than 2 and β greater than 3) one has that outer rotation curves can be flat as observed.

But the most puzzling problem up-to-date in cosmology is the necessity of adding "ad hoc" a dark energy or negative pressure (the so called by Einstein cosmological constant) to the main equation of General Relativity to account for the last measures on supernovae Ia and the fluctuations in the cosmic microwave background radiation which implies a flat accelerating expanding universe. The field equation of General Relativity was formulated by Einstein as the

generalization of the classic Poisson equation which relates the second derivative of the potential ϕ associated to the gravitational field with the assumed continuous mass distribution represented by the volume density ρ:

$$\Delta^2\phi + 4\pi G\rho = 0\,. \tag{16}$$

For comparison, the similar equation in General Relativity, which relates the mass and energy distribution with the differential changes in the geometry of the continuum space-time, is (see e. g. Einstein [18]):

$$\left(R_{\mu\nu} - \frac{1}{2}\,g_{\mu\nu}R\right) + \kappa\,T_{\mu\nu} = 0\,. \tag{17}$$

But for the last equation be coherent with the last independent measures of SN Ia and fluctuations of CMB radiation, we need to add a term $g_{\mu\nu}\Lambda$ to the left side of equation which represents near 73% of all the other terms. This problem is avoided naturally if we consider a discontinuous space-time, and then we re-formulate the equations by using the fractional derivative instead the full derivative. In that case, the second derivative is less than the full derivative, and then the cosmological constant is not needed at all to equilibrate the equations. In fact the μ-fractional derivative of the function r^λ is given by [19]:

$$D^\mu r^\lambda = \frac{\Gamma(\lambda+1)}{\Gamma(\lambda-\mu+1)}r^{\lambda-\mu} \tag{18}$$

for λ greater than -1, μ greater than 0. But as $\lambda\to-1$, $r^\lambda\to\propto\phi$ being ϕ the gravitational potential. And as one can see, taken a fixed value of λ, as μ increase, the μ-derivative decrease. Or to be more precise, if we assume that the constant to be added to the left side of Eq. (17) represents the 73% of all the matter and energy in the Universe, one has:

$$\lim_{\lambda\to-1}\frac{\Gamma(\lambda-\mu+1)R^{-\lambda-2}}{\Gamma(\lambda-2+1)R^{-\lambda-\mu}} \simeq 1.73\,, \tag{19}$$

where R is a characteristic scale-length of the Universe. And the relation (19) works for values of μ greater but very near 2, being 2 the value corresponding to the usual second derivative. So we conclude that taking a value, for the derivatives in the field equations, slightly greater than the usual 2, we are able of include the cosmological constant inside the new fractional derivative of the classical field equations.

4 Conclusions

The new theory of the General Interactivity can be applied to many fields of natural science and constitutes a new step forward in the approximation to the real behaviour of Nature. It assumes the necessity of explicitly taking into account the real history of a system and projecting to the future. However, it also takes into account the non-uniformity of the distribution of holes in the Nature and is therefore a theory of discontinuity. The new theory can account for naturally the needed amounts of dark matter and dark energy as a light modification of classical field equations.

Acknowledgements

This work was supported by project AYA2004-08251-CO2-01 of the Spanish Ministry of Education and Science, and P3/86 of the Instituto de Astrofísica de Canarias.

References

1. Casuso E. *I.J.M.P.A.*, 1999, v. 14, No. 20, 3239.
2. Zwicky F. *Hel. Phys. Acta*, 1933, v. 6, 110.
3. Sancisi R., van Albada T. S. In: *Dark Matter in the Universe*, (eds. Knapp G., Kormendy J.), I.A.U. Symp. No. 117, 67 Reidel, Dordrecht, 1987.
4. Battaner E., Florido E. *Fund. of Cosmic Phys.*, 2000, v. 21, 1.
5. Mc Kay T. A. et al. *ApJ*, 2002, v. 571, L85.
6. Riess A. G. et al. *AJ*, 1998, v. 116, 1009.
7. Perlmutter S. et al. *ApJ*, 1999, v. 517, 565.
8. de Bernardis P. et al. *Nature*, 2000, v. 404, 955.
9. Hanany S. et al. *ApJ*, 2000, v. 545, L5.
10. Halverson N. W. et al. *ApJ*, 2002, v. 568, 38.
11. Kirshner R. P. *Science*, 2003, v. 300, 1914.
12. Wilson K. G., Kogut J. *Physics Reports*, 1974, v. 12, No. 2, 75.
13. Simmoneau E., Varela A. M., Munoz-Tunon C. *J.Q.S.R.T.*, 1993, v. 49, 149.
14. Nakamura J. *ApJ*, 2000, v. 531, 739.
15. Chandrasekhar S. *Rev. Mod. Phys.*, 1943, v. 15(1), 20.
16. Binney J., Tremaine S. In: *Galactic Dynamics*, Princeton Univ. Press, 1987.
17. van Albada T. S., Bahcall J. N., Begeman K., Sancisi R. *ApJ*, 1985, v. 295, 305.
18. Einstein A. In: *El Significado de la Relatividad*, ed. Planeta-Agostini, Spain, 1985.
19. Oldham K. B., Spanier J. In: *The Fractional Calculus: Integrations and Differentiations of Arbitrary Order*, New York, Academic Press, 1974.

Phenomenological Model for Creep Behaviour in Cu-8.5 at.% Al Alloy

M. Abo-Elsoud

Mater. Sci. Lab., Physics Department, Faculty of Science, Beni-Suef University, Egypt

E-mail: maboelsoud24@yahoo.com

Creep experiments were conducted on Cu-8.5 at.% Al alloy in the intermediate temperature range from 673 to 873 K, corresponding to 0.46–0.72 T_m where T_m is the absolute melting temperature. The present analysis reveals the presence of two distinct deformation regions (climb and viscous glide) in the plot of $\log \dot{\varepsilon}$ vs. $\log \sigma$. The implications of these results on the transition from power-law to exponential creep regime are examined. The results indicated that the rate controlling mechanism for creep is the obstacle-controlled dislocation glide. A phenomenological model is proposed which assumes that cell boundaries with sub-grains act as sources and obstacles to gliding dislocations.

1 Introduction

The importance of accurate experimental data on the creep properties of polycrystalline metals and alloys is well known.

Creep resistance is an important attribute of high temperature alloys and mechanisms that control! creep in alloys must be well understood for design of alloys that resist creep. These mechanisms can be classified into different types depending on the values of the activation energy for creep and temperatures. Several of these mechanism were reviewed by Raj and Langdon [1].

The creep resistance of Cu was shown to increase as the Al content is increased although the creep increment was small above 8.5 at.% Al. The creep response of Cu-Al binary solid solutions has been described in one of two ways: (i) those alloys in which dislocation climb is the rate-controlling step during deformation and (ii) where dislocation glide becomes rate controlling due to solute drag on moving dislocations [2]. More detailed knowledge of dislocation processes in cell walls and for sub-boundaries in creep that could lead to a greater understanding of the creep mechanisms has been emphasized [3]. From out point of view, the two models which represent an important step in this direction are as follows: (a) the model of soft (i.e. sub-grain interior) and hard (i. e. sub-boundaries) regions introduced by Nix-Ilschner [4], and developed with considerable detail by Rodriguez et al. [5]; (b) the bowing-out model of sub-boundaries due to Argon and Takeuchi [6]. From an experimental point of view, Aldrete [7] measured local stresses in the sub-grain structure formed during steady state creep in Cu-16 at.% Al solid solution alloy. Their results show that the internal stress σ_i [3] mainly originates in cell wall regions.

The objective of this paper is to study the phenomenological model for creep behaviour in Cu-8.5 at.% Al alloy, and examine the mechanism controlling the creep regime at intermediate temperature region.

2 Experimental procedure

The Cu-8.5 at.% Al alloy was prepared from melting high purity copper and aluminum (99.99%) by aspiration through a quartz crucible of induction melted alloy under a helium atmosphere [8]. The cooling rate of the alloy is between $4{\times}10^2$ and $10^3\,\mathrm{K s^{-1}}$. The ingot was swaged in wire form of diameter 1 mm and ≈ 50 mm gauge length. The wire specimens were pre-annealed at 873 K for 1h to check what happens to the distribution of Al, and to remove the effects of machining with producing a stable uniform grain size [9], in a quartz ampoule after evacuating to at least $5.3{\times}10^4$ Pa. After this treatment the samples were considered to be precipitated [10]. Fairly reproducible and equiaxed grains were obtained from the heat treatment, and the average linear intercept grain size obtained from a statistical sample size of grains was $\cong 10\mu$m.

Creep tests were conducted at the intermediate temperature range from 673 to 873 K, corresponding to $0.46-0.72\,T_m$, with an accuracy of ± 1 K under constant stress condition in a home-made creep machine with a Andrade-Chalmers lever arm. All tests were conducted under a flowing argon atmosphere maintained at a slightly positive pressure.

Some temperature change tests were conducted in order to determine the activation energy for creep Q_c.

3 Results and discussion

All creep curves showed a normal primary stage and a reasonably well-established steady-state region. The duration of the tertiary stage was short and abrupt, although the contribution of the tertiary strain to the total strain was often quite large. Typical creep curves are shown in Fig. 1 for a temperature 773 K and different stress levels.

Usually creep tests are carried out on annealed samples; then we can assume that, during the first minutes of the test,

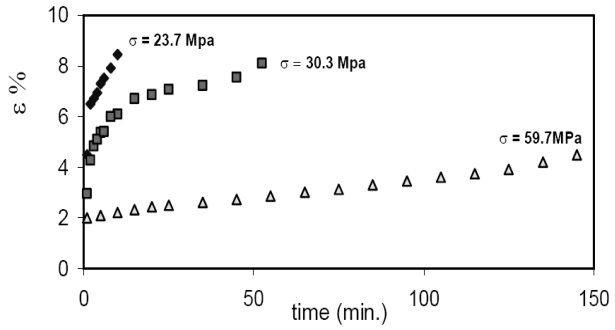

Fig. 1: Representative creep curves at different stress levels and at $T = 823\,\mathrm{K}$.

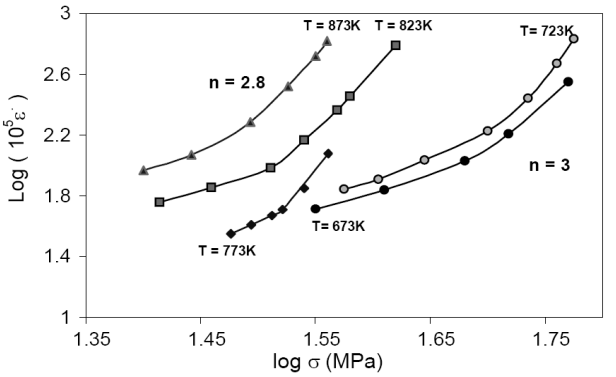

Fig. 2: Stress dependence of minimal creep rate at different temperatures. The creep rates show a change in slopes from $n = 3$ to $n = 2.8$ at the transition stresses.

the annihilation events are negligible as compared with the creation of dislocations. Therefore, considering that all the dislocations are mobile, the change ρ_m in is due to the creation of new dislocations. Also, according to Montemayor-Aldrete et al. [7] the creation rate $\dot{\rho}_m^+$ of dislocations is given as

$$\dot{\rho}_m^+ = \frac{\alpha\sigma\,\dot{\varepsilon}}{\bar{u}}\,, \qquad (1)$$

where $\bar{u}$ is the mean value for the self-energy of dislocations per unit length, α is the average geometrical factor relating the tensile deformation to the shear deformation for samples, and $\dot{\varepsilon}$ is the deformation rate.

Since the strain in the secondary region was often quite small, especially at the lower temperatures, it was necessary to assume that the minimum creep rate was representative of secondary behaviour. Fig. 2 shows the variation of the minimum creep rate $\dot{\varepsilon}$ with applied stress plotted logarithmically. As indicated, the stress exponent, n, $(n = \partial \ln \dot{\varepsilon}/\partial \ln \sigma_a)_{T,t}$ decreases from $\cong 3.2 \pm 0.2$ at the lowest temperature of 673 K to $\cong 2.8 \pm 0.2$ at temperature above $\cong 773\,\mathrm{K}$. These values of stress exponent are typical for a rate controlling process due to a transition from viscous glide mechanism to climb of dislocation along the shear planes [2]. However, Fig. 2 assumes implicitly that the power-law relationship is valid and this may not be true to for all of the datum

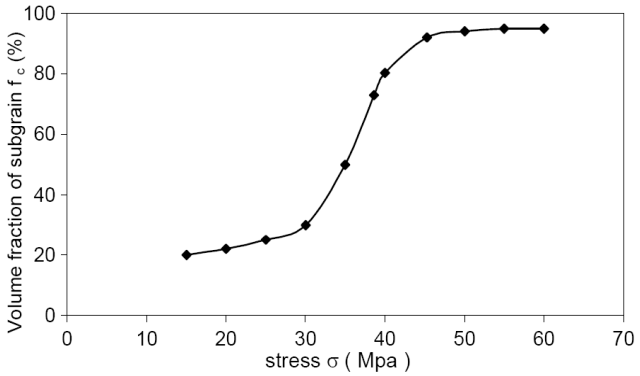

Fig. 3: The dependence of the volume fraction fc of subgrains near grain boundaries on applied stress at $T = 773\,\mathrm{K}$.

points. This observation suggested that there is a connection between creep behaviour and the internal microstructure of the primary sub-grains. It is found that the primary sub-grains become elongated in the transition region between power-law and exponential creep, and they often contain fewer secondary sub-boundaries, larger numbers of coarse-walled cells and a higher dislocation density in comparison to their equiaxed neighbors [1]. Similar microstructures consisting of cells and equiaxed and elongated sub-grains have also been observed in Al [9], Cu [11], Fe [12].

From a phenomenological point of view, the qualitative features of the our model consider that in the early primary transient stage of deformation the only difference between viscous glide and power-law creep is due to the dependence of the glide velocity on the effective stress σ_e. Here $\sigma_e = \sigma - \sigma_i$, with σ the applied stress and σ_i the internal stress. At the higher stress level in the power law creep regime, the apparent creep mechanism is determined by the relative volume fraction of climb-and viscous-glide-controlled regions as presented in Fig. 3. If the above arguments are reasonable, then it is suggested that the creep rate in a grain of a polycrystalline aggregate can be represented by summation of the viscous glide and climb rates as follows [13]:

$$\dot{\varepsilon}_{app} = (1 - f_c)\,\dot{\varepsilon}_g + f_c\,\dot{\varepsilon}_c\,, \qquad (2)$$

where $\dot{\varepsilon}_{app}$ is the apparent creep rate, and $\dot{\varepsilon}_g$ and $\dot{\varepsilon}_c$ are the rates of the viscous glide and climb processes respectively. The volume fraction of sub-grains near the boundary is f_c. The volume fraction of the region controlled by the viscous glide process is $1 - f_c$. If grain boundaries migrate only, the value of f_c becomes zero.

Fig. 4 shows a schematic representation of the deformation behaviour in the vicinity of grain boundaries and development of sub-grains in $n \approx 3$ stress region. It shows a large equiaxed primary sub-grain which is formed during power-law creep and subdivided by cells; for simplicity, secondary sub-boundaries are not shown (see Fig. 4a). Under steady-state conditions, a dislocation generated at a cell boundary under the action of a shear stress, τ, can glide across to the

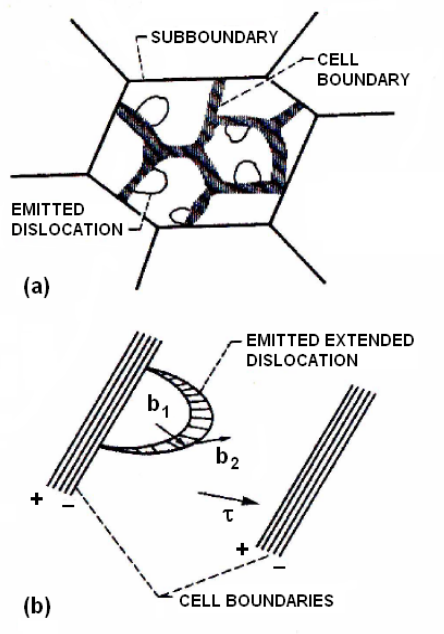

Fig. 4: A phenomenological model for creep showing (a) cells and dislocations within a sub-grain and (b) emission of extended dislocations from a cell wall; b_1 and b_2 are the Burgers vectors of the partial dislocations.

opposite boundary fairly easily (Fig. 4b), where its motion is obstructed or it is annihilated. This process is similar to mechanisms suggested for cyclic deformation [14] but unlike the earlier two phase creep models [2], the present mechanism is consistent with recent experimental observations [15] since it assumes that the cell rather than the sub-grain boundaries govern steady-state behaviour. This difference is important because, in order to accommodate strain inhomogeneity in the material, a cell boundary is more likely than a sub-boundary to breakup due to its smaller misorientation angle (about 0.1°), and thus it is more likely to release new dislocations into the sub-grain interior. In this way, the cell boundaries act as the major sources and sinks for dislocations during creep. The transition from power-law to exponential creep can be envisaged [4, 7] to occur when these microstructural changes are sufficiently large that they influence the nature and magnitudes of the internal stresses acting within the primary sub-grains, thereby resulting in an increase in their aspect ratio. The internal stresses within elongated sub-grains are expected to be higher than that within equiaxed sub-grain, and this difference can lead to sub-boundary migration if the sub-boundaries are mobile. This is consistent with experimental observations on many materials [16].

Fig. 5 shows a comparison of the experimental activation energies Q_c for the alloy with those predicted by the Nix-Ilschner model [4] for obstacle-controlled glide Q_g vs. normalized stress σ/G. It suggest that obstacle controlled dislocation glide is the dominant mechanism in Cu-8.5 at.% Al alloy

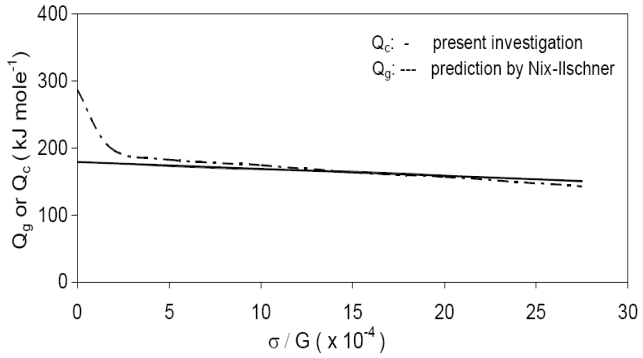

Fig. 5: A comparing between the experimental activation energies, Q_c, for Al-8.5 at.% Cu alloy, and the prediction by the Nix-Ilschner model [4] for obstacle-controlled glide, Q_g at $T = 773$ K.

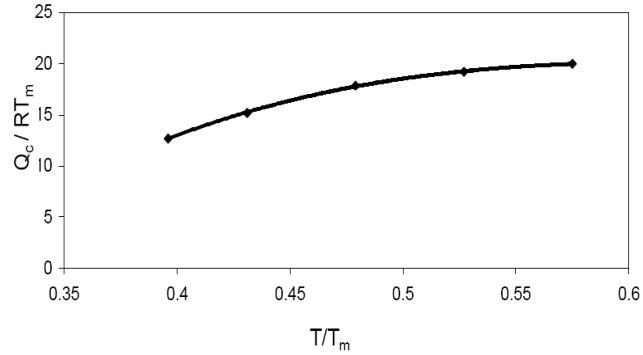

Fig. 6: The normalized activation energies, Q_c, dependence of the T/T_m for the increasing strain rates.

at intermediate temperature region when $\sigma/G \geqslant 5\times10^{-5}$, corresponding to the exponential creep regime [17].

Although the Nix-Ilschner model [4] is in excellent agreement with the experimental data, it is conceptually limited because since it assumes that the deformation processes occurring within the sub-grain interior (i. e. the soft regions) are coupled with recovery mechanisms taking place at the sub-boundaries (i. e. the hard regions). While this assumption predicts that the power-law and the exponential creep mechanisms will act independently, it dose not satisfy the strain compatibility conditions which must maintained between the hard and soft regions to ensure that the slowest deforming phase determines the overall creep rate in both deformation regimes. Support this phenomenological model is also found in Cottrell-Stokes type experiments [18].

Additionally, Fig. 6 reveals that the normalized activation energies, Q_g/RT_m, extrapolate smoothly to the values obtained at lower homologous temperatures where obstacle-controlled glide was established as the dominant deformation process.

4 Conclusion

1. A detailed analysis of creep data on Cu-8.5 at.% Al alloy, obtained at intermediate temperatures between

$0.46-0.72\,T_m$, showed that the obstacle-controlled glide is the rate-controlling mechanism in the transition from power-law to exponential creep regime.

2. A phenomenological model for creep is proposed which is based on the premise that cell boundaries in the sub-grain interior act as sources and obstacles for dislocations.
3. The soft and hard regions model for the internal stress σ_i for a power-law creep curve can only be explained by considering the contribution to σ_i arising from the cell wall dislocations, as well as from dislocations that do not belong to the cell walls.

References

1. Raj S. V. and Langdon T. G. *Acta Metall.*, 1991, v. 39, 1817.
2. Guyot P., Canova G., *Philos. Mag.*, 1999, v. A79, 2815.
3. Cadek J. *Mater. Sci. Eng.*, 1987, v. 94, 79.
4. Nix W. D. and Ilschner B. Strength of Metals and Alloys (ICSMA5), ed. by Haasen P., Gerold V. and Kostorz G., v. 3, p. 1503, Pergamon Press, Oxford, 1980.
5. Poddriguez P. P., Ibarra A., Iza-Mendia A., San Juan J. and No M. L. *Mater. Sci. and Eng.*, 2004, v. A378, 263–268.
6. Argon A. S. and Takeuchi S. *Acta Metall.*, 1981, v. 29, 1877.
7. Montemayor-Aldrete J. *Mater. Sci. and Eng.*, 1993, v. A160, 71–79.
8. Kang S. S., Dobois J. M. *Philos. Mag.*, 1992, v. A66, No. 1, 151.
9. Soliman M. S. J. *Mater. Sci.*, 1993, v. 28, 4483.
10. Murray J. L. *Int. Met. Rev.*, 1985, v. 30, 211.
11. Hasegawa T., Karashima S. *Metall. Trans.*, 1971, v. 2, 1449.
12. Ichihashi K., Oikawa H. *Trans. Japan Inst. Metals*, 1976, v. 17, 408.
13. Dong-Heon Lee, dong Hyuk Shin and Soo Woo Nam. *Mater. Sci. and Eng.*, 1992, v. A156, 43–52.
14. Mughrabi H. Strength of Metals and Alloys (ICSMA5), ed. by Haasen P., Gerold V. and Kostorz G., v. 3, p. 1615, Pergamon Press, Oxford, 1980.
15. Yuwei Xun, Farghalli, Mohamed A., *Acta Metr.*, 2004, v. 52, 4401–4412.
16. Caillard D. and Martin J. L. *Rev. Phys. Appl.*, 1987, v. 22, 169.
17. Raj S. V. and Langdon T. G. *Acta Metall.*, 1989, v. 37, 843.
18. Giacometti E., Balue N., Bonneville J. In: Dubois J. M., Thiel P. A., Tsai A. P., Urban K. (Eds.), *Quasicrystals, Proceedings of the Materials Research Society Symposium*, v. 553, p. 295, *Materials Research Society*, 1999.

Positron Annihilation Line Shape Parameters for CR-39 Irradiated by Different Alpha-Particle Doses

M. Abdel-Rahman*, M. Abo-Elsoud†, M. F. Eissa†, N. A. Kamel*, Y. A. Lotfy*, and E. A. Badawi*

*Physics Department, Faculty of Science, Minia University, Egypt
†Physics Department, Faculty of Science, Beni-suef University, Egypt
E-mail: maboelsoud24@yahoo.com <M. Abo-Elsoud>; emadbadawi@yahoo.com <E. A. Badawi>

Doppler broadening positron annihilation technique (DBPAT) provides direct information about the change of core and valance electrons in Polyallyl diglycol carbonate (CR-39). CR-39 is widely used as etched track type particle detector. This work aims to study the variation of line-shape parameters (S- and W-parameters) with different α-particle doses of ^{241}Am (5.486 MeV) on CR-39 samples at different energies. The relation between both line-shape parameters was also reported. The behavior of the line-shape S- and W-parameters can be related to the different phases.

1 Introduction

Positron Annihilation Technique (PAT) has been used to probe a variety of material properties as well as carry out research in solid state physics. Recently this technique has become established as a useful tool in material science and is successfully applied for investigation of defect structures present in metal alloys. PAT has been employed for the investigating Polymorphism in several organic materials [1] and it has emerged as a unique and potent probe for characterizing the properties of polymers [2].

Positron Annihilation Doppler Broadening Spectroscopy (PADBS) is a well established tool to characterize defects [3]. The 511 keV peak is Doppler broadened by the longitudinal momentum of the annihilating pairs. Since the positrons are thermalized, the Doppler broadening measurements provide information about the momentum distributions of electrons at the annihilation site.

Two parameters S (for shape), and W (for wings) [4] are usually used to characterize the annihilation peak. The S-parameter is more sensitive to the annihilation with low momentum valence and unbound electrons. The S-parameter defined by Mackenzie et al. [5] as the ratio of the integration over the central part of the annihilation line to the total integration. The W-parameter is more sensitive to the annihilation with high momentum core electrons and is defined as the ratio of counts in the wing regions of the peak to the total counts in the peak.

CR-39 is a polymer of Polyallyl diglycol carbonate (PADC) has been used in heavy ion research such as composition of cosmic rays, heavy ion nuclear reactions, radiation dose due to heavy ions and exploration of extra heavy elements. Some applications include studies of exhalation rates of radon from soil and building materials [6, 7] and neutron radiology [8]. When a charged particle passes through a polyallyl diglycol carbonate, $C_{12}H_{18}O_7$ (CR-39) a damage zone are created, this zone is called latent track. The latent track of the particle after chemical etching is called "etch pit" [9]. The etch pit may be seen under an optical microscope. Positron trapping in vacancies (the size of the etch pit in the CR-39 sample) results in an increase (decrease) in S (W) since annihilation with low momentum valence electrons is increased at vacancies.

2 Experimental technique

Various holder collimators with different heights are used to normally irradiate the INTERCAST CR-39 in air by α-particles [10]. Track detectors "CR-39" were normally irradiated in air by different α-particle energies from 0.1 μCi ^{241}Am source.

The heights of the holders are 12.47, 17.55, 21.58, 24.93, 28.7, 31.55 and 34.6 mm they would reduce the energy of 5.486 MeV α-particles from ^{241}Am to 4.34, 3.75, 3.3, 2.86, 2.3, 1.78 and 1.13 MeV, respectively. The irradiations were verified at 0.5, 2, 3, 4.5 min. After exposures, the detectors were etched chemically in 6.25 M NaOH solution at 70°C for 6 h. The simplest way to guide the positrons into the samples is to use a sandwich configuration. ^{22}Na is the radioactive isotope used in our experiment.

The positron source of 1 mCi free carrier ^{22}NaCl was evaporated from an aqueous solution of sodium chloride and deposited on a thin Kapton foil of 7.5 μm in thickness. The ^{22}Na decays by positron emission and electron capture (E. C.) to the first excited state (at 1.274 MeV) of ^{22}Na. This excited state de-excites to the ground state by the emission of a 1.274 MeV gamma ray with half life $T_{1/2}$ of 3×10^{-12} sec. The positron emission is almost simultaneous with the emission of the 1.274 MeV gamma ray while the positron annihilation is accompanied by two 0.511 MeV gamma rays. The measurements of the time interval between the emission of 1.274 MeV and 0.511 MeV gamma rays can

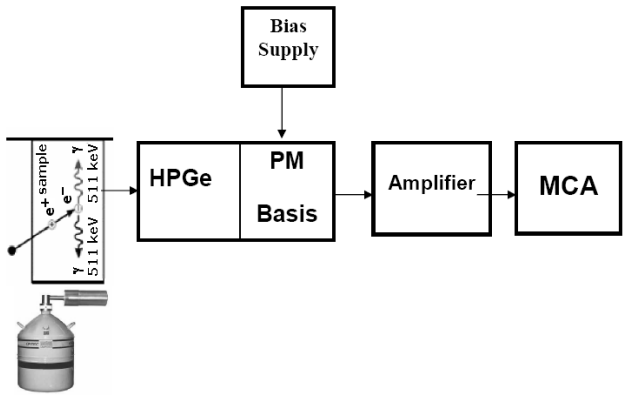

Fig. 1: Block diagram of HPGe-detector and electronics for Doppler broadening line shape measurements.

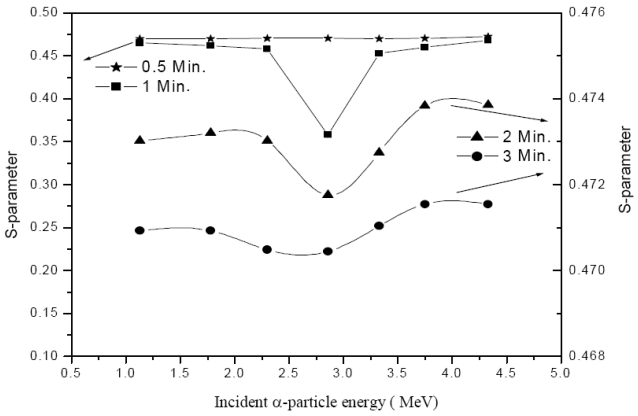

Fig. 2: The variation of S-parameter as a function of irradiation energy for 0.5, 1, 2 and 3 min. irradiation time.

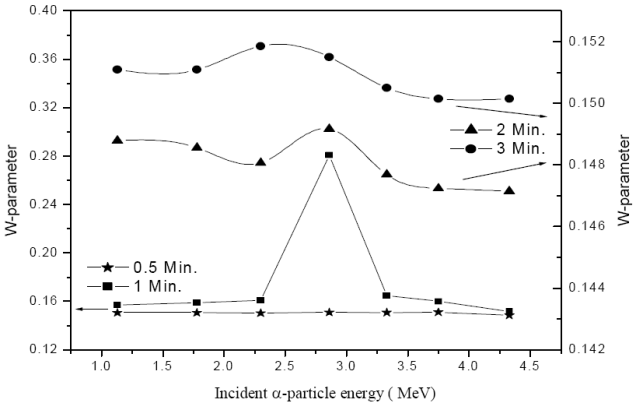

Fig. 3: The variation of W-parameter as a function of irradiation energy for 0.5, 1, 2 and 3 min irradiation time.

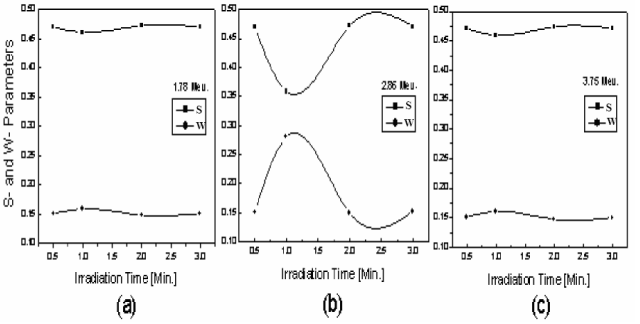

Fig. 4: The variation of S and W parameters as a function of irradiation time for CR-39 samples.

yield the lifetime τ of positrons. The source has to be very thin so that only small fractions of the positron annihilate in the source.

The system which has been used in the present work to determine the Doppler broadening S- and W-parameters consists of an Ortec HPGe detector with an energy resolution of 1.95 keV for 1.33 MeV line of ^{60}Co, an Ortec 5 kV bais supply 659, Ortec amplifier 575 and trump 8 k MCA. Figure 1, shows a schematic diagram of the experimental setup. Doppler broadening is caused by the distribution of the velocity of the annihilating electrons in the directions of gamma ray emission. The signal coming from the detector enters the input of the preamplifier and the output from the preamplifier is fed to the amplifier. The input signal is a negative signal. The output signal from the amplifier is fed to a computerized MCA. All samples spectrum are collected for 30 min.

3 Results and discussion

The Doppler broadening line-shape parameters were measured for irradiated CR-39 samples of different α-particle energies at different doses (0.5, 1, 2 and 3 min). The data of S-and W-parameters at 1 min were calculated by Abdel-Rahman et. al. [11]. The Doppler broadening line-shape S- and W-parameters are calculated using SP ver. 1.0 program [12] which designed to automatically analyze of the positron annihilation line in a fully automated fashion but the manual control is also available. The most important is to determine the channel with the maximum which is associated with the energy 511 keV. The maximum is necessary because it is a base for definition of the regions for calculations of S- and W-parameters.

The results of S- and W-parameters as a function of α-particle energy at different irradiation doses into CR-39 polymer are shown in Figures 2 and 3. From these figures one notice a linear behavior of S- and W-parameters obtained at minimum irradiation time of 0.5 min. The effect of such small irradiation time is very weak to make any variation in line-shape parameters. The values of S- and W-parameters are 47% and 15% respectively at 0.5 min. At longer time (1 min) the S-parameter has values around 46% while values of about 15% are obtained for W-parameter. An abrupt change at 1 min definitely observed at irradiation energy of 2.86 MeV of α-particles for both S- and W-parameters. At this energy a drastically decrease in the S-parameter with deviation of about $\Delta S = 11\%$ comparable with a drastically increase in the W-parameter with deviation of about $\Delta W = 13\%$ [11].

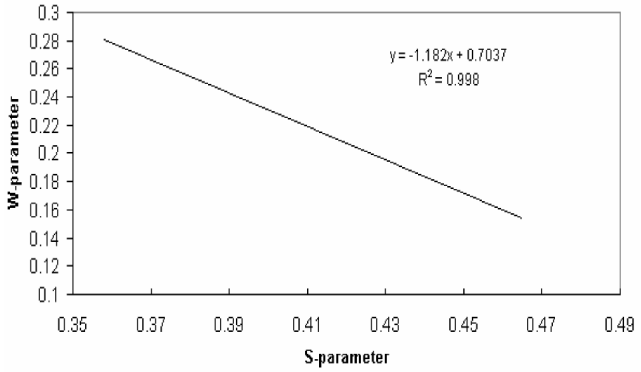

Fig. 5: The correlation between the W-parameter and S-parameter at irradiation time of 1 min.

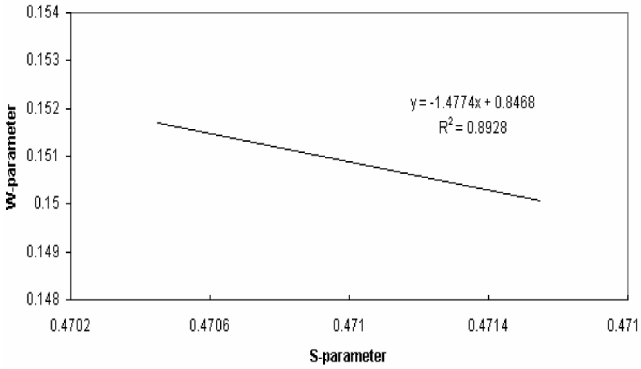

Fig. 6: The correlation between the W-parameter and S-parameter at irradiation time of 3 min.

The S-parameter decreases while W-parameter increases with increasing of irradiation time. Values of about 35% and 25% for S-parameter are obtained at 2 and 3 min respectively for lower energies. The deviation of both S- and W-parameters at 2.86 MeV become very small at longer time as measured at 2 and 3 min. The deviations of $\triangle$S and $\triangle$W reach values less than 0.1% at 3 min (notice different scale on Figures 2 and 3). The behavior of S- and W-parameters reveal an abrupt change at the position of the transition (1 min at 2.86 MeV). The behavior of the line-shape S- and W-parameters can be related to the different phases. Like many others molecular materials, the use of PAT also proven a very valuable in the study of phase transition in polymers.

To recognize more clear the effect of both irradiation time and energy, we take 3 values of energies from presented figures and draw them as a function of irradiation time. Figure 4 (a, b, and c) represent the S- and W-parameters as a function irradiation time for samples irradiated at energies of 1.78, 2.86 and 3.75 MeV respectively. It is much more clear from these figures a slightly change of S- and W-parameters are obtained only at 1 min at irradiation energies of 1.78 and 3.75 MeV. Much more pronounced change in both S- and W-parameters are obtained at the same irradiation time at energy of 2.86 MeV.

The values of W-parameter as a function of S-parameter at 1 and 3 min are plotted in Figs. 5 and 6. It is obvious from these Figures that W-parameter increases as S-parameter decreases for all irradiation times. In addition there are a good correlation with $r^2 = 0.998$ and 0.8928 between S-parameter and W-parameter for 1 and 3 min respectively.

4 Conclusion

The variation of line-shape parameters (S- and W-parameters) at different α-particle doses of ^{241}Am on CR-39 samples for different energies have been studied. The behavior of line-shape parameters at different α-particle doses reveals a pronounced decrease and increase in both S- and W-parameters respectively. A linear behavior of S- and W-parameters are obtained at minimum irradiation time of 0.5 min. An abrupt change of both line-shape parameters, obtained at 2.86 MeV and irradiation dose of 1 min. The W-parameter increases as S-parameter decreases for all irradiation times.

Acknowledgment

We thank Prof. Dr. M. A. Abdel-Rahman for his encouragements and support facilities during preparation of this work.

References

1. Walker W. W., Kline D. C. *J. Chem. Phys.*, 1974, v. 60, 4990.
2. Jean Y. C. In: A. Dupasquier and A. P. Mills Jr. (Eds), *Positron Spectroscopy of Solids*, IOS Publ., Amsterdam, 1995, 563–569.
3. Dupasquier A., Mills A. P. (Eds.) *Positron Spectroscopy of Solids*, IOS Publ., Amsterdam, 1995
4. Urban-Klaehen J. M., Quarles C. A. *J. Appl. Phys.*, 1999, v. 86, 355.
5. Mackenzie I. K., Eady J. A. and Gingerich R. R. *Phys. Lett.*, 1970, v. 33A, 279.
6. Sroor A., El-Bahia S. M., Ahmed F., Abdel-Haleem A. S. Natural radioactivity and radon exhalation rate of soil in southern Egypt. *Applied Radiation and Isotopes*, 2001, v. 55, 873–879.
7. Sharma N. and Virk H. S. Exhalation rate study of radon/thoron in some building materials. *Radiation Measurements*, 2001, v. 34, 467–469.
8. Majeed A. and Durrani S. A., High-energy neutron spectrum measurements using electrochemically etched CR-39 detectors with radiators and degraders. *Nucl. Track Radiat. Meas.*, 1991, v. 19, No. 1–4, pp. 489–494.
9. Durrani S. A., Bull R. K. Solid-state nuclear track, principles, methods and applications formation. Pergamon, Oxford, 1987.
10. Enge W. Introduction to plastic nuclear track detectors. *Nuclear Track*, 1980, No. 4, 283–308.
11. Abdel-Rahman M. A., Abdel-Rahman M., Abo-Elsoud M., Eissa M. F., Lotfy Y. A. and Badawi E. A. *Progress in Physics*, 2006, v. 3, 66–69.
12. http://www.ifj.edu.pl/∼mdryzek.

Progress in Physics is a quarterly issue scientific journal, registered with the Library of Congress (DC).

This is a journal for scientific publications on advanced studies in theoretical and experimental physics, including related themes from mathematics.

Electronic version of this journal:
http://www.geocities.com/ptep_online

Progress in Physics is peer reviewed and included in the abstracting and indexing coverage of: Mathematical Reviews and MathSciNet of AMS (USA), DOAJ of Lund University (Sweden), Zentralblatt MATH (Germany), Referativnyi Zhurnal VINITI (Russia), etc.

Department of Mathematics, University of New Mexico,
200 College Road, Gallup, NM 87301, USA

Printed in the United States of America

Issue 2006, Volume 3
US $ 20.00